

DISSERTATION

Gene expression changes in senescent human fibroblasts point
to the existence of a human telomere position effect

Genexpressionsänderungen in seneszenten menschlichen
Fibroblasten weisen auf die Existenz eines menschlichen
Telomerpositionseffektes hin

zur Erlangung des akademischen Grades
Doctor rerum medicinalium (Dr. rer. medic.)

vorgelegt der Medizinischen Fakultät
Charité – Universitätsmedizin Berlin

von

Kathrin Jäger

Erstbetreuung: Prof. Dr. med. Michael Walter

Datum der Promotion: 29.11.2024

Contents

List of figures	vi
List of abbreviations	vii
Abstract in English	1
Zusammenfassung in deutscher Sprache	2
1 Introduction	3
1.1 Aging.....	3
1.1.1 Aspects of aging	3
1.1.2 Telomeres and replicative aging.....	3
1.1.3 Telomerase	4
1.1.4 Telomere position effect.....	5
1.1.5 Stress and senescence.....	7
1.2 Diseases associated with telomere shortening - a selection.....	9
1.2.1 Hutchinson-Gilford-Progeria syndrome.....	9
1.2.2 Nijmegen Breakage syndrome	9
1.2.3 Werner syndrome	10
1.3 Protein phosphatase 2A	11
1.4 Aim of the work.....	13
2 Methods.....	15
2.1 Cell culture.....	15
2.2 Hydrogen peroxide treatment.....	16
2.3 Gene expression analysis via quantitative real-time PCR (qPCR)	16
2.4 Telomere length measurement	17
2.5 Three-dimensional fluorescence <i>in situ</i> hybridization (3D-FISH).....	17
2.6 Protein analyses.....	18
2.7 <i>PPP2R2C</i> knock down.....	19
2.8 Serum deprivation	19

2.9	Inhibitor tests	19
2.10	Statistical analysis.....	20
3.	Results	21
3.1	Chromosomal conservation of TPE-OLD candidates	21
3.2	Telomere length in relation to replicative aging.....	21
3.3	Gene expression changes in TPE-OLD candidate genes	22
3.4	Evidence of a telomere loop as a possible reason for gene silencing	23
3.5	Effect of <i>PPP2R2C</i> on the dephosphorylation of p70S6k independent of cellular mTOR levels.....	24
3.6	<i>PPP2R2C</i> silencing in HGP fibroblasts	24
3.7	Influence of chromatin modification on <i>PPP2R2C</i> mRNA expression.....	25
3.8	<i>PPP2R2C</i> expression in different cell types.....	26
3.9	Telomere position effect in NBS cells	26
4.	Discussion.....	28
4.1	Characterization of <i>PPP2R2C</i> as a TPE-OLD gene	28
4.2	Cell specificity of TPE-OLD	28
4.3	Direct influence of telomere shortening on the mTOR signaling pathway	29
4.4	Replicative aging as a tumor suppressor.....	30
4.5	Abnormalities in telomere kinetics in HGP and NBS	30
4.6	Limitations.....	31
5.	Conclusion	33
6.	Outlook.....	34
7.	Reference list.....	35
8.	Annex	45
	Eidesstattliche Erklärung	45
	Declaration of contribution to the selected publications.....	46
	Printed copies of selected publications.....	47

Curriculum vitae.....	172
List of publication.....	174
Acknowledgement.....	176

List of figures

- Figure 1 Telomere Position Effect
- Figure 2 Senescence signaling cascade
- Figure 3 Structural organization of protein phosphatase 2A
- Figure 4 Immortalization of human fibroblasts
- Figure 5 Exemplary representation of a cell nucleus analyzed with 3D-FISH

List of abbreviations

3D-FISH	Three-dimensional fluorescence <i>in situ</i> hybridization
DSB	Double strand break
HGP	Hutchinson-Gilford-Progeria
HUVEC	Human umbilical vein endothelial cell
LCL	Lymphoblastoid cell line
mTOR	Mammalian target of rapamycin
NBS	Nijmegen Breakage syndrome
p70S6k	p70 S6 kinase
PP2A	Protein phosphatase 2
qPCR	Quantitative real-time PCR
TERC	Telomerase RNA component
TERT	Telomerase reverse transcriptase
TL	Telomere length
TPE-OLD	Telomere Position Effect-Over Long Distances
TPE	Telomere position effect
SIS	Stress induced senescence
WS	Werner syndrome

Abstract in English

Every living organism ages. A distinction can be made between replicative aging (characterized by telomere shortening) and stress-induced aging (mainly caused by reactive oxygen compounds). In replicative aging, the telomeres shorten during each cell division, which is caused by incomplete replication during cell division. Several diseases have been shown to be affected directly or indirectly by telomere shortening. One of these diseases is Hutchinson-Gilford-Progeria, which is characterized by premature aging and mild telomere shortening. Another disease is the Nijmegen Breakage syndrome, which is a disease associated with more severe telomere attrition and markedly reduced telomere length. Telomeres are repetitive nucleotide sequences that act as protective caps at the ends of each chromosome. Each cell can divide for a certain number of times until it enters a stage called senescence or apoptosis. Most tumor and stem cells can express the gene telomerase (hTERT, human Telomerase Reverse Transcriptase), which can extend telomeres to some extent. Recently, the so-called Telomere Position Effect-Over Long Distances (TPE-OLD) has been described. Here, gene expression is directly controlled by telomere length.

In this work, different genes were screened for a TPE-OLD mechanism in human fibroblasts from Hutchinson-Gilford-Progeria patients and healthy children. In addition, primary cells were transfected with a vector to express hTERT and to artificially lengthen telomeres. In addition, lymphoblastoid cell lines and HUVEC were studied to further elucidate the cell specificity. For comparison, telomere-dependent differences in gene expression were also investigated in Nijmegen Breakage Syndrome cells.

The serine/threonine phosphatase *PPP2R2C* (a tumor suppressor gene) was identified as a TPE-OLD regulated gene. Gene expression is upregulated by telomere shortening and chromosome reorganization in pre-senescent cells and leads to dephosphorylation of p70S6 kinase and suppression of mTOR (mammalian target of rapamycin) by TPE-OLD.

The results suggest a metabolic adaptation process in older cells and a link between telomere length and gene expression regulation and mTOR suppression.

Zusammenfassung in deutscher Sprache

Jeder lebende Organismus altert. Man kann vereinfacht zwischen replikativer Alterung (begleitet von Telomerverkürzung) und stressinduzierter Alterung (überwiegend verursacht durch reaktive Sauerstoffverbindungen) unterscheiden. Bei der replikativen Alterung verkürzen sich die Telomere bei jeder Zellteilung, was auf eine unvollständige Replikation während der Zellteilung zurückzuführen ist. Viele chronische und einige erbliche Krankheiten werden durch Telomerverkürzung direkte oder indirekte beeinflusst. Eine dieser erblichen Modellkrankheiten ist die Hutchinson-Gilford-Progerie, die durch vorzeitige Alterung gekennzeichnet ist. Eine andere Krankheit ist das Nijmegen Breakage Syndrom, welches sich durch genetische Instabilität und durch eine drastisch reduzierte Telomerlänge auszeichnet. Telomere sind sich wiederholende Nukleotidsequenzen, die als Schutzkappen an den Enden der Chromosomen fungieren. Jede Zelle kann sich in einer bestimmten Anzahl teilen, bis sie in die Phase der Seneszenz oder die Apoptose übergeht. Im Vergleich dazu können die meisten Tumore und Stammzellen das Gen Telomerase (hTERT, human Telomerase Reverse Transkriptase) exprimieren, welches die Telomere partiell verlängern kann. Vor kurzem wurde der so genannte „Telomere Position Effect-Over Long Distances“ (TPE-OLD) beschrieben. Hier werden Gene direkt durch die Telomerlänge kontrolliert.

In dieser Arbeit wurden potenzielle Kandidaten-Gene auf einen TPE-OLD-Mechanismus in menschlichen Fibroblasten von Hutchinson-Gilford-Progerie und gesunden Kindern untersucht. Darüber hinaus wurden primäre Zellen mit einem hTERT enthaltenen Vektor zur künstlichen Verlängerung der Telomere transfiziert. Darüber hinaus wurden lymphoblastoide Zelllinien und HUVECs untersucht, um die Zellspezifität zu untersuchen. Telomer-abhängige Unterschiede in der Genexpression wurden zusätzlich in Nijmegen Breakage Syndrom-Zellen untersucht.

Die Serin/Threonin-Phosphatase *PPP2R2C* (ein Tumorsuppressor-Gen) wurde als ein durch TPE-OLD reguliertes Gen identifiziert, das durch die Telomerverkürzung und physikalische Umlagerung der chromosomalen Struktur in präseneszenten Zellen verstärkt exprimiert wurde, was zur Dephosphorylierung der p70S6-Kinase mit konsekutiver Unterdrückung von mTOR (mammalian target of rapamycin) führte.

Die Ergebnisse weisen auf eine metabolische Anpassung von älteren Zellen hin, bei denen die Telomerlänge einen Link zur Genexpressionregulierung und der mTOR-Suppression darstellt.

1 Introduction

1.1 Aging

1.1.1 Aspects of aging

Every living organism is undergoing the aging process. Aging is characterized by a progressive multisystemic loss of cell and organ function leading to the death of the organism. Chronic diseases such as diabetes mellitus, atherosclerosis, neurodegenerative diseases and also tumors are triggered or amplified by the aging process (1). In addition, exogenous factors such as an unhealthy lifestyle, excessive exposure to radiation or stress can accelerate aging (2, 3). Genetic and epigenetic factors also influence aging (4).

Two main types of aging processes can be distinguished in human cells: replicative aging (triggered by telomere shortening during each cell division) and stress-dependent mechanisms (SIS, stress-induced senescence). In this context, exogenous factors (pathogens, radiation, chemical carcinogens), endogenous factors (growth factors, alkylating reagents, reactive oxygen compounds) and replicative aging mechanisms (induced by telomere shortening) ultimately lead to DNA damage and reinforce each other. Different factors act cooperatively to induce overlapping signal transduction pathways. DNA damage causes transcriptional dysfunction and age-dependent functional impairment and leads to cellular senescence or apoptosis. (5, 6). Senescence refers to a cell state of growth arrest accompanied by functional decline (7), while apoptosis describes programmed cell death, mostly triggered by overlapping but stronger stimuli and signaling cascades than in senescence induction (8).

In replicative senescence, the telomere shortening during each cell division, which is caused by incomplete replication during cell division is the main trigger for cell cycle arrest (9). This aging process primarily occurs in large, long-lived organisms (such as humans).

1.1.2 Telomeres and replicative aging

Telomeres together with variety of specialized proteins form protective caps (loops) located at the end of all chromosomes and in human beings consist of the non-coding tandem repeat sequence (TTAGGG)_n (10). They provide genomic stability and protect DNA from degradation and recombination. They are also responsible for the positioning of the chromosomes within the cell nucleus. This is of particular importance for the pairing of

homologous chromosomes during early meiosis and cell division (11) but may also influence proper gene expression.

Every time a cell divides, telomeres shorten because of the so-called 'end-replication problem'. During cell division, part of the terminal DNA is lost. When a critical threshold of telomere sequence loss is reached, the loop structure is abolished and dysfunctional telomeres are formed. As a result, the protective function of telomeres is lost, leading to chromosome instability. Accumulation of such DNA damage then leads to senescence or apoptosis (12–14). The resulting constant telomere shortening leads to a limitation of cell division, referred to as replicative senescence (15). Each cell can divide itself for a certain number of times until it is sent to senescence or cell death. The number of times a cell can divide before it is sent to growth arrest due to its critical telomere length (TL) is described by the Hayflick limit (16).

When a critical telomere shortness is reached, the p53 pathway is activated with consecutive senescence or apoptosis (9). Intact telomeres are protected by the binding of specific telomere binding proteins called "shelterin complex." The shelterin complex supports the tertiary structure of telomeres and protects them from DNA-degrading enzymes (17). This complex is bound directly or indirectly to telomere sequences, thus forming a protein complex consisting of six proteins: TRF1 (telomeric repeat binding factor 1), TRF2 (telomeric repeat binding factor 2), TIN2 (TRF1 interacting nuclear factor 2), POT1 (protector of telomeres 1), RAP1 (Repressor/Activator protein 1), and TPP1 (POT1-TIN2 organizing protein (17). Shortening of telomeres and loss of these proteins results in detection of double-strand breaks (DSB) via specific stressor proteins (ATM / ATR) and end-to-end fusion of chromosomes, and eventually loss of genomic stability, activation of cell cycle checkpoints, and growth arrest (9).

It has been hypothesized that the entry of cells into senescence protects the body of large long-lived species from early tumorigenesis (12–14, 17).

As a consequence of telomere shortening, a connection with the occurrence of age-related diseases such as myocardial infarction (18), atherosclerosis (19) or Alzheimer's disease (20) has been described.

1.1.3 Telomerase

The TL of normal somatic cells decreases with each cell division. By contrast, stem cells, germline cells and cancer cells have found a way to avoid growth arrest. All these cells express the enzyme telomerase (21–23). Telomerase consists of two subunits: a RNA

template (TERC) (24) and a telomerase reverse transcriptase catalytic subunit (TERT) (25). TERT is a reverse transcriptase that extends the guanine-rich telomere sequences at the 3' - end of chromosomes by appending the repetitive (TTAGGG)_n sequence (12). The property of TERT has been exploited by introducing the catalytic subunit into cells that normally do not possess it. In this way, human skin fibroblasts can (under proper experimental conditions) be immortalized with the aid of the human TERT subunit (hTERT) (26). Compared to other immortalization methods, this procedure has the advantage of generating a juvenile cell type that is physiologically very close to the *in vivo* phenotype without altering the karyotype (for example immortalization using oncogenes). In addition, these cells retain contact inhibition capacity, cell cycle control, growth factor dependence, and a normal karyotype (27). In addition, it could be shown that in fibroblasts the initiation of senescence after immortalization with hTERT could significantly be delayed and the number of population doublings (PDs) of the cells in culture could be increased from 40-80 to over 120 PDs before senescence occurred (28).

1.1.4 Telomere position effect

In 1985, a mechanism called TPE (29), has been described first in *Drosophila melanogaster* (29) and then in *Saccharomyces cerevisiae* (30). This effect is defined as a suppression of gene expression in subtelomeric regions and a change in gene expression associated with progressive telomere shortening (9). This effect can in these organisms be observed up to 100 to 150 kb away from the telomere and describes the direct influence of telomere (length) on gene expression by heterochromatin spreading (30, 31).

The first evidence that a TPE may also exist in humans was demonstrated by a luciferase reporter gene near the telomere tandem sequence in HeLa cells (31). It was shown that the silencing effect correlates with TL, and, that the luciferase reporter is expressed at significantly lower levels inserted at telomeric regions than at intra chromosomal sites. In addition, artificial telomere lengthening with overexpression of *hTERT* was shown to cause a decrease in luciferase expression (31). This had similarly been shown previously by Gottschling et al. 1990 in yeast studies. Thus, genes located close to the telomeres can be silenced, at least under artificial *in vitro* conditions (30). In further studies, it has been shown that tertiary structures can also be influenced by telomeres, which in yeast can repress genes up to 20 kb away from the chromosome end (32).

In human cells, an influence of telomeres on gene expression was hypothesized to occur up to 10-15 Mb away from the chromosome end. This mechanism was called Telomere

Position Effect-Over Long Distance (TPE-OLD) (33), where genes located between the chromosome end and the affected gene are not affected by TPE. While in "classical" TPE the telomere impact is caused by the spreading of heterochromatin (34), in TPE-OLD genes a loop structure formation of telomeres including the interaction with the shelterin protein complex may bring the long telomeres close to the candidate genes, thus suppressing its activity (33). During telomere shortening, this structure is then released and the telomeres separate from the TPE-OLD gene, increasing gene expression of the TPE-OLD gene (fig. 1). In old cells with short telomeres, such an interaction cannot be maintained, which then leads to a change in gene expression (33, 35). By artificially lengthening telomeres with overexpression of *hTERT*, this mechanism was shown to be reversible under *ex vivo* conditions (31, 36).

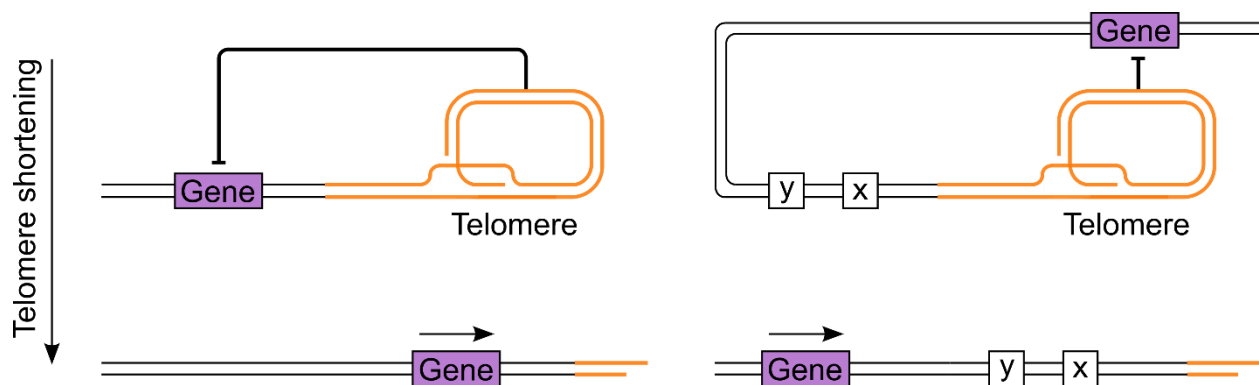


Figure 1: Telomere Position Effect. On the left panel the "classical" TPE is shown. A gene (violet) close to the telomere (orange) is repressed. Telomere shortening causes the suppressed gene to be expressed in aging cells. The TPE-OLD is shown on the right panel. Here, the gene (violet) is suppressed by telomere loops. Genes that are "far" away from the telomere end can be affected. Genes (x, y; white boxes) between the target gene (violet) and the telomere end (orange) are not affected. Shortening of telomeres by replicative aging opens the loop and the target gene is exposed. Own illustration.

To date, 16 TPE-OLD candidate genes have been identified in humans using gene expression analysis, three-dimensional fluorescence in situ hybridization (3D-FISH), and mapping of interaction with HI-C (32, 33, 36–38).

1.1.5 Stress and senescence

Oxidative stress by free radicals, UV irradiation and activation of oncogenic signaling pathways lead to immediate growth arrest *in vitro*, which resembles replicative senescence in many respects. The term 'Stress Induced Senescence' (SIS) was introduced for this phenomenon (39). This is caused by the induction of DNA DSBs and is primarily not dependent on TL (39). Telomere shortening is not necessarily associated with this response, and even artificial telomere elongation by reverse transcriptase telomerase (hTERT, human Telomerase Reverse Transcriptase) does not protect fibroblasts from stress-induced growth arrest (40).

SIS offers the possibility to induce cells into a state of senescence under experimental conditions by defined stress in a short period of time without the need to undergo numerous cell divisions. Both stress and frequent cell divisions, often at sites of increased proliferation such as heavily stressed vascular sections, can lead to senescence, and often both factors synergize to induce the aging process (9).

These different factors lead to senescence and are strongly overlapping. However, slightly different signaling pathways may trigger senescence at the molecular level. For example, telomere damage and shortening primarily leads to activation of the p53-p21-pRb cascade, similar to the response to DSB (9). DSB or short telomeres initially activate the ATR (ATM and Rad3 related) and ATM (Ataxia Teleangiectasia Mutated) kinases. These specific kinases regulate numerous proteins involved in the DNA damage response. The tumor suppressor protein p53, which is involved in senescence initiation, is activated by ATM / ATR. The activation of p21, a target of p53, leads to the inhibition of CDK2 / cyclin E. This prevents phosphorylation of the tumor suppressor protein pRb and induces cell cycle arrest (9).

DNA damage (41), cytotoxic substances (42), reactive oxygen species, and other stimuli can also lead to hypophosphorylation of Rb. This signaling pathway is mediated via the protein p16^{INK4a} and leads to the inhibition of CDK4 / CDK6 / cyclin D (43) (fig. 2).

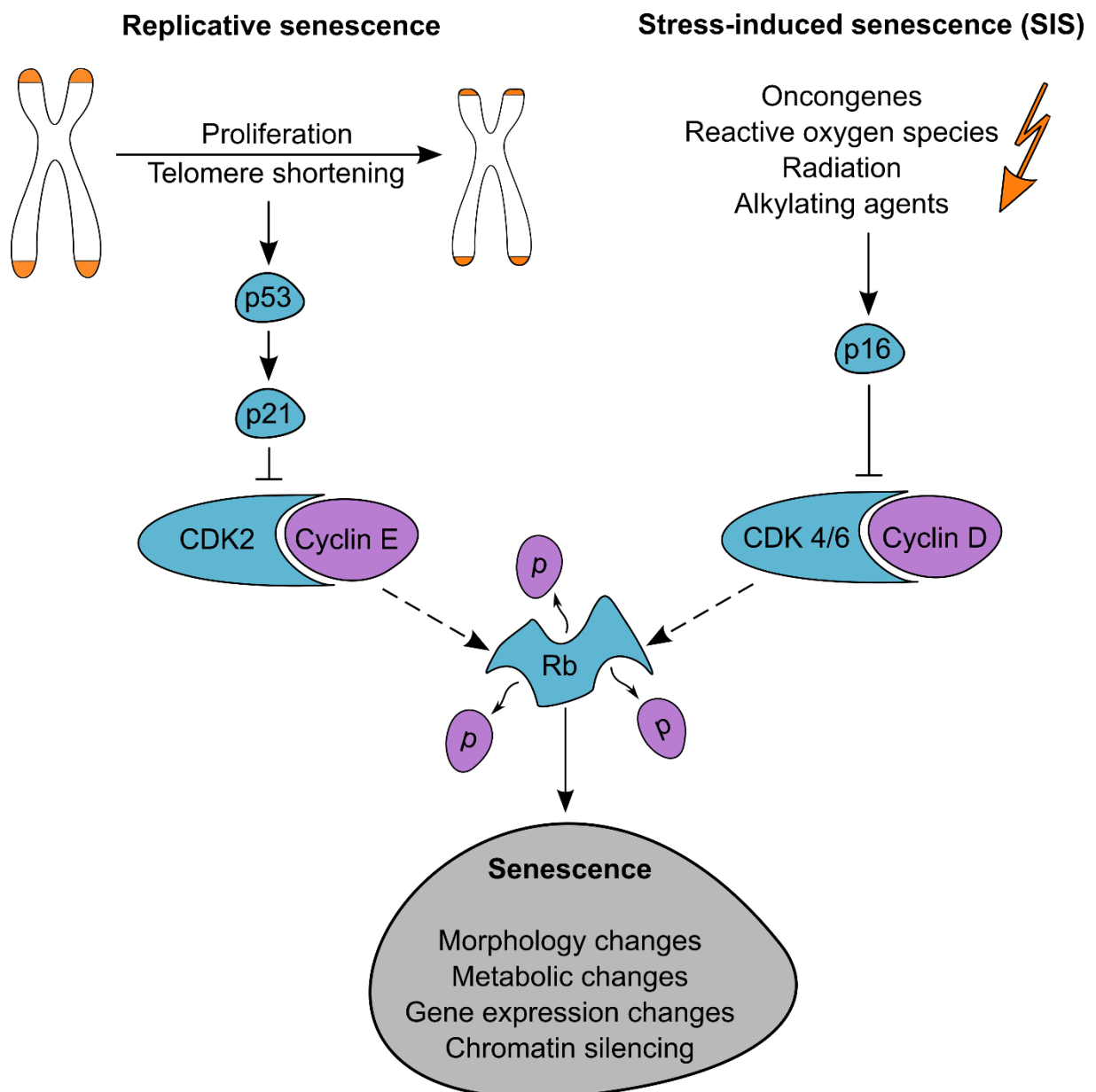


Figure 2: Senescence signaling cascade. Dysfunctional telomeres and / or telomere – independent signals (SIS) induce via p53 / p21 and p16 the hypophosphorylation of pRB and trigger senescence entry. Figure modified according to Jäger and Walter, 2016 (26).

P53 is considered the primary factor in senescence initiation. Studies have shown that a defective p53-pRb cascade avoids senescence and cells continue to grow despite shortened telomeres. It is therefore assumed that senescence serves as an important protection mechanism against the development of malignant tumors (44).

Another possibility would be that a possible TPE is lost due to the shortening of the telomeres. This would result in the lack of expression of genes, which under normal conditions may support a coordinated shut-down.

1.2 Diseases associated with telomere shortening - a selection

There are many different diseases caused by mutations in genes responsible for telomere stability (*TERT*, *TERC*, *DKC1*, *TINF2* and many more) and other mutations that indirectly destabilize telomeres, such as interference with chromosome anchoring during cell division, for example in Hutchinson-Gilford-Progeria (HGP) syndrome (27, 45–47).

Mutations in the *TERT* and *TERC* genes are the most common mutations leading to diseases affecting telomere biology. The symptoms manifest later in life. Diseases include dyskeratosis congenita, idiopathic pulmonary fibrosis, aplastic anemia, and familial liver cirrhosis. A mutation in *TRF2*, which directly affects the shelterin complex rarely, leads to direct shortening of telomeres. This may cause dyskeratosis congenita (46), Hoyeraal-Hreidarsson syndrome (46), and idiopathic pulmonary fibrosis (45).

In the following section, some secondary telomeropathies, which lead to premature aging, are described in more detail. Two of these diseases (HGP and NBS) were used as model diseases for premature aging and telomere shortening to varying degrees.

1.2.1 Hutchinson-Gilford-Progeria syndrome

The HGP syndrome is a very rare disorder in which the affected individuals age prematurely. The classic genotype is caused by a spontaneous *de novo* point mutation in the lamin A (*LMNA*) gene, resulting in a single nucleotide substitution mutation c.1824C > T in exon 11 associated with physical and disturbances in the nuclear envelope and misfolding of chromosomes anchored in the nuclear membrane (47). During the meantime other mutations have been described, which can lead to a Progeria like syndrome (48). HGP patients develop alopecia, postnatal growth retardation with sclerodermatous skin changes, loss of subcutaneous fat, atherosclerosis, and other age-associated symptoms particular in mesenchymal tissues. At an average age of 12.6 - 14.6 years, the patients die of heart attacks and strokes. (49). The cognitive development is normal and no increased incidence of cancer is observed during the short life time (49). Measurements of TLs in fibroblasts showed that they were moderately shortened compared to healthy fibroblasts (27), which may at least in part contribute to the clinical phenotype.

1.2.2 Nijmegen Breakage syndrome

NBS is a rare autosomal recessive disease caused by a mutation of the nibrin gene (*NBS2*) on chromosome 8 (50). This mutation causes the protein complex involved in the

DNA repair mechanism to be disturbed or incorrectly assembled. As a result, the whole mechanism comes to a standstill. In addition, the ATM cascade is disturbed in NBS and the cells can no longer enter regular apoptosis (51). Phenotypically, there are different malformations, because the mutation mostly affects the whole body. Already during pregnancy, a delayed development can be observed, which continues after birth. A small head is conspicuous, and it comes to malformations of the head and the brain. In addition, the immune system is affected, which, together with the disturbed DNA repair, leads to specific types of cancer (particularly leukemia, lymphoma) (52).

It appears that nibrin has an additional important role in telomere protection (53). There are experimental data suggesting a link between nibrin and dysfunctional telomeres (54). Both cultured fibroblast cells and B-lymphocytes from NBS patients have a markedly reduced TL (53). The exact role of nibrin in telomere homeostasis is however not understood.

1.2.3 Werner syndrome

Werner syndrome (WS), like HGP syndrome, is a progeroid disease. The mutation in *WRN* (Werner gene) is inherited in an autosomal recessive manner. This gene encodes one of the 5 RecQ helicases of the human genome. Nonsense mutations, insertions, and / or deletions or substitutions in the *WRN* gene result in genomic instability (55). Mutations in this gene are found in approximately 90% of cases clinically diagnosed as WS. The remaining 10% are operationally referred to as atypical WS and have other causes, for example, other mutations in the *LMNA* gene (56). Functionally, *WRN* appears to have a variety of different functions in DNA repair, recombination, replication, transcription, and regulation of telomere integrity, and thus appears to be centrally involved in the maintenance of genomic stability (57). Unlike HGP syndrome, the first symptoms do not appear before young adulthood. These include post-puberty dwarfism, premature graying of the hair, regression of the body tissue. The risk of developing malignant tumors is high, especially for sarcomas of mesenchymal origin and for melanomas not caused by sunlight exposure. The most frequent causes of death are malignancies or myocardial infarction caused by extensive and unusual form of arteriosclerosis (58). Studies have shown that although TL in young patients is accelerated telomere attrition occurs normal but in higher ages (59).

1.3 Protein phosphatase 2A

Studies have shown that dephosphorylation of multiple enzymes and signaling molecules by protein phosphatase 2A (PP2A), plays a key role in growth, differentiation and regulation of cell cycle and growth arrest at the cellular level (60). Moreover, PP2A is a tumor-suppressor and its inhibition can lead to tumor growth (61). A broad variety of protein kinases in cellular signal transduction cascades provide substrates for PP2A, including the p70S6 kinase (p70S6k) involved in cell cycle regulation (62).

PP2A is a serine/threonine phosphatase composed of different subunits. This holoenzyme consists three subunits: a structural (subunit A), a catalytic (subunit C) and a regulatory subunit (subunit B) (60). In mammals, both the structural and catalytic subunits have two isoforms, with the α isoform being more frequent than the β isoform (63). The variable regulatory subunit is further divided into four subfamilies, which consist numerous of isoforms and splice variants in this subfamily: B (α , β , γ , δ), B' (α , β , γ , δ , ϵ), B'' (α , β , γ , δ) and B''' (PR93, PR110) (64–68). Four isoforms of the regulatory subunit, two isoforms of the structural subunit and two isoforms of the catalytic subunit were investigated in more details in this study (fig.3).

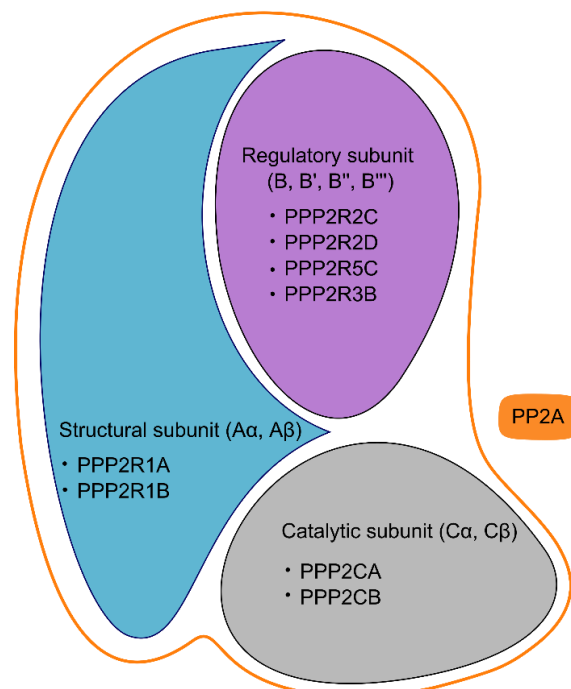


Figure 3. Structural organization of protein phosphatase 2A. PP2A consists of a structural subunit (A), a catalytic subunit (C), and a regulatory subunit (B). The respective subunits also consist of variable units (written in parentheses). Also shown are the genes that were further investigated in this work. Figure modified after Jäger et al., 2022 (69).

The isoforms display functional differences during development. While B α and B β are mostly found in cytosolic regions, the B γ isoform is enriched in the cytoskeletal fraction (70). Moreover, while the B α isoform is constantly expressed, the expression level of B β and B γ is highly variable during different developmental stages (70). The B β and B γ subunits are predominantly expressed in the brain (67), whereas the B α subunit is ubiquitously expressed (67). However, knowledge is incomplete in an under-examined field needing further research. Much less is known about serine / threonine specific phosphatase compared to kinases. Studies suggest that the B γ subunit (encoded by *PPP2R2C*) is a tumor-suppressor gene in glioblastoma (61) and prostate cancer (71), by suppressing the p70S6k in the mTOR pathway (61). A possible influence on the cognitive development was suggested sometimes in intellectual disability syndrome (72).

1.4 Aim of the work

Aging of human cells can occur via stress-dependent mechanisms (SIS, stress-induced senescence) and / or via replicative aging processes triggered by increasing telomere shortening, with a broad overlap of both mechanisms and signal transduction pathways. (5, 6).

Telomere attrition may induce a DNA damage signal that ultimately leads to cellular senescence. Recent data suggest that telomere attrition may modulate cell physiology and possibly also aging by a process called TPE; e.g., the telomere length and / or telomere structure-dependent silencing / activation of gene expression. A suspected but not yet proven function of a TPE is the induction of senescence (including cell cycle arrest) and/or the regulation of accompanying mechanisms in pre-senescent cells.

This work will further investigate candidate TPE genes involved in cell cycle regulation with the following questions:

- a) Can a TPE be shown / proven and is it specific?
- b) Can a functional relationship between TPE and senescence be shown?
- c) Do changes in TPE contribute to the phenotype of telomere diseases?

The following models and approaches were used for this purpose:

Human skin fibroblasts from HGP children, as a model for premature replicative senescence. Fibroblasts from healthy children were used as control group. Lymphoblastoid cell lines (LCL) and HUVEC were used to investigate possible cell-specificities.

Gene expression analyses were performed of both the candidate gene and genes between the candidate gene and the telomere region.

Comparative studies of primary and *hTERT*-immortalized HGP fibroblasts with artificially elongated telomeres were used to prove possible age-specific changes that arise from replicative processes triggered by telomere shortening. In order to prove successful immortalization, the growth curves of the primary cells and the immortalized cells as well as the TLs and telomeric activity were compared.

There are multiple other factors apart from telomere shortening, which may influence lifespan. A very important mechanism which converges from various factors is SIS. De-

spite different damage mechanisms, similar signaling pathways, including p53, are activated by both telomere-dependent and telomere-independent signals. As a model for SIS, cells were treated with hydrogen peroxide which is an established procedure to initiate cell stress. In parallel, the respective immortalized cell lines were used to prove which effects can possibly be compensated.

To show a loop structure of the telomere as a possible mechanism for gene silencing, specific probes were used for the investigated gene locus and were analyzed by 3D-FISH.

For all studies, the cells were compared at low and high PD numbers. In higher passages an increase of the postulated effect on gene expression was postulated.

2 Methods

The material and methods section gives a brief overview of the used techniques and employed cell lines. A detailed step-by-step guide for each method can be found in Jäger et al. 2022 (69), Habib et al. 2020 (73) and Jäger and Walter 2016 (26).

2.1 Cell culture

Primary fibroblasts from healthy children without obvious genetic defects, HGP fibroblast from the Progeria Research Foundation (PRF) Cell and Tissue Bank and one dermal fibroblast cell line from an apparently healthy adult donor were used. The primary cells were immortalized with retroviral supernatants obtaining a pBabePuro vector to stably express human telomerase as described in (26, 27, 74) (fig 4).

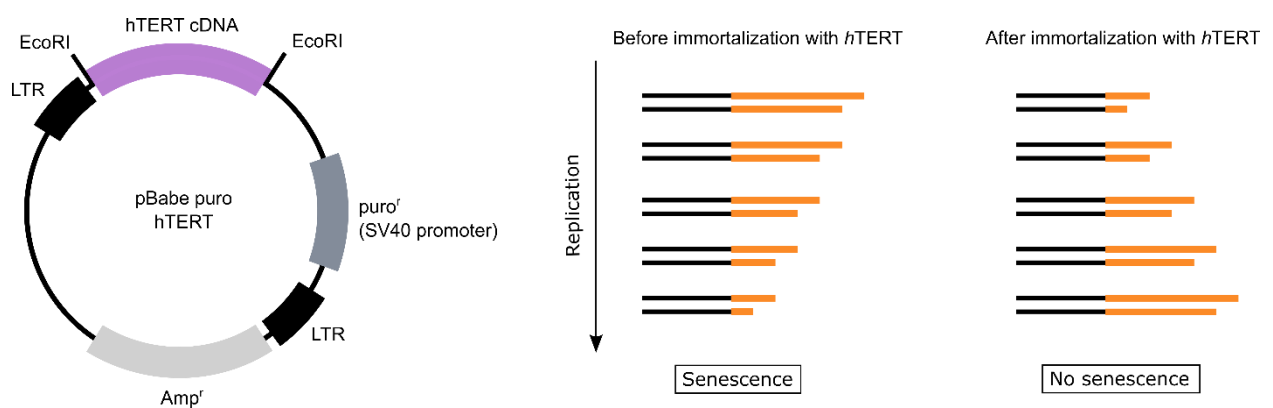


Figure 4. Immortalization of human fibroblasts. On the left side the construction of the vector is shown, which was used for the immortalization of the cells by retroviral supernatant (according to reference Yi et al., 1999 (75)). On the right site the suggested physiological effect of telomere elongation on senescence development is shown. In replicatively aging cells, telomeres (orange) shorten after each cell division until they reach a critical length which leads the cell into senescence. After immortalization with hTERT, telomeres are artificial elongated and cells escape senescence (own illustration).

Cells were analyzed at low and high PD number before and after immortalization. Furthermore, mRNA from healthy human fibroblast donors at different ages were analyzed. A detailed overview of the characteristics of the individual fibroblast cell lines are shown in Table S5 in (69). The fibroblast cell lines were cultivated in Dulbecco's modified Eagle's

medium (DMEM) high glucose (4.5 g/liter) with L-glutamine without pyruvate (Gibco, catalog no. 41965) supplemented with 10% fetal bovine serum (FBS; Biochrome), penicillin (100 U/ml), and streptomycin (100 µg/ml) (Biochrome, catalog no. A2212), hereafter referred to as “full medium” (69).

Moreover, 413 lymphoblastoid cell lines (LCL) from the BASE-II study were investigated (76, 77). The positive (standard) control for cells with long telomeres is originated from T-lymphoblastic leukemia cells (cell line 1301) and was a gift from S. Roura (ICREC Research Group, Germans Trias i Pujol Health Sciences Research Institute, Barcelona, Spain). Both the LCLs and the 1301 cell line were maintained in RPMI 1640 medium with L-glutamine (Gibco, catalog no. 11875-093) supplemented with 10% FBS (Biochrome), penicillin (100 U/ml), and streptomycin (100 µg/ml) (Biochrome, catalog no. In addition, fibroblasts and LCLs from NBS patients were analyzed as shown in detail in (69, 73). These cells were cultured in the mediums described above. HUVECs (Human Umbilical Vein Endothelial Cells, PromoCell, catalog no. C-12200) were cultivated in Endothelial Cell Growth Medium Kit (PromoCell, catalog no. C-22110) supplemented with penicillin (100 U/ml) and streptomycin (100 µg/ml) (Thermo Fisher Scientific, catalog no. 15140122). All cell lines were grown in a humidified incubator at 37°C and 5% CO₂. An ethical vote is available for all cell lines (69).

2.2 Hydrogen peroxide treatment

Cells from healthy children and the HGP cells were treated at ~ 100% confluence with 200 µM H₂O₂ for two hours. The cells were then washed with PBS and cultivated with full medium for 22 hours. A control was cultivated under identical conditions without H₂O₂. mRNA for qPCR analyses were isolated as described in (69). The relative expression level of each gene was normalized to the respective primary control at low PD number. One untreated cell dish for each PD and cell line was used for DNA isolation and TL measurement (69).

2.3 Gene expression analysis via quantitative real-time PCR (qPCR)

Total mRNA was isolated using the NucleoSpin RNA extraction kit (Macherey-Nagel, catalog no 740955). For mRNA quantification, 1µg of RNA was transcribed into cDNA according to protocol (M-MLV Reverse Transcriptase, RNase (H-), Promega, catalog no

M5301). A total of 10ng (5 ng/μl) was used for gene expression measurements. All Taq-Man probes used for qPCR were from Applied Biosystems. A total list of all utilized primers can be found in the supplementary section in (69) and in the methods parts in (73).

2.4 Telomere length measurement

For DNA isolation, a standard extraction kit (DNeasy Blood & Tissue Kit, Qiagen, catalog no. 69504) was used. TL measurement was carried out using a modified monochrome multiplex qPCR (MMqPCR) described before in Cawthon 2009 (78). To determine mean TL, the telomere-specific amplification, and the amplification of the housekeeping gene / single-copy gene are performed in one reaction well with one quantification measurement at different temperatures. The TL is expressed as an arbitrary unit and is given as the ratio of telomere to single copy gene. The qPCR was performed on a Bio-Rad CFX384 real-time C1000 thermal cycler (69, 73).

2.5 Three-dimensional fluorescence *in situ* hybridization (3D-FISH)

For the 3D-FISH analyses three control children cell lines and three HGP cell lines in high PD (with short telomeres) and high PD after immortalizations (long telomeres) were compared. Cells were cultivated until they reach a confluence ~ 100%. Slides for direct cell preparation were prepared following the protocol in (69). The Spectrum Orange-labeled RP11-462B2 BAC probe was used to label the *PPP2R2C* region on chromosome 4. To mark the subtelomeric 4p region, the Vysis TelVysion 4p Spectrum probe (Abbott, Vysis, catalog no. 30-252004) was used (69).

Image acquisition was performed as described in Jäger et al. 2022: “Using a confocal scanning laser microscope (LSM 880 AxioExaminer Z1 from Zeiss) at 405-nm excitation/415- to 480-nm emission for DAPI, 488-nm excitation/500- to 545-nm emission for Spectrum Green, and 561-nm excitation/565- to 640-nm emission for Spectrum Orange. A 63x numerical aperture 1.4 Plan-Apochromat oil immersion objective was used to capture optical sections at intervals of 0.3 μm. The pinhole was set to about 1 airy unit to achieve optical slices at all wavelengths with identical thickness. Images were processed using Imaris 9.3 software (Andor Bitplane)” (69). The distance between their gravity centers (distance between the closest probes in each target) was determined by 3D reconstruction and surface rendering of the spots and used for further statistical analysis (69). A total of 70 nuclei (140 distances) were evaluated for each experiment. Only nuclei that

showed 2 red and 2 green signals each and had regular DAPI staining and normal cell shapes were used for analysis (e.g., mitotic cells, or triploid cells were excluded) (fig.5) (69).

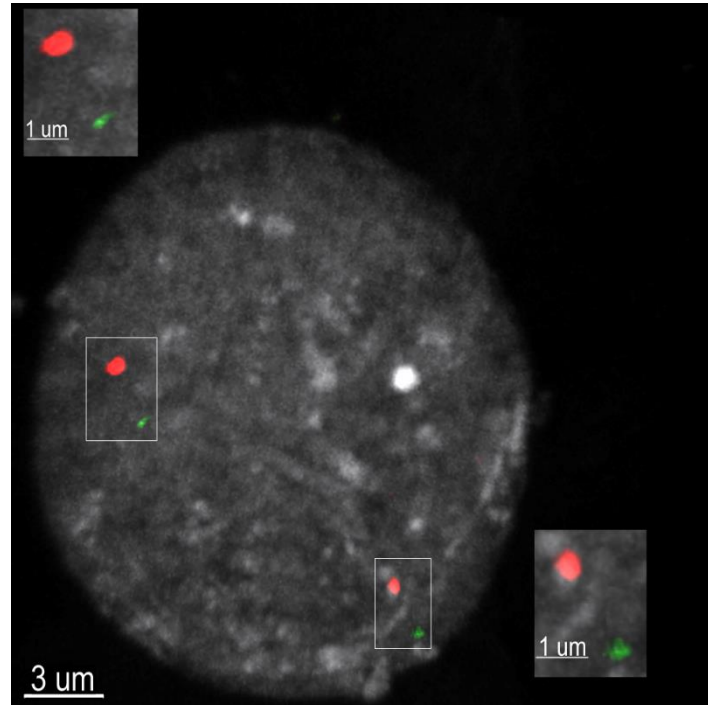


Figure 5. Exemplary representation of a cell nucleus analyzed with 3D-FISH. Red: *PPP2R2C* region on chromosome 4 labeled with RP11-462B2 BAC probe. Green: subtelomeric region labeled with Vysis TelVysion 4p probe. For better contrast, the cell nucleus was stained with DAPI and displayed here in gray. Distances were measured between red and green labeled spots. Own illustration.

2.6 Protein analyses

(These experiments were carried out by Dr. Juliane Mensch, Institute of Clinical Chemistry and Laboratory Medicine, Rostock University Medical Center, data shown in (69))

For protein analyses, cells were harvested at 100% confluence and were resuspended in 200 μl sucrose-hepes buffer with cComplete ULTRA Tablets EDTA-free (Roche, catalog no. 05892791001). The cell suspension was lysed by pipetting ten times up and down with a 26G insulin injection needle. The supernatant was used for protein concentration determination using Pierce BCA Protein Assay Kit (Thermo Fisher Scientific, catalog no. 23225). Albumin was used as standard. A total amount of 15 μg of the cell homogenate

was used for semi dry western blot analysis. The gels were transferred onto a polyvinylidene fluoride membrane. The primary antibodies were incubated overnight at 4°C. Subsequently, the membranes were incubated with the secondary antibodies for 1 hour at room temperature. A detailed description of the used antibodies and their incubation times are described in more detail in (69). The Image Studio Lite Quantification software (LiCore) was used for densitometric analysis.

2.7 *PPP2R2C* knock down

For this experiment one primary HGP cell line at high PD number was used. To knock-down *PPP2R2C* a Trilencer-27 Human siRNA Kit (OriGene, catalog no. SR303688) was used. To achieve maximum efficiencies, the provided different siRNAs were mixed. Cells at ~ 80% confluence were either treated with an end concentration in of 25 or 50 nM siRNA, according to the manufacturer's instructions. When the cells showed cellular stress signals (after approximately 7 hours), the medium was changed. The cells were harvested after 72 hours for gene expression analysis and protein determination. A control was cultured in full medium for the same time. The relative expression level of each gene was normalized to the control (69).

2.8 Serum deprivation

One healthy primary control cell line and the associated *hTERT* cell line were used for this experiment. Cells at ~ 95% confluence were either treated for 18 hours with DMEM without 10% FBS, or were treated with full medium for 17 hours and then treated 1h with PBS only. In addition, a control was carried along in each PD, which was cultured in full medium for 18 hours. Cells were then harvested for mRNA analysis and protein determination. The relative expression level of each gene was normalized to the respective control (69).

2.9 Inhibitor tests

Three different substances were used for the inhibitor assay: Trichostatin A (TSA) (inhibits histone deacetylases), 5-AzaC (leads to non-specific DNA demethylation) and resveratrol (induces instability of telomeric DNA). (79–81). In addition, the compound BCI-50 was used as a newly developed SIRT6 inhibitor (82). For these studies, only three of

the healthy control cell lines were used. Due to the low availability of the compound BCI-150, only one healthy cell line was used for this treatment. The exact experimental setup is described in the material and methods part in (69).

After the treatments, mRNA was isolated and qPCR for gene expression analyses were performed as described before. The relative expression level of each gene was normalized to that of the youngest cells (low PD) treated with DMSO (69).

2.10 Statistical analysis

Statistical analyses were performed with OriginPro 2018 (69). “Normally distributed variables are presented as the mean \pm SD or as the SEM. The two-sided exact Mann-Whitney *U* test was applied to evaluate differences between two independent groups in non-normally distributed variables. $P < 0.05$ was considered statistically significant” (69).

For 3D-FISH cut point analysis, the OptimalCutpoints package in R was used (the R analysis for 3D-FISH analysis were performed by Dr. Bruno Neuner) (69).

3. Results

3.1 Chromosomal conservation of TPE-OLD candidates

(These results have been achieved in cooperation with the Institute for Biostatistics and Informatics in Medicine and Ageing Research, Rostock University Medical Center, Dr. Steffen Möller, data shown in (69))

TPE-OLD candidate genes are often evolutionarily conserved at the end of telomeres in long-lived mammals but not in species with shorter life expectancies (Fig 1B in (69)). Among them are many genes that directly or indirectly influence cell growth and aging, including 20 genes, which belong to the group of serine/threonine specific phosphatases PPP1, PPP2 and PPP6. It was noticed that these regulatory subunits, despite being highly variable in sequence, are evolutionarily conserved at the end of the telomere in replicatively aging species. Four subunits belong to one family (PP2A) - namely *PPP2R2C*, *PPP2R2D*, *PPP2R5C*, and *PPP2R3B* – and showed relative to telomere local conservation within the postulated distance of a TPE-OLD gene (Fig S4 in (69)). Because of the role of the PP2A subunits in cell cycle control and the fact that these genes fit the criteria of a TPE-OLD gene, they were studied more detail (69).

3.2 Telomere length in relation to replicative aging

The TL of the used cell lines was measured at different PD numbers. Comparisons were made between primary young, still dividing cells at low PD and primary pre-senescent cells at high PD. The pre-senescent cells were thawed 10-15 passages before reaching senescence. Relative TL was measured by monochrome multiplex qPCR. In the young primary fibroblasts (PD 13 to 17) the relative TL was 0.48 - 0.81, in the pre-senescent control fibroblasts (PD 41 to 55) 0.15 - 0.24. In the young primary HGP fibroblasts (PD 19 to 20) 0.28 - 0.68, in the pre-senescent primary HGP fibroblasts (PD 34 to 42), 0.17 - 0.46 arbitrary units (table S5 in (69)).

The fibroblast cell lines were immortalized using a retroviral construct, which resulted in artificial lengthening of their telomeres with each cell division. In the immortalized control cells at low PD (PD 14 to 28 after immortalization), the relative TL was 0.6 - 1.18. Compared to the long-term immortalized control cells (PD 56 to 70), the TL was 1.59 - 2.91. In the immortalized HGP cells in low passage (PD 15 to 34), the relative TL was 0.67 -

1.44 and in the immortalized HGP cells at high PD (PD 57 to 63), the relative TL was 0.87 - 2.74 arbitrary units, respectively (table S5 in (69)).

Thus, telomeres were successively shortened in cells in higher PDs and there was a substantial artificial lengthening of telomeres in cells immortalized with *hTERT* for control cells 3.7-fold and for HGP cells 2.9-fold (table S5 in (69)).

3.3 Gene expression changes in TPE-OLD candidate genes

To investigate whether gene expression is regulated in dependence on TL, gene expression of PP2A subunits was measured in primary fibroblasts in low and high PDs, as well as in immortalized cell lines in the respective PDs. This was done in both control and HGP fibroblasts. Special attention was paid to the four regulatory subunits (*PPP2R2C*, *PPP2R2D*, *PPP2R3B*, and *PPP2R5C*). In addition, two catalytic subunits (*PPP2CA* and *PPP2CB*) and two structural subunits (*PPP1A* and *PPP1B*) were examined as controls. Only for the regulatory subunit *PPP2R2C* a clear dependence of TL on gene expression could be shown with an up-regulation of mRNA by 6.85 ± 1.79 -fold ($p \leq 0.01$) in control cells at high PD compared to low PD (i.e., when telomere was short). In HGP cells, the mRNA increases were lower up to 2.03 ± 0.27 -fold ($p \leq 0.01$) (fig. 3A in (69)). A substantial individual variation of each cell line was observed. In control cells, the minimum/maximum fold change was 2.76-fold / 16.99-fold, in HGP the minimum/ maximum fold change was 1.03-fold / 3.28-fold (fig. S6 in (69)).

Subsequently, gene expression of the immortalized cells was examined. Here, *PPP2R2C* mRNA measurements showed that in control cells after immortalization (with artificially extended telomeres), gene expression fell to the level of the primary young cells (or even lower) (0.4 ± 0.3 -fold vs. 6.8 ± 6.2 -fold, $p \leq 0.01$) In HGP cells, suppression of *PPP2R2C* gene expression (below basal level) was observed at very long telomeres (0.3 ± 0.2 -fold versus 2.0 ± 0.9 -fold, $p \leq 0.01$) (Fig 3B in (69)).

When comparing the TL of each cell line to *PPP2R2C* gene expression, an inverse correlation was observed in both control and HGP cells (Fig 3C in (69)).

To verify that the gene expression changes were causally related to telomere shortening, cells were additionally stressed with H_2O_2 to induce stress-induced senescence (SIS). Here, *p21* was used as a stress control (Fig. S6 in (69)).

Neither the structural PP2A subunits nor the catalytic PP2A subunits displayed any relationship between gene expression and TL. Moreover, no significant effect of SIS on

PPP2R2C mRNA expression could be shown. (Fig. S6 in (69)). In addition, genes located on chromosome 4p between *PPP2R2C* and the subtelomeric region were examined including *HTT* and *WFS1*. These genes were chosen because both genes are involved in aging processes (83, 84). However, no correlation was found between gene expression of these two genes and TL in old primary and immortalized fibroblasts (Fig.3 and Fig. S6 in (69)).

These data suggest that *PPP2R2C* gene expression change is selectively and directly related to TL.

3.4 Evidence of a telomere loop as a possible reason for gene silencing

Next, it was examined whether a telomere loop (and not the spread of heterochromatin) could be the cause of gene silencing of *PPP2R2C*.

To demonstrate that a telomere loop is present, high-resolution three-dimensional fluorescence hybridization (3D-FISH) was used to measure the distance between the subtelomeric region and the *PPP2R2C* locus. A TelVysion probe (~100 - 300 kb from telomere; green) was used to label the subtelomeric region and a BAC (bacterial artificial chromosome) was used to label the *PPP2R2C* locus (4.2 Mb from telomere; red). 140 distances for each cell line were analyzed. For cells with short telomeres, a significantly higher percentage of separated probes (S; distance between probes > 2.26 μm) than adjacent (A, distance between probes < 2.26 μm) probes could be detected (Fig. 4, Fig. S8A and Fig. S8B in (69)). A significant change in the distribution of total probe distances was observed. By contrast, in the immortalized cells with artificially elongated telomeres, more adjacent distances were observed (69).

The data demonstrate a physical loop as the most likely explanation for gene silencing in cells with long telomeres.

3.5 Effect of *PPP2R2C* on the dephosphorylation of p70S6k independent of cellular mTOR levels

(These results have been achieved in collaboration with Dr. Juliane Mensch, Institute of Clinical Chemistry and Laboratory Medicine, Rostock University Medical Center, data shown in (69))

The mTOR protein complex is a component of various signaling pathways, many of which are related to cell growth and cell cycle (85). *PPP2R2C* is able to dephosphorylate a downstream target of mTOR (61).

It was shown that in pre-senescent cells with short telomeres, the phosphorylation of p70S6k was reduced to $16 \pm 6\%$ relative to the levels of control fibroblasts in low PD (Fig. 5A, in (69), results analyzed by Dr. Juliane Mensch). No correlation was found between the growth rate and mTOR, and p70S6k expression levels, and no correlation was found between the growth rate and the phosphorylation level of p70S6k. However, a two-fold higher relative mTOR, p70S6k protein level was shown in the HGP fibroblasts compared to the control fibroblasts. The deactivating dephosphorylation of p70S6K was not disturbed in HGP cells; by contrast, it was rather enhanced (Fig S12 in (69), results archived from Dr. Juliane Mensch).

Next, it was investigated whether serum depletion in cell culture influenced the protein levels and mRNA expressions. Although there were reduced p70S6k and mTOR levels in the absence of serum, this reduction was much lower than the TL-dependent regulation of *PPP2R2C* mRNA. Thus, serum deficiency was excluded as a major factor in p70S6k phosphorylation (Fig. S13 in (69)).

siRNA (small interfering RNA) experiments were performed to further confirm the influence of *PPP2R2C* on p70S6k phosphorylation. It was shown that in pre-senescent HGP fibroblasts, the dephosphorylation of p70S6k was decreased by approximately 90% in *PPP2R2C* silenced cells (Fig S15 in (69)).

3.6 *PPP2R2C* silencing in HGP fibroblasts

(These results have been achieved in collaboration with Dr. Juliane Mensch, Institute of Clinical Chemistry and Laboratory Medicine, Rostock University Medical Center, data shown in (69))

HGP fibroblasts were used as a model for premature aging associated with telomere attrition. Because other work has shown that HGP cells exhibit moderately shortened TLs

(27, 86), it was hypothesized that altered TPE could contribute to the age-related phenomena in HGP.

A severe TPE-OLD defect for *PPP2R2C* could be excluded. In pre-senescent HGP cells p70S6k was almost completely dephosphorylated as it can be expected for TPE-OLD (Fig. 5A in (69), results archived from Dr. Juliane Mensch). Moreover, an inverse correlation between TL and *PPP2R2C* was shown (Fig. 3C in (69)). Although HGP fibroblasts showed consistently high mTOR protein levels (Fig S12 in (69), results archived from Dr. Juliane Mensch), p70S6k dephosphorylation was intact in HGP cells in high PD with short TL (Fig 5A in (69), results analyzed by Dr. Juliane Mensch).

Moreover, it was shown that TLs were shorter in HGP cells compared to control cells at comparable (low) PDs (TL 0.49 ± 0.08 in HGP versus 0.68 ± 0.07 in control groups; $P = 0.1$). In cells at high PD, the TLs of HGP fibroblasts were longer compared with the TLs of control cells (TL 0.33 ± 0.08 versus 0.19 ± 0.02 ; $P = 0.2$) (Fig. 3B, in (69)). These data may point to complex telomeric dysfunction in HGP cells. Apparently, the dynamics of TL-dependent chromosomal reorganization was altered in HGP, compared to control cells (table S6 in (69), calculation done by Bruno Neuner).

3.7 Influence of chromatin modification on *PPP2R2C* mRNA expression

Next, the influence of substances interfering with histone deacetylation and other modifications was investigated, since heterochromatin in mammals is dependent on heterochromatin spreading.

For this purpose, different substances such as TSA (an inhibitor of histone deacetylase), 5-AzaC (an inhibitor of DNA methyltransferase) and RSV (which causes instability of telomeric DNA) (79–81) were used. Only under the influence of RSV a weak increase of *PPP2R2C* mRNA (up to 1.6-fold) could be seen (Fig. S10 in (69)). No significant effect could be observed with the other inhibitors, excluding any significant and specific modulation of these substances. Therefore, a new SIRT inhibitor (compound BCI-150), which exclusively inhibits sirtuin 6 (SIRT6), was used (82). SIRT6 is thought to be involved in maintaining a silencing-competent chromatin structure of telomeres (87). Indeed, in hTERT immortalized cells, this SIRT6 inhibitor was able to increase *PPP2R2C* expression up to fivefold, suggesting that silencing of *PPP2R2C* depends on histone deacetylation mediated by SIRT6 (Fig. S10 in (69)).

3.8 *PPP2R2C* expression in different cell types

Next, it was investigated whether *PPP2R2C* is regulated in a cell-type specific manner, or similarly differentially expressed in other cell lines depending on TL. For this purpose, 413 lymphoblastoid cell lines from the Berlin Aging Study II were investigated. In this cell population, no correlation was found between TL and *PPP2R2C* gene expression, or any other TPE-OLD candidate gene (Fig. S17 in (69)).

Moreover, the same studies were performed in primary HUVECs. Compared with LCLs, up-regulation was detected in the following genes: *PPP2R2C*, *PPP2R2D*, *PPP2R5C*, *C1S*, and *SORBS2*. In addition, a reciprocal regulation was shown for *DSP*, e.g. the mRNA level was lower in old cells with short telomeres compared with young cells with longer telomeres (Fig. S18 in (69)).

Finally, the question arose whether upregulation of *PPP2R2C* may also occur *in vivo*. For this purpose, human skin fibroblasts from older donors were compared to very young and middle-aged donors. It was shown that the upregulation of *PPP2R2C* was significantly more pronounced in cells from old donors. (Fig. S19 in (69)).

Altogether, these data suggest that TPE-OLD is in part cell type specific. Data also suggest that replicative senescence *in vitro* resembles replicative senescence *in vivo* and that TPE-OLD is effective *in vivo*.

3.9 Telomere position effect in NBS cells

NBS is characterized by chromosome instability associated with immunodeficiency and a high predisposition to cancer (52). However, NBS also displays many symptoms of premature aging such as gray hair, café au lait spots and decline in mental function. This phenotype is at least in part caused by a dramatic (up to 40%) reduced TL (73). NBS therefore belongs to the severe (secondary) telomeropathies. The primary defect affects impaired DNA damage repair. This extreme telomere attrition may on one hand counteract cancerogenic effects to some extent (if the telomeres are still stable enough) but may also induce a progeroid phenotype. It could be shown that the TL-dependent gene expression change was attenuated in eight TPE-OLD candidate genes in NBS fibroblasts (BSG -61%, CACNA1A -91%, COL5A3 -92%, GAMT -35%, NOTCH3 -42%, OLFM2 -90%, and SCAMP4 -52%) and was even reversed in three growth promoting TPE-OLD

candidate genes (DDX39A 3.8-fold, RNASEH2A 15.1-fold, and UHRF1 12.5-fold), suggesting that TPE-OLD the normal senescence program is disturbed in this disease (Fig. 5 and Table S8 in (73)), further suggesting a physiological role of TPE-OLD.

4. Discussion

4.1 Characterization of *PPP2R2C* as a TPE-OLD gene

The studies showed that *PPP2R2C* was upregulated in cells with short telomeres, whereas suppression of gene expression was observed in cells with long telomeres. By contrast, exogenous stress (hydrogen peroxide) did not induce any change in gene expression. Thus, *PPP2R2C* expression was related to TL and was apparently not influenced by exogenous triggers such as SIS. As previously shown for other TPE-OLD genes (33, 36), 3D-FISH analysis revealed that the TEL-*PPP2R2C* probes were significantly closer to each other in cells with long telomeres than in cells with short telomeres (69). It has previously been shown that the length of telomeres on both alleles can vary (88). Also in this work, it could be seen in 3D-FISH studies that (presumably due to the bimodal TL distribution) both chromosomes are involved in the telomere loop.

Moreover, gene regulation by TL was specific and discontinuous. Genes located between the subtelomeric region and *PPP2R2C* (even closer to the telomere end than *PPP2R2C*) were not affected by this effect. In inhibitor experiments, compound BCI-160 (a recently developed SIRT inhibitor with high selectivity for SIRT6) (82) increased *PPP2R2C* gene expression up to fivefold in hTERT immortalized cells. Previously, SIRT6 was shown to be required for the repression of telomere-external reporter genes (87).

Altogether, these results suggest that silencing of *PPP2R2C* depends on histone deacetylation mediated by SIRT6 and is dependent on a loop – like chromosomal structure.

4.2 Cell specificity of TPE-OLD

It was shown that in both skin fibroblasts and in HUVEC cells, mRNA expression for *PPP2R2C* is directly regulated by TL. However, this effect could not be observed in LCLs, suggesting some kind of cell specificity (69).

Demanelis et al. has shown that TL varies in different tissues (89). Thus, *PPP2R2C* and possibly also other TPE-OLD candidates are likely not differentially expressed in all cell types to the same degree, possibly related to basal TL of the respective cell type. Explicitly there is a possibility that the three other TPE-OLD candidate genes of the PP2A subunit are induced in other cell types or metabolic states, but still affect similar signaling

pathways. In addition, non-comparable results may result from the fact that the used primer pairs cannot detect all induced splice variants; moreover, not all variants are yet known. Epigenetic mechanisms (DNA methylation, histone modifications in promoter region) (33) may additionally have an influence on TPE-OLD effects (69). Additionally, in LCLs the procedure for immortalization using EBV may have contributed to the lack of positive results. Unlike immortalization with hTERT, this immortalization method was reported to result in partially dysfunctional telomeres (90).

In facioscapulohumeral muscular dystrophy, it could be shown that a repositioning of a telomere-related gene created a TPE-OLD effect, which was age-dependent (89). Moreover, in fibroblasts from the three old donors, the *in vitro* effect of *PPP2R2C* regulation was most pronounced in the here described experiments (69). Altogether these data suggest a physiological function of *PPP2R2C* (and other TPE-OLD genes) in the aging organism, and that cell and tissue specificity may exist for TPE-OLD genes (69).

4.3 Direct influence of telomere shortening on the mTOR signaling pathway

(These results have been achieved in collaboration with Dr. Juliane Mensch, Institute of Clinical Chemistry and Laboratory Medicine, Rostock University Medical Center)

Both Fan et al. and Bluemn et al. have previously shown that overexpression of *PPP2R2C* can inhibit tumorigenesis and that repression of *PPP2R2C* can promote tumor cell proliferation (61, 71). This is mediated by the activity of p70S6k in the mTOR signaling pathway secondary to p70S6k phosphorylation / dephosphorylation. In this work, it was shown that upregulation of *PPP2R2C* in pre-senescent (but still dividing) fibroblasts resulted in almost complete dephosphorylation of p70S6k. In addition, there is an inverse correlation between *PPP2R2C* expression and TL and between the level of dephosphorylation of p70S6k and TL (69). Knockdown of *PPP2R2C* using siRNA reactivated mTOR-dependent metabolic genes in aged cells (69, 91, 92).

Altogether, the data shown here suggest that dephosphorylation of p70S6k has metabolism inhibiting (potentially protective) effect on pre-senescent fibroblasts in accordance with current models on mTOR (69). However, most of the experimental findings on the life-prolonging effect of mTOR suppression so far have been shown in mice, which have been genetically modified (93), and *Drosophila* (69, 94).

The results show a possible physiological *in vivo* function for mTOR suppression, namely adaptation to aging conditions in old cells with short telomeres (69).

4.4 Replicative aging as a tumor suppressor

The described results support the hypothesis that replicative aging acts as a tumor suppressor. A TPE-OLD gene was identified (*PPP2R2C*), which has previously been described as a tumor suppressor gene (61). To ensure tumor suppression over a long period of time, any negative aspects of replicative aging must be minimized. Apart from genetic instability syndromes (73), telomere attrition is not life-threatening in humans (95). Insofar, an additional adaptation beyond the DNA damage response which is inherent to replicative aging makes sense as protection mechanism against cancer (69).

Interestingly, Kim et al. had shown that h*TERT* itself is a TPE-OLD gene (33). Hypothetically, mild up-regulation of h*TERT* in old cells (with short telomeres) could contribute to cell stabilization without increasing tumor risk in the organism. However, this has to be shown in further experiments. In this regard, mTOR suppression (by *PPP2R2C*) could act synergistically to limit the risk of tumor formation in cells with a critical TL. Such concept does not exclude that under certain circumstances expression of h*TERT* and other TPE genes may lead to predisposition to cancer through uncontrolled derepression of transcription (69).

4.5 Abnormalities in telomere kinetics in HGP and NBS

HGP patients (at least during their short life time) do not develop cancer (49). In this work, it was shown that TL-dependent chromosomal rearrangement for *PPP2R2C* is not severely disturbed. Thus, intact mTOR suppression may even prevent an even worse phenotype (tumor formation at low age). However, various abnormalities were observed in HGP cells despite functional TPE-OLD. These include a higher rate of proliferation (cells grew faster and reached the stage of senescence earlier, Figs. S5, S16 in (69)), an overall reduced *PPP2R2C* suppression and high cell to cell variability. In addition, the dynamics in the change of TL-*PPP2R2C* distances of the probes was different compared to controls (Fig. S8 in (69)). An abnormal distribution of TLs at low and high PDs with quite normal average TLs has also been shown in other studies (69, 86, 96).

In contrast to HGP patients, NBS patients exhibit higher genetic instability and a high cancer rate (52). In NBS cells, with more severe telomere attrition the results suggest a

marked telomeric imbalance in TPE-OLD (73). The data from the NBS experiments further support the concept that a disease mechanism can be effective independent from the DNA damage response and long before the onset of cell death: an imbalance or dysfunction in telomere position effect which may contribute to the progeroid phenotype in HGP, NBS and possibly other diseases (73).

The data in this thesis can provide an explanation why HGP patients suffer from age-related symptoms but do not develop tumors. However, since HGP patients die very early (49, 97, 98), it cannot entirely be excluded that at an older age these patients would also develop cancer (73).

4.6 Limitations

This study has some limitations. First, skin fibroblasts from healthy children were used for the most experiments. HGP fibroblasts with short telomeres and premature aging were considered as an example of replicative senescence. For better comparability and to exclude pre-existing *in vivo* aging effects, samples from donors younger than <10 years were used. It should be noted however that the skin punches of healthy children were taken from children <1 year old, whereas the progeria children were between two and six years old. The slightly different age of donors could be an influencing factor, due to the lack of suitable control donors between the ages of two and seven years.

Second, cells were passaged in culture until they reached the stage of replicative senescence. Not all cell lines were examined in low and high PDs, since in some instances (as indicated in the manuscripts) only cell aliquots in higher PDs were available from the older donors. In the HUVECs, a comparable problem arose in high PDs. The HUVECs were grown up to passage 5, but not higher, because a slower growth rate and changes in cell morphology were observed. It was not entirely clear whether this limit represents the maximum level of PDs in cell culture.

Third, the human skin fibroblasts were immortalized using a retro-viral construct, resulting in artificial elongation of telomeres after each cell division. Immortalization by hTERT has the advantage of preserving contact inhibition, cell cycle control, growth factor dependence and normal karyotype compared to immortalization by oncogenes, irradiation or fusion with tumor cells (27, 28, 99). By contrast, primary B lymphocytes were immortalized with Epstein-Barr virus to generate immortalized lymphoblastoid cell lines. This procedure

elongates telomeres not only by telomerase but also by alternative lengthening of telomeres (ALT). This can lead to reduced telomere binding of proteins and subsequently to dysfunctional telomeres. (90). This could be a reason why the effects detected in human skin fibroblasts and LCLs, were not comparable, as described above.

Fourth, a disadvantage of hydrogen peroxide as stress trigger is its instability at room temperature and 37°C. Moreover, it cannot entirely be excluded that the cells had slightly different confluency when treated with H₂O₂, and / or had different metabolic states, which may in part influence the neutralization capacity.

Fifth, a monochromatic multiplex PCR was used for TL measurement (78). This allows a very low amount of DNA to be analyzed. Here, the telomere amplification product (T) is compared with the amount of a single-copy gene standard (S). The advantage of this method is that the amplification of both products is done in the same well. Thus, some measurement errors such as pipetting errors, can be excluded. Nevertheless, this method has pitfalls and disadvantages. For example, it only provides a determination of the relative mean TL of the entire material and does not give information on TL of individual cells or individual chromosomes.

Sixth, in the 3D-FISH analysis, only selected cell lines were used to investigate possible telomere loops. For this purpose, only the "extreme" TLs were compared in these experiments. This means that only cells at high PD (short telomeres) were compared with immortalized cells at high PD (with artificially extended telomeres). Thus, this is a simplification for better analysis and not a completely "natural" *in vivo* state.

Seventh, some of the primary cell lines grew slowly in culture and it was difficult to have enough material in all PDs to perform all experiments. The primary control cells came from the Children's Hospital Münster, while the HGP cells came from the Progeria Research Foundation (PRF) Cell and Tissue Bank, and therefore it was difficult to have a maximum of replicates for all experiments. For this reason, the Mann-Whitney *U* test was used for statistical analysis. Some statistical tests could not be applied due to the low number. The Mann-Whitney *U* test is a non-parametric test that does not assume a normal distribution. Exact 2-sided significance was used for calculations to have a maximum validity.

5. Conclusion

A telomere position effect was detected in human skin fibroblasts in a gene for a regulatory subunit of serine/threonine-specific phosphatase PP2 (*PPP2R2C*), suggesting a functional link between replicative aging and mTOR suppression in human fibroblasts.

In HGP cells, this mechanism is an effective but changed in dynamics in relation to the TL. Adequate upregulation of *PPP2R2C* in HGP is a possible explanation for lack of cancerogenesis because *PPP2R2C* is an effective tumor suppressor gene.

A mechanistic link between TL, TPE-OLD-mediated gene expression and mTOR suppression is a possible metabolic adaptation in older cells.

6. Outlook

Technical difficulties for the identification of TPE-OLD genes, cell specificity and other methodological challenges could be the reason for the sparse number of known TPE-OLD genes. To better understand the cell specificity aspect, other tissue types and other PP2A regulatory subunits as well as other TPE-OLD candidates need to be investigated. In addition, further structural experiments are required to better understand the influence of chromatin structure on TPE-OLD. As previously described, siRNA knockdown is temporary. In further studies, a knockout using CRISPR/Cas9 should be performed. In this work, only *in vitro/ ex vivo* models were used. It could be useful to investigate the mechanisms described here in further studies using appropriate animal models.

7. Reference list

1. López-Otín C, Blasco MA, Partridge L, Serrano M, Kroemer G. The hallmarks of aging. *Cell* 2013; 153(6):1194–217. Available from: URL: <https://www.ncbi.nlm.nih.gov/pmc/articles/PMC3836174/>.
2. Shammass MA. Telomeres, lifestyle, cancer, and aging. *Curr Opin Clin Nutr Metab Care* 2011; 14(1):28–34.
3. Fisher GJ, Kang S, Varani J, Bata-Csorgo Z, Wan Y, Datta S, Voorhees JJ. Mechanisms of photoaging and chronological skin aging. *Arch Dermatol* 2002; 138(11):1462–70.
4. Brunet A, Berger SL. Epigenetics of aging and aging-related disease. *The Journals of Gerontology Series A: Biological Sciences and Medical Sciences* 2014; 69 Suppl 1(Suppl 1):S17-20.
5. Hasty P, Vijg J. Aging. Genomic priorities in aging. *Science (New York, N.Y.)* 2002; 296(5571):1250–1.
6. Takahashi Y, Kuro-O M, Ishikawa F. Aging mechanisms. *Proc Natl Acad Sci U S A* 2000; 97(23):12407–8. Available from: URL: <https://www.pnas.org/doi/10.1073/pnas.210382097>.
7. Hayflick L, Moorhead PS. The serial cultivation of human diploid cell strains. *Experimental Cell Research* 1961; 25(3):585–621.
8. Kerr JF, Wyllie AH, Currie AR. Apoptosis: a basic biological phenomenon with wide-ranging implications in tissue kinetics. *Br J Cancer* 1972; 26(4):239–57.
9. Shay JW, Wright WE. Senescence and immortalization: role of telomeres and telomerase. *Carcinogenesis* 2005; 26(5):867–74.
10. Meyne J, Ratliff RL, Moyzis RK. Conservation of the human telomere sequence (TTAGGG)_n among vertebrates. *Proc Natl Acad Sci U S A* 1989; 86(18):7049–53.
11. Shampay J, Szostak JW, Blackburn EH. DNA sequences of telomeres maintained in yeast. *Nature* 1984; 310(5973):154–7.
12. Greider CW, Blackburn EH. Identification of a specific telomere terminal transferase activity in tetrahymena extracts. *Cell* 1985; 43(2):405–13.

13. Greider CW, Blackburn EH. A telomeric sequence in the RNA of *Tetrahymena* telomerase required for telomere repeat synthesis. *Nature* 1989; 337(6205):331–7.
14. Levy MZ, Allsopp RC, Futcher A, Greider CW, Harley CB. Telomere end-replication problem and cell aging. *Journal of Molecular Biology* 1992; 225(4):951–60.
15. Wynford-Thomas D, Kipling D. The end-replication problem. *Nature* 1997; 389(6651):551. Available from: URL: <https://www.nature.com/articles/39210>.
16. Hayflick L. The limited in vitro lifetime of human diploid cell strains. *Experimental Cell Research* 1965; 37(3):614–36.
17. Diotti R, Loayza D. Shelterin complex and associated factors at human telomeres. *Nucleus* 2011; 2(2):119–35.
18. Brouillette S, Singh RK, Thompson JR, Goodall AH, Samani NJ. White cell telomere length and risk of premature myocardial infarction. *Arterioscler Thromb Vasc Biol* 2003; 23(5):842–6.
19. Okuda K, Khan MY, Skurnick J, Kimura M, Aviv H, Aviv A. Telomere attrition of the human abdominal aorta: relationships with age and atherosclerosis. *Atherosclerosis* 2000; 152(2):391–8. Available from: URL: [https://www.atherosclerosis-journal.com/article/S0021-9150\(99\)00482-7/fulltext](https://www.atherosclerosis-journal.com/article/S0021-9150(99)00482-7/fulltext).
20. Zglinicki T von, Serra V, Lorenz M, Saretzki G, Lenzen-Grossimlghaus R, Gessner R, Risch A, Steinhagen-Thiessen E. Short telomeres in patients with vascular dementia: an indicator of low antioxidative capacity and a possible risk factor? *Lab Invest* 2000; 80(11):1739–47.
21. Kim NW, Piatyszek MA, Prowse KR, Harley CB, West MD, Ho PL, Coviello GM, Wright WE, Weinrich SL, Shay JW. Specific association of human telomerase activity with immortal cells and cancer. *Science (New York, N.Y.)* 1994; 266(5193):2011–5.
22. Hiyama K, Hirai Y, Kyoizumi S, Akiyama M, Hiyama E, Piatyszek MA, Shay JW, Ishioka S, Yamakido M. Activation of telomerase in human lymphocytes and hematopoietic progenitor cells. *J Immunol* 1995; 155(8):3711–5.
23. Morrison SJ, Prowse KR, Ho P, Weissman IL. Telomerase Activity in Hematopoietic Cells Is Associated with Self-Renewal Potential. *Immunity* 1996; 5(3):207–16.

24. Feng J, Funk WD, Wang SS, Weinrich SL, Avilion AA, Chiu CP, Adams RR, Chang E, Allsopp RC, Yu J. The RNA component of human telomerase. *Science (New York, N.Y.)* 1995; 269(5228):1236–41.
25. Nakamura TM, Morin GB, Chapman KB, Weinrich SL, Andrews WH, Lingner J, Harley CB, Cech TR. Telomerase catalytic subunit homologs from fission yeast and human. *Science (New York, N.Y.)* 1997; 277(5328):955–9.
26. Jäger K, Walter M. Therapeutic Targeting of Telomerase. *Genes (Basel)* 2016; 7(7).
27. Ouellette MM, McDaniel LD, Wright WE, Shay JW, Schultz RA. The establishment of telomerase-immortalized cell lines representing human chromosome instability syndromes. *Hum Mol Genet* 2000; 9(3):403–11. Available from: URL: <https://pubmed.ncbi.nlm.nih.gov/10655550/>.
28. Forsyth NR, Evans AP, Shay JW, Wright WE. Developmental differences in the immortalization of lung fibroblasts by telomerase. *Aging Cell* 2003; 2(5):235–43. Available from: URL: <https://pubmed.ncbi.nlm.nih.gov/14570231/>.
29. Levis R, Hazelrigg T, Rubin GM. Effects of genomic position on the expression of transduced copies of the white gene of *Drosophila*. *Science (New York, N.Y.)* 1985; 229(4713):558–61.
30. Gottschling DE, Aparicio OM, Billington BL, Zakian VA. Position effect at *S. cerevisiae* telomeres: Reversible repression of Pol II transcription. *Cell* 1990; 63(4):751–62.
31. Baur JA, Zou Y, Shay JW, Wright WE. Telomere position effect in human cells. *Science (New York, N.Y.)* 2001; 292(5524):2075–7.
32. Robin JD, Ludlow AT, Batten K, Magdinier F, Stadler G, Wagner KR, Shay JW, Wright WE. Telomere position effect: regulation of gene expression with progressive telomere shortening over long distances. *Genes Dev* 2014; 28(22):2464–76.
33. Kim W, Ludlow AT, Min J, Robin JD, Stadler G, Mender I, Lai T-P, Zhang N, Wright WE, Shay JW. Regulation of the Human Telomerase Gene TERT by Telomere Position Effect-Over Long Distances (TPE-OLD): Implications for Aging and Cancer. *PLoS Biol* 2016; 14(12):e2000016.
34. Kyrion G, Liu K, Liu C, Lustig AJ. RAP1 and telomere structure regulate telomere position effects in *Saccharomyces cerevisiae*. *Genes Dev* 1993; 7(7A):1146–59.

35. Lange T de. Shelterin: the protein complex that shapes and safeguards human telomeres. *Genes Dev* 2005; 19(18):2100–10.
36. Robin JD, Ludlow AT, Batten K, Gaillard M-C, Stadler G, Magdinier F, Wright WE, Shay JW. SORBS2 transcription is activated by telomere position effect-over long distance upon telomere shortening in muscle cells from patients with facioscapulohumeral dystrophy. *Genome Res* 2015; 25(12):1781–90.
37. Lou Z, Wei J, Riethman H, Baur JA, Voglauer R, Shay JW, Wright WE. Telomere length regulates ISG15 expression in human cells. *Aging (Albany NY)* 2009; 1(7):608–21.
38. Stadler G, Rahimov F, King OD, Chen JCJ, Robin JD, Wagner KR, Shay JW, Emerson CP, Wright WE. Telomere position effect regulates DUX4 in human facioscapulohumeral muscular dystrophy. *Nat Struct Mol Biol* 2013; 20(6):671–8.
39. Volonte D, Galbiati F. Polymerase I and transcript release factor (PTRF)/cavin-1 is a novel regulator of stress-induced premature senescence. *Journal of Biological Chemistry* 2011; 286(33):28657–61.
40. Gorbunova V, Seluanov A, Pereira-Smith OM. Expression of human telomerase (hTERT) does not prevent stress-induced senescence in normal human fibroblasts but protects the cells from stress-induced apoptosis and necrosis. *J Biol Chem* 2002; 277(41):38540–9.
41. Shapiro GI, Edwards CD, Ewen ME, Rollins BJ. p16INK4A participates in a G1 arrest checkpoint in response to DNA damage. *Mol Cell Biol* 1998; 18(1):378–87.
42. Schmitt CA, Fridman JS, Yang M, Lee S, Baranov E, Hoffman RM, Lowe SW. A senescence program controlled by p53 and p16INK4a contributes to the outcome of cancer therapy. *Cell* 2002; 109(3):335–46.
43. Hara E, Smith R, Parry D, Tahara H, Stone S, Peters G. Regulation of p16CDKN2 expression and its implications for cell immortalization and senescence. *Mol Cell Biol* 1996; 16(3):859–67.
44. Beauséjour CM, Krtolica A, Galimi F, Narita M, Lowe SW, Yaswen P, Campisi J. Reversal of human cellular senescence: roles of the p53 and p16 pathways. *The EMBO Journal* 2003; 22(16):4212–22. Available from: URL: <https://www.embo-press.org/doi/full/10.1093/emboj/cdg417>.

45. Armanios MY, Chen JJ-L, Cogan JD, Alder JK, Ingersoll RG, Markin C, Lawson WE, Xie M, Vulto I, Phillips JA, Lansdorp PM, Greider CW, Loyd JE. Telomerase mutations in families with idiopathic pulmonary fibrosis. *N Engl J Med* 2007; 356(13):1317–26.
46. Marrone A, Walne A, Tamary H, Masunari Y, Kirwan M, Beswick R, Vulliamy T, Dokal I. Telomerase reverse-transcriptase homozygous mutations in autosomal recessive dyskeratosis congenita and Hoyeraal-Hreidarsson syndrome. *Blood* 2007; 110(13):4198–205.
47. Sandre-Giovannoli A de, Bernard R, Cau P, Navarro C, Amiel J, Boccaccio I, Lyonnet S, Stewart CL, Munnich A, Le Merrer M, Lévy N. Lamin a truncation in Hutchinson-Gilford progeria. *Science (New York, N.Y.)* 2003; 300(5628):2055. Available from: URL: <https://pubmed.ncbi.nlm.nih.gov/12702809/>.
48. Gordon LB, Brown WT, Collins FS, editors. GeneReviews® [Internet]. University of Washington, Seattle; 2019.
49. Hennekam RCM. Hutchinson-Gilford progeria syndrome: review of the phenotype. *Am J Med Genet A* 2006; 140(23):2603–24.
50. Varon R, Vissinga C, Platzer M, Cerosaletti KM, Chrzanowska KH, Saar K, Beckmann G, Seemanová E, Cooper PR, Nowak NJ, Stumm M, Weemaes CM, Gatti RA, Wilson RK, Digweed M, Rosenthal A, Sperling K, Concannon P, Reis A. Nibrin, a novel DNA double-strand break repair protein, is mutated in Nijmegen breakage syndrome. *Cell* 1998; 93(3):467–76.
51. Difilippantonio S, Nussenzweig A. The NBS1-ATM connection revisited. *Cell Cycle* 2007; 6(19):2366–70.
52. Krüger L, Demuth I, Neitzel H, Varon R, Sperling K, Chrzanowska KH, Seemanova E, Digweed M. Cancer incidence in Nijmegen breakage syndrome is modulated by the amount of a variant NBS protein. *Carcinogenesis* 2007; 28(1):107–11. Available from: URL: <https://academic.oup.com/carcin/article/28/1/107/2476261>.
53. Ranganathan V, Heine WF, Ciccone DN, Rudolph KL, Wu X, Chang S, Hai H, Ahearn IM, Livingston DM, Resnick I, Rosen F, Seemanova E, Jarolim P, DePinho RA, Weaver DT. Rescue of a telomere length defect of Nijmegen breakage syndrome cells requires NBS and telomerase catalytic subunit. *Current Biology* 2001; 11(12):962–6.

54. Rai R, Hu C, Broton C, Chen Y, Lei M, Chang S. NBS1 Phosphorylation Status Dictates Repair Choice of Dysfunctional Telomeres. *Mol Cell* 2017; 65(5):801-817.e4.
55. Yu CE, Oshima J, Fu YH, Wijsman EM, Hisama F, Alisch R, Matthews S, Nakura J, Miki T, Ouais S, Martin GM, Mulligan J, Schellenberg GD. Positional cloning of the Werner's syndrome gene. *Science (New York, N.Y.)* 1996; 272(5259):258-62.
56. Chen L, Lee L, Kudlow BA, Dos Santos HG, Sletvold O, Shafeghati Y, Botha EG, Garg A, Hanson NB, Martin GM, Mian IS, Kennedy BK, Oshima J. LMNA mutations in atypical Werner's syndrome. *The Lancet* 2003; 362(9382):440-5.
57. Rossi ML, Ghosh AK, Bohr VA. Roles of Werner syndrome protein in protection of genome integrity. *DNA Repair (Amst)* 2010; 9(3):331-44.
58. Takemoto M, Mori S, Kuzuya M, Yoshimoto S, Shimamoto A, Igarashi M, Tanaka Y, Miki T, Yokote K. Diagnostic criteria for Werner syndrome based on Japanese nationwide epidemiological survey. *Geriatr Gerontol Int* 2013; 13(2):475-81.
59. Schulz VP, Zakian VA, Ogburn CE, McKay J, Jarzebowicz AA, Edland SD, Martin GM. Accelerated loss of telomeric repeats may not explain accelerated replicative decline of Werner syndrome cells. *Hum Genet* 1996; 97(6):750-4. Available from: URL: <https://link.springer.com/article/10.1007/BF02346184>.
60. Janssens V, Goris J. Protein phosphatase 2A: a highly regulated family of serine/threonine phosphatases implicated in cell growth and signalling. *Biochem J* 2001; 353(Pt 3):417-39.
61. Fan Y-L, Chen L, Wang J, Yao Q, Wan J-Q. Over expression of PPP2R2C inhibits human glioma cells growth through the suppression of mTOR pathway. *FEBS Lett* 2013; 587(24):3892-7.
62. Westphal RS, Coffee RL, Marotta A, Pelech SL, Wadzinski BE. Identification of kinase-phosphatase signaling modules composed of p70 S6 kinase-protein phosphatase 2A (PP2A) and p21-activated kinase-PP2A. *J Biol Chem* 1999; 274(2):687-92.
63. Xing Y, Xu Y, Chen Y, Jeffrey PD, Chao Y, Lin Z, Li Z, Strack S, Stock JB, Shi Y. Structure of protein phosphatase 2A core enzyme bound to tumor-inducing toxins. *Cell* 2006; 127(2):341-53.
64. Moreno CS, Park S, Nelson K, Ashby D, Hubalek F, Lane WS, Pallas DC. WD40 repeat proteins striatin and S/G(2) nuclear autoantigen are members of a novel family of

- calmodulin-binding proteins that associate with protein phosphatase 2A. *J Biol Chem* 2000; 275(8):5257–63.
65. Wera S, Hemmings BA. Serine/threonine protein phosphatases. *Biochem J* 1995; 311 (Pt 1):17–29.
66. Tanabe O, Nagase T, Murakami T, Nozaki H, Usui H, Nishito Y, Hayashi H, Kagamiyama H, Takeda M. Molecular cloning of a 74-kDa regulatory subunit (B" or delta) of human protein phosphatase 2A. *FEBS Lett* 1996; 379(1):107–11.
67. Zolnierowicz S, Csontos C, Bondor J, Verin A, Mumby MC, DePaoli-Roach AA. Diversity in the regulatory B-subunits of protein phosphatase 2A: identification of a novel isoform highly expressed in brain. *Biochemistry* 1994; 33(39):11858–67. Available from: URL: <https://pubmed.ncbi.nlm.nih.gov/7918404/>.
68. McCright B, Virshup DM. Identification of a new family of protein phosphatase 2A regulatory subunits. *J Biol Chem* 1995; 270(44):26123–8.
69. Jäger K, Mensch J, Grimmig ME, Neuner B, Gorzelniak K, Türkmen S, Demuth I, Hartmann A, Hartmann C, Wittig F, Sporbert A, Hermann A, Fuellen G, Möller S, Walter M. A conserved long-distance telomeric silencing mechanism suppresses mTOR signaling in aging human fibroblasts. *Sci Adv* 2022; 8(33):eabk2814.
70. Strack S, Zaucha JA, Ebner FF, Colbran RJ, Wadzinski BE. Brain protein phosphatase 2A: developmental regulation and distinct cellular and subcellular localization by B subunits. *J Comp Neurol* 1998; 392(4):515–27.
71. Bluemn EG, Spencer ES, Mecham B, Gordon RR, Coleman I, Lewinshtein D, Mostaghel E, Zhang X, Annis J, Grandori C, Porter C, Nelson PS. PPP2R2C loss promotes castration-resistance and is associated with increased prostate cancer-specific mortality. *Mol Cancer Res* 2013; 11(6):568–78.
72. Backx L, Vermeesch J, Pijkels E, Ravel T de, Seuntjens E, van Esch H. PPP2R2C, a gene disrupted in autosomal dominant intellectual disability. *Eur J Med Genet* 2010; 53(5):239–43.
73. Habib R, Kim R, Neitzel H, Demuth I, Chrzanowska K, Seemanova E, Faber R, Digweed M, Voss R, Jäger K, Sperling K, Walter M. Telomere attrition and dysfunction: a potential trigger of the progeroid phenotype in nijmegen breakage syndrome. *Aging (Albany NY)* 2020; 12(12):12342–75.

74. Kannenberg F, Gorzelniak K, Jäger K, Fobker M, Rust S, Repa J, Roth M, Björkhem I, Walter M. Characterization of cholesterol homeostasis in telomerase-immortalized Tangier disease fibroblasts reveals marked phenotype variability. *J Biol Chem* 2013; 288(52):36936–47.
75. Yi X, Tesmer VM, Savre-Train I, Shay JW, Wright WE. Both transcriptional and posttranscriptional mechanisms regulate human telomerase template RNA levels. *Mol Cell Biol* 1999; 19(6):3989–97.
76. Bertram L, Böckenhoff A, Demuth I, Düzel S, Eckardt R, Li S-C, Lindenberger U, Pawelec G, Siedler T, Wagner GG, Steinhagen-Thiessen E. Cohort profile: The Berlin Aging Study II (BASE-II). *Int J Epidemiol* 2014; 43(3):703–12.
77. Gerstorf D, Bertram L, Lindenberger U, Pawelec G, Demuth I, Steinhagen-Thiessen E, Wagner GG. Editorial. *Gerontology* 2016; 62(3):311–5.
78. Cawthon RM. Telomere length measurement by a novel monochrome multiplex quantitative PCR method. *Nucleic Acids Res* 2009; 37(3):e21.
79. Komashko VM, Farnham PJ. 5-azacytidine treatment reorganizes genomic histone modification patterns. *Epigenetics* 2010; 5(3):229–40.
80. Marks PA, Richon VM, Rifkind RA. Histone deacetylase inhibitors: inducers of differentiation or apoptosis of transformed cells. *J Natl Cancer Inst* 2000; 92(15):1210–6.
81. Rusin M, Zajkiewicz A, Butkiewicz D. Resveratrol induces senescence-like growth inhibition of U-2 OS cells associated with the instability of telomeric DNA and upregulation of BRCA1. *Mechanisms of ageing and development* 2009; 130(8):528–37.
82. Parenti MD, Grozio A, Bauer I, Galeno L, Damonte P, Millo E, Sociali G, Franceschi C, Ballestrero A, Bruzzone S, Del Rio A, Nencioni A. Discovery of novel and selective SIRT6 inhibitors. *J Med Chem* 2014; 57(11):4796–804.
83. Sakakibara Y, Sekiya M, Fujisaki N, Quan X, Iijima KM. Knockdown of *wfs1*, a fly homolog of Wolfram syndrome 1, in the nervous system increases susceptibility to age- and stress-induced neuronal dysfunction and degeneration in *Drosophila*. *PLoS Genet* 2018; 14(1):e1007196.
84. Machiela E, Jeloka R, Caron NS, Mehta S, Schmidt ME, Baddeley HJE, Tom CM, Polturi N, Xie Y, Mattis VB, Hayden MR, Southwell AL. The Interaction of Aging and

- Cellular Stress Contributes to Pathogenesis in Mouse and Human Huntington Disease Neurons. *Front Aging Neurosci* 2020; 12:524369.
85. Saxton RA, Sabatini DM. mTOR Signaling in Growth, Metabolism, and Disease. *Cell* 2017; 168(6):960–76.
86. Decker ML, Chavez E, Vulto I, Lansdorp PM. Telomere length in Hutchinson-Gilford progeria syndrome. *Mechanisms of ageing and development* 2009; 130(6):377–83. Available from: URL: <https://pubmed.ncbi.nlm.nih.gov/19428457/>.
87. Tennen RI, Bua DJ, Wright WE, Chua KF. SIRT6 is required for maintenance of telomere position effect in human cells. *Nat Commun* 2011; 2:433.
88. Baird DM, Rowson J, Wynford-Thomas D, Kipling D. Extensive allelic variation and ultrashort telomeres in senescent human cells. *Nat Genet* 2003; 33(2):203–7.
89. Demanelis K, Jasmine F, Chen LS, Chernoff M, Tong L, Delgado D, Zhang C, Shinkle J, Sabarinathan M, Lin H, Ramirez E, Oliva M, Kim-Hellmuth S, Stranger BE, Lai T-P, Aviv A, Ardlie KG, Aguet F, Ahsan H, Doherty JA, Kibriya MG, Pierce BL. Determinants of telomere length across human tissues. *Science (New York, N.Y.)* 2020; 369(6509).
90. Kamranvar SA, Chen X, Masucci MG. Telomere dysfunction and activation of alternative lengthening of telomeres in B-lymphocytes infected by Epstein-Barr virus. *Oncogene* 2013; 32(49):5522–30. Available from: URL: <https://www.nature.com/articles/onc2013189>.
91. Zhang J, Gao Z, Ye J. Phosphorylation and degradation of S6K1 (p70S6K1) in response to persistent JNK1 Activation. *Biochim Biophys Acta* 2013; 1832(12):1980–8.
92. Khan AA, Betel D, Miller ML, Sander C, Leslie CS, Marks DS. Transfection of small RNAs globally perturbs gene regulation by endogenous microRNAs. *Nat Biotechnol* 2009; 27(6):549–55.
93. Harrison DE, Strong R, Sharp ZD, Nelson JF, Astle CM, Flurkey K, Nadon NL, Wilkinson JE, Frenkel K, Carter CS, Pahor M, Javors MA, Fernandez E, Miller RA. Rapamycin fed late in life extends lifespan in genetically heterogeneous mice. *Nature* 2009; 460(7253):392–5.
94. Hahn K, Miranda M, Francis VA, Vendrell J, Zorzano A, Telemann AA. PP2A regulatory subunit PP2A-B' counteracts S6K phosphorylation. *Cell Metab* 2010; 11(5):438–44.

95. Steenstrup T, Kark JD, Verhulst S, Thinggaard M, Hjelmborg JVB, Dalgård C, Kyvik KO, Christiansen L, Mangino M, Spector TD, Petersen I, Kimura M, Benetos A, Labat C, Sinnreich R, Hwang S-J, Levy D, Hunt SC, Fitzpatrick AL, Chen W, Berenson GS, Barbieri M, Paolisso G, Gadalla SM, Savage SA, Christensen K, Yashin AI, Arbeevev KG, Aviv A. Telomeres and the natural lifespan limit in humans. *Aging (Albany NY)* 2017; 9(4):1130–42. Available from: URL: <https://pubmed.ncbi.nlm.nih.gov/28394764/>.
96. Li Y, Zhou G, Bruno IG, Cooke JP. Telomerase mRNA Reverses Senescence in Progeria Cells. *J Am Coll Cardiol* 2017; 70(6):804–5.
97. Baker PB, Baba N, Boesel CP. Cardiovascular abnormalities in progeria. Case report and review of the literature. *Archives of pathology & laboratory medicine* 1981; 105(7):384–6. Available from: URL: <https://pubmed.ncbi.nlm.nih.gov/6894691/>.
98. Gordon LB, Massaro J, D'Agostino RB, Campbell SE, Brazier J, Brown WT, Kleinman ME, Kieran MW. Impact of farnesylation inhibitors on survival in Hutchinson-Gilford progeria syndrome. *Circulation* 2014; 130(1):27–34.
99. Yang J, Chang E, Cherry AM, Bangs CD, Oei Y, Bodnar A, Bronstein A, Chiu CP, Herron GS. Human endothelial cell life extension by telomerase expression. *J Biol Chem* 1999; 274(37):26141–8. Available from: URL: <https://pubmed.ncbi.nlm.nih.gov/10473565/>.

8. Annex

Eidesstattliche Erklärung

„Ich, Kathrin Jäger, versichere an Eides statt durch meine eigenhändige Unterschrift, dass ich die vorgelegte Dissertation mit dem Thema: „Gene expression changes in senescent human fibroblasts point to the existence of a human telomere position effect; Genexpressionsänderungen in seneszenten menschlichen Fibroblasten weisen auf die Existenz eines menschlichen Telomerpositionseffekts hin“ selbstständig und ohne nicht offengelegte Hilfe Dritter verfasst und keine anderen als die angegebenen Quellen und Hilfsmittel genutzt habe.

Alle Stellen, die wörtlich oder dem Sinne nach auf Publikationen oder Vorträgen anderer Autoren/innen beruhen, sind als solche in korrekter Zitierung kenntlich gemacht. Die Abschnitte zu Methodik (insbesondere praktische Arbeiten, Laborbestimmungen, statistische Aufarbeitung) und Resultaten (insbesondere Abbildungen, Graphiken und Tabellen) werden von mir verantwortet.

Ich versichere ferner, dass ich die in Zusammenarbeit mit anderen Personen generierten Daten, Datenauswertungen und Schlussfolgerungen korrekt gekennzeichnet und meinen eigenen Beitrag sowie die Beiträge anderer Personen korrekt kenntlich gemacht habe (siehe Anteilserklärung). Texte oder Textteile, die gemeinsam mit anderen erstellt oder verwendet wurden, habe ich korrekt kenntlich gemacht.

Meine Anteile an etwaigen Publikationen zu dieser Dissertation entsprechen denen, die in der untenstehenden gemeinsamen Erklärung mit dem/der Erstbetreuer/in, angegeben sind. Für sämtliche im Rahmen der Dissertation entstandenen Publikationen wurden die Richtlinien des ICMJE (International Committee of Medical Journal Editors; www.icmje.org) zur Autorenschaft eingehalten. Ich erkläre ferner, dass ich mich zur Einhaltung der Satzung der Charité – Universitätsmedizin Berlin zur Sicherung Guter Wissenschaftlicher Praxis verpflichte.

Weiterhin versichere ich, dass ich diese Dissertation weder in gleicher noch in ähnlicher Form bereits an einer anderen Fakultät eingereicht habe.

Die Bedeutung dieser eidesstattlichen Versicherung und die strafrechtlichen Folgen einer unwahren eidesstattlichen Versicherung (§§156, 161 des Strafgesetzbuches) sind mir bekannt und bewusst.“

Datum

Unterschrift

Declaration of contribution to the selected publications

Kathrin Jäger contributed the following to the below listed publications:

Publication 1: Jäger K, Mensch J, Grimmig ME, Neuner B, Gorzelniak K, Türkmen S, Demuth I, Hartman A, Hartmann C, Wittig F, Sporbert A, Hermann A, Fuellen G, Möller S, Walter M. A Conserved Long-Distance Telomeric Silencing Mechanism Suppresses mTOR Signaling in Aging Human Fibroblasts. *Science Advances* 2022; 8 (33): eabk2814. DOI: 10.1126/sciadv.abk2814

Contribution in detail:

- Planning, organization and performing of experiments shown in Figure 5, 4B and C, S4 – S6, S8A and S8B, S10, S11, S15, S17 – S19; Table S5, S7.
- Processing and evaluation of data, interpretation of results, preparation of tables and figures shown in: Figure 3, 4B and C, S4 – S6, S8A and S8B, S10, S11, S15, S17 – S19; Table S5, S7.
- Writing the manuscript (together with M. Walter) and working on the final version of the paper.

Publication 2: Habib R, Kim E, Neitzel H, Demuth I, Chrzanowska K, Seemanova E, Faber R, Dig-weed M, Voss R, Jäger K, Sperling K, Walter M. Telomere attrition and dysfunction: a potential trigger of the progeroid phenotype in nijmegen breakage syndrome. *Aging* 2020,12(12):12342-12375. DOI: 10.18632/aging.103453

Contribution in detail:

- Planning, organization and performing of experiments shown in Figure 5, Supplementary Figure 3
- Processing and evaluation of data, interpretation of results, preparation of figures shown in: Figure 5, Supplementary Figure 3
- Revising the manuscript and working on the final version of the paper, to the part of gene expression measurement of TPE-OLD candidate genes.

Publication 3: Jäger K and Walter M. Therapeutic Targeting of Telomerase. *Genes (Basel)* 2016; 7(7):39. DOI: 10.3390/genes7070039

Contribution in detail:

- Co-writing the manuscript

Unterschrift des Doktoranden/der Doktorandin

Printed copies of selected publications

Publication 1: A Conserved Long-Distance Telomeric Silencing Mechanism Suppresses mTOR Signaling in Aging Human Fibroblasts.

Jäger K, Mensch J, Grimmig ME, Neuner B, Gorzelniak K, Türkmen S, Demuth I, Hartman A, Hartmann C, Wittig F, Sporbert A, Hermann A, Fuellen G, Möller S, Walter M.

Science advances 2022; 8 (33): eabk2814

DOI: 10.1126/sciadv.abk2814

Impact factor (2022): 14.136

CANCER

A conserved long-distance telomeric silencing mechanism suppresses mTOR signaling in aging human fibroblasts

Kathrin Jäger^{1,2}, Juliane Mensch^{1,2}, Maria Elisabeth Grimmig¹, Bruno Neuner³, Kerstin Gorzelniak⁴, Seval Türkmen^{5,6}, Ilja Demuth^{7,8}, Alexander Hartmann¹, Christiane Hartmann⁹, Felix Wittig¹⁰, Anje Sporbert¹¹, Andreas Hermann^{9,12,13}, Georg Fuellen¹⁴, Steffen Möller¹⁴, Michael Walter^{1,2*}

Telomeres are repetitive nucleotide sequences at the ends of each chromosome. It has been hypothesized that telomere attrition evolved as a tumor suppressor mechanism in large long-lived species. Long telomeres can silence genes millions of bases away through a looping mechanism called telomere position effect over long distances (TPE-OLD). The function of this silencing mechanism is unknown. We determined a set of 2322 genes with high positional conservation across replicatively aging species that includes known and candidate TPE-OLD genes that may mitigate potentially harmful effects of replicative aging. Notably, we identified *PPP2R2C* as a tumor suppressor gene, whose up-regulation by TPE-OLD in aged human fibroblasts leads to dephosphorylation of p70S6 kinase and mammalian target of rapamycin suppression. A mechanistic link between telomeres and a tumor suppressor mechanism supports the hypothesis that replicative aging fulfills a tumor suppressor function and motivates previously unknown antitumor and antiaging strategies.

INTRODUCTION

Telomeres are repetitive nucleotide sequences that protect the natural ends of linear chromosomes (1). The exact role of telomeres in aging is still a matter of debate. Successive telomere attrition during cell divisions provides a molecular mechanism that determines replicative life span (1, 2), which ultimately leads to cellular senescence. Telomere shortening was proposed to be a tumor suppressor mechanism a long time ago (2, 3). Successive telomere attrition during replication (4) eventually triggers the DNA damage response when telomeres become critically shortened, leading to cell cycle arrest and replicative senescence. It is believed that this mechanism acts as a tumor suppressor mechanism in humans and other large, long-lived

species (2) at the cost of possible negative effects in later life (5). Clinical observations support this concept as most clinically detectable cancers have reactivated telomerase (1). Nevertheless, there is still much controversy about the functional and physiological role of replicative aging. A main reason is the double-edged role of telomere attrition (6). Excessive shortening of the telomere is itself tumorigenic. Short telomeres are found in premalignancies and may increase genetic instability and tumor formation in mice (7).

In 2001, a process called telomere position effect (TPE), i.e., the reversible silencing of telomeric genes, was demonstrated in human HeLa cells using a luciferase reporter (8). Together, 16 genes were identified using cultivated myoblasts and fibroblasts, which are differentially expressed in young cells (with long telomeres) versus old cells (with short telomeres). Most of these genes are silenced in young cells (with long telomeres) and become expressed when telomeres are short (table S1). Re-elongation of telomeres in cells with short telomeres by exogenous expression of the *hTERT* gene (active telomerase) results in expression patterns similar to those in young cells with long telomeres (9, 10). As the silencing mechanism acts via looping structures up to at least 15 Mb away from the telomere, as experimentally proven for the five genes, *C1S*, *DSP*, *ISG15* (10, 11), *SORBS2* (9), and *hTERT* (12), it was named telomere position effect over long distance (TPE-OLD) (Fig. 1A). Not much is known about the functional details of TPE-OLD. The ability to regulate genes by telomere length (TL) in a preemptive fashion, e.g., without induction of a strong DNA damage signal from critically short telomeres, may have important implications for the regulation of subtle age-dependent adjustments, which prompted us to study these interrelationships in more detail.

We used a bioinformatics approach to identify TPE-OLD candidate genes and investigated gene expression of candidates in human fibroblasts at high population doublings (PDs) (with short telomeres) and in *hTERT* immortalized fibroblasts (with long telomeres). Fibroblasts from patients with Hutchinson-Gilford progeria (HGP) were used as a model for accelerated telomere attrition. HGP cells display

¹Institute of Clinical Chemistry and Laboratory Medicine, Rostock University Medical Center, University of Rostock, Rostock, Germany. ²Charité-Universitätsmedizin Berlin, corporate member of Freie Universität Berlin, Humboldt-Universität zu Berlin, and Berlin Institute of Health, Institute of Laboratory Medicine, Clinical Chemistry and Pathobiochemistry, Berlin, Germany. ³Charité-Universitätsmedizin Berlin, corporate member of Freie Universität Berlin, Humboldt-Universität zu Berlin, and Berlin Institute of Health, Department of Anesthesiology and Intensive Care Medicine, Berlin, Germany. ⁴Unfallkrankenhaus Berlin, Institute of Laboratory Medicine, Berlin, Germany. ⁵LNS Hematooncogenetics, National Center of Genetics Luxembourg, Dudelange, Luxembourg. ⁶Charité-Universitätsmedizin Berlin, corporate member of Freie Universität Berlin, Humboldt-Universität zu Berlin, and Berlin Institute of Health, Institute of Medical Genetics and Human Genetics, Berlin, Germany. ⁷Charité-Universitätsmedizin Berlin, corporate member of Freie Universität Berlin, Humboldt-Universität zu Berlin, and Berlin Institute of Health, Department of Endocrinology and Metabolism, Berlin, Germany. ⁸Berlin Institute of Health at Charité-Universitätsmedizin Berlin, BCRT - Berlin Institute of Health Center for Regenerative Therapies, Berlin, Germany. ⁹Translational Neurodegeneration Section "Albrecht-Kossel", Department of Neurology, Rostock University Medical Center, University of Rostock, 18147 Rostock, Germany. ¹⁰Institute of Pharmacology and Toxicology, Rostock University Medical Center, University of Rostock, Rostock, Germany. ¹¹Advanced Light Microscopy, Max Delbrück Center for Molecular Medicine, Berlin, Germany. ¹²Deutsches Zentrum für Neurodegenerative Erkrankungen (DZNE) Rostock/Greifswald, Rostock, Germany. ¹³Center for Transdisciplinary Neurosciences Rostock (CTNR), University Medical Center Rostock, Rostock, Germany. ¹⁴Institute for Biostatistics and Informatics in Medicine and Ageing Research, Rostock University Medical Center, Rostock, Germany.

*Corresponding author. Email: michael.walter@med.uni-rostock.de

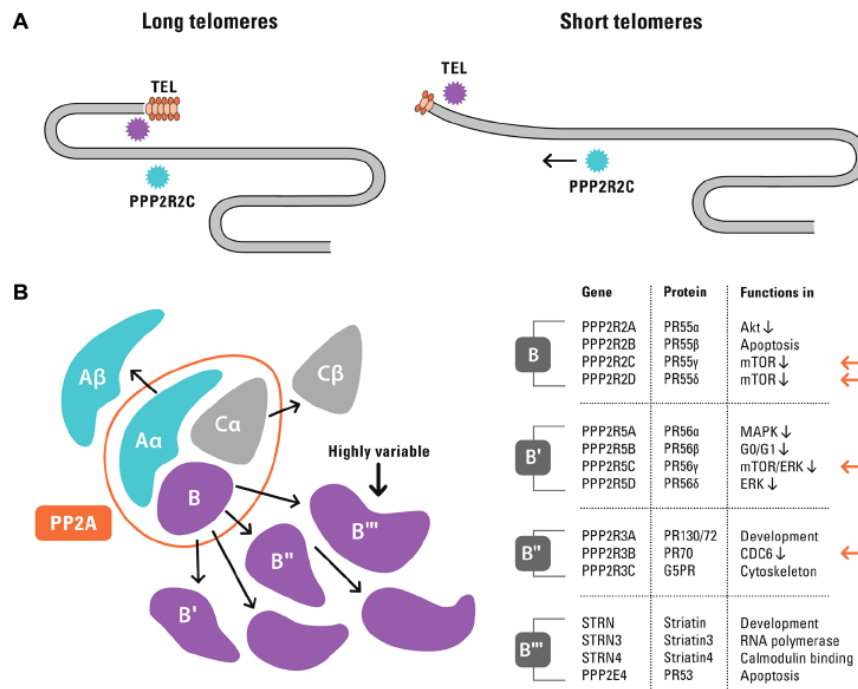


Fig. 1. TPE-OLD concept and protein phosphatase 2A holoenzyme subunits as TPE-OLD candidates. (A) TPE-OLD concept. Telomeres may loop to specific loci to regulate gene expression, a process termed “telomere position effect over long distances” (9, 10, 12). The effect extends to a distance of at least 15 Mb from the telomere and may regulate gene expression in an age-dependent manner. (B) Schematic representation of the structural (A α and A β), regulatory (B, B', B'', and B''') and catalytic (C α and C β) subunits forming the PP2A holoenzyme. The enzyme is composed of one of two homologous catalytic subunits, one of two homologous structural subunits, and 1 of at least 15 highly variable regulatory subunits. The included table summarizes functional roles of the regulatory subunits. Red arrows indicate the TPE-OLD candidates, all displaying similar regulatory functions, as indicated by (21–24). MAPK, mitogen-activated protein kinase; ERK, extracellular signal-regulated kinase.

shorter telomeres and abnormal TL distribution (13, 14). Patients with HGP show many phenomena of normal aging at young age but a low cancer incidence and no age-related neurodegeneration (15). We identified 2322 TPE-OLD candidate genes, many of which are involved in cell cycle control, metabolic regulation, and stress response. We used one of these candidates (*PPP2R2C*) to show a mechanistic link between telomere attrition and a tumor suppressor mechanism that acts long before telomere-driven DNA damage signaling occurs, driving a tumor suppressor effect based on attenuated mammalian target of rapamycin (mTOR) signaling. *PPP2R2C* encodes PR55 γ , a regulatory subunit of the serine/threonine-specific phosphatase (PP2A) with a wide variety of substrates involved in the regulation of cell cycle and metabolism (Fig. 1B) (16, 17). Our findings suggest an important functional role of TPE-OLD in aging cells and support the hypothesis that replicative aging fulfills a tumor suppressor function.

RESULTS

Genomic positional conservation analysis identifies previously unidentified TPE-OLD candidate genes

We first sought to identify candidate genes that might be affected by TPE-OLD by using a bioinformatics approach. Thinking in terms of biological mechanisms, most phenomena are gradual and the distinction between replicatively aging species and other species can be expected to be gradual as well. While some species are “clearly

aging replicatively,” this attribute is difficult to assign in many cases. When selecting the species, we therefore adopted the simplest possible definition. The criteria for categorizing a species as having “assumed TL-dependent replicative aging” were set as TL < 20 kb, undetectable telomerase levels, and no stasis (stress associated senescence), as previously proposed by Gomes *et al.* (18). By using these criteria, we noted that the 16 known or suggested TPE-OLD genes reported in the literature (9–12) appeared to be preserved at two telomeric positions in “replicatively aging species,” that is, in species which undergo TL-dependent replicative aging (18), including both primates and nonprimates (at 0.2 to 7.5 Mb and at 13 to 17 Mb) (Fig. 2A and fig. S1). No such conservation was observed in organisms that do not undergo TL-dependent aging.

We used the Ensembl genome database to screen for other genes presenting a similar conserved position as this set of genes with established TPE-OLD. We selected possible candidates on the basis of positional conservation, at most 1 Mb apart, and anywhere within 17 Mb of the telomere, e.g., the maximum distance discussed in the literature for TPE-OLD effects. Using this approach, we identified 2322 novel TPE-OLD candidates (fig. S3 and table S2). Gene set enrichment analysis found that many candidates are involved in proliferation, metabolism, and stress response and/or are regulated by transcription factors involved in proliferation, metabolism, development, and response to stress and DNA damage (table S3) (19, 20). Accordingly, gene families associated with transcriptional regulation,

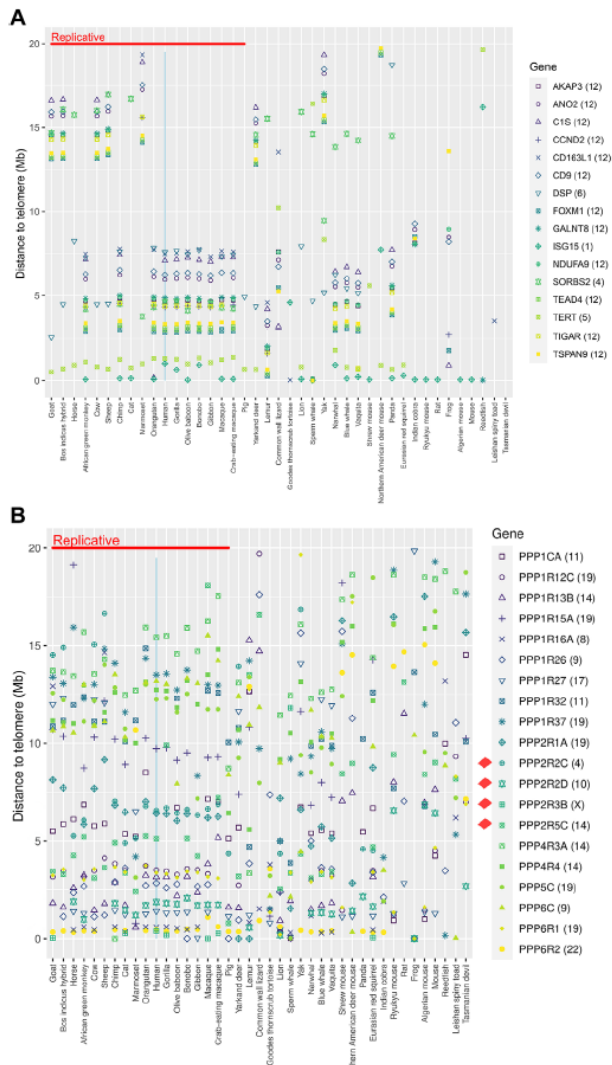


Fig. 2. Conserved genomic positions of known TPE-OLD genes and identification of TPE-OLD candidate genes encoding PP2A subunits. (A) Telomeric distances for established TPE-OLD genes. The figure shows the distance to the closest telomere in megabases for all genes for which a TPE-OLD was already proposed in the literature, capped at 20 Mb. Genes are distinguished by their symbol, supported by color. Species are separated horizontally, sorted by the median distance to telomeres for all genes in the genome. Only species with a median gene distance to the telomeres of above 15 Mb are shown, which is close to the maximal distance of established TPE-OLD genes from the telomere. Species proposed to age replicatively [as defined in Results and in (18)] are grouped on the left. The data presented in this figure serve as a reference for the preservation of telomeric distances below 20 Mb and for the differences between replicatively and nonreplicatively aging species that can be expected for TPE-OLD genes. We find the telomeric distances among established TPE-OLD genes to be preserved across species such that these appear as horizontal patterns on the left. The number in parentheses behind the gene name indicates the human chromosome coding for that gene. (B) Telomeric distances for TPE-OLD candidates among PP1A and PP2A subunits. This figure presents a selection of those genes that appear clustered below 20 Mb. The four genes that have been investigated here are marked in the legend.

cell growth, and response to stress were overrepresented in the group of TPE-OLD candidates (table S4). Thus, changes in the activity of these genes in aging cells may point to a regulated adaptive process, which prompted us to investigate one of the highly ranked groups of TPE-OLD candidates more closely.

Several regulatory subunit genes of the cell growth regulator PP2A are TPE-OLD candidates

Focusing on genes strongly related to cell growth and aging, 20 of the TPE-OLD candidate genes encode subunits of serine/threonine-specific phosphatases PPP1, PPP2, and PPP6 and display the typical positional conservation with respect to the telomere (Fig. 2B and figs. S2 to S3). These PPPs code for key regulators of cell division, protein synthesis, and tumor suppression. The most abundant enzyme, PP2A, accounts for up to 1% of total cell protein in some tissues and has more than 300 substrates involved in cell cycle and metabolism, regulating major cell cycle pathways and checkpoints (16, 17). The full activity, substrate specificity, and subcellular localization of the PP2A phosphatase are determined by diverse regulatory subunits (Fig. 1B) (16, 17). We observed that although the catalytic subunits (*PPP2CA* and *PPP2CB*) have high sequence conservation, their chromosomal positions were not conserved among species; in contrast, the telomeric distance of many regulatory subunit genes, which are much more diverse in sequence, tended to be evolutionarily conserved among species with TL-dependent replicative aging. In particular, we noticed that four regulatory subunits of PP2A, namely, *PPP2R2C*, *PPP2R2D*, *PPP2R5C*, and *PPP2R3B* (21–24), were locally preserved within the suggested TPE-OLD range at distinct positions relative to the telomere (fig. S4). No telomeric conservation (or any other conservation of chromosomal location) of these genes was observed in species that do not undergo TL-dependent replicative aging (Fig. 2B and fig. S4). Given these observations and the role of PP2A in cell cycle regulation, we focused on these four PP2A regulatory subunit genes as TPE-OLD candidates in our next experiments.

Expression of the PP2A regulatory subunit gene *PPP2R2C* is markedly up-regulated in healthy presenescent fibroblasts but is not up-regulated in stress-induced senescence

We examined telomere-associated changes in gene expression and cell physiology in old but still replicating (presenescent) cells. The presenescence stage (reached after high PDs) of primary cells was established by culturing cells until the final cell cycle arrest and, for the experiments, thawing frozen samples from 10 to 15 PDs before the suggested final arrest. The presenescent fibroblasts had already shortened telomeres [TL ratio (TLR) 0.15 to 0.24 versus TLR 0.48 to 0.81 in their young derivatives] but did not yet have the typical signs of senescent cells, even if their growth rate was already weakened (growth profiles are shown in fig. S5). These cells were compared with the respective replicatively young healthy cells. The same procedure was done with cells from patients with HGP, which are considered a model for accelerated telomere attrition and premature aging (13). TL was quantified as relative TLR, compared to single-copy gene standard, using an established polymerase chain reaction (PCR) method. Fibroblast cell lines were classified either as “young primary control cells” (low PDs 13 to 17, TLR 0.48 to 0.81), as “presenescent primary control cells” (high PDs 41 to 55, TLR 0.15 to 0.24), as “young primary HGP cells” (low PDs 19 to 20, TLR 0.28 to 0.68), or as “presenescent primary HGP cells” (high PDs 34 to 42, TLR 0.17 to 0.46; table S5).

SCIENCE ADVANCES | RESEARCH ARTICLE

First, we compared TL and gene expression levels of all relevant PP2A subunits in young (L for low PD in Fig. 3 and fig. S6) and presenescent (H for high PD in Fig. 3 and fig. S6) healthy controls and in HGP fibroblasts. Specifically, we analyzed the four PP2A regulatory subunits that appeared preserved within the suggested TPE-OLD range at distinct positions relative to the telomere (*PPP2R2C*, *PPP2R2D*, *PPP2R5C*, and *PPP2R3B*), the two structural

(*PPP1A* and *PPP1B*), and the two catalytic subunits (*PPP2CA* and *PPP2CB*).

No influence of TL on gene expression was detected for any structural or catalytic subunit (Fig. 3). Among the regulatory telomeric PP2A subunit genes, *PPP2R2C* displayed a consistently up-regulated level of mRNA in healthy fibroblasts with short telomeres (6.85 ± 1.79 -fold, $P \leq 0.01$ at 5 to 15 PDs before senescence),

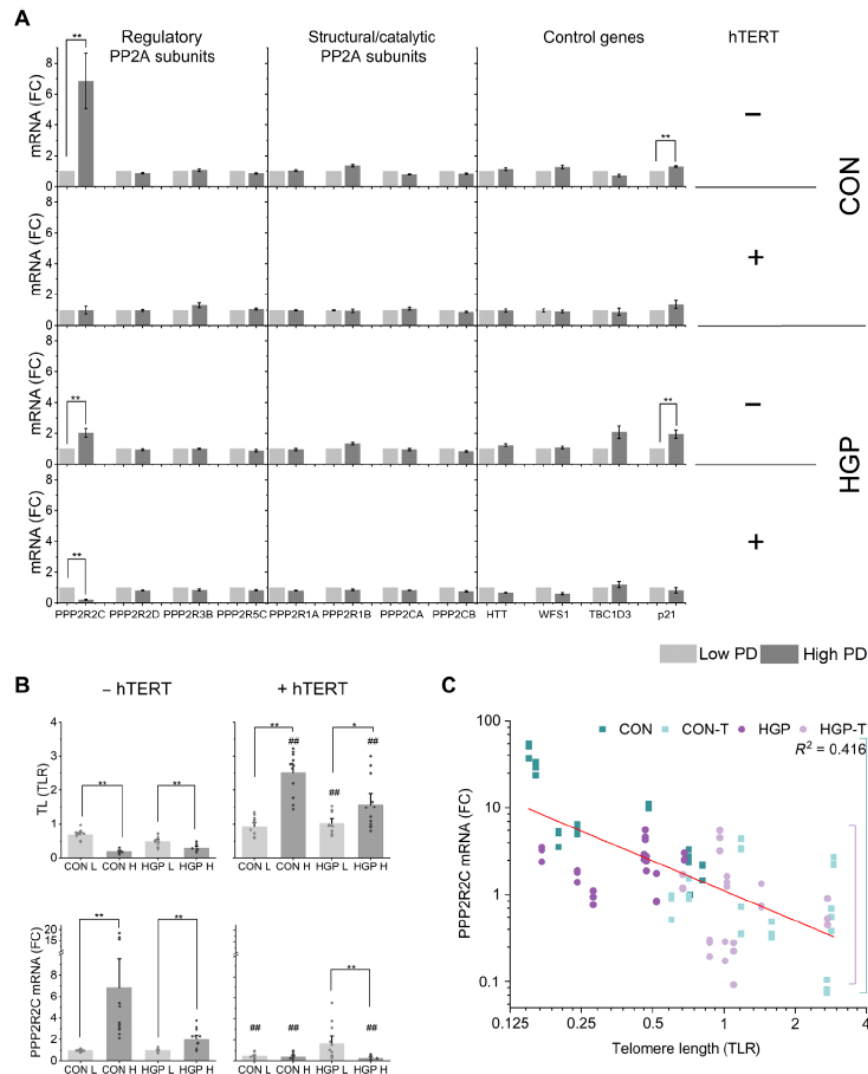


Fig. 3. TL-dependent mRNA levels of regulatory, structural, and catalytic PP2A subunits in control (CON) and progeria (HGP) fibroblasts. (A) Quantitative PCR (qPCR) analysis of primary (–hTERT) and immortalized (+hTERT) control (CON) and HGP cells at low (L) and high (H) PD. *Cyclophilin A* was used as normalization control. *WFS1* and *HTT* represent internal controls, *p21* represents a stress marker, and *TBC1D3* represents a potential confounder, as described in Results. All values were normalized to the level (=100%) of mRNA in cells at L PD. Results are shown as means \pm SEM. Mann-Whitney *U* test was used: * $P < 0.05$ and ** $P < 0.01$ for L PD versus H PD. Six of 2394 measurements were excluded because mRNA was undetectable. (B) Average TL and *PPP2R2C* mRNA levels of CON and HGP cells at L and H PD before (–hTERT) and after (+hTERT) immortalization. TL was measured as relative TLR using monochrome multiplex qPCR (MMqPCR), as described in Materials and Methods. mRNA values were normalized to the level (=100%) of *PPP2R2C* mRNA in primary L PD cells. Results are shown as means \pm SD. * $P < 0.05$ and ** $P < 0.01$ for L PD versus H PD. ## $P < 0.01$ for +hTERT versus –hTERT (Mann-Whitney *U* test). Each assay in (A) and (B) was performed in biological quadruplicate and technical triplicate. (C) Negative correlation between TL and *PPP2R2C* mRNA levels. All values were normalized to the mRNA level (=100%) of cell line 707 at L PD. Data are shown for 48 separate measurements from $n = 16$ cell lines [8 primary and 8 immortalized (T)], excluding one measurement with undetectable mRNA. FC, fold change.

with some interassay and interindividual variation (minimum/maximum observed fold change 2.76-fold/16.99-fold). The PP2A subunit genes *PPP2R2D*, *PPP2R5C*, and *PPP2R3B* were not up-regulated in fibroblasts under the conditions described here (Fig. 3A) and therefore were not analyzed further. In fibroblasts derived from patients with HGP, *PPP2R2C* mRNA levels increased 2.03 ± 0.27 -fold, $P \leq 0.01$, in high PD cells relative to low PD cells (Fig. 3A) (minimum/maximum observed fold change 1.03-fold to 3.28-fold; fig. S6).

Next, we measured gene expression in hTERT-immortalized cells (i.e., cells with artificially elongated telomeres) at low and high PDs. Cells that had recently been immortalized were classified as “immortalized cells at low PD” (PD 14 to 28 after hTERT immortalization in healthy cells with TLR 0.6 to 1.18; PD 15 to 34 after hTERT immortalization in HGP cells with TLR 0.67 to 1.44), and cells with a substantial number of PDs after immortalization were classified as “immortalized cells at high PD” (PD 56 to 70 after hTERT immortalization in healthy cells with TLR 1.59 to 2.91; PD 57 to 63 after hTERT immortalization in HGP cells with TLR 0.87 to 2.74).

After immortalization, the *PPP2R2C* mRNA level in healthy fibroblasts was decreased to that of young cells or even lower (0.4 ± 0.3 -fold versus 6.8 ± 6.2 -fold, $P \leq 0.01$) (Fig. 3B). In HGP fibroblasts, the *PPP2R2C* mRNA level declined to below basal levels in hTERT-immortalized HGP fibroblasts (0.3 ± 0.2 -fold versus 2.0 ± 0.9 -fold, $P \leq 0.01$), but with a substantial delay (at high PD after immortalization only). Together, we found an inverse relationship between *PPP2R2C* expression and TL in both control and HGP fibroblasts (Fig. 3C).

In addition to replicative senescence, several factors can accelerate and/or trigger cell senescence, including various forms of stress like oxidative stress. Such acute stress is not primarily driven by the shortening of telomeres and may occur completely independently of TL and replicative senescence (25, 26). Using sublethal H_2O_2 concentrations, we triggered stress-induced senescence to investigate the specificity of the phenomena described here. Cyclin-dependent kinase inhibitor p21 was used to monitor the stress-inducible premature senescence (SIPS) (27). We stimulated fibroblasts with H_2O_2 at concentrations capable of inducing a typical stress response (SIPS), as indicated by induction of *p21* mRNA (fig. S6) and the cellular stress marker β -galactosidase [i.e., senescence-associated β -galactosidase (SA- β -Gal)] (fig. S7). SA- β -Gal measurements were additionally confirmed by a highly sensitive spectrophotometric method [4-methylumbelliferyl- β -D-galactopyranoside (MUG)], an alternative for SA- β -Gal staining and subjective visual quantification that measures enzyme activity in cell lysates. We observed nonsignificant increases in *PPP2R2C* at the mRNA level in some experiments but found that H_2O_2 stimulation did not induce a significant *PPP2R2C* mRNA increase (fig. S6), while it did increase SA- β -Gal measurements, suggesting that oxidative stress is not a stimulus for *PPP2R2C* mRNA expression.

Together, these data showed that the expression of the PP2A regulatory subunit gene *PPP2R2C* is markedly up-regulated in healthy presenescent fibroblasts but is not up-regulated in SIPS. We found a lower relative increase in *PPP2R2C* mRNA in HGP cells compared to healthy controls but no marked deviation from the inverse relationship between TL and *PPP2R2C* expression.

Histone-dependent telomere looping but not long-range heterochromatin spreading is responsible for the silencing of *PPP2R2C*

We were next interested to explore the mechanism linking telomere shortening with *PPP2R2C* mRNA expression. Classical TPE in

Saccharomyces cerevisiae and *Drosophila melanogaster* regulates genes in a manner proportional to the proximity to telomeric repeats through heterochromatin spreading and is not effective over longer telomere distances (28). To exclude spreading of the TPE in a continuous fashion (as in classical TPE), we examined the expression of other genes located between *PPP2R2C* and the telomere. We did not find a correlation between TL and the expression of genes such as *WFS1* and *HTT*, which also have some functional relationship with aging and survival (29, 30), in high-PD and low-PD cells with and without hTERT immortalization (Fig. 3 and fig. S6). Thus, telomere attrition did not influence *WFS1* or *HTT* expression, although the chromosomal locations of these genes are more telomeric than the one of *PPP2R2C*, indicating that long-range heterochromatin spreading is not responsible for the silencing of *PPP2R2C*.

Next, we examined whether telomere shortening causes a change in chromatin organization involving the *PPP2R2C* locus. According to the TPE-OLD concept, there is a loop structure formed by long chromosomes in presenescent cells that opens or even completely disappears as telomeres shorten. Thus, as chromosomal reorganization occurs in cells with short telomeres, one would expect a higher percentage of separated (“S”; distance between probes $>2.26 \mu\text{m}$) probes and a lower percentage of adjacent (“A”; distance between probes $<2.26 \mu\text{m}$) probes. We used a high-resolution three-dimensional fluorescence in situ hybridization imaging (3D-FISH) to measure the distance between a bacterial artificial chromosome (BAC) probe containing the *PPP2R2C* locus (red; 4.2 Mb from the telomere) and a TelVysion probe containing the conserved subtelomeric region of 4p (green; ~ 100 to 300 kb from the telomere; Fig. 4). Consistent with our proposed mechanism, we observed a continuous and highly significant change in the overall distribution of the distances between the two loci in cells with long versus short TLs (Fig. 4 and figs. S8 and S9). This pattern persisted even when we examined the shortest and longest probe distances separately for each cell line (fig. S8D) to correct for the known bimodal distribution of TLs in fibroblasts (31).

In the yeast, expression of telomeric genes is modulated by chromatin modification in response to starvation and heat shock stress and is part of an important regulatory network (28). Moreover, changes in telomeric chromatin in late-passage human cells have been linked to cellular senescence (32). Heterochromatin in mammalian cells is normally dependent on histone deacetylation. We therefore investigated the influence of treatment with substances interfering with histone modifications on *PPP2R2C* mRNA levels (fig. S10). We did not find significant changes after treatment with trichostatin A (TSA), an inhibitor of histone deacetylases (33), and we did also not find a change after treatment of fibroblasts with 5-azacytidine (5-AzaC), which results in nonspecific overall DNA demethylation leading to a reorganization of genomic histone modification patterns (34). Resveratrol (RSV), which may induce instability of telomeric DNA (35), slightly increased *PPP2R2C* mRNA levels in hTERT-immortalized fibroblasts, by up to 1.6-fold.

Because TSA, 5-AzaC, and RSV lack specificity, we aimed for a more specific modulation. In *S. cerevisiae*, the nicotinamide adenine dinucleotide-dependent histone deacetylase Sir2 (silent information regulator 2) has a key role in generating and maintaining silent chromatin near telomeres (36). This epigenetic silencing of telomere-proximal genes is lost with replicative yeast aging, concomitant with aberrant hyperacetylation of subtelomeric sequences. The mammalian Sir2 homolog sirtuin 6 (SIRT6) has recently been shown to be required for repression of an endogenous telomere-proximal gene,

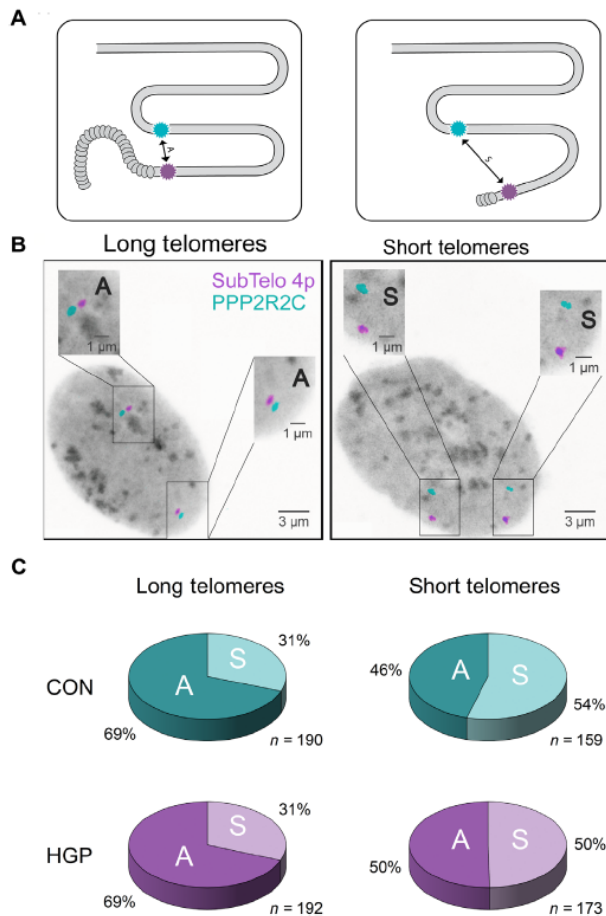


Fig. 4. Identification of *PPP2R2C* as a TPE-OLD gene: Chromosomal reorganization. (A) Graphical illustration of the TPE-OLD effect with long and short telomeres. (B) Confocal images of 3D-FISH processed with IMARIS. Gray, 4',6-diamidino-2-phenylindole (DAPI); turquoise, BAC RP11-762B2 targeting the gene *PPP2R2C*; magenta, TelVysion (TEL) probe targeting subtelomeric 4p (100 to 300 kb from the telomere of chromosome 4p). A, adjacent; S, separated. (C) Overall distribution of TEL-*PPP2R2C* probe distances for both healthy control cells and progeria cells. The proportion of probe distances ≤ 2.26 and > 2.26 μm is shown in circle diagrams. The number of experiments includes all data points, after deducting the points with fewer than or more than four signals (instead of two red and two green signals each), irregular DAPI staining (e.g., mitotic cells) and abnormal cell shape (252 of total 1680 distances were excluded). Images were acquired using 405-nm excitation/415- to 480-nm emission for DAPI, 488-nm excitation/500- to 545-nm emission for Spectrum Green, and 561-nm excitation/565- to 640-nm emission for Spectrum Orange. Images were then processed using Imaris 9.3 software (Andor Bitplane).

suggesting a key role for SIRT6 in maintaining a silencing-competent chromatin structure at natural telomeres (37). Compound BCI-150, a new SIRT inhibitor with selectivity for SIRT6 but not for SIRT1 and SIRT2 (38), enhanced the expression of *PPP2R2C* up to fivefold in *hTERT*-immortalized cells (fig. S10). As SIRT6 was found to be required for repression of telomere-proximal reporter genes in human cells (37), this finding suggests that silencing of *PPP2R2C* is dependent on histone deacetylation mediated by SIRT6.

P70S6K dephosphorylation and downstream effects in presenescent fibroblasts are directly related to *PPP2R2C* up-regulation regardless of basal mTOR levels

The protein encoded by *PPP2R2C* (PR55 γ) inhibits p70S6K, a downstream target of mTOR, via dephosphorylation (21). Together with S6 ribosomal protein (S6RP) and initiation factor and 4E-binding protein 1, p70S6K is the most important downstream target of mTOR, and its Thr³⁸⁹ phosphorylation status closely correlates with its kinase activity in vivo (39).

In presenescent human fibroblasts, telomere attrition was associated with markedly decreased phosphorylation of p70S6K to $16 \pm 6\%$ of the levels of young healthy control cells (Fig. 5A). It has previously been shown that inhibition of p70S6K may secondarily decrease Akt phosphorylation (40). Accordingly, we observed a lower level of Akt protein in the phosphorylated state in both presenescent healthy controls and (to a lesser degree) HGP cells (Fig. 5C). Immortalization of cells with telomerase, which recovered cell growth (fig. S5), also recovered the p70S6K phosphorylation pattern (Fig. 5A) and the Akt phosphorylation pattern (Fig. 5C) in both cell types in a TL-dependent manner (fig. S11).

mTOR mediates and integrates growth signals; thus, mTOR and protein synthesis are tightly regulated and coupled to cell growth rates. We examined the possibility that a lower p70S6K degree of phosphorylation occurs secondary to a lower need for protein synthesis and a lower growth-related mTOR and p70S6K activity. We therefore related cell growth rates to the protein amounts of Akt, mTOR, and p70S6K (fig. S12). We found no evidence of a relationship between the growth rates, the expression of mTOR, p70S6K, and Akt, and the degree of p70S6K phosphorylation. By contrast, the HGP fibroblasts with reduced growth rates had approximately twofold higher relative mTOR, p70S6K, and Akt protein levels compared to control presenescent cells. Despite this inappropriately high mTOR activation, the deactivating dephosphorylation of p70S6K was not disturbed but was enhanced (red arrow in fig. S12). In another experiment, we examined the influence of serum starvation on total and phosphorylated p70S6K and mTOR protein and mRNA levels. As shown in fig. S13, this treatment led to slightly decreased levels of p70S6K and mTOR, reduction of which, however, was much lower than the TL-dependent up-regulation of *PPP2R2C* and the resulting decrease in p70S6K phosphorylation in aged cells. Thus, serum starvation was not a major determinant of p70S6K phosphorylation in presenescent fibroblasts.

Phosphorylation at Thr³⁸⁹ activates p70S6K and increases cellular protein synthesis via phosphorylation of the S6RP; correspondingly, dephosphorylation inhibits protein synthesis. Inhibition of mTOR (and p70S6K) decreases the protein levels of many metabolic targets and may thus decelerate senescence entry. We therefore analyzed the metabolic marker arylsulfatase A (ARSA), in primary presenescent cells. The protein product (fig. S14, right) and resulting activity (middle panel) of ARSA, which is regulated by mTOR and p70S6K and is strongly inhibited by the prototype mTOR inhibitor rapamycin (41), were suppressed in aged fibroblasts.

To further confirm the role of *PPP2R2C* in p70S6K phosphorylation in fibroblasts, we performed inhibitor experiments using *PPP2R2C*-specific small interfering RNA (siRNA). Upon treatment of presenescent fibroblasts with siRNA (both 25 and 50 nM) for 7 hours and an incubation time of 48 hours after siRNA removal, the dephosphorylation of p70S6K was inhibited by approximately 90% in HGP cells (fig. S15). In parallel, increased mRNA levels of

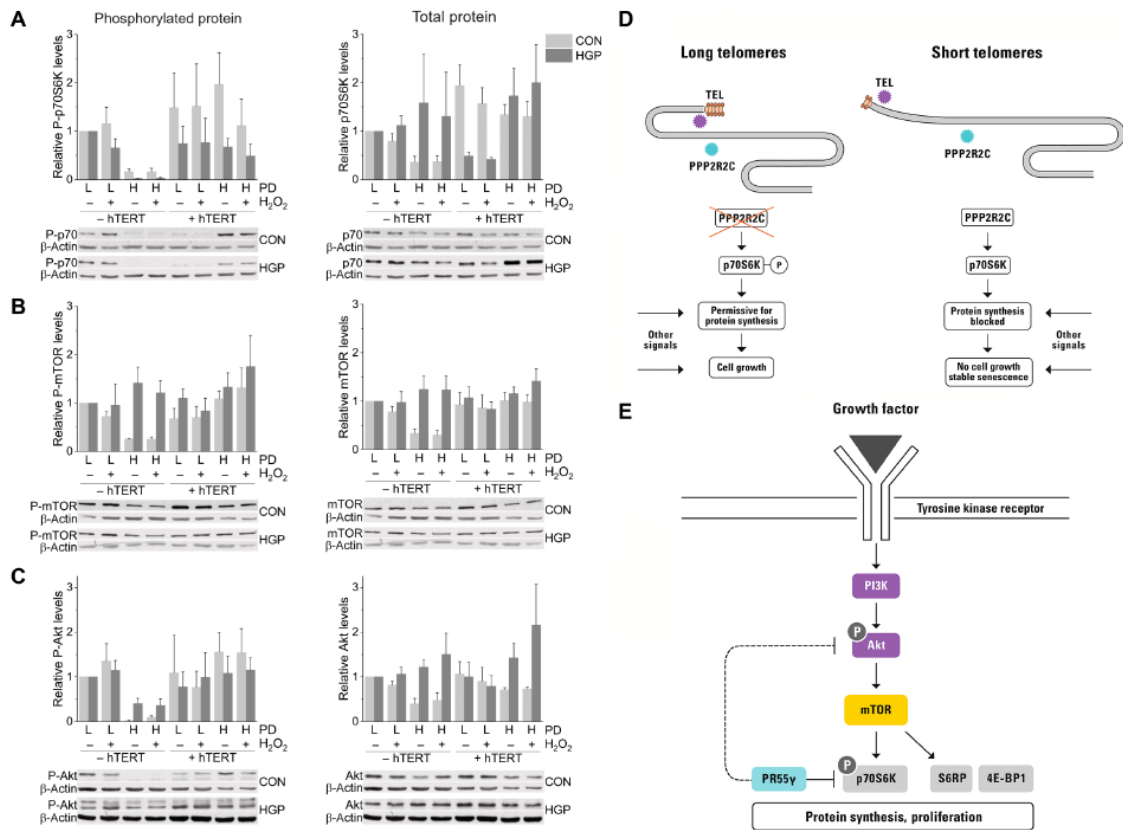


Fig. 5. Influence of TL on mTOR signaling. (A to C) Total and phosphorylated protein levels of (A) p70S6K, (B) mTOR, and (C) Akt. Western blot analysis was performed from primary (–hTERT) and hTERT-immortalized cells (+hTERT) at low (L) and high (H) PDs in the absence or presence of H₂O₂ (200 μM; 2 hours), as indicated. Light gray columns, healthy CON fibroblasts; dark gray columns, HGP fibroblasts. All protein levels were normalized to the protein levels of β-actin. Protein/β-actin ratios were expressed relative to those in low-PD cell samples (which were set at a value of 1). Means ± SEM, *n* = 4 cell lines per column (with two to three independent blots each). Each β-actin belongs to the same membrane as the respective protein (fig. S21). (D) Schematic summary of the suggested protective effect of TPE-OLD on PPP2R2C (PR55_γ for the protein) induction. (E) Schematic illustration of the Akt/mTOR/p70S6K pathway. PR55_γ-mediated dephosphorylation of p70S6K has a direct inhibitory effect on protein synthesis and may thus stabilize cells in presenescence. Inhibition of p70S6K may additionally lead to a lower degree of Akt phosphorylation (40). Magenta, oncogenes; turquoise, tumor suppressors; gray, not characterized. PI3K, phosphatidylinositol 3-kinase; 4E-BP1, 4E-binding protein 1.

genes whose transcription is likely dependent on p70S6K phosphorylation were observed and the total amount of p70S6K was moderately reduced. Together, these findings are in accordance with previous data on p70S6K and show that TL-dependent up-regulation of PPP2R2C leads to metabolic and proliferative suppression in aged cells. Our data support the notion that PR55_γ, which is encoded by PPP2R2C, causes dephosphorylation of p70S6K and thereby contributes to inhibition of cellular function in presenescent fibroblasts with short telomeres.

TL-dependent silencing of PPP2R2C and possible downstream effects were not severely affected in HGP fibroblasts despite abnormalities in telomere attrition kinetics

Fibroblasts from patients with HGP were used as a model for suggested accelerated telomere attrition. The mean TL in HGP fibroblasts is slightly shorter than normal, and the TL distribution is abnormal.

Normal or even longer telomeres have been described in approximately one-third of all cells (13, 14). We therefore hypothesized that changes in TPEs may at least in part explain these aging-related phenomena. However, we could exclude a severe abnormality in TPE-OLD (for PPP2R2C) in HGP.

p70S6K was almost completely unphosphorylated in presenescent HGP cells (Fig. 5A); we observed an inverse relationship between TL and PPP2R2C mRNA expression (Fig. 3C), and dephosphorylation of p70S6K occurred in aged HGP cells with shorter telomeres (Fig. 5A) despite constantly high levels of total mTOR protein levels in these cells (fig. S12), which together excludes a severe abnormality in TL-dependent silencing of PPP2R2C by TPE-OLD.

There were, however, various indications of some subtle “telomeric dysfunction” in HGP cells. For example, in cells from patients with HGP but not controls, telomeres tended to be shorter in young cells (TLR 0.49 ± 0.08 in HGP versus 0.68 ± 0.07 in controls at low PD; *P* = 0.1) but longer in presenescent cells (TLR 0.33 ± 0.08 versus

0.19 ± 0.02 at high PD; $P = 0.2$) (Fig. 3B). TL-dependent chromosomal reorganization in HGP fibroblasts was slightly (~10%) but not significantly different from that in controls (table S6). In line with the abnormal TL distribution, there was a higher variability in other features examined in HGP cell lines. Two HGP cell lines (HGADFN 127 and HGADFN 164) showed only moderate chromosomal reorganization, whereas the third cell line (HGADFN 178) displayed the most severe reorganization among all cells (fig. S9). Moreover, we found a lower relative increase in *PPP2R2C* mRNA in HGP cells compared to healthy controls (2.03 ± 0.27 versus 6.85 ± 1.79 -fold, $P = 0.02$; Fig. 3B), and the suppression of Akt phosphorylation was reduced in HGP cells compared to the controls ($41 \pm 11\%$ versus $2 \pm 1\%$ of phosphorylation levels in young cells, $P = 0.029$; Fig. 5C). We also observed higher overall proliferation rates (figs. S5 and S16) and an approximately 2-fold higher activity level of the mTOR target ARSA ($P = 0.04$) and an approximately 1.5-fold higher ARSA protein level compared to control cells (difference not significant) (fig. S14), associated with a higher degree of senescence. Primary HGP cells grew faster and senesced after fewer rounds of replication than healthy control cells (fig. S5). We observed a higher fraction of cells in the G₂-M phase of the cell cycle (fig. S14) typical for senescent cells (42), higher levels of the senescence markers MUG and SA-β-Gal (fig. S7), elevated levels of mTOR in presenescence, and elevated levels of *TBC1D3* (Fig. 3 and fig. S6), an amplifier of EGF receptor response. Together, these findings indicate that HGP cells have higher proliferation stress than controls. Although a severe abnormality in TPE-OLD (for *PPP2R2C*) can be excluded, TL heterogeneity and/or dysfunction may lead to altered TPE-OLD dynamics that may contribute to a higher degree of proliferation stress.

TL-dependent silencing of *PPP2R2C* and established TPE-OLD candidates in other cell types and in fibroblasts from aged cell donors

To investigate TL-dependent expression of *PPP2R2C* in a different human cell type, we assessed the expression of *PPP2R2C* and TLs in 413 lymphoblastoid cell lines (LCLs) established from B lymphocytes from participants of the Berlin Aging Study II (BASE-II) (43, 44), using the reverse transcription PCR (RT-PCR) and monochrome multiplex quantitative PCR (MMqPCR) approaches used for fibroblasts above. LCLs are expected to represent cells with a very broad TL distribution. Using this cell population, we did not observe a correlation between *PPP2R2C* expression and TL (fig. S17). We did also not find an increased mRNA expression for the other TPE-OLD candidates in LCLs. In primary human umbilical vein endothelial cells (HUVECs), by contrast, we found mRNA up-regulations for *PPP2R2C*, *PPP2R2D*, *PPP2R5C*, *C1S*, and *SORBS2*; we found a reciprocal regulation (lower mRNA levels in aged cells) for *DSP* and no significant changes or inconclusive results for *TERT*, *ISG15*, and *PPP2R3B* (fig. S18). In human fibroblasts, we could confirm most of the previously established TPE-OLD genes as being differentially expressed (higher expression in aged cells with short telomeres), but we could not show differential regulation for *PPP2R5C*, *PPP2R2D*, and *PPP2R3B*. Together, these data suggest that cell specificity is to be noted for TPE-OLD and/or that other factors may influence the expression of these TPE-OLD genes, particularly in LCLs (fig. S18).

We lastly asked whether up-regulation of *PPP2R2C* also plays a role in vivo and thus compared fibroblasts derived from very young up to very old individuals. We found that up-regulation of *PPP2R2C*

is evidently more pronounced in the cells from very old donors, compared to young and middle-aged cell donors, further suggesting a physiological function in the aging organism and that in vitro replicative senescence resembles in vitro senescence (fig. S19).

DISCUSSION

A simple tool predicts known and candidate TPE-OLD genes

We presented a heuristic strategy that can be applied to identify potentially protective TPE-OLD candidate genes. Most of these candidate genes are not known to be involved in senescence or apoptosis entry but code for proteins involved in proliferation, metabolism, tumor suppression, and stress response. Moreover, many TPE-OLD candidates are regulated by transcription factors involved in proliferation, development, and stress response. For example, the functions of the AP2 family of transcription factors are the cell type-specific stimulation of proliferation and the suppression of terminal differentiation (45). Sp1 both activates and suppresses the expression of a number of essential oncogenes and tumor suppressors, as well as genes involved in proliferation, differentiation, DNA damage response, and senescence (46).

Only 1 of the 11 human genes associated with the Gene Ontology (GO) term “chromatin silencing at telomere” (GO:0006348) was found within the group of TPE-OLD candidate genes, *DOT1L*, which encodes a histone H3K79 methyltransferase and is essential for mammalian heterochromatin structure. Hence, the group of 2322 genes described here likely belongs to a previously unknown category with regulation being dependent on TL. Our tool allows other researchers to identify and investigate possible TPE-OLD genes for unidentified antitumor and antiaging strategies.

The gene encoding for the protein phosphatase 2A subunit PR55γ (*PPP2R2C*) is a TPE-OLD gene and subject to long-range telomere regulation in human fibroblasts

PPP2R2C up-regulation was dependent on telomere attrition but not on exogenous stress triggers such as H₂O₂. Complete gene silencing was achieved by telomere elongation. Using 3D-FISH analysis, we showed that TEL-*PPP2R2C* probes were significantly closer together in cells with long telomeres than in cells with short telomeres, demonstrating telomere-dependent chromatin reorganization. In accordance with other investigations, changes in TPE-OLD gene expression were discontinuous (e.g., not involving genes positioned closer to the telomere), and the reestablishment of gene suppression after hTERT introduction occurred with some delay (as some time is required for elongation) (47).

Notably, BCI-150, a recently developed SIRT inhibitor with selectivity for SIRT6 versus SIRT1 and SIRT2 (38), enhanced the expression of *PPP2R2C* up to fivefold in hTERT-immortalized cells. As SIRT6 is required for repression of telomere-proximal reporter genes in human cells (37), this finding suggests that silencing of *PPP2R2C* is dependent on histone deacetylation mediated by SIRT6. The bimodality in 3D-FISH experiments suggested that both chromosomes are involved in telomere loopings, in accordance with the reported bimodal distribution of TLs in fibroblasts, with TL differences of up to 6.5 kb between homologous chromosomes, likely due to stochastic elements in telomere inheritance (31). Together, these findings demonstrated a mechanistic link between TPE-OLD and a tumor suppressor gene that acts long before telomere-driven DNA damage signaling occurs.

Telomere attrition leads to suppression of mTOR signaling via dephosphorylation of p70S6K

It has previously been shown that overexpression of *PPP2R2C* inhibited cancer cell proliferation both in vitro and in vivo through the suppression of the activity of S6K in the mTOR pathway (21). Vice versa, low *PPP2R2C* expression was associated with an increased likelihood of cancer recurrence and cancer-specific mortality in prostate cancer (48). In accordance with these data, we showed that *PPP2R2C* up-regulation led to almost complete dephosphorylation of p70S6K in presenescent but still replicating fibroblasts, and we found inverse relationships between TL and *PPP2R2C* expression and between TL and the dephosphorylation grade of p70S6K and Akt, respectively. Dephosphorylation of p70S6K likely delays senescence entry via metabolic suppression. The protein synthesis of rapamycin-sensitive proteins was suppressed in presenescent fibroblasts. By contrast, inhibition of *PPP2R2C* by siRNA may reinduce mTOR/p70S6K-dependent genes in aged cells. In parallel, we observed a decline in total p70S6K protein, which may occur because of phosphorylation-dependent degradation events, as previously described (49). However, we cannot entirely exclude unspecific transfection events (50). More specific and complete knockout and over-expression strategies using CRISPR-Cas9 technologies may further elucidate possible beneficial effects of *PPP2R2C*.

The combination of expansion-stimulation signals and inhibition of cell division (51) is a well-known factor in the transition to an unstable hypermetabolic state, which may occur without effective down-regulation of cell metabolism (52). Our data corroborate other findings and suggest an overall protective effect of p70S6K dephosphorylation in presenescent cells. This molecular pathway and the life-prolonging effects of mTOR suppression have been discussed in great detail. However, most findings so far were obtained by use of genetic manipulation in mice (53, 54) and flies (55) or mTOR inhibition in human and rodent cell lines or in *Caenorhabditis elegans*. We show a possible physiological function and mechanism for mTOR suppression in vivo and identify short telomeres as an upstream trigger for mTOR suppression.

The effects of *PPP2R2C* regulation by TL supports the hypothesis that replicative aging fulfills a tumor suppressor function in vivo

The here-described findings strongly argue for a tumor suppressor function of replicative aging. We identified a direct tumor suppressor gene under influence of TPE-OLD. A protective effect that mitigates the pitfalls of telomere attrition, namely, ongoing mitogenic stress, is plausible and supports the hypothesis that a main function of replicative aging is tumor suppression. As a prerequisite for an overall positive net effect (tumor suppression for a sufficiently long period of time), possible negative aspects of replicative aging must be minimized. Telomere attrition is, genetic instability syndromes (56) notwithstanding, generally not life-threatening in humans and also not in mice nor in *C. elegans* (57–59).

The expression of the *hTERT* gene itself is possibly regulated by TPE-OLD (12), further pointing to a regulatory role of telomeric gene expression. Gene silencing may have evolved as a mechanism to suppress undesired gene expression after embryonal development. It is tempting to speculate, but awaits further experimental proof, that limited up-regulation of *hTERT* in a cell with critically short telomeres may stabilize the cell without undermining the tumor suppressor effect of telomere attrition in general; “mild” *hTERT*

up-regulation and mTOR suppression may synergize to limit the tumorigenic risk in cells with critically short telomeres. These data do not exclude the possibility that the induction of *hTERT* or other TPE-OLD genes may paradoxically impinge on the predisposition to cancer through uncontrolled transcriptional derepression.

HGP fibroblasts display functional *PPP2R2C* TPE-OLD effects but abnormalities in telomere attrition kinetics

Our experimental data did not indicate severe deficiency of TL-dependent chromosomal reorganization in HGP. Thus, functional chromosomal reorganization may prevent an even worse phenotype, which is in line with the low cancer rates among patients with HGP (15).

Despite functional TPE-OLD in HGP fibroblasts, HGP cell lines display some abnormalities such as reduced mean *PPP2R2C* mRNA levels, higher proliferation rates, a reduced degree of Akt suppression, elevated variability of TL in 3D-FISH experiments, less marked changes in telomere *PPP2R2C* probe distances between low- and high-PD cells, and a slightly lower suppression of the metabolic marker ARSA. These observations are plausible in view of the greater heterogeneity in TL and abnormal TL distribution in HGP found in this and other studies; normal or even longer telomeres have been described in approximately one-third of all cells in other studies despite shorter average TLs (13, 14). Accordingly, we detected shorter telomeres in young HGP cells and even longer telomeres in presenescent cells, which corresponds to an overall “narrower” and shifted TL and *PPP2R2C* expression range. Primary (but not *hTERT*-transfected) HGP cells grew faster and senesced earlier after fewer rounds of replication (figs. S5 and S16). Altered dynamics in gene activation/silencing may contribute to attenuated metabolic suppression, which is known to accelerate senescence entry (52).

HGP fibroblasts age much faster in vitro and show constitutive activation of mTOR signaling, whereas the dephosphorylation of p70S6K is apparently intact. Preliminary data suggest more pronounced alterations in other TPE-OLD genes. Together, these data point to telomeric abnormalities in HGP and may help to explain why patients with HGP do not develop tumors but many signs of premature aging. Because of the early death of patients with HGP, it cannot entirely be ruled out that an increased risk of cancer could arise with older age in these patients. To investigate telomere clinical phenotype interrelationships more closely, cells from patients with Nijmegen breakage syndrome (56), which is characterized by chromosome instability, could be helpful. In fibroblasts from these patients, there were also indications of telomeric imbalances in TPE-OLD associated with accelerated telomere attrition (56). The patients tend to have progeroid symptoms, but, in contrast to patients with HGP, they have shorter telomeres, a higher degree of genetic instability, and a high cancer rate.

The TPE-OLD mechanism is evolutionary conserved, likely as a response to negative effects of replicative aging

Several lines of evidence support our hypothesis that TPE-OLD is an evolutionarily conserved response to replicative aging. First, we did not find an equal distribution of TPE-OLD genes along the ends of the chromosomes, indicating a highly conserved telomeric localization. Second, TPE-OLD candidates have functional similarities and are often involved in the control of proliferation and metabolism or stress responses. We anticipate that many other genes beyond the known ones such as *PPP2R2C* are protectively activated by

SCIENCE ADVANCES | RESEARCH ARTICLE

TPE-OLD as the cells of humans and other large, long-lived species age. We observed telomeric clustering of many other genes related to stress and aging, including interleukins (fig. S20), tumor suppressor genes, and genes coding for *FOX* (forkhead box) transcription factors involved in insulin signaling and longevity and heat shock factor 1 (*HSF1*), the master regulator of proteotoxic stress, but we did not find such clusters for genes involved in development, such as *HOX* genes or for the cell death gene and canonical driver of inflammation nuclear factor $\text{NF-}\kappa\text{B}$, which is in agreement with our concept that TPE-OLD is effective in presenescent cells and triggers protective processes but does not trigger apoptosis. Third, there are obvious similarities to classical TPE. The main function of classical TPE is protection against acute cellular stress. Notably, *CDC55*, the ortholog of *PPP2R2C* in yeast, is located in relative proximity to the yeast telomere (<150,000 base pairs), a site at which classical TPE with heterochromatin spreading and silencing of adjacent genes can be effective. *CDC55* encodes YGL190C, which dephosphorylates and antagonizes the protein Tap42, mediating the effects of rapamycin on the yeast Tor protein kinase (60). *CDC55* stabilizes yeast cells during starvation-induced stress and down-regulates metabolic functions (61). This mechanism is strongly reminiscent of the metabolic effect of p70S6K inhibition in humans. We thus suggest that TPE in yeast and TPE-OLD in large, long-lived species have a common functional and mechanistic origin (Fig. 6).

TPE-OLD effects are cell type specific and/or may display further levels of regulation

A differential regulation of *PPP2R2C* mRNA could be demonstrated for HUVECs and fibroblasts but not for LCLs. Moreover, a differential regulation of most known TPE-OLD genes could be shown for HUVECs and fibroblasts but not for LCLs suggesting cell specificity and/or peculiarities in LCLs.

Considering cell type specificity, the three other PP2A subunit TPE-OLD candidates affect similar pathways, and all potentially attenuate cell proliferation via mTOR inhibition (Fig. 1B), raising the possibility that these subunits may be induced in other metabolic states or in other cell types. Findings from facioscapulohumeral muscular dystrophy, in which a genetic defect results in repositioning of an active gene near telomeres or subtelomeric sequences and the phenotype is altered in an age-dependent manner (9), suggest cell and tissue specificity for TPE-OLD. TL varies greatly across tissue types (62); hence, similar functions may be performed by different subunits with genomic positions appropriate for the basal TL of their respective cell types.

There are various other possible explanations for discrepant findings in different cell types. It is possible that splice variants are induced, some of which undetectable with the used universal primer pairs. In addition, epigenetic mechanisms may influence TPE-OLD effects including DNA methylation and histone modifications in promoter regions (12), which are difficult to control experimentally. For example, in Epstein-Barr virus-transformed lymphoblastoid cells, the immortalization procedure may have contributed to the inability to reproduce established TPE-OLD effects. In these cells, telomeres are elongated both by telomerase and by alternative lengthening of telomeres, which may result in dysfunctional telomeres with a reduction in telomere binding proteins (63). We were interested that the *in vitro* effects of *PPP2R2C* were most pronounced in cells from three very old donors, further suggesting a physiological function of TPE-OLD (*PPP2R2C*) in the aging organism.

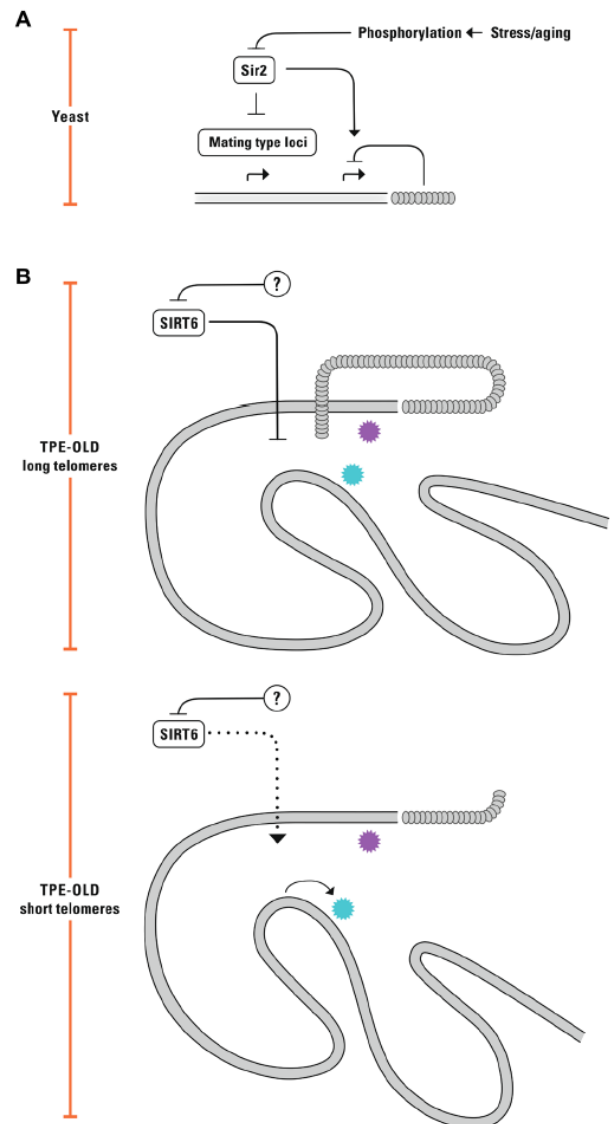


Fig. 6. Similarities between TPE and TPE-OLD and possible phylogenetic relationships. (A) TPE-OLD and TPE in yeast may share mechanistic and functional aspects. In *S. cerevisiae*, under optimal growth conditions, most subtelomeric genes are silenced by the histone-binding silent information regulator (SIR) complex (in this species, largely independent of TL). Nutrition starvation, heat shock, or chemical treatment can induce hyperphosphorylation of Sir proteins and a subsequent decrease in silencing (28). (B) Mechanistic and functional similarities of TPE in yeast and TPE-OLD in mammals and other vertebrates may be due to common evolutionary heritage, with SIRT6 (the mammalian homolog of Sir2) retaining its ancestral role as a cofactor for gene silencing in young and growing cells in the same way as Sir2 acts as a silencing factor in yeast, with stress serving as its inhibitor via phosphorylation events.

Cell specificity together with redundancy and methodological challenges (e.g., the difficulty in detecting these subtle effects without artificial cell manipulation) may explain why TPEs have thus far not been reported for human cells on a larger scale. Other tissues and other PP2A regulatory subunits and other TPE-OLD candidates

must be examined to unravel cell specific effects. More structural experiments are required for a better understanding of how chromatin architecture may influence TPE-OLD. These experiments include combining chromatin interaction maps with epigenome and transcriptome datasets for studying long-range control of gene expression. Another limitation of the here-described approach are possible misassignments to the classes of replicatively and nonreplicatively aging species, respectively. For example, there is little data on the cetaceans, and it seems possible that the blue whale, the narwhal, and the vaquita also age replicatively. For each new TPE-OLD candidate, confirmatory studies should be performed to confirm TPE-OLD effects experimentally and to rule out piggybacking by gene synteny as a cause for the telomeric location, e.g., the physical colocalization of genetic loci that are not disrupted during evolution.

In conclusion, we have identified a physiological trigger (telomere attrition) for a well-known aging-protection mechanism (mTOR suppression). This mechanistic link between short telomeres and tumor suppression points to a tumor suppressor function of replicative aging. We identified a large number of new TPE-OLD candidate genes, and we present a heuristic strategy that can be applied to easily identify candidate TPE-OLD genes. TPE-OLD genes are potential targets for intervention in cancer- and aging-related processes. Their activation may have a protective effect when telomeres shorten, but they do not necessarily have beneficial effects under all circumstances, such as in disease-associated cellular states.

MATERIALS AND METHODS

Experimental design

Genes with potential for TPE-OLD were screened in silico with cross-species data from the Ensembl genome database. We focused on a group of genes that shows preserved telomeric distances and that is strongly related to cell growth and aging.

The aim of further investigations was to examine telomere-associated changes in gene expression and cell physiology in old but still replicating (presenescent) cells before the point of cell cycle arrest. The presenescence stage (high PDs of primary cells) was established by culturing cells until the final cell cycle arrest and thawing frozen samples from 10 to 15 PDs before the final arrest for experiments.

Retrieval of gene-telomere distances for human genes and their orthologs

We retrieved the gene-telomere distances from the public MySQL database of Ensembl Mart version 100 (released April 2020) (64). Orthologs were accepted as determined by Ensembl Compara (65) by the “one2one,” “one2many,” or “many2many,” definitions. A species was included into the analysis if it was one of the established model organisms (*S. cerevisiae* and *C. elegans*) or if its median gene-telomere distance was at least 7.5 Mb, i.e., the median distance for fruitfly, as a threshold for the quality of genome assemblies in Ensembl to avoid false positives at the ends of chromosomal fragments. To facilitate interpretation, species are indicated by their common name. Scatter plots were created with R (66) version 4.0.1 and the ggplot2 package; heatmaps were created with the gplots (67) package for custom selection of genes from gene families with known gene-position effects. Telomeres are not annotated in Ensembl. As the biological anchor to define the gene-telomere distance for our analysis, we chose the location of the gene on the same chromosome arm

that is closest to the telomere, i.e., the first (p arm) or last (q arm) coding sequence for each chromosome.

Determination of preserved telomeric distances and selection of TPE-OLD candidates

For each gene, we determined at which distance to the telomeres the largest number of orthologs are located, where the maximum allowed pairwise distance between chromosomal positions was set to 1 Mb. We allow for two such 1-Mb-wide regions for each gene. The sum of the number of orthologs covered in these two regions determines the rank of that gene as a TPE-OLD candidate. For Fig. 1B and figs. S1 to S3, we thus grouped the chromosomal positions of the orthologs using a parameter-free complete linkage tree, using the R function `hclust`, for which we provided a custom distance function and then used the routine “`cutree`.” We systematically iterated over all human genes in Ensembl 104 with at least 12 orthologs in all completely sequenced “replicatively aging” species.

In the scatter diagrams of Fig. 2, the species on the *x* axis are sorted primarily by replicatively aging versus “nonreplicatively aging” and secondarily by their median gene-telomere distance. Scatter plots represent genes by a unique symbol and show telomeric distance on the *y* axis. Positions above 20 Mb are clipped in the scatter plot.

All R and shell scripts contributing to this manuscript are available online (68) to facilitate updates with upcoming releases of Ensembl or custom gene selections. The criteria for categorizing a species as having assumed TL-dependent replicative aging (marked by green color) were set as TL < 20 kb, undetectable telomerase levels, and no stasis, as described previously (18).

Gene set enrichment analysis

Gene enrichment analysis was performed by g:profiler as described in (19). Briefly, an enrichment score (ES) is calculated that reflects the degree to which a set *S* is overrepresented at the extremes (top or bottom) of the entire ranked list *L*. The statistical significance (nominal *P* value) of the ES is estimated by using an empirical phenotype-based permutation test procedure that preserves the complex correlation structure of the gene expression data. The proportion of false positives is controlled by calculating the false discovery rate by comparing the tails of the observed and null distributions for the normalized ES.

Cells and cell culture lines

Human primary dermal fibroblast cell lines were obtained from The Progeria Research Foundation (PRF) Cell and Tissue Bank. The HGP cell lines were HGADFN003, HGADFN127, HGADFN164, and HGADFN178. All HGP cell lines displayed the classical HGP mutation [LMNA Exon 11, heterozygous c.1824C > T (p.Gly608Gly)] [more details in (69)]. We did not examine cell lines with nonclassical or multiple mutations (exclusion criterion). Histograms of mutational analysis sequenced by the PRF Cell and Tissue Bank are available on request. Healthy child control dermal fibroblast cell lines (707, 731, 778, and 811) were a gift from the Children’s Hospital of Münster (Professor Thorsten Marquardt). These fibroblasts were from children in whom a genetic disease has been excluded and a nongenetic cause for their symptoms had been found. Cultures from all cell lines have tested negative for mycoplasma contamination. Ethical approval for the establishment of the cell lines and informed consent were obtained from the children’s parents. One human primary

dermal fibroblast cell line from an adult donor (N14) was a gift from E. Orso, University of Regensburg. The characteristics of all fibroblast cell lines are summarized in table S5.

All human fibroblasts were maintained in Dulbecco's modified Eagle's medium (DMEM) high glucose (4.5 g/liter) with L-glutamine without pyruvate (Gibco, catalog no. 41965) supplemented with 10% fetal bovine serum (FBS; Biochrome), penicillin (100 U/ml), and streptomycin (100 µg/ml) (Biochrome, catalog no. A2212), hereafter referred to as "fibroblast medium." In addition, we analyzed mRNA from healthy human fibroblast donors at different ages.

The 1301 cell line (derived from T lymphoblastic leukemia) was a gift from S. Roura (ICREC Research Group, Institut d'Investigació en Ciències de la Salut Germans Trias i Pujol, Barcelona, Spain). All other LCLs were established from BASE-II participants. We analyzed a subgroup of 413 participants of the BASE-II selected on the basis of the availability of LCLs. BASE-II is a prospective multidisciplinary and multi-institutional study that investigates factors associated with aging trajectories in Berlin (43, 70). All participants gave written informed consent to the study protocol that was approved by the Ethics Committee of the Charité-Universitätsmedizin Berlin (number of the ethical approval: EA2/029/09). Both the 1301 cell line and LCLs from the BASE-II study were maintained in RPMI 1640 medium with L-glutamine (Gibco, catalog no. 11875-093) supplemented with 10% FBS (Biochrome), penicillin (100 U/ml), and streptomycin (100 µg/ml) (Biochrome, catalog no. A2212). All cells were grown at 37°C in a humidified incubator containing 5% CO₂.

HUVECs were obtained from PromoCell (catalog no. C-12200; LOT no.: 449Z004) and cultivated using the Endothelial Cell Growth Medium Kit (catalog no. C-22110) from the same company. Penicillin (100 U/ml) and streptomycin (100 µg/ml) from Thermo Fisher Scientific (catalog no. 15140122) were added to the medium. HUVECs at several passages were grown in a humidified incubator at 37°C and 5% CO₂. Expansion, cell cultivation, and experiments were performed in T75 cell culture flasks (Sarstedt, catalog no. 83.3911.302). High cell densities were selected for subsequent harvesting.

hTERT immortalization

Fibroblasts were infected with retroviral supernatants from a packaging cell line (PA317-TERT) that stably expresses human telomerase cloned into a pBabePuro vector according to methods previously described (47, 71). The vector and packaging cell line were a gift from W. Wright (UTSW Medical School, Dallas, TX, USA). After a 2-week selection with puromycin according to established protocols (47), infection and selection were checked by determination of hTERT expression using real-time PCR and measurement of TL as described (72).

Test points for measurements

Test points for the fibroblast cell lines were classified either as "primary cells at low population doubling (PD)" (PD 13 to 20) or as "primary cells at high PD" (PD 34 to 55). The presenescence stage (high PDs of primary cells) was established by culturing cells until the final cell cycle arrest and thawing frozen samples from 10 to 15 PDs before the final arrest for experiments. Cells that had recently been immortalized were classified as immortalized cells at low PD (PD 14 to 34 after hTERT immortalization), and cells with a substantial number of PDs after immortalization were classified as immortalized cells at high PD (PD 55 to 70 after hTERT immortalization). The fibroblasts were immortalized in medium PDs, at about the

same time interval before senescence (mean PD of immortalization in controls PD 37 and in HGP PD 20).

Hydrogen peroxide treatment

Cells from eight fibroblast cell lines (HGADFN003, HGADFN127, HGADFN164, HGADFN178, 707, 731, 778, and 881) were grown to 100% confluence in 10-cm dishes. For H₂O₂ treatment, two culture dishes of each cell line were treated for 2 hours with 200 µM H₂O₂ in 10 ml of fibroblast medium; an additional three dishes were processed identically but without H₂O₂. After 2 hours of incubation, the cells were washed with 5 ml of PBS (Gibco, catalog no. 14190250) and incubated in fresh fibroblast medium for another 22 hours. Subsequently, cells from one H₂O₂ dish and from one untreated dish (as a control) for each of the eight cell lines were harvested for Western blot analyses. In addition, cells from the H₂O₂-stressed dish and one other untreated dish for each of the eight cell lines were harvested for gene expression analyses. Cells from the third untreated dish for each cell line were harvested for TL measurement.

Quantitative real-time PCR

For mRNA quantification, total RNA was isolated using a standard extraction kit (Macherey-Nagel NucleoSpin RNA, catalog no. 740955) and quantified with a NanoDrop ND 1000 spectrophotometer. Complementary DNA (cDNA) synthesis was carried out following the manufacturer's instructions [M-MLV Reverse Transcriptase, RNase (H-), Promega, catalog no. M5301]. One microgram of mRNA was used for the reverse transcriptase reaction.

qPCR was carried out using TaqMan Universal Master Mix II, no. UNG (catalog no. 4440040) from Applied Biosystems and following the manufacturer's manual. The cDNA samples (5 ng/µl) were assayed in triplicate; the nontemplate control (water) was analyzed in duplicate in a 384-well plate. The assay was carried out using a Bio-Rad CFX384 real-time C1000 thermal cycler with the following thermal cycling profile: 10 min at 95°C, followed by 50 cycles at 95°C for 15 s and 1 min at 60°C with signal acquisition. For gene expression quantification of the potential TPE and control genes, the gene expression TaqMan assays from Applied Biosystems were used. Primer characteristics are summarized in table S7. The $\Delta\Delta C_t$ method was used for relative quantification. The relative expression level of each gene was normalized to its level in untreated low-PD cells. The mean and SEM were calculated from technical duplicates or triplicates of biological replicates.

TL measurement

A standard extraction kit (DNeasy Blood & Tissue Kit, Qiagen, catalog no. 69504) was used for DNA extraction. Mean TL was determined using the modified MMqPCR method as described previously (73). This technique enables telomere-specific and single-copy gene (reference) amplification in a single reaction well with quantification measurements at different temperatures. The ratio of telomere to single-copy gene content (TLR) is taken as a relative measure of TL and is expressed in arbitrary units. The DNA samples (20 ng/µl, as a single copy) and a reference DNA standard (186.6 to 0.09 ng) were assayed in triplicate on different plates. A nontemplate control (water) and positive control (human leukemia cell line 1301 DNA) were prepared in duplicate and run on every plate. The assay was performed using a Bio-Rad CFX384 real-time C1000 thermal cycler with the following thermal cycling profile: 1 cycle of 15 min at 95°C; 2 cycles of 15 s at 94°C; 1 cycle of 15 s at 49°C; 40 cycles of 15 s at

SCIENCE ADVANCES | RESEARCH ARTICLE

94°C; 1 cycle 10 s at 62°C; and 1 cycle 15 s at 72°C with T signal acquisition, 10 s at 85°C, and 15 s at 89°C with signal acquisition. The reagents for PCR were used at the following final concentrations: 1 U of titanium Taq DNA polymerase per reaction with the provided titanium Taq PCR buffer (catalog no. 639208), 0.75× SYBR Green I (Sigma-Aldrich), 0.2 mM of each deoxynucleotide triphosphate, 1 mM dithiothreitol, 1 M betaine, 900 nM of each telomere primer (telg and telc), and 300 nM of each single-copy gene primer (albu and albd). Primer sequences are shown in table S7.

All samples were measured in triplicate, and the average of the three measurements was used to report the mean TL for each sample. The intra-assay coefficients of variation were <0.3 for all samples.

SA-β-Gal staining

The four HGP patient fibroblast cell lines and two control cell lines (731 and/or 811) were used for SA-β-Gal staining. Determination of β-galactosidase activity was performed using a histochemical staining kit from Sigma-Aldrich (catalog no. CS0030). The procedure was performed according to the manufacturer's recommendations. Briefly, cells were transferred into two wells of a 12-well plate and cultivated in fibroblast medium for approximately 1 day (to approximately 50 to 70% confluence). Cells in one well were treated with 200 μM H₂O₂ in 2 ml of fibroblast medium for 1.5 hours, washed with 1 ml of PBS, and incubated for another 4 hours in fibroblast medium followed by staining. Untreated cells were stained in the absence of H₂O₂. For the staining procedure, the cells were first washed twice with 1 ml of PBS per well and then fixed for 6 to 7 min at room temperature (RT) with 500 μl of 1× fixation buffer [10× fixation buffer (catalog no. F1797) diluted with H₂O]. The final concentrations in the cell dishes were 2% formaldehyde, 0.2% glutaraldehyde, 7.04 mM Na₂HPO₄, 1.47 mM KH₂PO₄, 0.13 M NaCl, and 2.68 mM KCl. Continuing the staining procedure, the cells were then washed again three times with 1 ml per well of PBS and incubated overnight at 37°C without CO₂ in 500 μl of staining mixture [10× staining solution (catalog no. S5818), reagent B (catalog no. R5272), reagent C (catalog no. R5147), X-gal solution (catalog no. X3753)]. The staining mixture was filtered through a 0.2-μm filter before use to remove aggregates. The percentage of SA-β-Gal-positive cells was ascertained by counting all visible cells in four fields of view of a light microscope at ×50 magnification. The counting was performed independently by two different individuals who were blinded to the treatment. Four dishes were excluded from analysis because of complete cell death after H₂O₂ treatment. The mean and SD were formed by using technical duplicates and biological replicates.

MUG assay

The four HGP patient fibroblast cell lines and two control cell lines (731 and/or 811) were used for the MUG assay. This highly sensitive spectrophotometric method is an alternative for SA-β-Gal staining and subjective visual quantification that measures enzyme activity in cell lysates (69). In this assay, β-galactosidase acts on the substrate MUG to produce 4-methylumbelliferone galactosidase, which can be detected fluorometrically (74). For each cell line, approximately 3.2 × 10⁶ cells were transferred into two 5-cm culture dishes (i.e., ca. 1.6 × 10⁶ cells per dish) and were cultivated to 50 to 70% confluence. One dish of each cell line was treated with 200 μM H₂O₂ in 3 ml of fibroblast medium for 1.5 hours and then incubated in normal fibroblast medium for another 4 hours. The following steps were executed according to the protocol by Gary and Kindell (75). The

cells were washed six times with 1 ml of PBS, lysed with 200 μl of lysis buffer [5 mM CHAPS, 40 mM citric acid, and 40 mM sodium phosphate (pH 6)], and transferred into 1.5-ml Eppendorf tubes using a cell scraper. The cells were vortexed for 20 s and centrifuged at 12,000g for 5 min at RT. The supernatant was frozen at 20°C until analysis. For measurements, 100 μl of the lysate was transferred into a reaction tube and mixed with 50 μl of lysis buffer and 150 μl of 2× reaction buffer [40 mM citric acid, 40 mM sodium phosphate, 300 mM NaCl, 10 mM mercaptoethanol, and 4 mM MgCl₂ (pH 6), stored at 4°C]; 1.7 mM MUG (Sigma-Aldrich, catalog no. M1633, stored at -20°C) was added immediately before use. The reaction solution was incubated for 3 hours at 37°C. After 3 hours, 50 μl of the reaction solution was withdrawn and transferred to a new Eppendorf tube containing 500 μl of stopping solution (400 mM Na₂CO₃) to inhibit the enzymatic reaction. Then, 150 μl of the solution was transferred into a well of a 96-well plate. Fluorescence was measured in duplicate with Fluoroskan Ascent FL (Thermo Fisher Scientific) at 360-nm excitation and 465-nm emission. The protein concentration of the lysate was determined using bicinchoninic acid (BCA) assay (with human albumin as the standard), and the fluorescence signal was normalized to the total protein concentration. Typical concentrations were in the range of 0.3 to 1.0 μg/ml. The results are displayed as relative fluorescence units per milligram (RFU/mg). The mean and SD were calculated from technical duplicates of biological replicates.

Western blotting

Fibroblast cell lines grown to confluence in a 7-cm dish (~5 × 10⁶ cells) were washed with 5 ml of 0.1% EDTA/PBS and then detached with 400 μl of trypsin/EDTA (Gibco, catalog no. 25200-056). The cells were removed in 7 ml of fibroblast medium and centrifuged at 1200g for 5 min at RT. The supernatant was discarded, and the pellet was resuspended in 1 ml of PBS, transferred to a 1.5-ml Eppendorf tube, and centrifuged again at 1200g for 5 min. The supernatant was discarded, and the cells were resuspended in 200 μl of sucrose-Hepes buffer [SHC buffer; 0.2 M sucrose, 0.02 M Hepes (pH 7.3), and cComplete ULTRA Tablets EDTA-free (Roche, catalog no. 05 892 791 001)] and lysed by pipetting the cell suspension up and down 10 times in a syringe through a 26G insulin injection needle. After 10-s centrifugation at 6000g to remove unlysed cell debris, the supernatant was aliquoted into Eppendorf tubes and stored at -80°C until analysis.

Protein concentrations were measured using the Pierce BCA Protein Assay Kit (Thermo Fisher Scientific, catalog no. 23225) with albumin as the standard. Then, 15 μg of the cell homogenate was mixed with 2× sample buffer [0.1 M Tris (pH 6.8), 8% (w/v) SDS, 40% (w/v) glycerol, bromophenol blue (0.2 mg/ml), and 20% β-mercaptoethanol]. SDS-polyacrylamide gel electrophoresis was performed with 7.5 and 10% polyacrylamide gels. The gels were transferred to polyvinylidene fluoride membranes (Millipore, catalog no. IPVH00010).

The membranes were incubated with primary antibodies against phospho-p70 S6 kinase (Thr³⁸⁹) (108D2) rabbit monoclonal antibody (mAb) (Cell Signaling Technology, catalog no. 9234) (1:2000), phospho-mTOR (Ser²⁴⁴⁸) (D9C2) XP rabbit mAb (Cell Signaling Technology, catalog no. 5536) (1:1000), and phospho-Akt (Ser⁴⁷³) rabbit mAb (Cell Signaling Technology, catalog no. 9271) (1:1000), all diluted in BSA-blocking solution [5% BSA, 0.1% Tween 20, 20 mM Tris, and 0.15 M NaCl (pH 7.5)], overnight at 4°C. The membranes were then incubated with goat anti-rabbit IgG (H + L)-horseradish peroxidase (HRP)-conjugated (Bio-Rad, catalog no. 1706515) (1:5000)

secondary antibody for 1 hour at RT. Blots were exposed to CL-XPosure Films (Thermo Fisher Scientific, catalog no. 34089) with a homemade enhanced chemiluminescence (ECL) solution using 2 ml of solution A [50 mg of luminol (Fluka, catalog no. 09253) in 200 ml 0.1 M tris solution (pH 8.6)] and 0.2 ml solution B [11 mg of para-coumaric acid (Sigma-Aldrich, catalog no. 501-98-4) in 10 ml of dimethyl sulfoxide (DMSO)] supplemented with 1 μ l of 30% H₂O₂ before use for each membrane. All blots were stripped with glycine stripping buffer (100 mM glycine and 320 mM HCl) for 30 min at 60°C.

Membranes were incubated overnight at 4°C with primary antibodies against p70 S6 kinase clone 20-10C-6, rabbit mAb (Millipore, catalog no. 05-781R) (1:6000); mTOR (7C10) rabbit mAb (Cell Signaling Technology, catalog no. 2983) (1:1000); Akt (C-20) (Santa Cruz Biotechnology, catalog no. sc-1618) (1:500); and mouse monoclonal anti- β -actin (clone AC-15, Sigma-Aldrich, catalog no. A5441) (1:80,000), all of which were diluted in milk-blocking solution [5% skimmed milk powder, 0.1% Tween 20, 20 mM tris, and 0.15 M NaCl (pH 7.5)]. As secondary antibodies, we used goat anti-mouse IgG (H + L)-HRP conjugate (Bio-Rad, catalog no. 1706516), goat anti-rabbit IgG (H + L)-HRP conjugate (Bio-Rad, catalog no. 1706515), rabbit anti-goat immunoglobulins, and polyclonal HRP (DakoCytomation, catalog no. P0449) at a dilution of 1:40,000 for β -actin and 1:5000 for all others. Incubation time was 1 hour at RT. Blots were developed as described above.

For ARSA experiments, the membranes were incubated overnight at 4°C with human anti-ARSA/ARSA antibody (R&D Systems, catalog no. MAB2485) (1:1000) diluted in milk-blocking solution, as described above. The secondary antibody goat anti-mouse IgG (H + L)-HRP conjugate (Bio-Rad, catalog no. 1706516) (1:5000) was incubated for 1 hour. Blots were exposed to CL-XPosure Films (Thermo Fisher Scientific, catalog no. 34089) on SuperSignal West Femto Maximum Sensitivity Substrate (Thermo Fisher Scientific, catalog no. 34096). Blots were stripped and incubated with monoclonal anti- β -actin antibody as described above.

Densitometric analysis was performed using Image Studio Lite Quantification Software (LI-COR). The mean and SEM values were calculated from biological quadruplicates and technical replicates, all normalized to β -actin.

Three-dimensional fluorescence in situ hybridization

Three fibroblast cell lines of patients with HGP (HGADFN127, HGADFN164, and HGADFN178) and three control cell lines (707, 731, and 778) were used for 3D-FISH experiments. Cell pairs with short and long telomeres were used for 3D-FISH analyses. Fibroblasts were cultivated in a T25 flask until they reached 100% confluence. The cells were then trypsinized and centrifuged, and the cell pellets were solubilized in PBS.

For slide preparation, cells were treated following established protocols for direct cell nucleus preparation. Briefly, the cell suspension was mixed carefully with 0.9% NaCl in a 1:1 ratio. After 10-min centrifugation at 210g at RT, the supernatant was discarded, and the cell pellet was incubated with 5 ml of 0.4% KCl solution (preheated to 37°C) for 10 min at RT. Then, 2 ml of ice-cold fixing solution (methanol/acetic acid 3 + 1) was added, and the whole mixture was centrifuged again.

The pelleted cells were fixed in 5 ml of ice-cold fixing solution. First, 1 ml of fixation solution was added dropwise and carefully mixed. The rest of the fixation solution was then slowly added and carefully mixed again. The fixing solution was changed five times

immediately. Last, the supernatant was aspirated and the cell pellet was resuspended. After fixation, 10 μ l of cell suspension was carefully dropped onto a slide, incubated for 15 min at 80°C on a heating plate, and washed briefly with PBS. For pepsin digestion, slides were incubated with pepsin solution [50 μ l of pepsin (Sigma-Aldrich, catalog no. 1.07192.001) and 100 ml of 0.01 N HCl] for 10 min at 37°C. The slides were washed with PBS and then incubated for 3 min with PBS/MgCl₂. The slides were then incubated for 10 min with 1% formaldehyde, followed by 3 min with PBS at RT and then 2 min at RT in ascending ethanol (70–85–100%); last, the slides were dried at RT.

For hybridization, 2 μ l of probe was added to the hybridization field. The Vysis TelVysion 4p spectrum probe (Abbott, Vysis, catalog no. 30-252004) was used for detection of the 4p subtelomeric region. For detection of the *PPP2R2C* region on the chromosome, RP11-462B2 BAC (Illumina) labeled with Spectrum Orange was used. Slides were then covered carefully with a cover glass and sealed with Fix-O-Gum (Marabu, catalog no. 29010017000). The codenaturation step was carried out for 5 min at 80°C on a heating plate. The slide was then incubated for 24 hours in a 37°C water bath protected from light. For the final washing step, the cover glass was removed carefully, and the slides were incubated for 2 min in 0.4 \times SSC/0.3% IGEPAL[®] CA-630 (Sigma-Aldrich, catalog no. 13021) solution at 73°C, briefly washed with 2 \times SSC/0.1% IGEPAL solution, and then washed with PBS at RT. The ethanol series described above was repeated, and the slides were air-dried. One drop of Vectashield/4',6-diamidino-2-phenylindole (DAPI) mixture (Vectashield, Vector, #H-1000; DAPI, Sigma-Aldrich, catalog no. 10236276001) was pipetted onto the slides and covered with a cover glass.

Images were acquired with a confocal scanning laser microscope (LSM 880 AxioExaminer Z1 from Zeiss) using 405-nm excitation/415- to 480-nm emission for DAPI, 488-nm excitation/500- to 545-nm emission for Spectrum Green, and 561-nm excitation/565- to 640-nm emission for Spectrum Orange. A 63 \times numerical aperture 1.4 Plan-Apochromat oil immersion objective was used to capture optical sections at intervals of 0.3 μ m. The pinhole was set to about 1 airy unit to achieve optical slices at all wavelengths with identical thickness. Images were then processed using Imaris 9.3 software (Andor Bitplane). A total of 70 cell nuclei (140 distances) were analyzed for each experiment. Cells with fewer or more than four signals (two red and two green signals each), irregular DAPI staining (e.g., mitotic cells), and abnormal cell shape were excluded from further analysis (excluded data points are available on request). The distance between their gravity centers (distance between the closest probes in each target) was determined by 3D reconstruction and surface rendering of the spots and used for further statistical analysis.

Binary and ordinal data are shown as absolute numbers and percentages. Continuous variables are displayed as the mean (SD) when normally distributed and the median (range) when not normally distributed. As the distance between the gravity centers after 3D reconstruction in the nuclei was not normally distributed, log transformation of both distances (AB and CD) was applied. Hierarchical linear models were used to estimate the impact of immortalization on the distance between gravity centers. We allowed random variation between cells, and cells were nested within cell lines. The results are displayed together with their *P* values and 95% confidence intervals (table S6). Distances were divided into deciles (0.7258, 1.090, 1.3442, 1.606, 1.93, 2.28, 2.773, 3.49, and 4.451 μ m) for graphical presentation (figs. S8, C, and D, and S9). To evaluate the optimal cut

point for the distinction between cells with or without immortalization (Fig. 4 and fig. S8, A and B), the R package “OptimalCutpoints” (76) was used. The optimal cut point was 2.26 μm . The area under the curve with this cut point was 0.63 with a sensitivity of 52% and a specificity of 69%.

PPP2R2C knockdown via 27-mer siRNA duplex

The knockdown of *PPP2R2C* was conducted using the Trilencer-27 Human siRNA Kit (OriGene; SR303688). The provided siRNAs were mixed to maximize knock-down efficiency. Cells were grown in DMEM containing 10% FBS (Biochrome), penicillin (100 U/ml), and streptomycin (100 $\mu\text{g}/\text{ml}$) (Biochrome, catalog no. A2212) in T25 flasks.

Primary cells of the cell line HGADFN127 were used at high PD for this experiment.

When cells reached a confluence of approximately 80%, siRNAs was added to a final concentration of 25 or 50 nM in the medium, following the instructions provided by the manufacturer. siRNA-containing medium was replaced by normal medium as soon as the cells started to show signs of cellular stress (7 hours). Cells were harvested 72 hours after removal of siRNA-containing medium and lysed for protein and mRNA isolation as described above.

Serum deprivation

For serum deprivation experiments, the 811 primary and *hTERT* immortalized cell lines were used. Cells were grown in two T75 flasks and treated at ~95% confluence for 18 hours in DMEM without pyruvate supplemented with 10% FBS and penicillin (100 U/ml) and streptomycin (100 $\mu\text{g}/\text{ml}$), and for 17 hours in DMEM supplemented with 10% FBS, and then 1 hour only in PBS. Cells were harvested for protein and RNA isolation as described. The cDNA samples (5 ng/ μl) were assayed in triplicate; the nontemplate control (water) was analyzed in duplicate in a 384-well plate. For gene expression quantification, the following TaqMan assays were used: *PPP2R2C* (Applied Biosystems, catalog no. Hs00902099_m1) and *mTOR* (Applied Biosystems, catalog no. Hs00234508_m1). Human *PPIA* (*cyclophilin A*) (Applied Biosystems, catalog no. 4333763F) was used as the endogenous control. The $\Delta\Delta\text{Ct}$ method was used for relative quantification.

Inhibitor tests

Three fibroblast cell lines from healthy individuals (707, 731, and 778) were used for TSA/5-AzaC and RSV experiments. TSA inhibits histone deacetylases (33). 5-AzaC results in nonspecific overall DNA demethylation (34) and RSV induces instability of telomeric DNA (35).

For TSA and 5-AzaC treatment, cells were grown in four 100 mm by 20 mm tissue culture dishes (Falcon, catalog no. 353003), denoted by letters A to D, from 25% initial confluence to 70% final confluence (A to D; A: DMSO control, B: TSA only; C: 5-AzaC only; D: TSA and 5-AzaC). 5-AzaC (1 $\mu\text{g}/\text{ml}$; Sigma-Aldrich, catalog no. A2385) dissolved in full medium was added to dishes C and D. The cells were then incubated in 5% CO_2 for 48 hours at 37°C. After 48 hours of incubation, TSA (0.2 $\mu\text{g}/\text{ml}$) (Sigma-Aldrich, catalog no. T8552) dissolved in DMSO was added to dishes B and D. To control for nonspecific DMSO side effects and to create comparable conditions, DMSO was added to dishes A and C at this time point. After 24 hours of incubation, the old medium was discarded, and fresh medium was added. After another 24 hours of equilibration incubation, the mRNA was isolated, and qPCR was performed as described.

For RSV treatment, cells were grown in four wells (A, B, C, and D) of a six-well tissue culture plate (Falcon, catalog no. 353046) and incubated in 5% CO_2 for 24 hours at 37°C. RSV (Merck, catalog no. 554325) in DMSO was added to fresh medium at different concentrations: A: 0 μM RSV (DMSO-only control); B: 0.25 μM RSV; C: 1.0 μM RSV; and D: 10 μM RSV. After a total 48-hour incubation, mRNA was isolated, and qPCR was performed.

The healthy cell line 778 was used for SIRT6 inhibitor treatment. Compound BCI-150 is a recently developed SIRT inhibitor with selectivity for SIRT6 versus SIRT1 and SIRT2 (38). Cells were grown in two wells (A and B) of a six-well tissue culture plate and incubated in 5% CO_2 for 24 hours at 37°C. Subsequently, the SIRT6 inhibitor BCI-150 (Asiner Ltd., catalog no. SYN 17739303), a gift from A. Del Rio (Institute of Organic Synthesis and Photoreactivity, National Council, Bologna, Italy), was added to well B at a concentration of 50 μM (in DMSO) in fresh medium. Only DMSO was added to well A (control). The cells were incubated for another 48 hours; mRNA was isolated as described above, and qPCR was performed.

qPCR was carried out using TaqMan Universal Master Mix II, no UNG (catalog no. 4440040) from Applied Biosystems following the manufacturer’s manual. The cDNA samples (5 ng/ μl) were assayed in triplicate; the nontemplate control (water) was analyzed in duplicate in a 384-well plate. The assay was carried out using a Bio-Rad CFX384 real-time C1000 thermal cycler with the following thermal cycling profile: 10 min at 95°C, followed by 50 cycles at 95°C for 15 s and 1 min at 60°C with signal acquisition. For gene expression quantification of the potential TPE gene *PPP2R2C*, a TaqMan assay (Applied Biosystems, catalog no. Hs00902099_m1) was used. Human *PPIA* (*cyclophilin A*) (Applied Biosystems, catalog no. 4333763F) was used as the endogenous control. The $\Delta\Delta\text{Ct}$ method was used for relative quantification. The relative expression level of each gene was normalized to that of the youngest cells (low PD) treated with DMSO.

Distribution of cells in the growth phase

Fibroblasts were cultivated on 100 mm by 20 mm tissue culture dishes (Falcon, catalog no. 353003) to ~70 to 80% confluence. For cell synchronization, cells were cultivated for 24 hours with DMEM/1% penicillin/streptomycin and 0.1% fetal calf serum. After 24 hours, the cells were harvested and prepared for cell cycle analyses. The cell pellets were resuspended in 500 μl of 70% ethanol and incubated at 4°C for 24 hours. The cells were centrifuged and resuspended in 200 μl of PBS with propidium iodide (50 $\mu\text{g}/\text{ml}$) (Sigma-Aldrich, catalog no. 25535-16-4) and ribonuclease A (25 $\mu\text{l}/\text{ml}$) (Macherey-Nagel, catalog no. 740505.50) and then incubated in the dark at RT for 30 min. The cell suspension was added to a fluorescence-activated cell sorting (FACS) Falcon and filled with 200 μl of PBS. Ten thousand cells were counted for routine FACS analyses (FACSCalibur).

Arylsulfatase activity

The arylsulfatase, an enzyme activity in protein homogenates, was determined following a modified protocol according to Böhringer *et al.* (77). For this purpose, 25 μg of total protein isolated as described in (78) was diluted in 50 μl of SHC buffer and 50 μl of reaction buffer [10 mM 4-nitrocatecholsulfate, 10% (w/v) NaCl, 0.3% (v/v) Triton X-100 (Sigma-Aldrich), and bovine serum albumin (1 mg/ml; Sigma-Aldrich)], in 0.5 M sodium acetate (pH 5.0) was added, followed by incubation at 37°C for 6 hours. The reaction was terminated by adding 800 μl of stop buffer (1 M NaOH), and the 4-nitrocatechol

SCIENCE ADVANCES | RESEARCH ARTICLE

released by ARSA was assessed at 515 nm using a spectrophotometer (Pharmacia Biotech) against water. As a blank, a similar assay was immediately stopped with 250 μ l of 0.5 N NaOH and absorption read again. The difference between absorptions read for reacted and blank assay was transformed to the activity unit pmol nitrocatecholsulfate degraded per minute.

Other statistical analysis

The package OptimalCutpoints in R 3.6.1 (79) was used for all scatter diagrams and for 3D-FISH cut point analysis. The code for data retrieval for scatter diagrams and heat maps is available at <https://bitbucket.org/ibima/tpe-old> and was programmed with R 3.6.1 (79). Statistical analyses were conducted using OriginPro 2018 and SPSS for Windows (IBM Corp. Released 2017. IBM SPSS Statistics for Windows, Version 25.0. Armonk, NY: IBM Corp). Normally distributed variables are shown as the means \pm SD or as the SEM as indicated. The two-sided exact Mann-Whitney *U* test was applied to evaluate differences between two independent groups in non-normally distributed variables. *P* < 0.05 was considered statistically significant.

SUPPLEMENTARY MATERIALS

Supplementary material for this article is available at <https://science.org/doi/10.1126/sciadv.abk2814>

[View/request a protocol for this paper from Bio-protocol.](#)

REFERENCES AND NOTES

- J. W. Shay, W. E. Wright, Telomeres and telomerase: Three decades of progress. *Nat. Rev. Genet.* **20**, 299–309 (2019).
- J. Campisi, Senescent cells, tumor suppression, and organismal aging: Good citizens, bad neighbors. *Cell* **120**, 513–522 (2005).
- J. W. Shay, Role of telomeres and telomerase in aging and cancer. *Cancer Discov.* **6**, 584–593 (2016).
- C. B. Harley, A. B. Futcher, C. W. Greider, Telomeres shorten during ageing of human fibroblasts. *Nature* **345**, 458–460 (1990).
- J. Maciejowski, T. de Lange, Telomeres in cancer: Tumour suppression and genome instability. *Nat. Rev. Mol. Cell Biol.* **18**, 175–186 (2017).
- J. A. Hackett, C. W. Greider, Balancing instability: Dual roles for telomerase and telomere dysfunction in tumorigenesis. *Oncogene* **21**, 619–626 (2002).
- M. A. Blasco, H. W. Lee, M. P. Hande, E. Samper, P. M. Lansdorp, R. A. DePinho, C. W. Greider, Telomere shortening and tumor formation by mouse cells lacking telomerase RNA. *Cell* **91**, 25–34 (1997).
- J. A. Baur, Y. Zou, J. W. Shay, W. E. Wright, Telomere position effect in human cells. *Science* **292**, 2075–2077 (2001).
- J. D. Robin, A. T. Ludlow, K. Batten, M. C. Gaillard, G. Stadler, F. Magdinier, W. E. Wright, J. W. Shay, SORBS2 transcription is activated by telomere position effect-over long distance upon telomere shortening in muscle cells from patients with facioscapulohumeral dystrophy. *Genome Res.* **25**, 1781–1790 (2015).
- J. D. Robin, A. T. Ludlow, K. Batten, F. Magdinier, G. Stadler, K. R. Wagner, J. W. Shay, W. E. Wright, Telomere position effect: Regulation of gene expression with progressive telomere shortening over long distances. *Genes Dev.* **28**, 2464–2476 (2014).
- Z. Lou, J. Wei, H. Riethman, J. A. Baur, R. Voglauer, J. W. Shay, W. E. Wright, Telomere length regulates ISG15 expression in human cells. *Aging* **1**, 608–621 (2009).
- W. Kim, A. T. Ludlow, J. Min, J. D. Robin, G. Stadler, I. Mender, T.-P. Lai, N. Zhang, W. E. Wright, J. W. Shay, Regulation of the human telomerase gene *TERT* by telomere position effect-over long distances (TPE-OLD): Implications for aging and cancer. *PLoS Biol.* **14**, e2000016 (2016).
- M. L. Decker, E. Chavez, I. Vulto, P. M. Lansdorp, Telomere length in Hutchinson-Gilford progeria syndrome. *Mech. Ageing Dev.* **130**, 377–383 (2009).
- Y. Li, G. Zhou, I. G. Bruno, J. P. Cooke, Telomerase mRNA reverses senescence in progeria cells. *J. Am. Coll. Cardiol.* **70**, 804–805 (2017).
- L. B. Gordon, F. G. Rothman, C. López-Otin, T. Misteli, Progeria: A paradigm for translational medicine. *Cell* **156**, 400–407 (2014).
- N. Włodarchak, Y. Xing, PP2A as a master regulator of the cell cycle. *Crit. Rev. Biochem. Mol. Biol.* **51**, 162–184 (2016).
- M. Kiely, P. A. Kiely, PP2A: The wolf in sheep's clothing? *Cancer* **7**, 648–669 (2015).
- N. M. V. Gomes, O. A. Ryder, M. L. Houck, S. J. Charter, W. Walker, N. R. Forsyth, S. N. Austad, C. Venditti, M. Pagel, J. W. Shay, W. E. Wright, Comparative biology of mammalian telomeres: Hypotheses on ancestral states and the roles of telomeres in longevity determination. *Aging Cell* **10**, 761–768 (2011).
- ELIXIR, *g-Profiler*, version e104_eg51_p15_3922dba; organism: *hsapiens* (2 June 2021); <https://bit.cs.ut.ee/gprofiler/gost>.
- J. Reimand, M. Kull, H. Peterson, J. Hansen, J. Vilo, g-Profiler—a web-based toolset for functional profiling of gene lists from large-scale experiments. *Nucleic Acids Res.* **35**, W193–W200 (2007).
- Y.-L. Fan, L. Chen, J. Wang, Q. Yao, J.-Q. Wan, Over expression of PPP2R2C inhibits human glioma cells growth through the suppression of mTOR pathway. *FEBS Lett.* **587**, 3892–3897 (2013).
- H.-H. Li, X. Cai, G. P. Shouse, L. G. Piluso, X. Liu, A specific PP2A regulatory subunit, B56 γ , mediates DNA damage-induced dephosphorylation of p53 at Thr55. *EMBO J.* **26**, 402–411 (2007).
- Z. Yan, S. A. Fedorov, M. C. Mumby, R. S. Williams, PR48, a novel regulatory subunit of protein phosphatase 2A, interacts with Cdc6 and modulates DNA replication in human cells. *Mol. Cell. Biol.* **20**, 1021–1029 (2000).
- S. Yu, L. Li, Q. Wu, N. Dou, Y. Li, Y. Gao, PPP2R2D, a regulatory subunit of protein phosphatase 2A, promotes gastric cancer growth and metastasis via mechanistic target of rapamycin activation. *Int. J. Oncol.* **52**, 2011–2020 (2018).
- Y. Zhao, A. Tyshkovskiy, D. Muñoz-Espín, X. Tian, M. Serrano, J. P. de Magalhães, E. Nevo, V. N. Gladyshev, A. Seluanov, V. Gorbunova, Naked mole rats can undergo developmental, oncogene-induced and DNA damage-induced cellular senescence. *Proc. Natl. Acad. Sci. U.S.A.* **115**, 1801–1806 (2018).
- T. Cindrova-Davies, N. M. E. Fogarty, C. J. P. Jones, J. Kingdom, G. J. Burton, Evidence of oxidative stress-induced senescence in mature, post-mature and pathological human placentas. *Placenta* **68**, 15–22 (2018).
- J. R. Baker, C. Vuppasetty, T. Colley, A. I. Papaloannou, P. Fenwick, L. Donnelly, K. Ito, P. J. Barnes, Oxidative stress dependent microRNA-34a activation via PI3K α reduces the expression of sirtuin-1 and sirtuin-6 in epithelial cells. *Sci. Rep.* **6**, 35871 (2016).
- A. Ottaviani, E. Gilson, F. Magdinier, Telomeric position effect: From the yeast paradigm to human pathologies? *Biochimie* **90**, 93–107 (2008).
- Y. Sakakibara, M. Sekiya, N. Fujisaki, X. Quan, K. M. Iijima, Knockdown of *wfs1*, a fly homolog of Wolfram syndrome 1, in the nervous system increases susceptibility to age- and stress-induced neuronal dysfunction and degeneration in *Drosophila*. *PLoS Genet.* **14**, e1007196 (2018).
- E. Machiela, R. Jeloka, N. S. Caron, S. Mehta, M. E. Schmidt, H. J. E. Baddeley, C. M. Tom, N. Polturi, Y. Xie, V. B. Mattis, M. R. Hayden, A. L. Southwell, The interaction of aging and cellular stress contributes to pathogenesis in mouse and human huntington disease neurons. *Front. Aging Neurosci.* **12**, 524369 (2020).
- D. M. Baird, J. Rowson, D. Wynford-Thomas, D. Kipling, Extensive allelic variation and ultrashort telomeres in senescent human cells. *Nat. Genet.* **33**, 203–207 (2003).
- R. J. O'Sullivan, S. Kubicek, S. L. Schreiber, J. Karlseder, Reduced histone biosynthesis and chromatin changes arising from a damage signal at telomeres. *Nat. Struct. Mol. Biol.* **17**, 1218–1225 (2010).
- P. A. Marks, V. M. Richon, R. A. Rifkin, Histone deacetylase inhibitors: Inducers of differentiation or apoptosis of transformed cells. *J. Natl. Cancer Inst.* **92**, 1210–1216 (2000).
- V. M. Komashko, P. J. Farnham, 5-Azacytidine treatment reorganizes genomic histone modification patterns. *Epigenetics* **5**, 229–240 (2010).
- M. Rusin, A. Zajkovic, D. Butkiewicz, Resveratrol induces senescence-like growth inhibition of U-2 OS cells associated with the instability of telomeric DNA and upregulation of BRCA1. *Mech. Ageing Dev.* **130**, 528–537 (2009).
- W. Dang, K. K. Steffen, R. Perry, J. A. Dorsey, F. B. Johnson, A. Shilatifard, M. Kaeberlein, B. K. Kennedy, S. L. Berger, Histone H4 lysine 16 acetylation regulates cellular lifespan. *Nature* **459**, 802–807 (2009).
- R. I. Tennen, D. J. Bua, W. E. Wright, K. F. Chua, SIRT6 is required for maintenance of telomere position effect in human cells. *Nat. Commun.* **2**, 433 (2011).
- M. D. Parenti, A. Grozio, I. Bauer, L. Galeno, P. Damonte, E. Millo, G. Sociali, C. Franceschi, A. Ballestrero, S. Bruzzone, A. Del Rio, A. Nencioni, Discovery of novel and selective SIRT6 inhibitors. *J. Med. Chem.* **57**, 4796–4804 (2014).
- Q. P. Weng, M. Kozlowski, C. Belham, A. Zhang, M. J. Comb, J. Avruch, Regulation of the p70 S6 kinase by phosphorylation in vivo. Analysis using site-specific anti-phosphopeptide antibodies. *J. Biol. Chem.* **273**, 16621–16629 (1998).
- X. Wang, P. Yue, H. Tao, S.-Y. Sun, Inhibition of p70S6K does not mimic the enhancement of Akt phosphorylation by rapamycin. *Heliyon* **3**, e00378 (2017).
- J. F. Gera, I. K. Mellingerhoff, Y. Shi, M. B. Rettig, C. Tran, J. H. Hsu, C. L. Sawyers, A. K. Lichtenstein, AKT activity determines sensitivity to mammalian target of rapamycin (mTOR) inhibitors by regulating cyclin D1 and c-myc expression. *J. Biol. Chem.* **279**, 2737–2746 (2004).
- V. Gire, V. Dulic, Senescence from G2 arrest, revisited. *Cell Cycle* **14**, 297–304 (2015).

43. L. Bertram, A. Böckenhoff, I. Demuth, S. Düzel, R. Eckardt, S. C. Li, U. Lindenberger, G. Pawelec, T. Siedler, G. G. Wagner, E. Steinhagen-Thiessen, Cohort profile: The Berlin Aging Study II (BASE-II). *Int. J. Epidemiol.* **43**, 703–712 (2014).
44. S. Herwest, C. Albers, M. Schmiester, B. Salewski, W. Hopfenmüller, A. Meyer, L. Bertram, I. Demuth, The hSNM1B/Apollo variant rs11552449 is associated with cellular sensitivity towards mitomycin C and ionizing radiation. *DNA Repair* **72**, 93–98 (2018).
45. D. Eckert, S. Buhl, S. Weber, R. Jäger, H. Schorle, The AP-2 family of transcription factors. *Genome Biol.* **6**, 246 (2005).
46. K. Beishline, J. Azizkhan-Clifford, Sp1 and the 'hallmarks of cancer'. *FEBS J.* **282**, 224–258 (2015).
47. M. M. Ouellette, L. D. McDaniel, L. E. Wright, J. W. Shay, R. A. Schultz, The establishment of telomerase-immortalized cell lines representing human chromosome instability syndromes. *Hum. Mol. Genet.* **9**, 403–411 (2000).
48. E. G. Bluem, E. S. Spencer, B. Mecham, R. R. Gordon, I. Coleman, D. Lewinshtein, E. Mostaghel, X. Zhang, J. Annis, C. Grandori, C. Porter, P. S. Nelson, PPP2R2C loss promotes castration-resistance and is associated with increased prostate cancer-specific mortality. *Mol. Cancer Res.* **11**, 568–578 (2013).
49. J. Zhang, Z. Gao, J. Ye, Phosphorylation and degradation of S6K1 (p70S6K1) in response to persistent JNK1 Activation. *Biochim. Biophys. Acta* **1832**, 1980–1988 (2013).
50. A. A. Khan, D. Betel, M. L. Miller, C. Sander, C. S. Leslie, D. S. Marks, Transfection of small RNAs globally perturbs gene regulation by endogenous microRNAs. *Nat. Biotechnol.* **27**, 549–555 (2009).
51. M. Ogrodnik, H. Salmonowicz, D. Jurk, J. F. Passos, Expansion and cell-cycle arrest: Common denominators of cellular senescence. *Trends Biochem. Sci.* **44**, 996–1008 (2019).
52. M. V. Blagosklonny, Geroconversion: Irreversible step to cellular senescence. *Cell Cycle* **13**, 3628–3635 (2014).
53. C. Selman, J. M. A. Tullet, D. Wieser, E. Irvine, S. J. Lingard, A. I. Choudhury, M. Claret, H. Al-Qassab, D. Carmignac, F. Ramadani, A. Woods, I. C. A. Robinson, E. Schuster, R. L. Batterham, S. C. Kozma, G. Thomas, D. Carling, K. Okkenhaug, J. M. Thornton, L. Partridge, D. Gems, D. J. Withers, Ribosomal protein S6 kinase 1 signaling regulates mammalian life span. *Science* **326**, 140–144 (2009).
54. D. E. Harrison, R. Strong, Z. D. Sharp, J. F. Nelson, C. M. Astle, K. Flurkey, N. L. Nadon, J. E. Wilkinson, K. Frenkel, C. S. Carter, M. Pahor, M. A. Javors, E. Fernandez, R. A. Miller, Rapamycin fed late in life extends lifespan in genetically heterogeneous mice. *Nature* **460**, 392–395 (2009).
55. K. Hahn, M. Miranda, V. A. Francis, J. Vendrell, A. Zorzano, A. A. Teleman, PP2A regulatory subunit PP2A-B' counteracts S6K phosphorylation. *Cell Metab.* **11**, 438–444 (2010).
56. R. Habib, R. Kim, H. Neitzel, I. Demuth, K. Chrzanoska, E. Seemanova, R. Faber, M. Digweed, R. Voss, K. Jäger, C. Sperling, M. Walter, Telomere attrition and dysfunction: A potential trigger of the progeroid phenotype in nijmegen breakage syndrome. *Aging* **12**, 12342–12375 (2020).
57. T. Steenstrup, J. D. Kark, S. Verhulst, M. Thinggaard, J. V. B. Hjelmberg, C. Dalgård, K. O. Kyvik, L. Christiansen, M. Mangino, T. D. Spector, I. Petersen, M. Kimura, A. Benetos, C. Labat, R. Sinnreich, S. J. Hwang, D. Levy, S. C. Hunt, A. L. Fitzpatrick, W. Chen, G. S. Berenson, M. Barbieri, G. Paolisso, S. M. Gadalla, S. A. Savage, K. Christensen, A. I. Yashin, K. G. Arbee, A. Aviv, Telomeres and the natural lifespan limit in humans. *Aging* **9**, 1130–1142 (2017).
58. M. J. P. Simons, Questioning causal involvement of telomeres in aging. *Ageing Res. Rev.* **24**, 191–196 (2015).
59. M. Raices, H. Maruyama, A. Dillin, J. Karlseder, Uncoupling of longevity and telomere length in *C. elegans*. *PLoS Genet.* **1**, e30 (2005).
60. Y. Jiang, J. R. Broach, Tor proteins and protein phosphatase 2A reciprocally regulate Tap42 in controlling cell growth in yeast. *EMBO J.* **18**, 2782–2792 (1999).
61. O. Medvedik, D. W. Lamming, K. D. Kim, D. A. Sinclair, MSN2 and MSN4 link calorie restriction and TOR to sirtuin-mediated lifespan extension in *Saccharomyces cerevisiae*. *PLoS Biol.* **5**, e261 (2007).
62. K. Demanelis, F. Jasmine, L. S. Chen, M. Chernoff, L. Tong, D. Delgado, C. Zhang, J. Shinkle, M. Sabarinathan, H. Lin, E. Ramirez, M. Oliva, S. Kim-Hellmuth, B. E. Stranger, T.-P. Lai, A. Aviv, K. G. Ardlie, F. Aguet, H. Ahsan; GTEx Consortium, J. A. Doherty, M. G. Kibriya, B. L. Pierce, Determinants of telomere length across human tissues. *Science* **369**, eaaz6876 (2020).
63. S. A. Kamranvar, X. Chen, M. G. Masucci, Telomere dysfunction and activation of alternative lengthening of telomeres in B-lymphocytes infected by Epstein-Barr virus. *Oncogene* **32**, 5522–5530 (2013).
64. J. Zhang, S. Haider, J. Baran, A. Cros, J. M. Guberman, J. Hsu, Y. Liang, L. Yao, A. Kasprzyk, BioMart: A data federation framework for large collaborative projects. *Database (Oxford)* **2011**, bar038 (2011).
65. J. Herrero, M. Muffato, K. Beal, S. Fitzgerald, L. Gordon, M. Pignatelli, A. J. Vilella, S. M. J. Searle, R. Amode, S. Brent, W. Spooner, E. Kulesha, A. Yates, P. Flicek, Ensembl comparative genomics resources. *Database* **2016**, bav096 (2016).
66. H. Wickham, *ggplot2: Elegant Graphics for Data Analysis* (Springer-Verlag, 2016).
67. G. R. Warnes, B. Bolker, L. Bonebakker, R. Gentleman, W. Huber, A. Liaw, T. Lumley, M. Maechler, A. Magnusson, S. Moeller, M. Schwartz, B. Venables, T. Galli, 'ggplots: Various R Programming Tools for Plotting Data' (R package version 3.1.1., 2020); <https://cran.r-project.org/web/packages/ggplots/index.html>.
68. *ibima / tpe-old — Bitbucket* (29 August 2021); <https://bitbucket.org/ibima/tpe-old/src/master/>.
69. S. Campbell, The Progeria Research Foundation Cell Bank. <https://www.progeriaresearch.org/cell-and-tissue-bank/>, 20 July 2022.
70. D. Gerstorff, L. Bertram, U. Lindenberger, G. Pawelec, I. Demuth, E. Steinhagen-Thiessen, G. G. Wagner, Behavioural Science Section/The Berlin Aging Study II-An overview. *Editorial. Gerontology* **62**, 311–315 (2016).
71. F. Kannenberg, K. Gorzelniak, K. Jäger, M. Fobker, S. Rust, J. Repa, M. Roth, I. Björkhem, M. Walter, Characterization of cholesterol homeostasis in telomerase-immortalized Tangier disease fibroblasts reveals marked phenotype variability. *J. Biol. Chem.* **288**, 36936–36947 (2013).
72. B. Neuner, A. Lenfers, R. Kelsch, K. Jäger, N. Brüggmann, P. van der Harst, M. Walter, Telomere length is not related to established cardiovascular risk factors but does correlate with red and white blood cell counts in a German blood donor population. *PLoS ONE* **10**, e0139308 (2015).
73. R. M. Cawthon, Telomere length measurement by a novel monochrome multiplex quantitative PCR method. *Nucleic Acids Res.* **37**, e21 (2009).
74. J. B. McGuire, T. J. James, C. J. Imber, S. D. St. Peter, P. J. Friend, R. P. Taylor, Optimisation of an enzymatic method for β -galactosidase. *Clin. Chim. Acta* **326**, 123–129 (2002).
75. R. K. Gary, S. M. Kindell, Quantitative assay of senescence-associated β -galactosidase activity in mammalian cell extracts. *Anal. Biochem.* **343**, 329–334 (2005).
76. M. López-Ratón, M. X. Rodríguez-Álvarez, C. C. Suárez, F. Gude-Sampedro, OptimalCutpoints: An R package for selecting optimal cutpoints in diagnostic tests. *J. Stat. Softw.* **61**, 1–36 (2014).
77. J. Böhringer, R. Santer, N. Schumacher, F. Gieseke, K. Cornils, M. Pechan, B. Kustermann-Kuhn, R. Handgretinger, L. Schöls, K. Harzer, I. Krägeloh-Mann, I. Müller, Enzymatic characterization of novel arylsulfatase A variants using human arylsulfatase A-deficient immortalized mesenchymal stromal cells. *Hum. Mutat.* **38**, 1511–1520 (2017).
78. Z. Darzynkiewicz, G. Juan, DNA content measurement for DNA ploidy and cell cycle analysis. *Current protocols in cytometry*, **7**, cy0705s00 (2001).
79. R Core Team, *R: A Language and Environment for Statistical Computing* (R Foundation for Statistical Computing, 2020).

Acknowledgments: We thank W. Wright and J. Shay (University of Texas Southwestern Medical Center, Dallas) for providing reagents and advice. This work would not have been possible without the positive encouragement from W. Wright. We thank M. Hanna (Mercury Medical Research and Writing), U. Kornak (University of Göttingen), and E. Steinhagen-Thiessen (Charité Berlin and University of Rostock) for proofreading the manuscript. The manuscript was edited at Springer Nature Author Services. We thank K. Tränkner (WriteNow, Berlin, Germany) for preparing the schematic drawings. We thank M. Haschke, B. Köttgen, S. Zigan, and K. Binder (Charité-Universitätsmedizin Berlin) for technical support. We thank A. del Rio (Institute of Organic Synthesis and Photoactivity, Bologna, Italy) for providing the SIRT inhibitor (compound BCI-150). We are grateful for financial and technical support from Labor Berlin. We thank J. Reunert, T. Marquardt, and E. Orso for providing control cells. We thank also all co-PIs from the BASE-II research project (L. Bertram, D. Gerstorff, U. Lindenberger, G. Pawelec, E. Steinhagen-Thiessen, and G. G. Wagner). Support for computing equipment was provided by the European Union [EFRE (European Fund for Regional Development)]. **Funding:** This work was supported by Sonnenfeld Stiftung grant (to K.J.), European Union's Horizon 2020 research and innovation program grant 633589 (to S.M. and G.F.), German Federal Ministry of Education and Research (Bundesministerium für Bildung und Forschung, BMBF) grant 03VP06230 (to G.F.), German Federal Ministry of Education and Research (Bundesministerium für Bildung und Forschung, BMBF) grants for the BASE-II research project nos. 16SV5536K, 16SV5537, 16SV5538, 16SV5837, 01UW0808, 01GL1716A, and 01GL1716B (to I.D.), Hermann and Lilly Schilling-Stiftung für medizinische Forschung im Stiftungsverband (to A.He.), and Stiftung für Pathobiochemie und Molekulare Diagnostik (to M.W.). **Ethics statement:** All procedures were performed in accordance with the ethical standards of the responsible committee. The cell lines were either established with the ethical approval of the Ethics Committee of the "Ärztammer Westfalen Lippe" and the Medical Faculty of the University of Münster (S. Vi. Walter), the University of Rostock (A2019-0134, A.He.; A2019-0134), and the consent of the participants or their parents (for children) or approved by the local Ethics committees of the Technische Universität Dresden (EK45022009) and the University Medical Center Rostock (A2019-0134). The HGP cell lines were a gift from the Progeria Research Foundation [L. Gordon; the PRF Cell and Tissue Bank is Institutional Review Board (IRB) approved by the Rhode Island Hospital Committee on the Protection of Human Subjects, Federal Wide Assurance FWA00001230, study CMTT#0146-09] and were collected according to the regulations of the Progeria Research Foundation. All participants from the BASE-II study gave written informed consent to the study protocol that was approved by the Ethics

SCIENCE ADVANCES | RESEARCH ARTICLE

Committee of the Charité-Universitätsmedizin Berlin (number of the ethical approval: EA2/029/09). **Author contributions:** Conceptualization: M.W. Methodology: K.J., J.M., S.M., B.N., K.G., S.T., I.D., A.S., M.W., F.W., C.H., A.Ha., and M.E.G. Visualization: K.J., J.M., M.E.G., S.M., and M.W. Supervision: M.W., G.F., and S.M. Writing—original draft: K.J. and M.W. Writing—review and editing: S.M., B.N., G.F., A.Ha., A.He., K.J., and M.W. **Competing interests:** The authors declare that they have no competing interests. **Data and materials availability:** All data needed to evaluate the conclusions in the paper are present in the paper and/or the Supplementary Materials and at <https://doi.org/10.5281/zenodo.6477501>. All program codes for the presented TPE-OLD candidate gene selection and analyses are freely available online at <https://doi.org/10.5281/zenodo.6477501>. Because of concerns for participant privacy, BASE-II data are available only upon reasonable request. External scientists may apply to the Steering Committee of BASE-II for data access. Please refer to the BASE-II website (www.base2.mpg.de/7549/data-documentation) for additional information. Please contact L. Müller, scientific coordinator, at lmuller@mpib-berlin.mpg.de. The progeria cell lines can be provided by the Progeria Research Foundation Inc. pending scientific review and a completed material transfer agreement. Requests for the progeria cell lines should be submitted to the Progeria Research Foundation. Both the two youngest and two oldest donors shown in fig. S19A can be provided by Coriell Institute pending scientific review and a completed material transfer agreement. Requests for the cell lines should be submitted to the Coriell Institute.

Submitted 14 October 2021
Accepted 5 July 2022
Published 17 August 2022
10.1126/sciadv.abk2814

ScienceAdvances

A conserved long-distance telomeric silencing mechanism suppresses mTOR signaling in aging human fibroblasts

Kathrin JägerJuliane MenschMaria Elisabeth GrimmigBruno NeunerKerstin GorzelniaKSeval TürkmenIlja DemuthAlexander HartmannChristiane HartmannFelix WittigAnje SporbertAndreas HermannGeorg FuellenSteffen MöllerMichael Walter

Sci. Adv., 8 (33), eabk2814. • DOI: 10.1126/sciadv.abk2814

View the article online

<https://www.science.org/doi/10.1126/sciadv.abk2814>

Permissions

<https://www.science.org/help/reprints-and-permissions>

Downloaded from <https://www.science.org> at Universitaet Rostock on October 10, 2022

Use of this article is subject to the [Terms of service](#)

Science Advances (ISSN) is published by the American Association for the Advancement of Science, 1200 New York Avenue NW, Washington, DC 20005. The title *Science Advances* is a registered trademark of AAAS.
Copyright © 2022 The Authors, some rights reserved; exclusive licensee American Association for the Advancement of Science. No claim to original U.S. Government Works. Distributed under a Creative Commons Attribution NonCommercial License 4.0 (CC BY-NC).

Supplementary Materials for

A conserved long-distance telomeric silencing mechanism suppresses mTOR signaling in aging human fibroblasts

Kathrin Jäger *et al.*

Corresponding author: Michael Walter, michael.walter@med.uni-rostock.de

Sci. Adv. **8**, eabk2814 (2022)
DOI: 10.1126/sciadv.abk2814

The PDF file includes:

Figs. S1 to S22
Tables S1 and S3 to S7
Legend for table S2
References

Other Supplementary Material for this manuscript includes the following:

Table S2

Fig. S1

Telomeric distances of known TPE-OLD genes. For each human gene, the dendrogram presents the maximum linkage tree of its orthologues, calculated based on their telomeric distance. Only species with replicative aging are considered. The height of a connecting bar represents the maximal difference in telomeric distance. The red bar is drawn at 1 Mb and represents where the tree is cut into subtrees. The number of genes in the two largest subtrees determines the rank of that gene in the TPE-OLD candidate list. The green dots represent the distance of an orthologue to the telomere. For example, C1S has two preserved telomeric distances: ~7 Mb from the telomere (dog, bonobo, African green monkey, gorilla, human, gibbon, chimp, macaque, olive baboon) and ~16 Mb from the telomere (sheep, hybrid indicine cattle, goat, hybrid cattle, cattle).

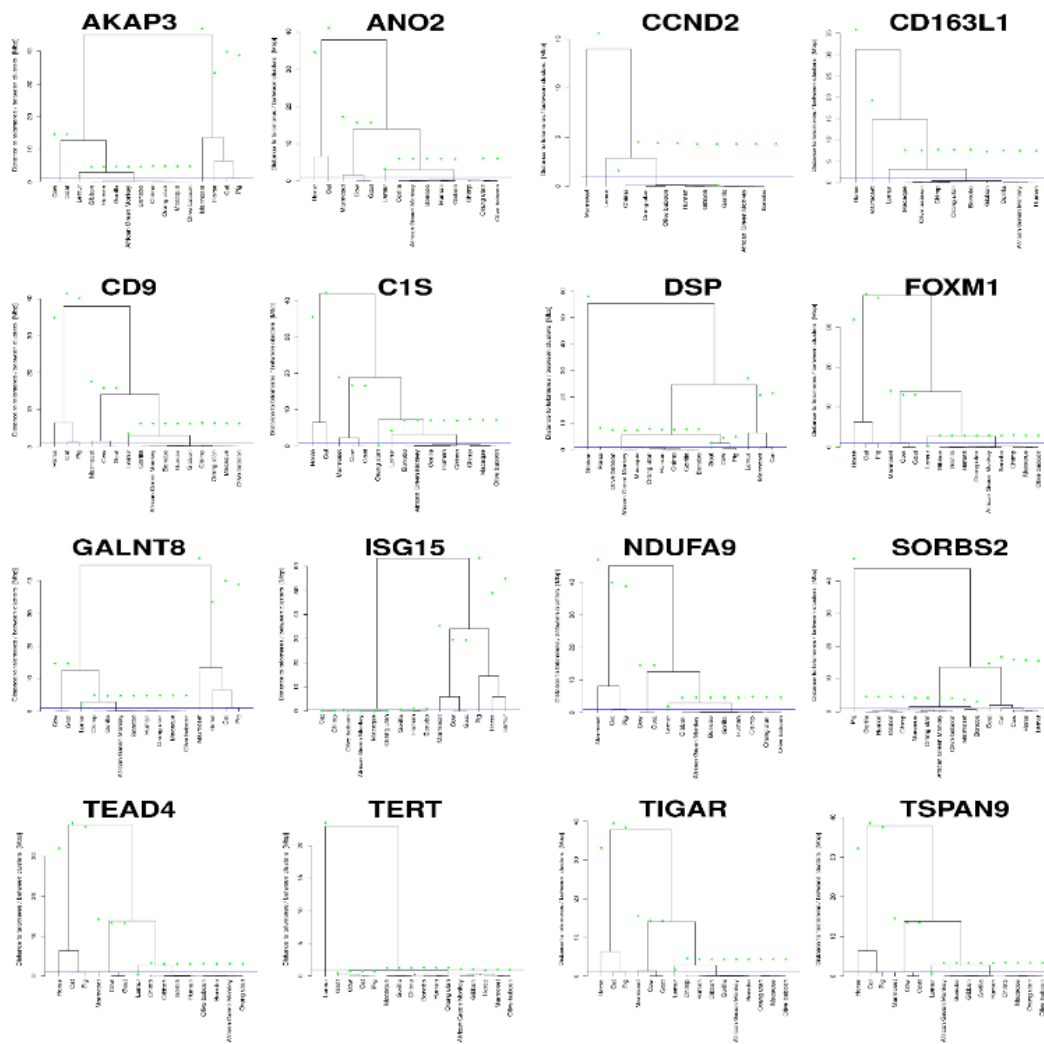


Fig. S2

Telomeric distances of selected serine/threonine specific phosphatases (PPP) that are candidates for TPE-OLD. Analogous to Figure S1, this figure presents dendrograms for the telomeric distances of selected subunits of PP2A.

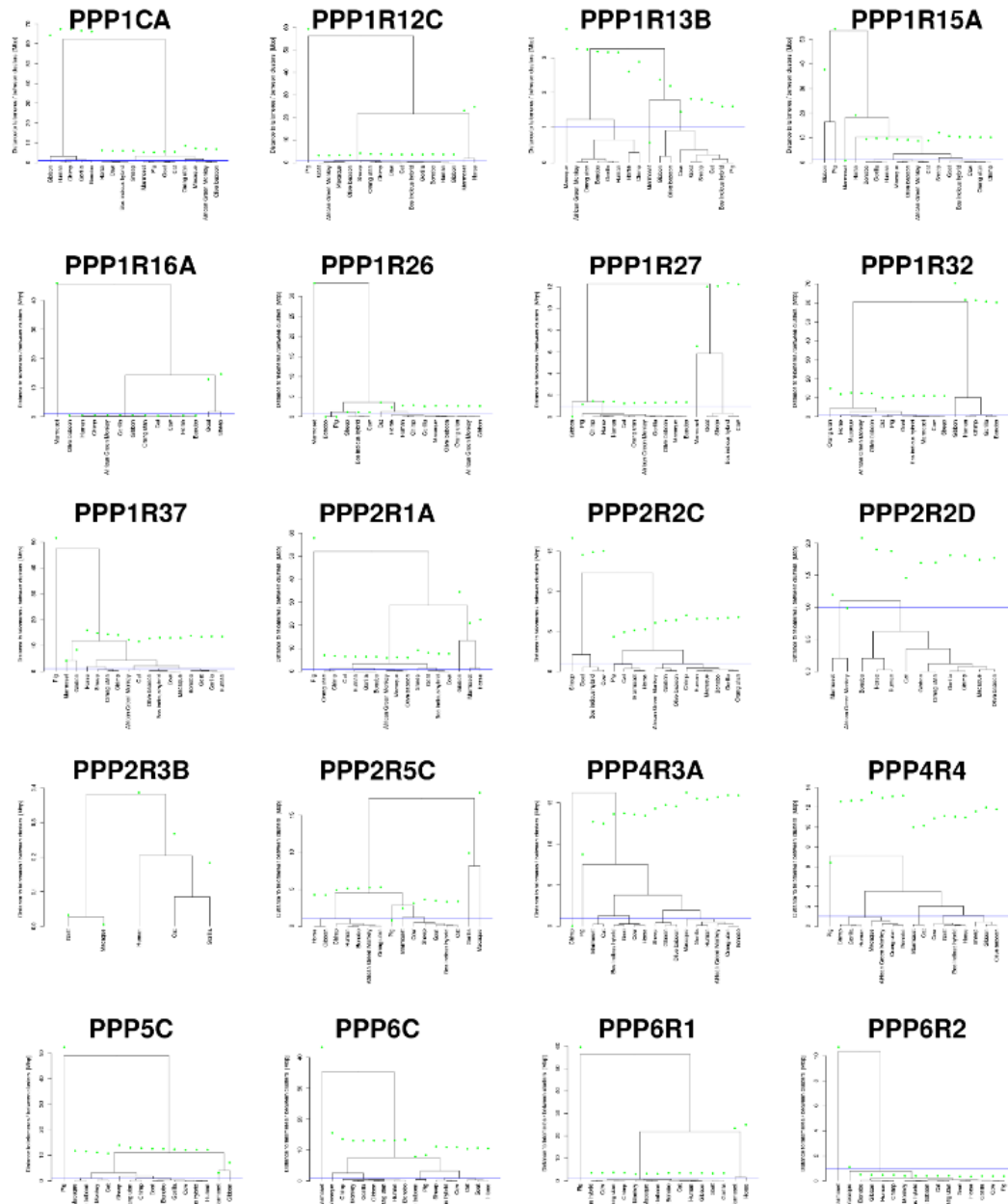


Fig. S4

TPE-OLD concept, PP2A holoenzyme structure and genomic localization of PP2A subunits. (A), Genomic localization of regulatory PP2A subunits. **(B),** Genomic localization of structural and catalytic PP2A subunits. Higher primates and other long-lived species with replicative aging retain the location of genes encoding some regulatory PP2A subunits at the end of their chromosomes. The location of each gene is shown in a schematic representation. Only the subtelomeric areas (up to 10 Mb) are drawn to scale, not the middle range. Each bar represents an individual chromosome; each color represents one PP2A subunit. The location of the genes relative to the telomeres is marked on the chromosome.

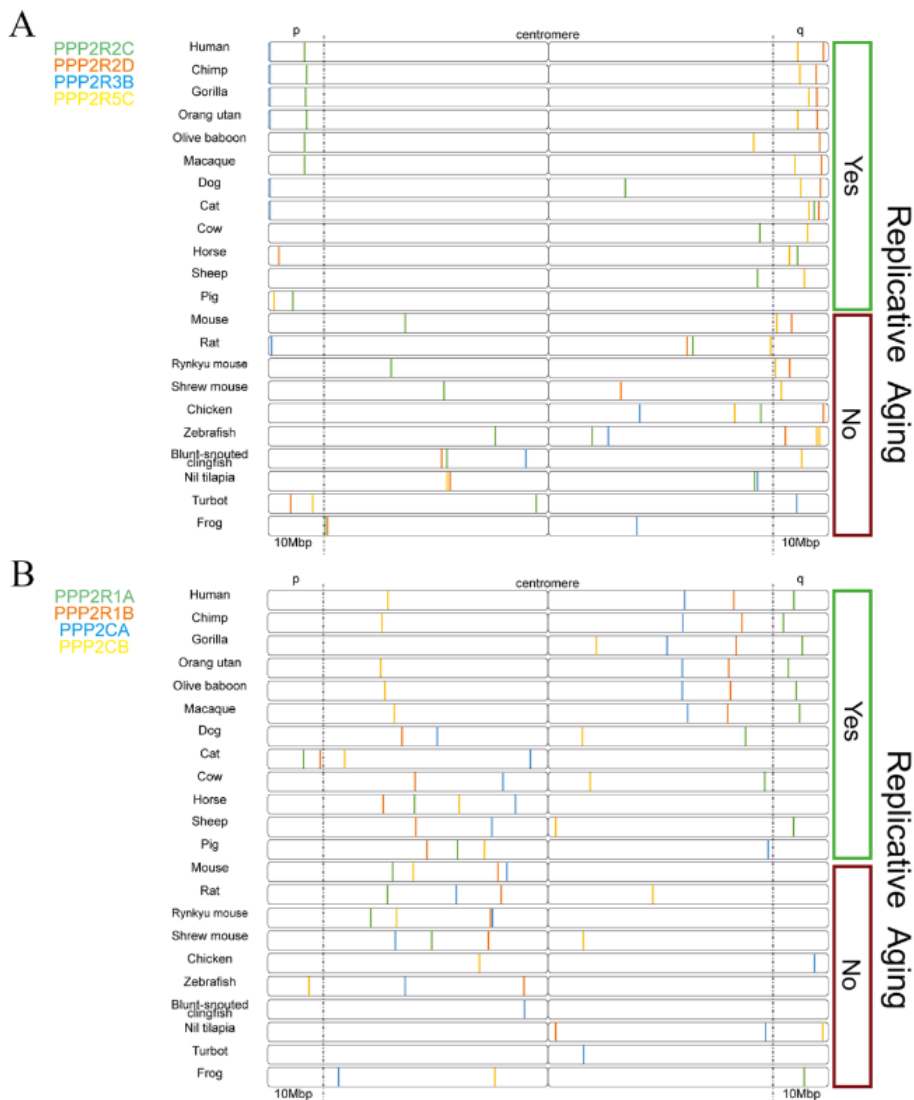


Fig. S5**Growth curves of primary (-hTERT) and immortalized (+hTERT) fibroblast cell lines.**

CON, healthy controls (turquoise symbols: squares N707, triangles 731, circles 778, rhombuses 811). HGP, Hutchinson-Gilford progeria fibroblasts (magenta symbols: squares HGADFN003, triangles HGADFN164, circles HGADFN127, rhombuses HGADFN178). L, low population doubling (PD); H, high PD.

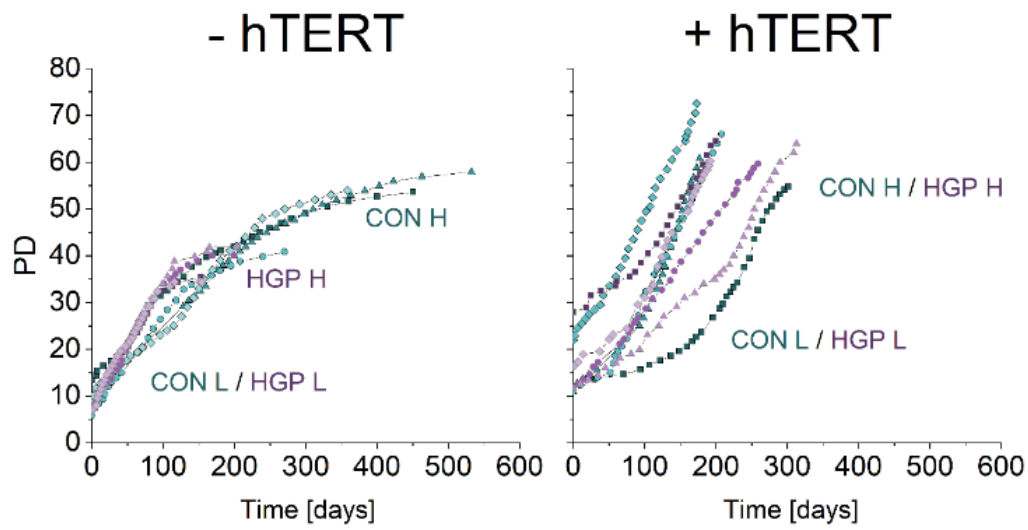
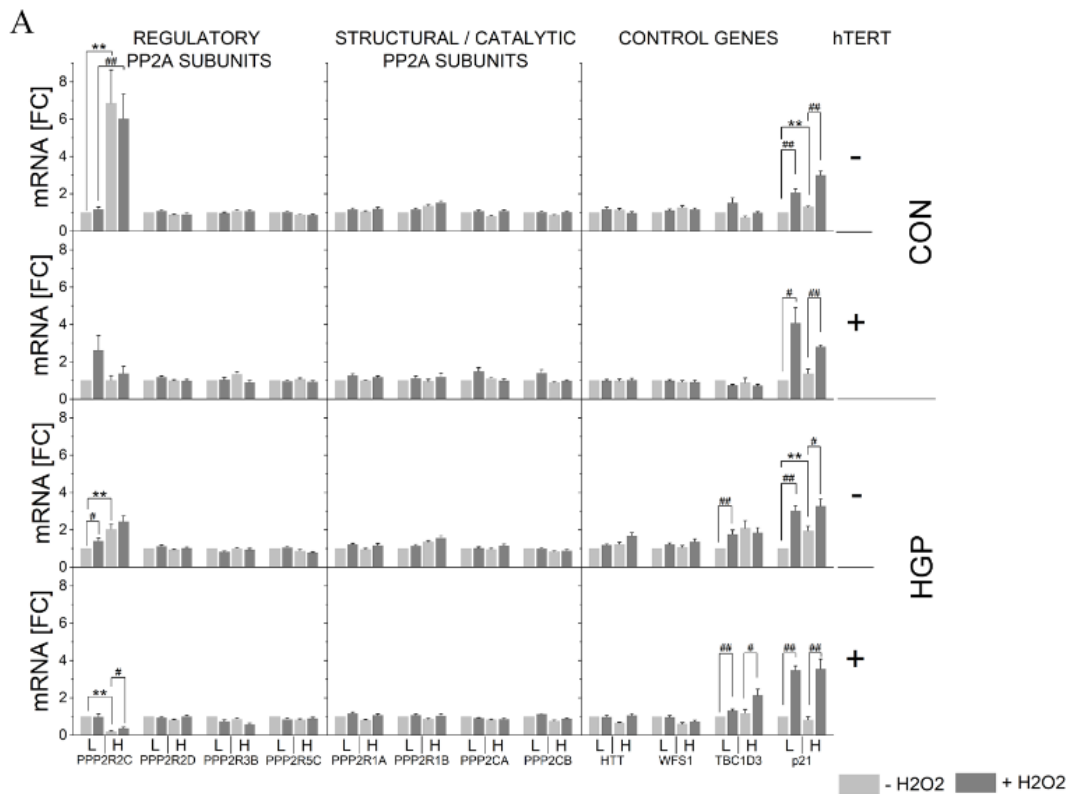


Fig. S6

Telomere length- and stress-dependent mRNA levels of regulatory, structural and catalytic PP2A subunits and control genes in healthy control (CON) and Progeria (HGP) cells. qPCR analysis of healthy CON and HGP fibroblasts at low (L) and high (H) PD was performed under basal conditions (10% FCS), in the absence of H₂O₂ (light gray columns) and in the presence of H₂O₂ (200 μM; 2 h, gray columns). *Cyclophilin A* was used as an internal normalization control. *WFS1* and *HTT* represent internal controls, e.g., genes between *PPP2R2C* and the telomere. *P21* was used as a marker for stress-inducible activation. *TBC1D3* is a potential confounder that may influence mTOR signaling and the HGP phenotype. All values were normalized to the level (= 100%) of mRNA in young cells (PD 13–20). Each assay was performed in biological quadruplicates and technical replicates and is shown as the mean ± SEM. The Mann-Whitney U test was employed to assess statistical significance. * indicates $p < 0.05$ and ** $p < 0.01$ for low PD vs high PD; # indicates $p < 0.05$ and ## $p < 0.01$ for -H₂O₂ vs. +H₂O₂ (A) Overall summarized data. (B) Data shown for all individual controls separately and in (C) for all individual HGP cell lines separately (with 3 technical replicates each).



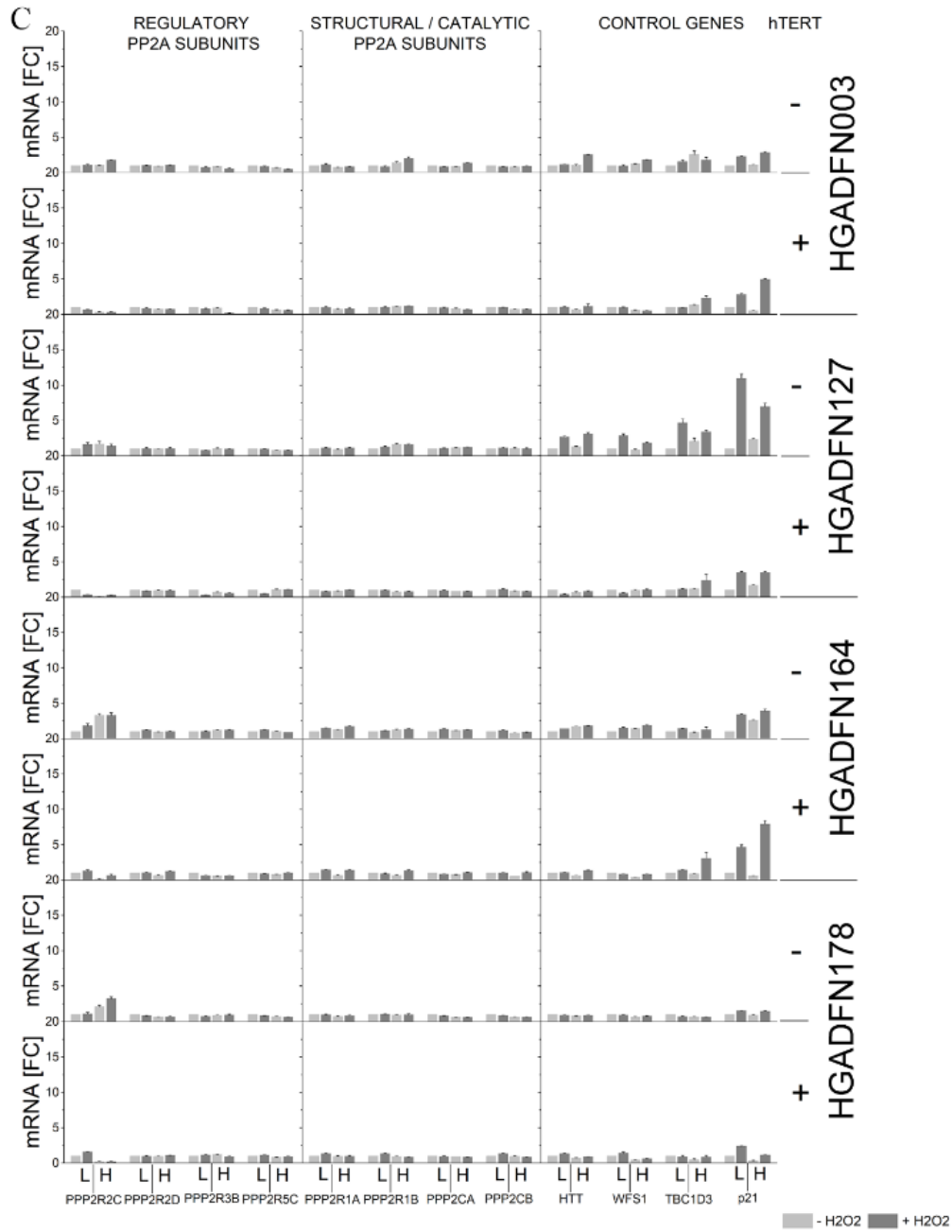


Fig. S7

Senescence associated- β -galactosidase as a marker for telomere length- and stress-dependent senescence. The number of senescence-associated β -galactosidase (SA- β -Gal)-positive cells (**A, C, E-H**) and the SA- β -Gal levels of cell extracts (measured fluorometrically as MUG) (**C, D**) were determined in primary and immortalized cells using two healthy control cell lines (light gray) and four HGP cell lines (gray) in the absence and presence of H_2O_2 (200 μM , 2 h), as described in the Materials and Methods. (**E**), Representative SA- β -Gal staining of HGP cells (low PD) in the absence of H_2O_2 . (**F**), Representative SA- β -Gal staining of HGP cells (high PD) in the absence of H_2O_2 . (**G**), Representative SA- β -galactosidase staining of immortalized HGP cells (low PD) in the absence of H_2O_2 . (**H**), Representative SA- β -Gal staining of immortalized HGP cells (high PD) in the absence of H_2O_2 . L, low PD; H, high PD, as indicated. The percentages of SA- β -Gal-positive cells were ascertained by counting five visual fields under a light microscope at 50x magnification by two different individuals independently and blinded.

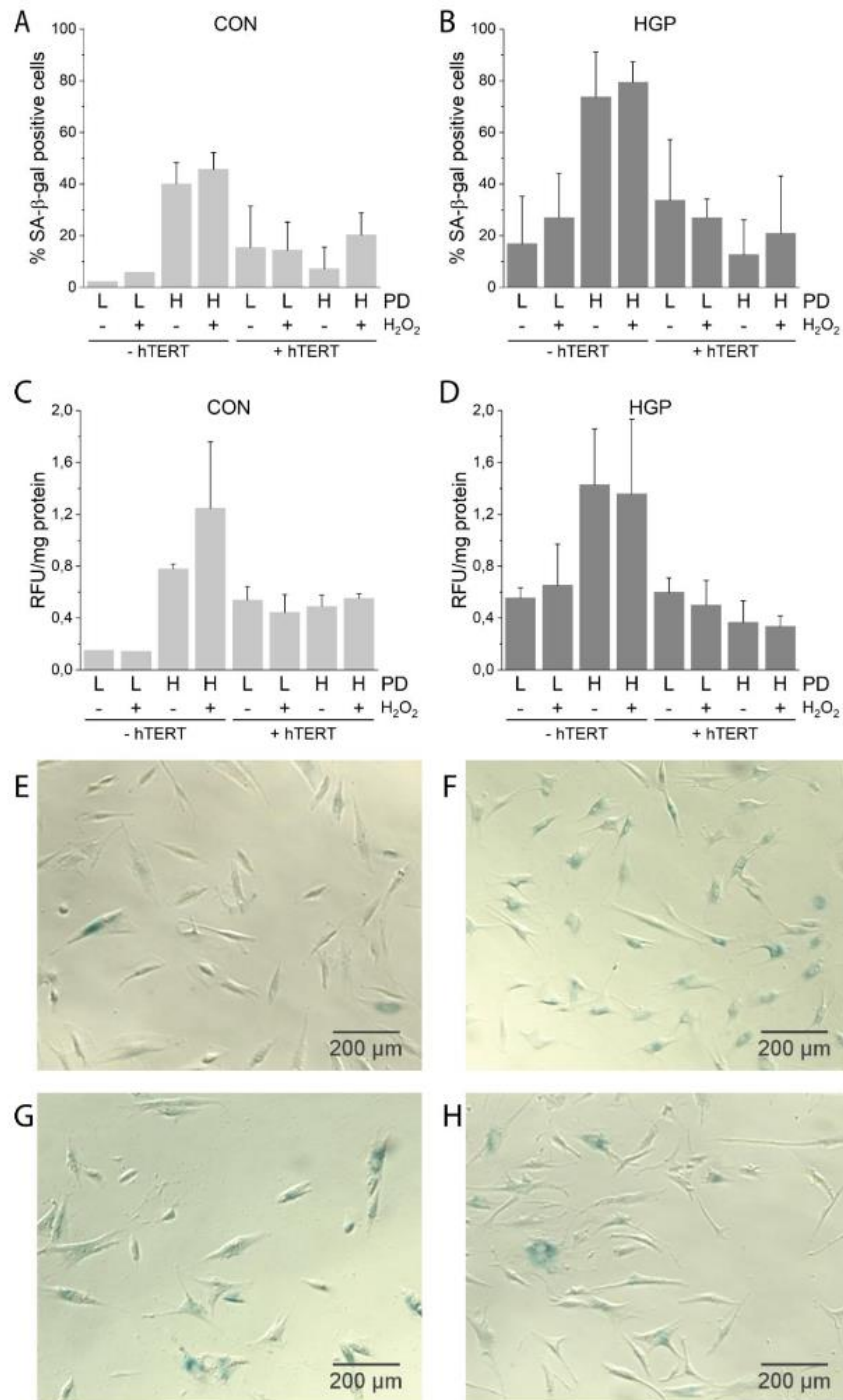


Fig. S8

Telomere length-dependent chromosomal reorganization of pre-senescent and *hTERT*-immortalized fibroblast cell lines. (A), Overall distribution of TEL-*PPP2R2C* probe distances for healthy control cells (n=208, 224, 266 for 707, 731 and 778). (B), Overall distribution of TEL-*PPP2R2C* probe distances for HGP cells (n=250, 236, 244 for HGADFN127, HGADFN164 and HGADFN176). The proportion of probe distances $\leq 2.26 \mu\text{m}$ and $> 2.26 \mu\text{m}$ are shown in circle diagrams. Adjacent (A) and separated (S) as indicated. (C), Stacked bar charts for all distances for all healthy controls (n=698) and all HGP cells (n=730), and the same data separated for the respective shortest and longest distances in each cell. The mean distances were stratified by cell lines and by immortalization status. Fibroblasts with short telomeres (-*hTERT*) show a shift to greater distances relative to cells with long telomeres (+*hTERT*); χ^2 test for trend, $p \leq 0.001$. The x-axis presents the deciles of distances from decile 1 = lowest 10% of distances to the highest decile, decile 10 = highest 10% of distances. (D), Pairwise (allele specific) TEL-*PPP2R2C* probe distances with the respective shortest and longest difference in each cell for CON (n=698) and HGP (n=730).

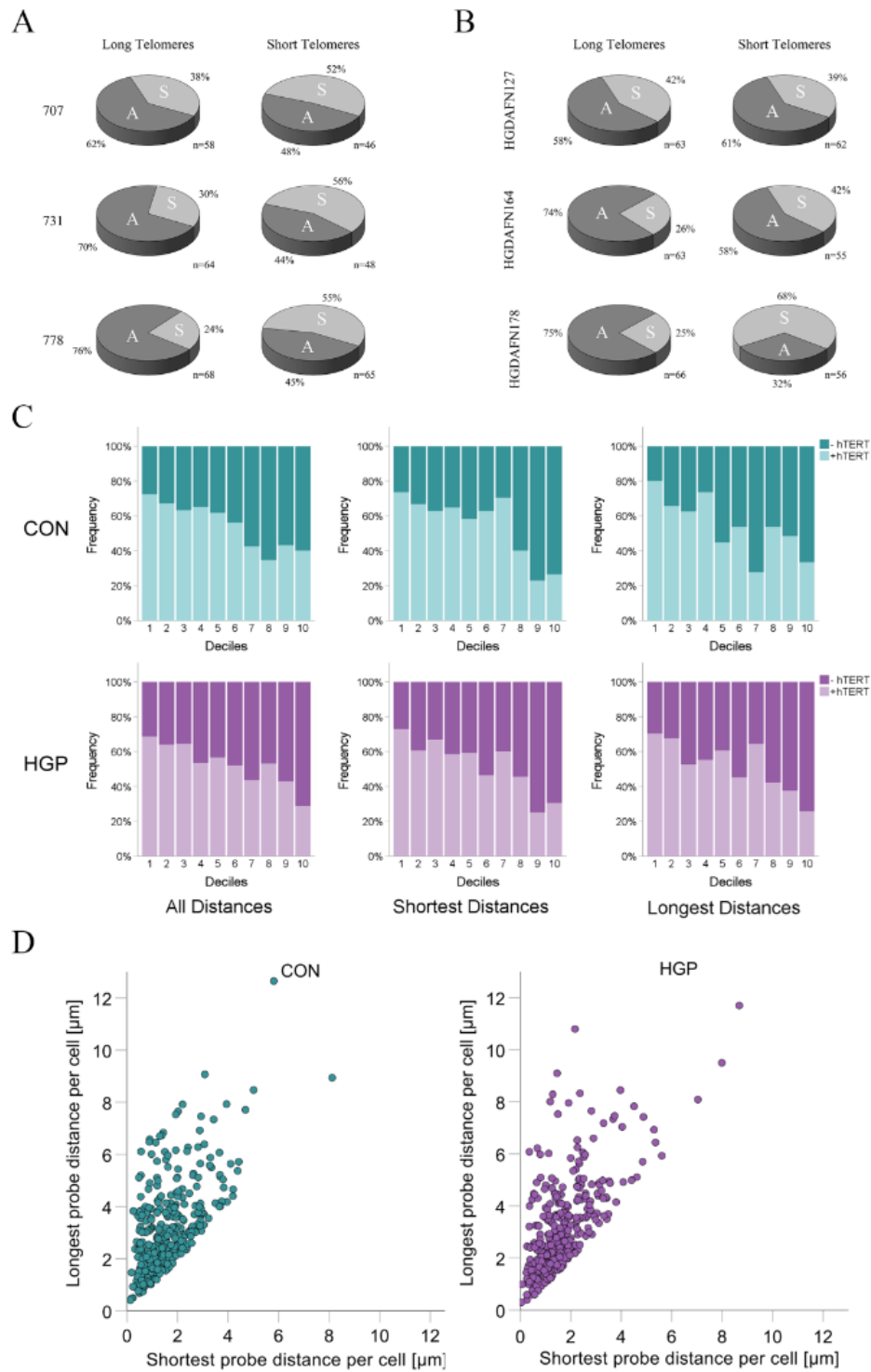


Fig. S9

Original data for all TEL-*PPP2R2C* probe distances for healthy controls and HGP cell lines. Distances were divided into deciles (0.7258 μm , 1.090 μm , 1.3442 μm , 1.606 μm , 1.93 μm , 2.28 μm , 2.773 μm , 3.49 μm , 4.451 μm) for graphical presentation. Horizontal lines indicate the bounds of deciles. The cut-off value for separation of A and S was 2.26 μm for all cell lines.

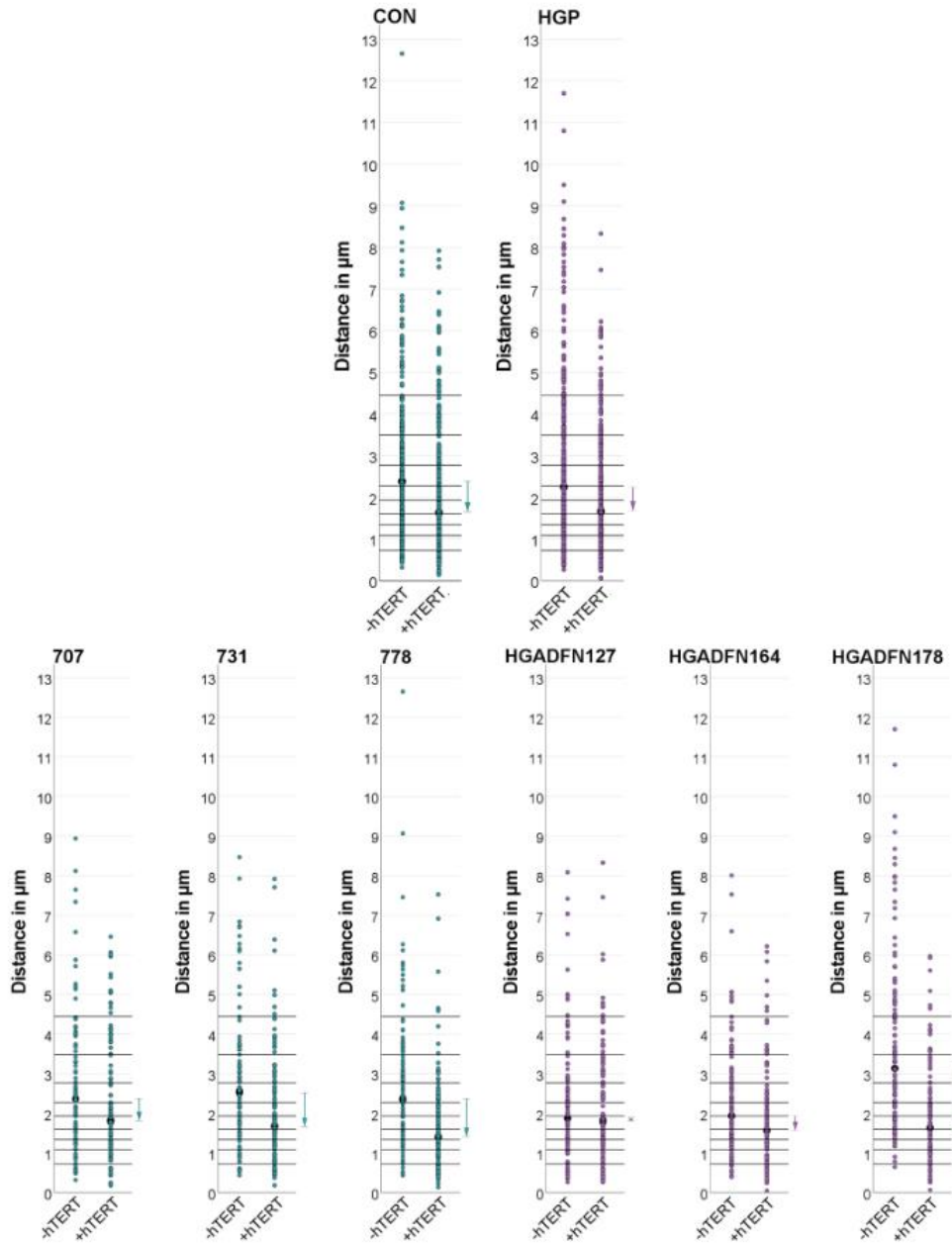


Fig. S10

Influence of chromatin modulators on *PPP2R2C* expression. Human fibroblasts were treated for the indicated time with the following: 1.) TSA at 0.2 $\mu\text{g/ml}$ (gray; n=3 cell lines, 3 technical replicates each), 5-AzaC at 1 $\mu\text{g/ml}$ (dark gray; n=3 cell lines, 3 technical replicates each), or both inhibitors (black); 2) resveratrol at a concentration of 0.25 μM (gray; n=3 cell lines, 3 technical replicates each), 1.0 μM (dark gray), or 10.0 μM (black); 3) 50 μM compound BCI-150 (dark gray) or the respective amounts of vehicle DMSO (light gray; all experiments n=3 cell lines, 3 technical replicates each). All values were normalized to the level (= 100%) of mRNA in primary cells (PD 13–17) in the absence of inhibitor. Each assay was performed in both biological and technical triplicates and is shown as the mean \pm SEM. The Mann-Whitney U test was used to assess statistical significance. * indicates $p < 0.05$ and ** $p \leq 0.01$. The experiment with compound BCI-150 was performed in technical triplicates for one cell line. *Cyclophilin A* was used as an internal normalization control. 11 of 288 measurements were excluded because of nondetectable mRNA.

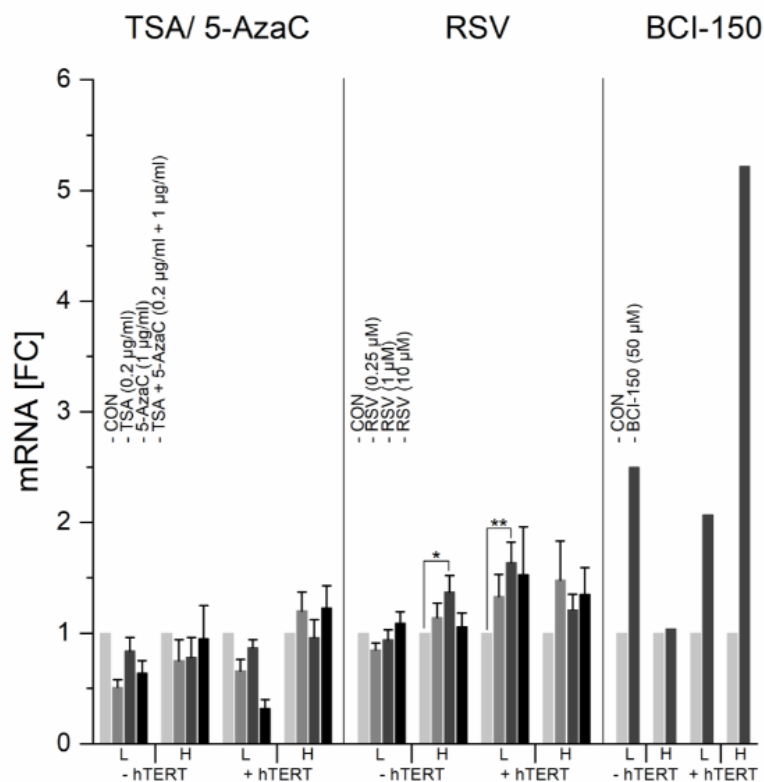


Fig. S11

Correlation between TL and degree of phosphorylation of (A) Akt and (B) p70S6K.
All protein levels were normalized to the protein levels of β -actin. PR, protein ratio.

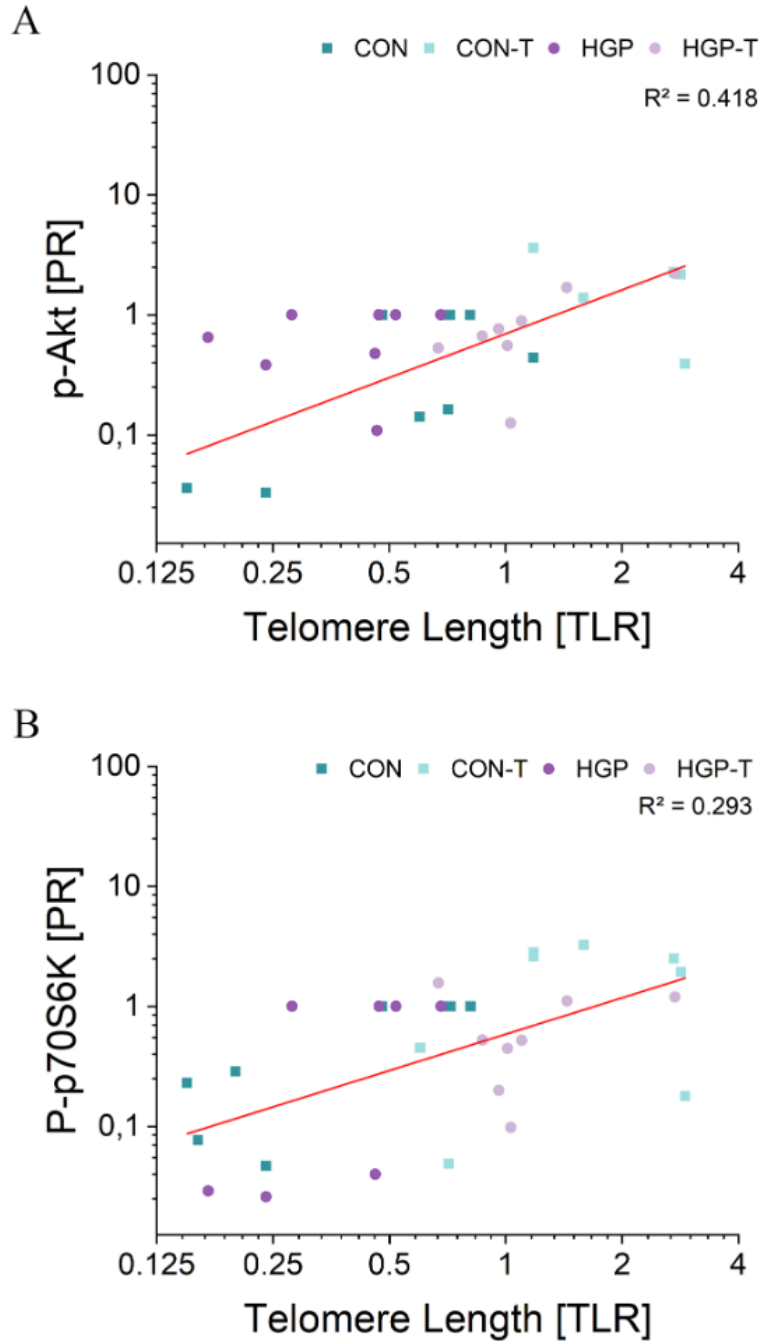


Fig. S13

Serum starvation is not a major determinant of p70S6K phosphorylation in aged fibroblasts *in vitro*. (A) Immunoblot analysis of total and phosphorylated p70S6K in immortalized control fibroblasts with long telomeres (L) and in aged control fibroblasts with short telomeres (S) without (-) or with (+) serum starvation, as described in Materials and Methods. The healthy control cell line 811 was used;. Attributable to artifacts in the Western blot densitometric analysis of protein signal was not possible, β -Actin was used as reference for input control. (B) qPCR analysis of the same healthy control cell line was performed once (with technical triplicates) for *mTOR* and *PPP2R2C* under identical conditions as in (A). *Cyclophilin A* was used as an internal normalization control.

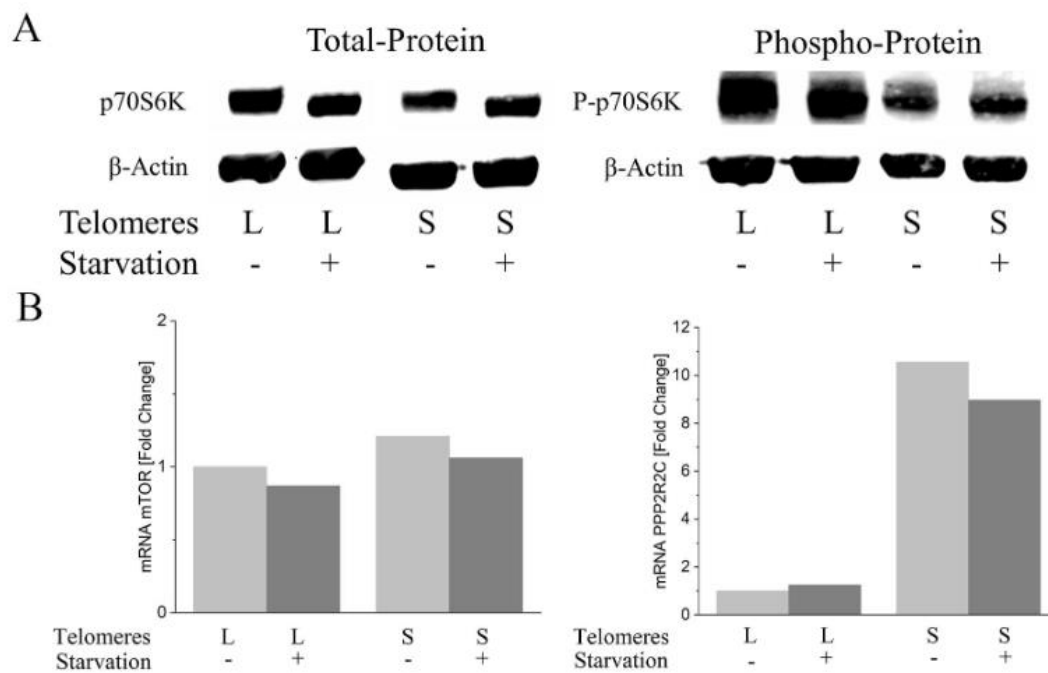


Fig. S14

Lack of metabolic suppression and cell stress in HGP fibroblasts. (A), Cellular levels of the senescence marker MUG (left panel) compared to the metabolic marker arylsulfatase A (activity in the middle panel and protein in the right panel), as shown for primary pre-senescent cells. The protein product and resulting activity of *ARSA*, which is regulated by mTOR and p70S6K and is strongly inhibited by the prototype mTOR inhibitor rapamycin, is not suppressed in pre-senescent HGP cells. Data show the mean values of three controls (707, 731, 811) and three HGP cell lines (HGADFN127, HGADFN164, HGADFN178). The Mann-Whitney *U* test was used to assess statistical significance. * indicates $p \leq 0.05$. **(B)**, Cell cycle distribution of healthy primary control cells (upper left), primary HGP cells (upper right), healthy control cells after *hTERT* immortalization (lower left), and HGP cells after *hTERT* immortalization (lower right), as described in Materials and Methods. G0/G1-phase (dark gray), S-phase (gray) and G2/M-phase (light gray). HGP cells had a higher percentage of cells in the G2/M phase and a lower percentage of cells in the S phase, which is typical for high proliferation stress. The *ARSA* activity levels were not increased in young HGP fibroblasts (low PDs) and were not increased in *hTERT* immortalized cells.

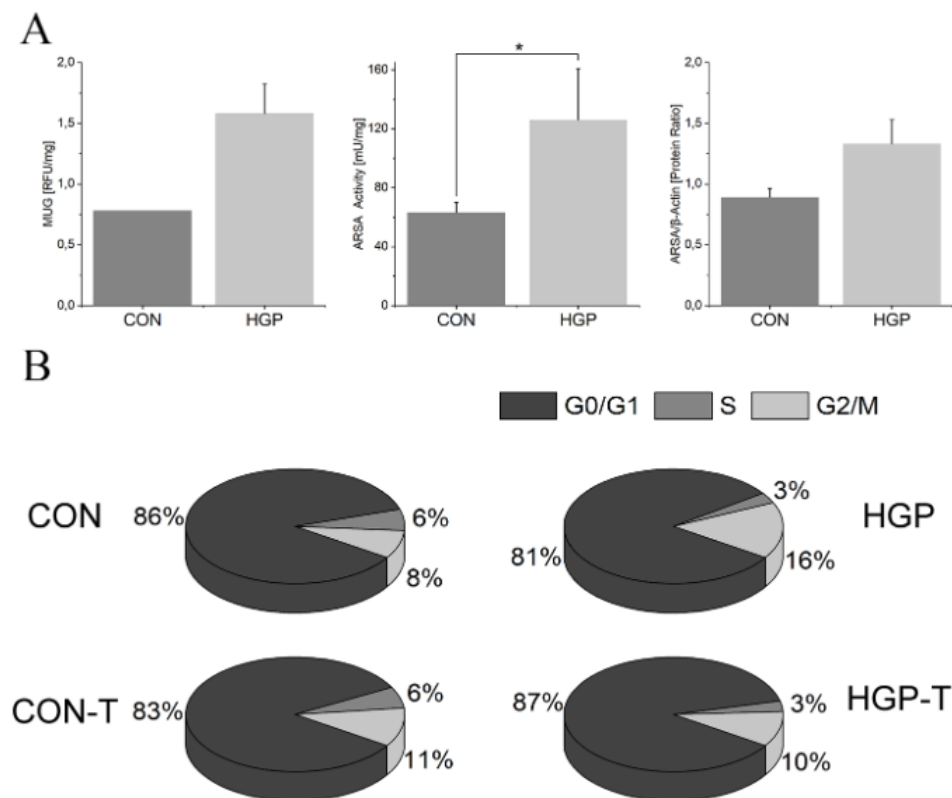
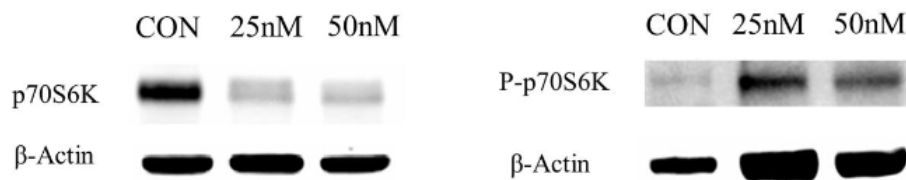


Fig. S15

PPP2R2C knock down by siRNA and induction of protein synthesis (A), Western blot analysis: effects of *PPP2R2C* knock down via siRNA in fibroblasts derived from a HGP affected individual. Depicted levels of total and phosphorylated p70S6K protein without and with siRNA treatments in two different concentrations. β -actin serves as a loading control. For densitometric illustration of blots β -actin was used as reference for input control. PR, protein ratio (**B**) mRNA levels of genes whose transcription is likely under control of p70S6K. *Cyclophilin A* was used as an internal normalization control. All values were normalized to the level (=100%) of mRNA in untreated cells (CON). For each gene the significance was calculated against the control (CON) of this gene. Assay was performed in duplicate using technical triplicates (total of six measurements). Data are shown as the mean \pm SD. The Mann-Whitney U test was employed to assess statistical significance. * indicates $p < 0.05$ and ** $p \leq 0.01$.

A



B

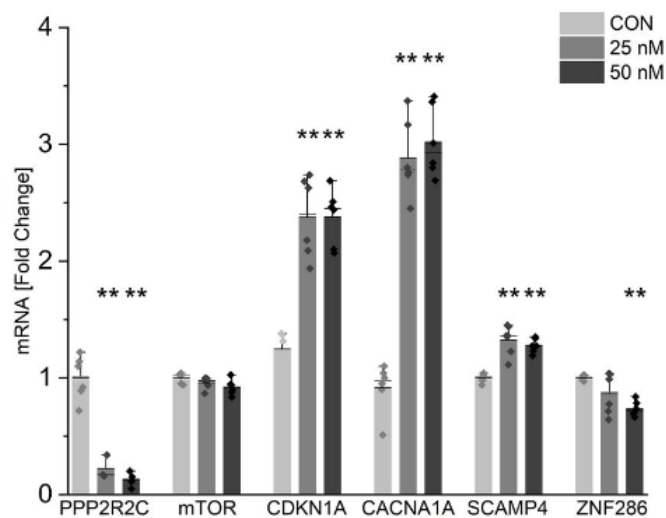


Fig. S16

Cell proliferation in control and HGP fibroblasts. First derivatives of growth curves of control and progeria cell lines before (bold line) and after *hTERT* immortalization (faint line). Progeria cell lines show a faster proliferation rate with an earlier stop of cell growth compared to healthy control cell lines. No smoothing was applied. CON, healthy controls; HGP, Hutchinson-Gilford progeria cells.

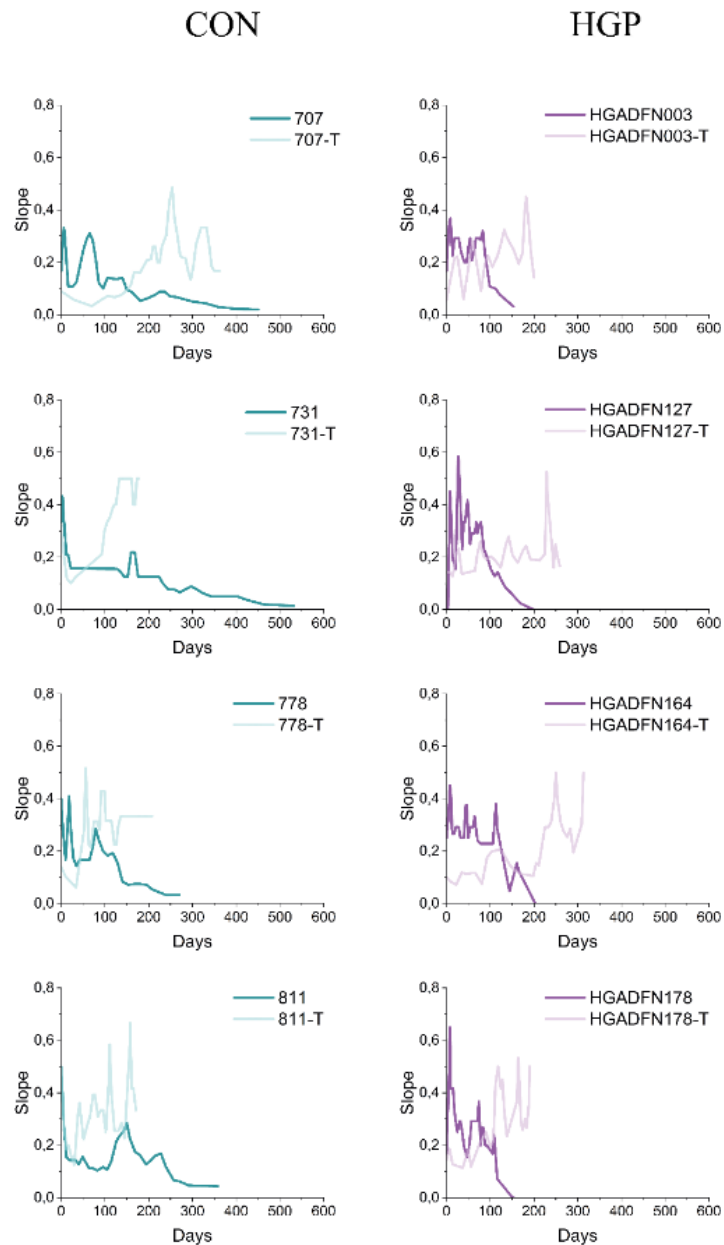


Fig. S17

Amount of *PPP2R2C* mRNA in lymphoblastoid cells (LCLs) from participants of the BASE-II correlated with telomere length, as measured by monochrome multiplex qPCR, which is described in the Materials and Methods section. All values are normalized to the level (=100%) of mRNA of the median of the TL. Data are shown for 413 LCLs (each analyzed in technical triplicates).

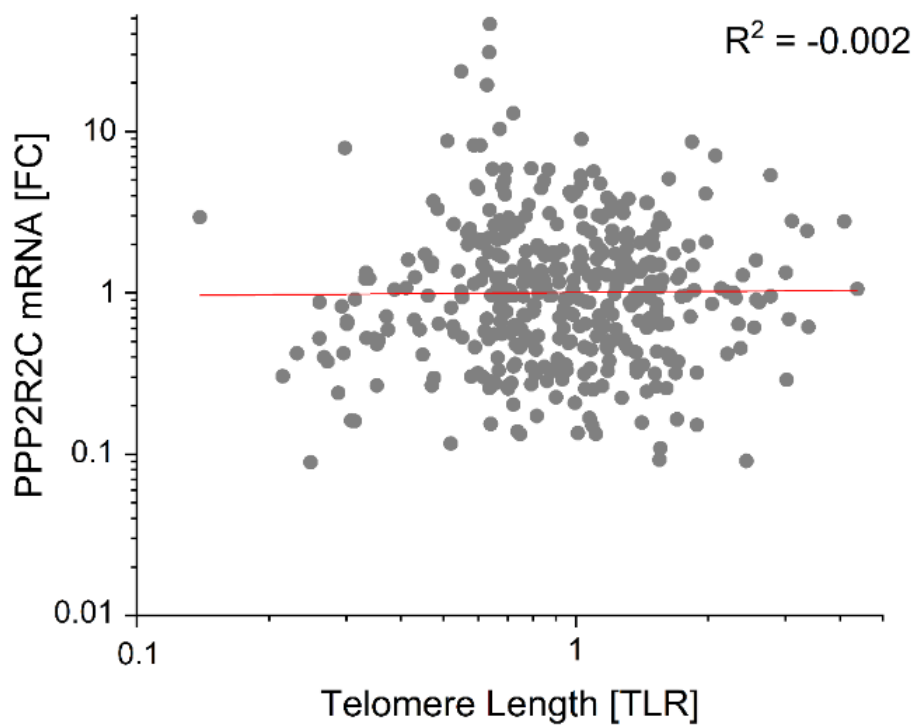


Fig. S18

mRNA levels of the four PPP TPE-OLD candidates and all confirmed TPE-OLD genes in LCLs and HUVECs with long and short telomeres. qPCR analysis was performed under basal conditions (10% FCS), in cells with long telomeres (low PDs in HUVECs) and in cells with short telomeres (high PDs in HUVECs). TL was measured by monochrome multiplex qPCR, as previously described. *Cyclophilin A* was used as an internal normalization control. All values were normalized to the level (=100%) of mRNA in cells with long telomeres. P-values indicate significance of the difference for assays done in duplicate using technical triplicates (total of six measurements). Data are shown as the mean \pm SD, the mean and median are shown. The Mann-Whitney U test was employed to assess statistical significance. * indicates $p < 0.05$ and ** $p \leq 0.01$ for an increase relative to low PD/long telomeres; # indicates $p < 0.05$ and ## $p \leq 0.01$ for a decrease relative to low PD/long telomeres (**A**) Overall summarized data shown for LCLs (**B**) Overall summarized data shown for HUVECs. For HUVECs the TL was measured in technical triplicates, the average of the three measurements (performed on different days) was used to report the mean TL.

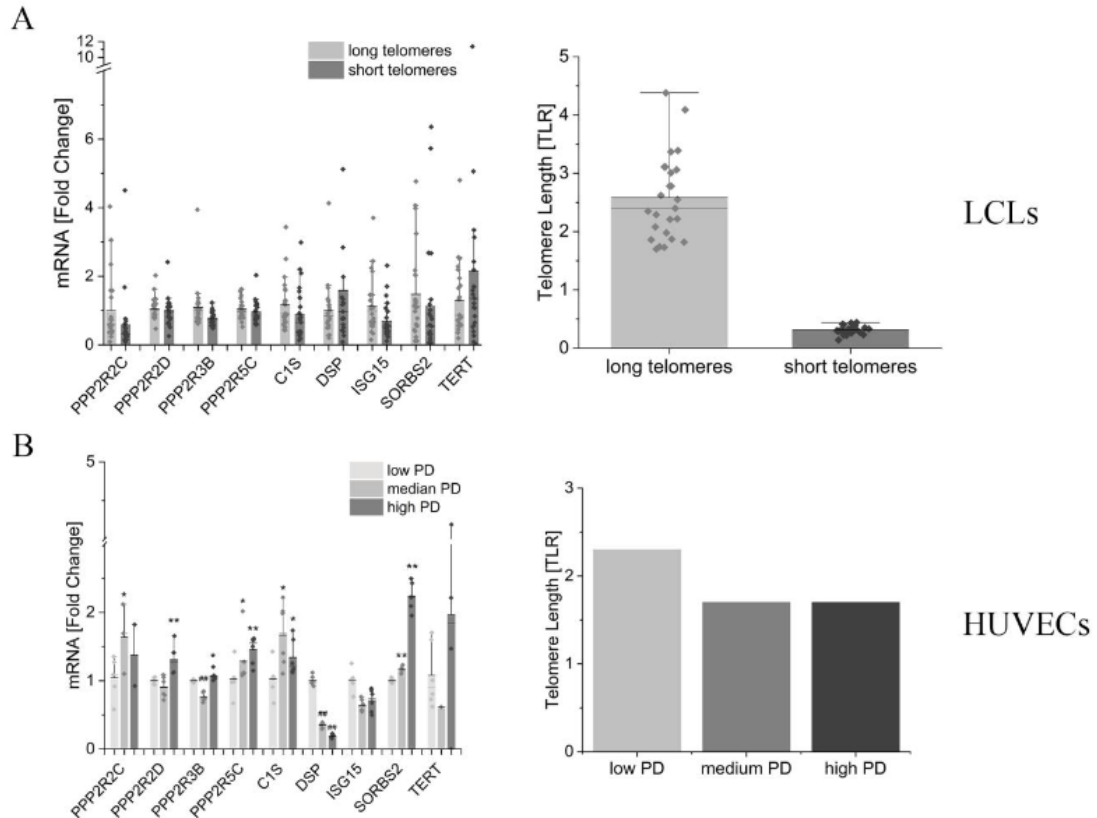
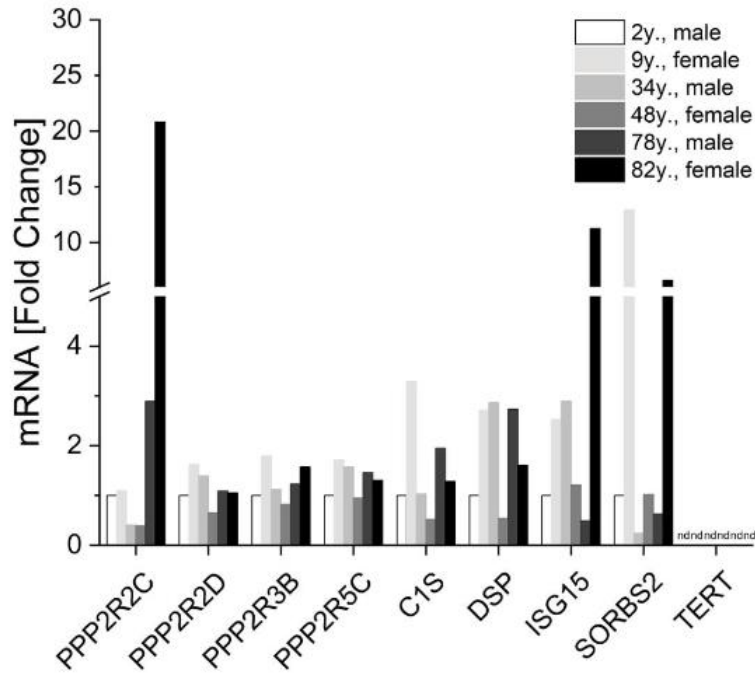


Fig. S19

mRNA levels of *PPP2R2C* in fibroblasts derived from cell donors of different ages. qPCR analysis was performed under basal conditions (10% FCS), in cells with long telomeres and in cells with short telomeres from donors of different ages. *Cyclophilin A* was used as an internal normalization control. All values were normalized to the level (=100%) of mRNA in cells with long telomeres. All assays were done twice and are shown as mean of technical triplicates **(A)**, qPCR data derived from samples of an array expression experiment (A. Herman group). Cells were harvested at high PDs >35. **(B)**, Data derived from samples of an independent experiment (M. Walter group) of different cell donors derived from children and one middle-aged woman (cell line N14 in Table S7). Cells were harvested at both low PD and high PDs. *Cyclophilin A* was used as an internal normalization control. All values were normalized to the level (=100%) of mRNA in cells with long telomeres. n.d., not detectable

A



B

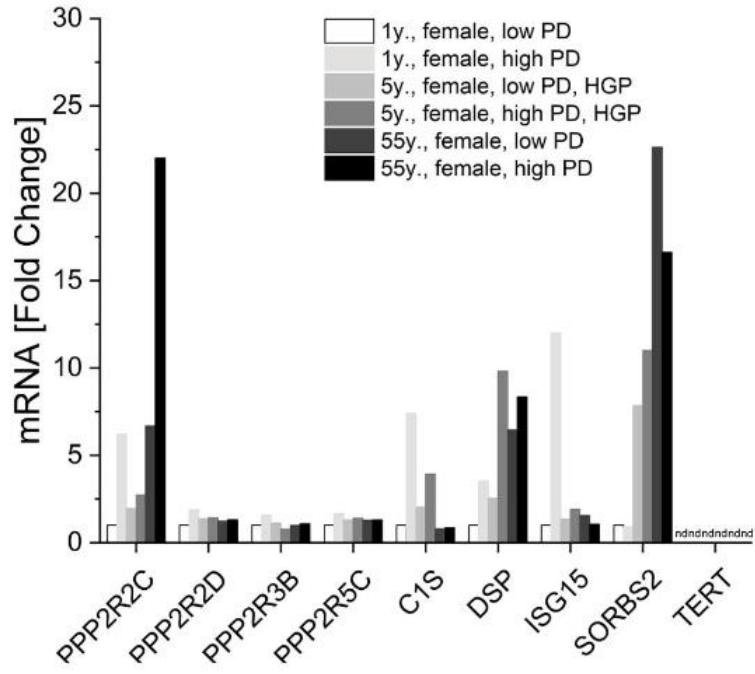
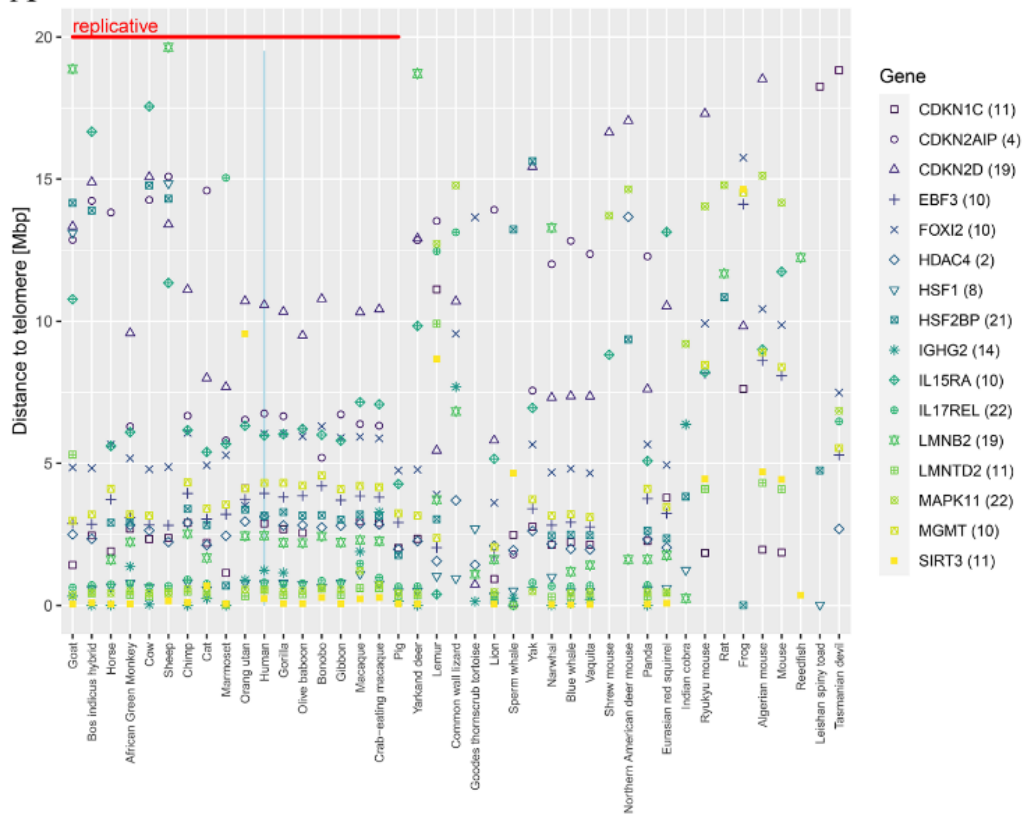


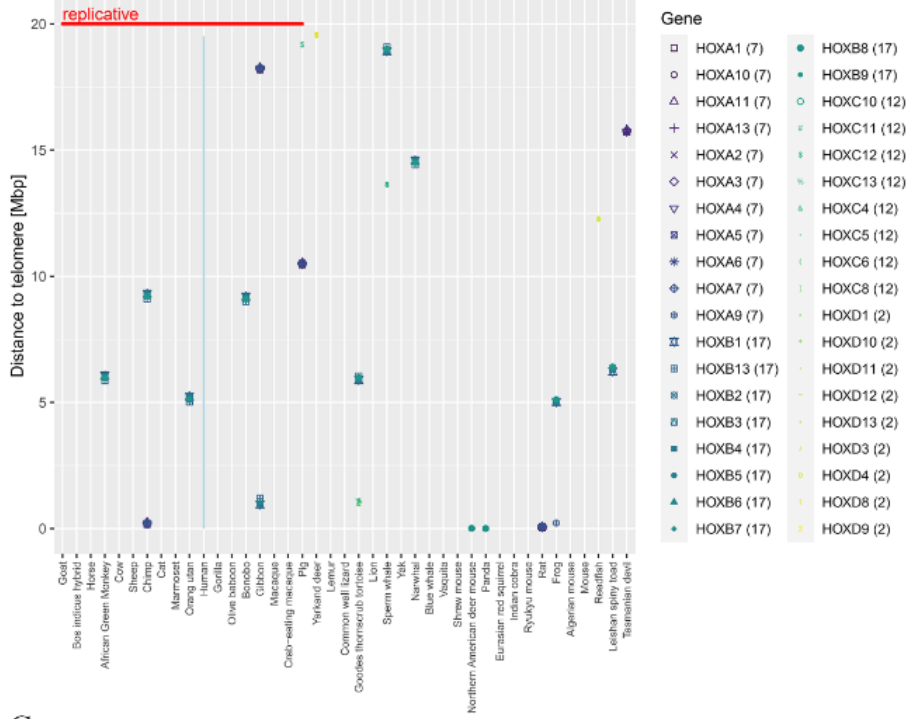
Fig. S20**Selected genes and gene families sorted by species and distance to telomeres:**

Telomeric distances for TPE-OLD candidate genes. The figure shows the distance to the closest telomere in Mb for selected TPE-OLD candidate genes. Genes are distinguished by their symbol, supported by color. Species are separated horizontally, sorted by the median distance to telomeres for all genes in the genome. Species proposed to age replicatively are grouped on the left. Telomeric distances among TPE-OLD genes are preserved across species such that these appear as horizontal lines on the left. The number in parentheses behind the gene name indicates the human chromosome coding for that gene.

(A) TPE-OLD candidate genes often code for factors involved in cell cycle regulation, tumor suppression, stress response, immune defense and metabolic regulation. Examples for TPE-OLD candidates are tumor suppressor genes (*EBF*, *CDKN1C*, *CDKN2D*), stress response genes and metabolic regulators (*HSF1*, *MAPK11*, *FOXI2*), regulators of epigenetic silencing (*SIRT3*, *HDAC4*), DNA damage response genes (*HSF2BP*, *MGMT*, *CDKN2AIP*), defense response genes (*IL17REL*, *IL15RA*, *IGHG2*) but also genes coding for proteins whose expression increases or declines during aging for unknown reasons such as some coagulation factors or lamins (*LMNB2*). Within the respective gene group, only individual members are TPE-OLD candidates. Some gene families seem to have no TPE-OLD genes at all such as *HOX* (B) and *NF- κ B* (C).

A

B



C

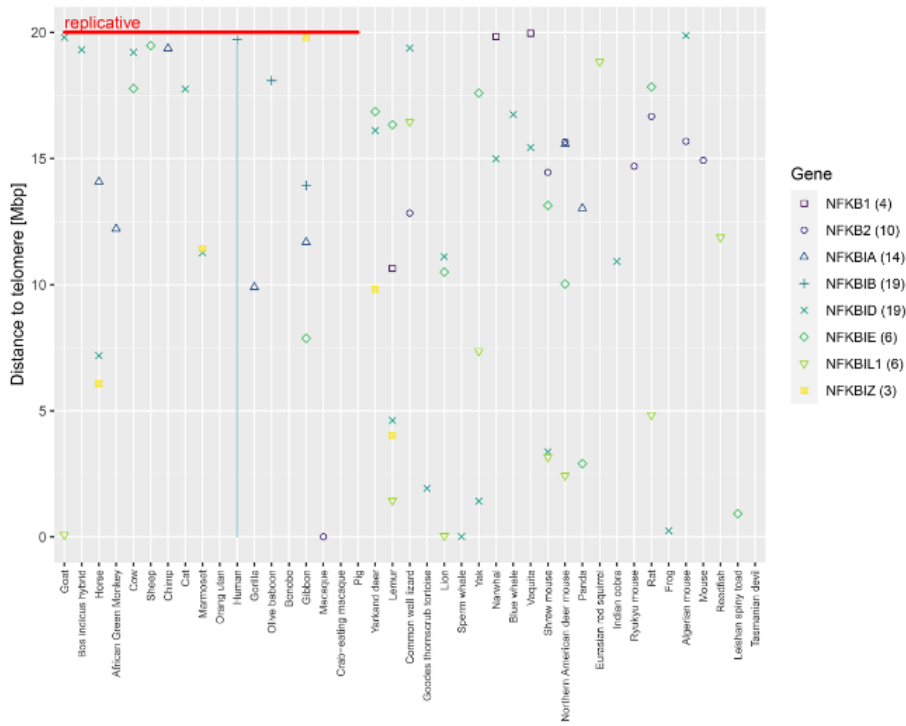
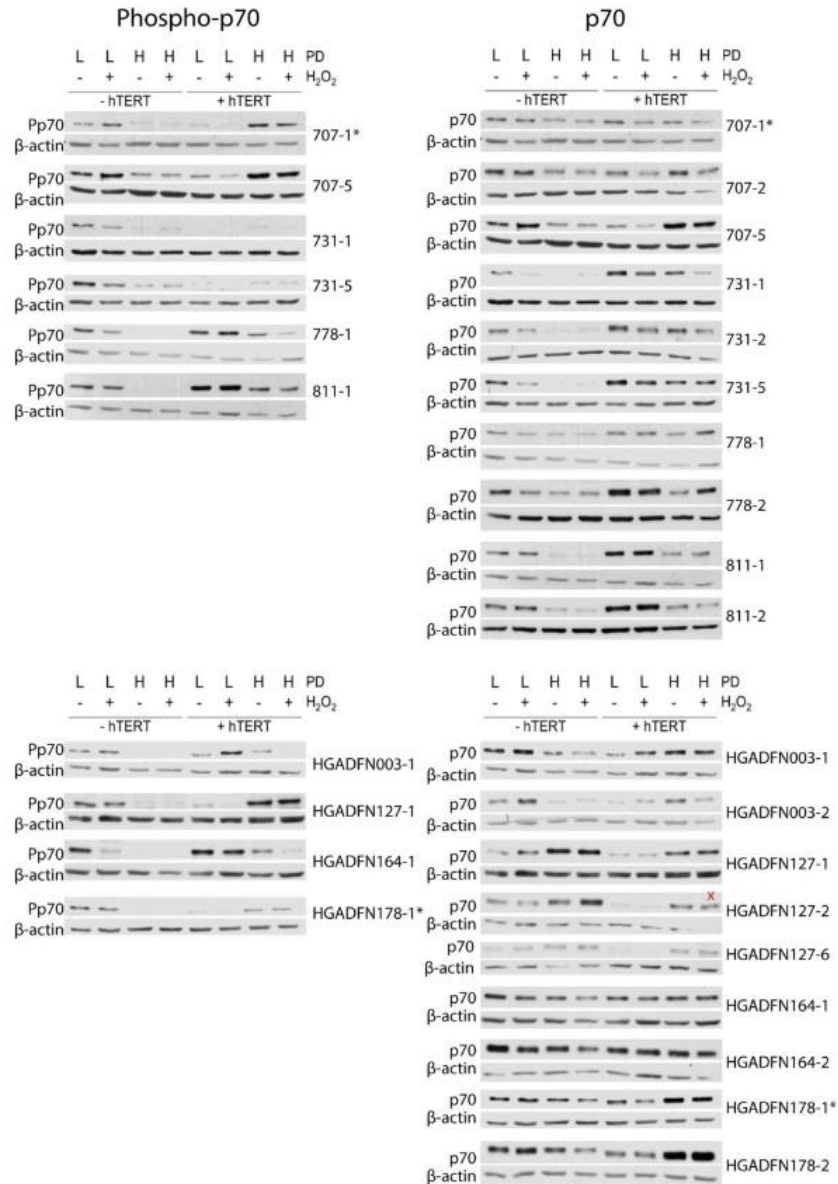
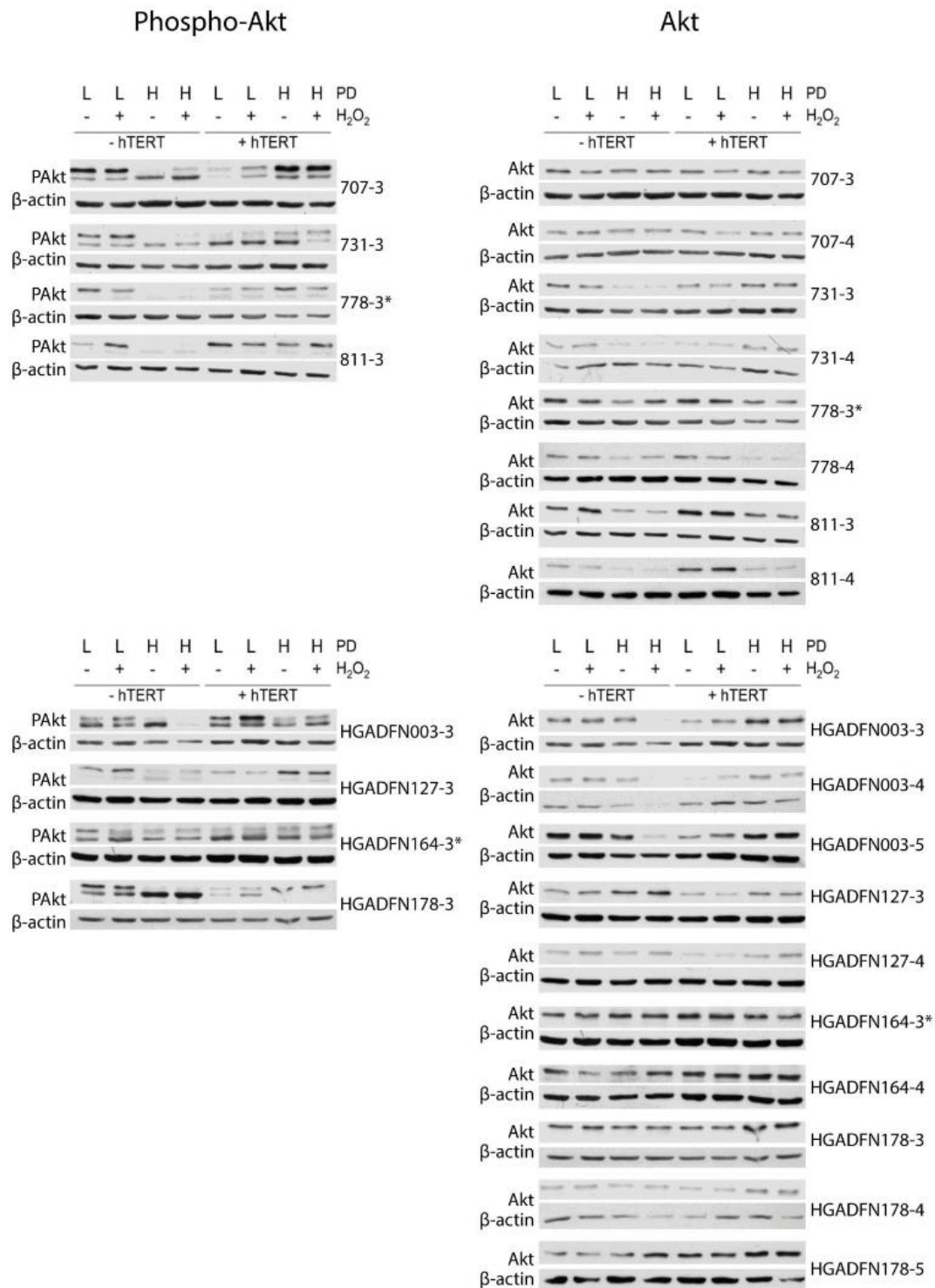


Fig. S21

Original Western blot data. Original Western blots of Fig. 5. *Indicates the blots shown for Fig. 5a-c. The blots (per cell line) are numbered according to their order of preparation. Blots with the same cell line and number were incubated with different antibodies. Red crosses indicate single lanes that were excluded from analysis because of loss of sample due to edge effects.





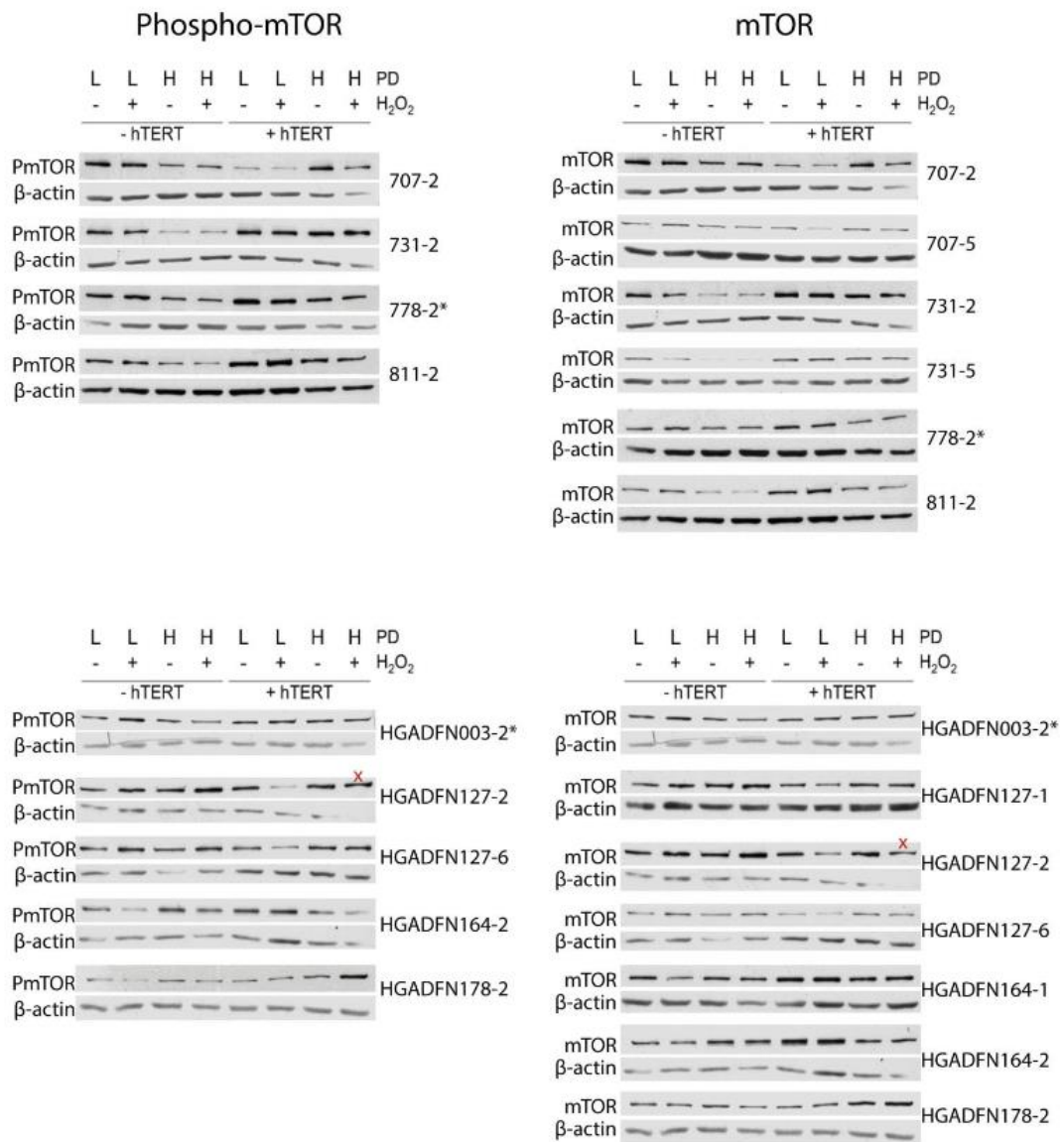


Fig. S22

Original Western blot data. Original Western blots of Figs. S13 and S15. **(A)** Serum starvation indicated with + or – sampled for cells with short telomeres (S) and long telomeres (L). **(B)** Original data for the *PPP2R2C* siRNA experiment: effect on p70S6K and P-p70S6K with different siRNA concentrations.

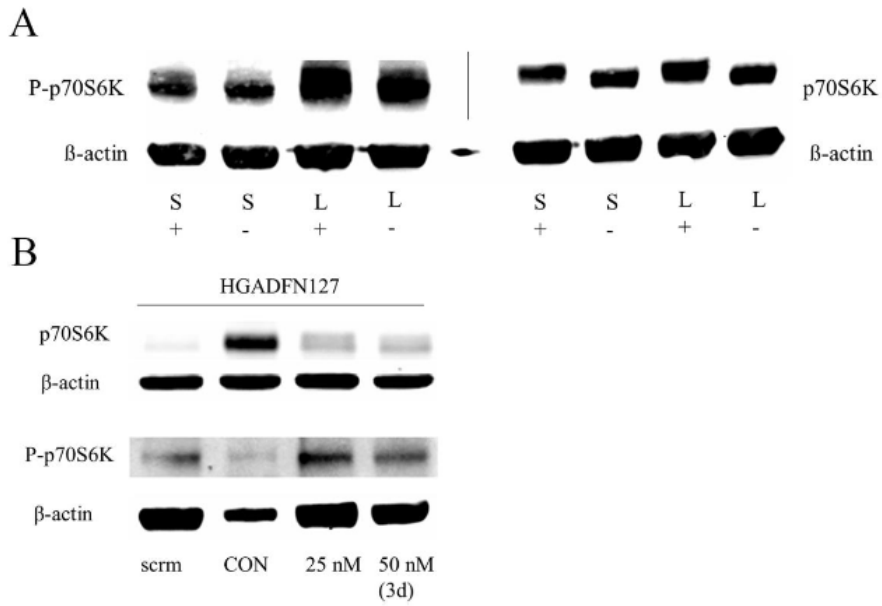


Table S1.

Regulation of gene expression with progressive telomere shortening in established and new TPE-OLD candidates. Green color, previously known or suggested TPE-OLD genes; dark green; TPE effect additionally confirmed by FISH; blue color, members of the phosphatase (PP2A) family investigated in this study

	Myoblasts¹	Fibroblasts^{1,2}	LCL	HUVEC
AKAP3	↑	n/a	n/a	n/a
ANO2	↑	n/a	n/a	n/a
C1S	↑	↑	~	↑
CCND2	↑	↑	n/a	n/a
CD163L1	↑	n/a	n/a	n/a
CD9	↓	n/a	n/a	n/a
DSP	↑	↑	~	↓
FOXM1	↓	n/a	n/a	n/a
GALNT8	↑	n/a	n/a	n/a
ISG15	↑	↑	~	~
NDUFA9	↑	n/a	n/a	n/a
SORBS2	(↑)	n/a	n/a	↑
TEAD4	↓	↓	n/a	n/a
TERT	n/a	(↑)	~	~
TIGAR	↑	n/a	n/a	n/a
TSPAN9	↑	n/a	n/a	n/a
PPP2R2C	n/a	↑	~	↑
PPP2R2D	n/a	~	~	↑
PPP2R3B	n/a	~	~	~
PPP2R5C	n/a	~	~	↑


n/a, no data available; ↑, higher expression in cells with short telomeres; ↓, lower expression in cells with short telomeres; ~, no significant change or inconclusive results; brackets, detectable in pathogenic context only (SORBS2) or for not full-length mRNA (TERT); 1, from references Robin et al. (SORBS2) (9), Robin et al. (all others) (10); 2, from references Kim et al. (TERT) (12); Lou et al (ISG15) (11).

Table S2: Ranking of TPE-OLD candidate genes. This table presents all 2322 genes that are TPE-OLD candidate genes, ranked by the number of orthologues that are at the same telomeric distance. The first two columns (x and y) provide the mean of the telomeric distances of the two 1 Mb-wide chromosomal regions that contain most of the orthologues. The columns num.x and num.y show the respective number of orthologues covered by that region and num.xy is the sum of these two, by which the gene is ranked. The next column indicates the human chromosome on which the gene is located and the last column indicates the name of the gene.


Table S2 is available as an excel file at: <https://doi.org/10.5281/zenodo.6477501>

Table S3.**Gene set enrichment analysis of all TPE-OLD candidate genes with g:Profiler**

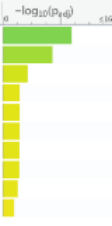
Genes from Table S1 were entered into g:Profiler (19, 20); p values are color-coded from yellow (insignificant) to blue (highly significant).

GO:MF		stats			
Term name	Term ID	P _{adj}			Show evidence codes
arylsulfatase activity	GO:0004065	2.020×10 ⁻²			
protein binding	GO:0005515	2.315×10 ⁻²			
sulfuric ester hydrolase activity	GO:0008484	4.509×10 ⁻²			


1 to 3 of 3 |< < Page 1 of 1 > >|

GO:BP		stats			
Term name	Term ID	P _{adj}			Show evidence codes
cellular metabolic process	GO:004237	8.043×10 ⁻³			
metabolic process	GO:0008152	2.237×10 ⁻²			

1 to 2 of 2 |< < Page 1 of 1 > >|

GO:CC		stats			
Term name	Term ID	P _{adj}			Show evidence codes
cytoplasm	GO:0005737	2.164×10 ⁻¹⁰			
intracellular anatomical structure	GO:0005622	1.119×10 ⁻⁷			
membrane-bounded organelle	GO:0043227	3.605×10 ⁻⁴			
intracellular organelle lumen	GO:0070013	4.534×10 ⁻³			
organelle lumen	GO:0043233	4.534×10 ⁻³			
membrane-enclosed lumen	GO:0031974	4.534×10 ⁻³			
intracellular membrane bounded organelle	GO:0043231	4.978×10 ⁻³			
organelle	GO:0043226	5.650×10 ⁻³			
cytosol	GO:0005829	9.236×10 ⁻³			
intracellular organelle	GO:0043229	3.040×10 ⁻²			

1 to 10 of 10 |< < Page 1 of 1 > >|

KEGG		stats			
Term name	Term ID	P _{adj}			Show evidence codes
Metabolic pathways	KEGG:01100	2.467×10 ⁻³			
Thermogenesis	KEGG:04114	4.447×10 ⁻³			
Diabetic cardiomyopathy	KEGG:05415	1.633×10 ⁻²			

1 to 3 of 3 |< < Page 1 of 1 > >|

REAC		stats		
Term name	Term ID	Padj	$-\log_{10}(P_{adj})$	Show evidence codes
Gamma carboxylation, hypusine formation and arylsulfatase...	REAC:R-HSA-16...	3.379×10^{-3}		

1 to 1 of 1 < > Page 1 of 1 >

MIRNA		stats		
Term name	Term ID	Padj	$-\log_{10}(P_{adj})$	Show evidence codes
hsa-miR-331-3p	MIRNA:hsa-miR...	2.184×10^{-3}		
hsa-miR-6791-5p	MIRNA:hsa-miR...	1.554×10^{-2}		
hsa-miR-106b-3p	MIRNA:hsa-miR...	2.118×10^{-2}		
hsa-miR-615-3p	MIRNA:hsa-miR...	2.258×10^{-2}		

1 to 4 of 4 < > Page 1 of 1 >

HPA		stats		
Term name	Term ID	Padj	$-\log_{10}(P_{adj})$	Show evidence codes
bronchus	HPA:0060000	1.601×10^{-2}		
placenta; decidua cells[Low]	HPA:0380511	4.132×10^{-2}		

1 to 2 of 2 < > Page 1 of 1 >

CORUM		stats		
Term name	Term ID	Padj	$-\log_{10}(P_{adj})$	Show evidence codes
CBP complex	CORUM:642	1.218×10^{-2}		

1 to 1 of 1 < > Page 1 of 1 >

HP		stats		
Term name	Term ID	Padj	$-\log_{10}(P_{adj})$	Show evidence codes
Mitochondrial inheritance	HP:0001427	5.562×10^{-6}		
Ventricular preexcitation	HP:0004309	1.289×10^{-4}		
Centrocecal scotoma	HP:0000576	2.278×10^{-3}		
Diffuse cerebral atrophy	HP:0002506	3.105×10^{-3}		
Leber optic atrophy	HP:0001112	4.145×10^{-3}		
Wolff-Parkinson-White syndrome	HP:0001716	6.781×10^{-3}		
Ragged-red muscle fibers	HP:0003200	7.181×10^{-3}		
Central retinal vessel vascular tortuosity	HP:0007768	1.348×10^{-2}		
Retinal arterial tortuosity	HP:0000631	1.348×10^{-2}		
Postural tremor	HP:0002174	2.490×10^{-2}		
Mitochondrial respiratory chain defects	HP:000125	3.118×10^{-2}		
Impaired visuospatial constructive cognition	HP:0010794	3.579×10^{-2}		
Stroke-like episode	HP:0002401	3.607×10^{-2}		
Slow decrease in visual acuity	HP:0007924	3.724×10^{-2}		

1 to 14 of 14 < > Page 1 of 1 >

Table S4

Functional gene groups

GENE FAMILY	ALL GENES	TPE GENES	RR	FUNCTION	INVOLVED IN
ZNF	388	99	1.609	DNA binding proteins	transcriptional regulation, development, protein degradation, DNA repair
SNO	293	60	1.291	glutamine amidotransferases	pyridoxine biosynthesis, response to nutrient limitation
KCN	97	19	1.235	potassium channels	antagonism of insulin secretion
RAB	89	17	1.205	small G proteins	vesicular transport; organelle formation; cell growth and development
PPP	81	16	1.246	serine/threonine phosphatases	cell growth and energy metabolism
MRP	79	16	1.277	ATP-binding cassette transmembrane proteins	export of organic anions and drugs
WDR	62	16	1.628	WDR domain proteins	DNA damage sensing; DNA repair, protein degradation, epigenetic regulation and immunity
FBX	62	12	1.221	F-box proteins	protein degradation and hematopoiesis
ADA	58	14	1.522	adenosine deaminases	purine metabolism; immunity
SER	57	17	1.881	serine proteases	myeloid and lymphoid immunity, embryological growth and synaptic plasticity
POL	55	13	1.491	DNA polymerases	DNA repair
FOX	54	11	1.285	transcription factors	cell growth and development
MAG	48	14	1.840	cancer-associated proteins	stress adaptation
ABC	46	9	1.234	ATP binding proteins	drug resistance
UBE	43	11	1.613	ubiquitination factors	protein degradation
ZBT	43	10	1.467	DNA binding proteins	development
IL1	42	8	1.201	cytokines	regulation of immune and inflammatory responses to infections or sterile insults
TBC	40	11	1.734	GAP domain proteins	cell growth
GAL	39	11	1.779	galactose transfer proteins	metabolism; innate and adaptive immunity
CFA	38	8	1.328	poly(ADP-ribose) polymerases	ADP ribosylation; tumor suppressor mechanisms
GOL	36	21	3.680	Golgi proteins	vesicular transport and Golgi architecture
SCA	36	11	1.927	transcription factors	neuroprotection
PRK	35	7	1.261	serine/threonine kinases	regulation of meiosis and mitosis
MET	34	8	1.484	receptor tyrosine kinases	cell growth
CAC	31	9	1.831	calcium channels	cell-to-cell communication, neurotransmission and neuroprotection
FGF	31	7	1.424	growth factors	cell growth
PRS	28	11	2.478	phosphoribosylpyrophosphate synthetases	ATP dependent cellular metabolism, cell growth and DNA repair
CHR	28	7	1.698	CHR domain proteins	transcriptional regulation of the cell cycle
SH3	26	7	1.698	SH3 domain proteins	signaling pathways regulating the cytoskeleton and cell growth (Ras, Src)
ZFP	25	7	1.786	DNA binding proteins	regulation of transcriptional and translational processes
IGH	23	19	5.211	immunoglobulin heavy locus proteins	adaptive immunity
KLK	19	10	3.320	serine proteases	innate immunity and tissue specific functions (neural plasticity, amyloid hydrolysis)
LCN	9	9	6.308	transcriptional regulators	cell growth, DNA repair, ubiquitination and tumor suppression

Genes are aggregated to their first three letters that commonly indicate a gene family. The column "ALL GENES" presents the number of members in the whole genome, the "TPE-GENES" column the number among the selected TPE-OLD candidates. RR is the ratio of the relative frequency in the TPE-OLD subset to the relative frequency in the genome. The PPP genes are among the most abundant of TPE-OLD candidates.

Table S5.
Control and patient fibroblast cell lines

Cell Line	Age, Sex	Molecular Defect	Primary Cells*		Immortalized Cells*	
			PD Low	PD High	PD Low	PD High
707	5 month, female	no	17 [0.72]	54 [0.20]	18 [0.60]	70 [1.59]
731	5 month, male	no	13 [0.71]	55 [0.15]	16 [0.71]	56 [2.91]
778	8 month, male	no	15 [0.48]	41 [0.16]	14 [1.18]	66 [2.72]
811	1 month, female	no	15 [0.81]	49 [0.24]	28 [1.18]	63 [2.84]
HGADFN003	2 years 0 month, male	Exon 11 mutation C->T, clinically affected	19 [0.68]	34 [0.46]	34 [1.44]	63 [0.87]
HGADFN127	5 years 0 month, female	Exon 11 mutation C->T, clinically affected	19 [0.52]	40 [0.24]	15 [0.96]	57 [2.74]
HGADFN164	4 years 8 month, female	Exon 11 mutation C->T, clinically affected	19 [0.28]	42 [0.17]	15 [0.67]	64 [1.10]
HGADFN178	6 years 11 month, female	Exon 11 mutation C->T, clinically affected	20 [0.47]	34 [0.28]	22 [1.03]	59 [1.54]
N14	55 years, female	no	18 [1.11]	39 [0.78]		52 [2.65]
Young1 [#]	2 years, male	no		42		
Young5 [#]	9 years, female	no		38		
Midage1 [#]	34 years, male	no		43		
Midage3 [#]	48 years, female	no		40		
Old1 [#]	78 years, male	no		37		
Old2 [#]	82 years, female	no		40		

* Mean telomere length in brackets next to the PD (population doubling number). Telomere length was measured using a monochrome multiplex qPCR. The PD was calculated as follows: $((\text{current cell number} / \text{previous cell number})^{\log})^{0.3}$. # These cell lines were only analyzed in high passage.

Table S6.**Log-transformed distance between the gravity centers after 3D-reconstruction**

Results of hierarchical linear models. The table shows the results of hierarchical linear models (HLMs) with the intracellular probe distances in gravity centers after 3D reconstruction as dependent variables. There was no significant difference between progeria cell lines and control cell lines before immortalization (mean difference -0.03, $p=0.72$), and immortalized cells showed significantly lower distances than nonimmortalized cells: mean difference = -0.34, $p < 0.0001$. The effect of immortalization did not differ between progeria cell lines and control cell lines: mean difference after immortalization: 0.03, $p = 0.76$. Similar results were found for all shortest and longest probe pair distances per cell.

Parameter	Distance AB		Distance CD		Combined distance AB and CD [#]	
	β (95%-confidence interval)	p-value	β (95%-confidence interval)	p-value	β (95%-confidence interval)	p-value
Progeria cells versus control cells	-0.03 (-0.22 to 0.16)	0.76	-0.04 (-0.25 to 0.17)	0.72	-0.03 (-0.22 to 0.15)	0.72
Immortalisation versus no immortalisation	-0.38 (-0.52 to -0.25)	< 0.0001	-0.29 (-0.41 to -0.17)	< 0.0001	-0.34 (-0.43 to -0.25)	< 0.0001
Immortalisation in Progeria cells versus immortalisation in control cells	0.04 (-0.15 to 0.23)	0.67	0.004 (-0.17 to 0.17)	0.97	0.02 (-0.11 to 0.15)	0.76

Distances AB (shortest probe distance) and CD (longest probe distance) nested within cells and cells nested within cell lines.

Publication 2: Telomere attrition and dysfunction: a potential trigger of the progeroid phenotype in nijmegen breakage syndrome.

Habib R, Kim E, Neitzel H, Demuth I, Chrzanowska K, Seemanova E, Faber R, Digweed M, Voss R, **Jäger K**, Sperling K, Walter M.

Aging 2020;12(12):12342-12375

DOI: 10.18632/aging.103453

Impact factor (2021): 5.95

Telomere attrition and dysfunction: a potential trigger of the progeroid phenotype in nijmegen breakage syndrome

Raneem Habib^{1,2}, Ryong Kim^{2,3}, Heidemarie Neitzel², Ilja Demuth^{4,5}, Krystyna Chrzanowska⁶, Eva Seemanova⁷, Renaldo Faber⁸, Martin Digweed², Reinhard Voss⁹, Kathrin Jäger^{10,11}, Karl Sperling^{2,*}, Michael Walter^{10,11,*}

¹Department of Human Genetics, Ruhr-University Bochum, Bochum, Germany

²Institute of Medical and Human Genetics, Charité - Universitätsmedizin Berlin, Berlin, Germany

³Institute of Clinical Chemistry, Red-Cross General Hospital, Pyongyang, Democratic People's Republic of Korea

⁴Department of Endocrinology and Metabolism, Charité – Universitätsmedizin Berlin, Corporate Member of Freie Universität Berlin, Humboldt-Universität zu Berlin, Berlin Institute of Health, Germany

⁵Charité - Universitätsmedizin Berlin, BCRT - Berlin Institute of Health Center for Regenerative Therapies, Berlin, Germany

⁶Department of Medical Genetics, The Children's Memorial Health Institute, Warsaw, Poland

⁷Department of Clinical Genetics, Institute of Biology and Medical Genetics, Second Medical School, Charles University, Prague, Czech Republic

⁸Center for Prenatal Medicine, Leipzig, Germany

⁹Integrated Functional Genomics, Interdisciplinary Center for Clinical Research, University of Münster, Münster, Germany

¹⁰Institute of Clinical Chemistry and Laboratory Medicine, University of Rostock, Rostock, Germany

¹¹Institute of Laboratory Medicine, Clinical Chemistry and Pathobiochemistry, Charité – Universitätsmedizin Berlin, Corporate Member of Freie Universität Berlin, Humboldt-Universität zu Berlin, Berlin Institute of Health, Germany

*Co-senior authors

Correspondence to: Michael Walter; **email:** michael.walter@med.uni-rostock.de

Keywords: nijmegen breakage syndrome, telomere-position effect over long distances, alternative lengthening of telomeres, nibrin, DNA repair

Received: January 8, 2020

Accepted: May 27, 2020

Published: June 20, 2020

Copyright: Habib et al. This is an open-access article distributed under the terms of the Creative Commons Attribution License (CC BY 3.0), which permits unrestricted use, distribution, and reproduction in any medium, provided the original author and source are credited.

ABSTRACT

Background: Nibrin, as part of the NBN/MRE11/RAD50 complex, is mutated in Nijmegen breakage syndrome (NBS), which leads to impaired DNA damage response and lymphoid malignancy.

Results: Telomere length (TL) was markedly reduced in homozygous patients (and comparably so in all chromosomes) by ~40% (qPCR) and was slightly reduced in NBS heterozygotes older than 30 years (~25% in qPCR), in accordance with the respective cancer rates. Humanized cancer-free NBS mice had normal TL. Telomere elongation was inducible by telomerase and/or alternative telomere lengthening but was associated with abnormal expression of telomeric genes involved in aging and/or cell growth. Lymphoblastoid cells from NBS patients with long survival times (>12 years) displayed the shortest telomeres and low caspase 7 activity.

Conclusions: NBS is a secondary telomeropathy. The two-edged sword of telomere attrition enhances the cancer-prone situation in NBS but can also lead to a relatively stable cellular phenotype in tumor survivors. Results suggest a modular model for progeroid syndromes with abnormal expression of telomeric genes as a molecular basis.

Methods: We studied TL and function in 38 homozygous individuals, 27 heterozygotes, one homozygous fetus, six NBS lymphoblastoid cell lines, and humanized NBS mice, all with the same founder *NBN* mutation: c.657_661del5.

INTRODUCTION

Nijmegen breakage syndrome (NBS) was first described in 1981 in two patients in Nijmegen, in the east of the Netherlands [1]. It is characterized by chromosome instability associated with microcephaly, immunodeficiency, hypersensitivity to ionizing irradiation, and a high predisposition to cancer [2–4]. NBS also displays other symptoms of aging such as postnatal growth retardation, decline in mental function, gray hair, telangiectasias and café au lait spots. Nibrin, a DNA double-strand break (DSB) repair protein, is defective [5, 6], and more than 90% of NBS patients are homozygous for a founder mutation: c.657_661del5 [6–8]. Risk of death from lymphoma is elevated ~1000-fold; by the age of 20, more than 40% of patients have developed a malignant disease, predominantly of lymphoid origin. Even heterozygous carriers of the founder mutation have an increased risk of cancer [8]. In some areas of the world, the *NBN* gene became the most important cancer-predisposing gene [7].

Nibrin is part of the nibrin/Mre11/Rad50 (MRN) complex, which is involved in the repair of DNA double strand breaks (DSBs), the processing of DSBs in immune gene rearrangements, and meiotic recombination [9]. The important role of this complex in mediating the ATM-dependent repair of DSBs probably explains the predisposition to cancer and immunodeficiency in NBS. It is unclear, however, why the incidence of cancer is so much higher in NBS than in other genetic instability syndromes. Nibrin is multifunctional and may also play an important role in protecting the telomeres from inappropriate DNA repair. Telomeric DNA is an evolutionarily highly conserved repetitive sequence that plays a crucial role both in cellular senescence and in carcinogenesis. The exact role of the MRN complex and nibrin in particular in telomere homeostasis is not clear, even though there have been some groundbreaking experimental findings in recent years pointing to a key function in the response to dysfunctional telomeres [10, 11]. Unlike in *S. cerevisiae*, mammalian MRN is not required for association of telomerase to short telomeres [12]. However, experimental *in vitro* and animal data suggest that the MRN complex is required for activation of the ATM-dependent repair of dysfunctional telomeres, the resection of telomeric DNA to create the single-stranded 3' overhang and for stabilization of telomeric T-loops, which is required for telomere replication and elongation [13, 14]. Telomeres recruit Mre11, phosphorylated nibrin, and ATM, which is important for protection and repair of telomeres [15, 16]. The MRN complex protects the leading-strand ends from non-homologous end joining (NHEJ) [17], whereby the telomeres seem to recruit Mre11, phosphorylated nibrin and ATM in every G2 phase of the cell cycle and thus

promote the formation of a chromosome end protection complex and a localized DNA damage response [18]. It was proposed that nibrin is required for the proper assembly of the MRN complex, which includes ubiquitination of nibrin upon DSBs [19] and may indirectly influence ATM activation by Mre11 and Rad50 [20].

We therefore hypothesized that NBS is a telomeropathy [21, 22], and that telomere abnormalities may accelerate cancer manifestation. Shorter telomeres have been described in individual NBS cases, for both NBS lymphocytes [23, 24] and fibroblasts [25]. Nonetheless, a systematic investigation has not yet been carried out, and the importance of MRN in general and nibrin in particular for telomere length and function are unclear.

RESULTS

Telomere lengths in human NBS cells and in humanized NBS mice

Relative leukocyte TLs of blood DNA from 38 NBS homozygotes, 27 heterozygotes, and 108 control individuals were measured by qPCR. The mean relative TL of NBS-homozygotes was ~40% shorter in two age-matched groups (1-10 and 11-20 years) than in the control group ($p < 0.05$). We found mildly (~25%) reduced TLs in older NBS heterozygotes (>30 years old; $p = 0.1$) but not in younger heterozygotes (Figure 1 and Supplementary Tables 1–3).

For Q-FISH analysis, six NBS lymphoblastoid cell lines derived from three individuals with extremely short survival after cancer manifestation (<3 years), and from three individuals with remarkably long survival (>12 years) were analyzed. All six lymphoblastoid cell lines had TLs that were markedly reduced (by ~60-75%) relative to healthy controls ($p < 0.05$). Rather short telomeres were found on chromosomes 17, 19, and 20, but this pattern is also a characteristic of normal diploid cells [26], and no preferred shortening of a particular chromosome was observed (Figures 2 and 3).

A positive correlation was found between the TL measured by Q-FISH and the TL measured by qPCR ($r = 0.96$); (Supplementary Figure 1). Regression analysis was applied to transform the qPCR data into absolute TLs. In the formula $y = 3.4(X) + 10.11$, y represents the predicted TRF (Terminal Restriction Fragment) value in kb, X represents the qPCR (T/S) value. The qPCR data and the TRF values showed a moderate correlation ($r = 0.64$; Supplementary Figure 2).

A rather uniform TL distribution has been described for most fetal tissues of healthy individuals [27]. In

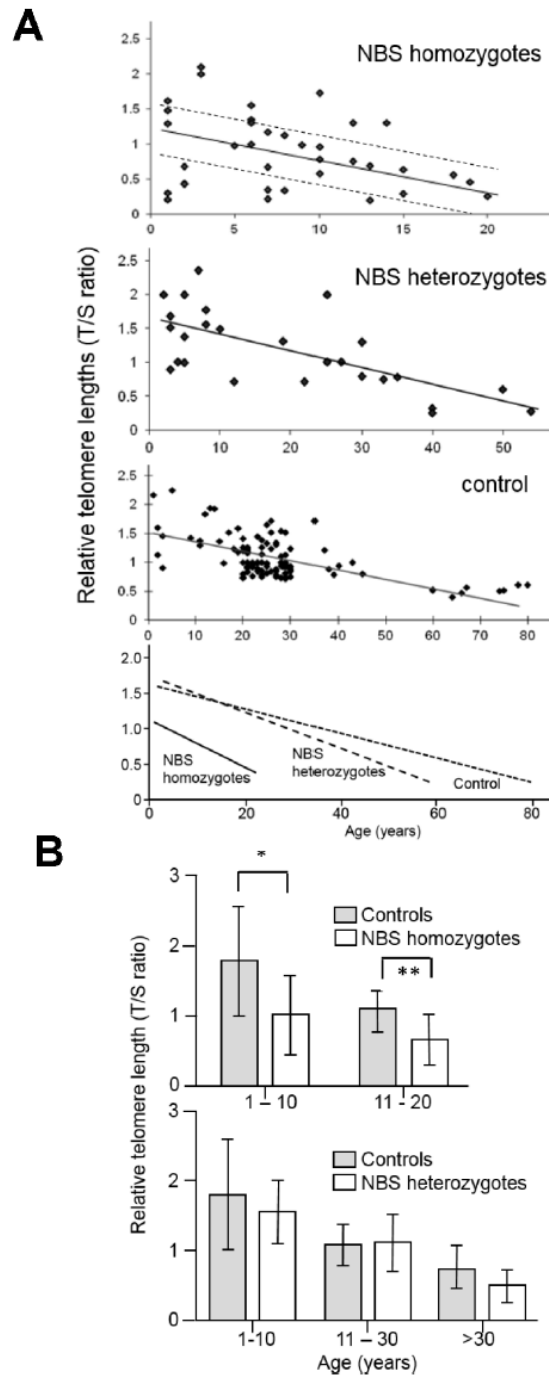


Figure 1. (A) Relative telomere length (TL) as a function of age in NBS homozygotes, heterozygotes, and control individuals. Relative TL (T/S ratio) was analyzed from blood samples of 38 NBS homozygotes, 27 NBS heterozygotes, and 108 control individuals by quantitative polymerase chain reaction (qPCR). The dashed lines separate the NBS homozygotes in those with long, medium, and short TL. Below: regression curves standardized for age. Original after thesis Raneem Habib [28]. (B) Comparison of TL, as analyzed by qPCR, of NBS homozygotes, heterozygotes, and controls. The comparison was made for age-matched groups (mean values and standard deviation). * indicates $p < 0.01$; ** indicates $p < 0.001$.

contrast, we found considerable differences in TLs between different fetal tissues: spinal cord and brain tissues had the longest telomeres, while fibroblasts and skin had the shortest, suggesting substantial telomere attrition in these tissues before birth (Figure 4B).

The common human NBN mutation c.657_661del5 is hypomorphic, allowing low-level, functionally relevant, truncated nibrin protein to be formed through an alternative initiation of translation. This is relevant because a loss of function leads to early embryonic lethality in mice [29]. *Nbn*^{-/-} mice with the human NBS allele display most of the human NBS characteristics with one exception: humanized NBS mice are not prone to early tumorigenesis [29]. The humanized mice analyzed in this investigation expressed the human *NBN* gene, generated by the introduction of the human allele including the 5 bp deletion into *Nbn*-deficient

mice (*Nbn*^{-/-}*NBN*^{del5}). The T/S ratio of control and *Nbn*-deficient mice showed some variability but we did not find significant differences in the TLs between the mice with the NBN founder mutation and the mice with the wild type allele (Figure 4A).

Genetic instability in human NBS cells

The NBS cell lines exhibited spontaneous aberrations, such as chromatid breaks and translocations, as previously described [1–6]. The NBS cell lines in this study displayed a markedly increased rate of chromatid breaks after irradiation (Supplementary Table 4). In one cell line (94P0307) we did find telomere fusions that had not been described in previous NBS studies. All individual telomeres of this line were shorter than those of the control line 06P0131 with one exception: the telomere of the p arm of one chromosome 19, which

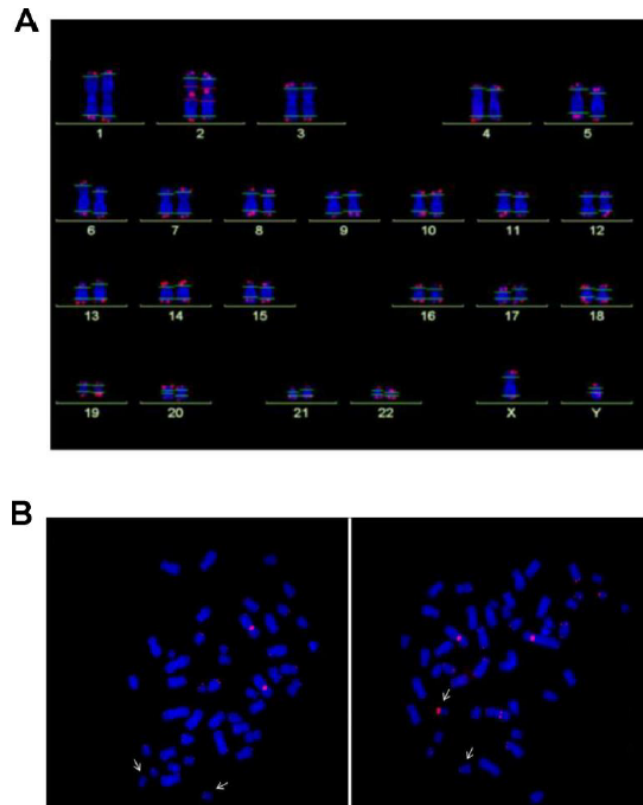


Figure 2. (A) Analysis of telomere length by Q-FISH. Normal karyogram with single telomeres stained for telomere repeats (Q-FISH) and a repetitive region in the centromeric region of chromosome 2. The horizontal lines overlaid on each chromosome define the measurement areas. (B) Metaphases of the NBS LCL 94P0307 after Q-FISH of the NBS cell line 94P0307 with very short telomeres and a telomere fusion. The arrows point to chromosomes 19. Left panel, Metaphase with weak telomeric fluorescence of both chromosomes 19; Right panel, Metaphase with one chromosome 19 with a brightly fluorescent telomere of the p-arm. The other bright signal is the reference region of chromosome 2. Original after thesis Raneem Habib [28].

showed an enormous variability in length (Figure 2B; Figure 3 and Supplementary Table 5), due to cellular mosaicism. This telomere was brightly fluorescent in approximately 70% of the metaphases with decreasing tendency during cultivation. The difference in relative T/C values was approximately 11:1 for the two chromosomes 19 (Supplementary Table 6). The expression of *hTERT* was weak in this and all other lymphoblastoid lines analyzed, close to the lower detection limit (Supplementary Figure 3), pointing to alternative lengthening of telomeres (ALT) as the most likely mechanism of telomere elongation in this cell line. Telomere dysfunction-driven genome damage associated with chromosomal break-fusion-bridge cycles and double-strand breaks are frequent in ALT cell lines [30]. In this context, we were interested that the cell line 94P0307 had twice as many aberrations (chromatid breaks and translocations) compared to the other two cell lines with long survival (Supplementary Table 4 and Supplementary Figure 4).

Abnormal regulation of telomeric genes in NBS cells

We investigated possible functional consequences of telomere elongation on 19p and of the expression of telomeric genes *per se*. Telomeres may loop to specific loci to regulate gene expression; this process is called TPE-OLD (telomere position effect over long distances) [31]. Individual genes or gene regulators close to the telomeres are silenced in young cells (with long telomeres) and become expressed when telomeres are short. Re-elongation of short telomeres in cells by exogenous expression of the *hTERT* gene (active telomerase) normally results in reorganization of functional telomeres and expression patterns similar to those in young cells with long telomeres, up to 10-15 Mbp away from the telomere [31]. We were interested to know if long 19p telomeres might influence the mRNA expression of telomeric genes. Using Affymetrix cDNA microarray analyses and fibroblasts from healthy volunteers and Hutchinson Gilford progeria (HGP) patients we identified ten genes on 19p that were differentially regulated at the level of mRNA in pre-senescent cells (with short telomeres) and in *hTERT* immortalized cells (with long telomeres) and that were not differentially regulated by UV-B irradiation as a model for stress-induced senescence (Supplementary Table 7 and Supplementary Figures 5–8).

As shown in Figure 5 and Supplementary Table 8, differential regulation in array experiments was confirmed by qPCR for all ten genes in the healthy control fibroblasts. The extremely elongated telomere of 19p in the lymphoblastoid cell line did not show any suppressive or enhancing effect on mRNA level (Figure 5). By contrast, the expression of all TPE-OLD

candidate genes was markedly altered in pre-senescent NBS fibroblasts. We observed lower mRNA levels for *BSG* (-61%), *GAMT* (-35%), *SCAMP4* (-52%), *OLFM2* (-90%), *COL5A3* (-92%), *CACNA1A* (-91%) and *NOTCH 3* (-42%), and we observed increases for *UHRF1* (12.5-fold), *RNASEH2A* (15.1-fold), and *DDX39A* (3.8-fold) in pre-senescent NBS compared to pre-senescent control fibroblasts. The telomere-dependent regulation was even reversed for *UHRF1*, *RNASEH2A*, *CACNA1A* and *DDX39A*. All TPE-OLD candidates encode proteins involved in senescence or cell growth. *BSG* encodes the metalloproteinase EMMPRIN that may trigger matrix metalloprotease and cytokine production and plays an important role in heart remodeling in aging mice [32]. The *GAMT* gene product guanidinoacetate methyltransferase catalyzes creatine synthesis, which may help to replenish cellular ATP [33], possibly for senescence-associated secretory phenotype (SASP) [34]. *SCAMP4* gene product secretory carrier membrane protein is a direct player in SASP [35]. The *OLFM2* gene product olfactomedin 2 is an age-dependent regulator of cell differentiation and regulates axonal growth [36]. *COL5A3* induces collagen synthesis and is involved in age-dependent tissue remodeling [37]. *CACNA1A* regulates calcium entry age-dependently and plays a role in neurodegeneration [38]. *NOTCH3* functions as a tumor suppressor by controlling p21-mediated cellular senescence [39]. By contrast, *UHRF1* is a negative regulator of senescence. Cellular senescence can be induced by phosphorylation and inactivation of UHRF1 [40]. *RNASEH2A* enhances migration and invasion and may play a role in cancerogenesis [41]. *DDX39A* is a RNA helicase and Telomeric Repeat Factor 2 (TRF2)-interacting protein with suspected roles in both cancer and longevity [42]. Altogether, these data suggest abnormal regulation of telomeric aging genes in NBS cells.

Relationship between telomeres length, disease progression, and cell pathology

There was no significant correlation between the TL and either the age at cancer manifestation or age at death (Table 1, Supplementary Table 9). This result was surprising insofar as we expected a worse phenotype in patients with short telomeres. Thus we explored the possibility that short telomeres may have stabilized the phenotype in a senescence-like state in all or in individual patients. To test this possibility, we measured caspase 7 activity as a surrogate marker for apoptosis. Senescent fibroblasts resist apoptosis by downregulating caspases. As shown in Table 2, caspase activity was significantly higher in the three cell lines derived from patients with shorter survival and longer telomeres compared to those with longer survival and shorter telomeres (2.8-fold; $P < 0.05$, 48h after 10 mg/ml

bleomycin). The cell line 94P0307 with the shortest telomeres displayed an extremely low (almost undetectable) caspase activity. Moreover, the cell lines derived from patients with shorter survival displayed on average twice as many chromatid breaks as the cells from patients with long survival (Supplementary Table 4). Altogether these data point to a more stable

phenotype with a higher “degree” of senescence in cells from patients with long survival.

There is a close functional link between ATM and nibrin [43]. As shown in Table 2, the radionimetic bleomycin induction of ATM-Ser 1981 phosphorylation was not significantly different among cell lines with

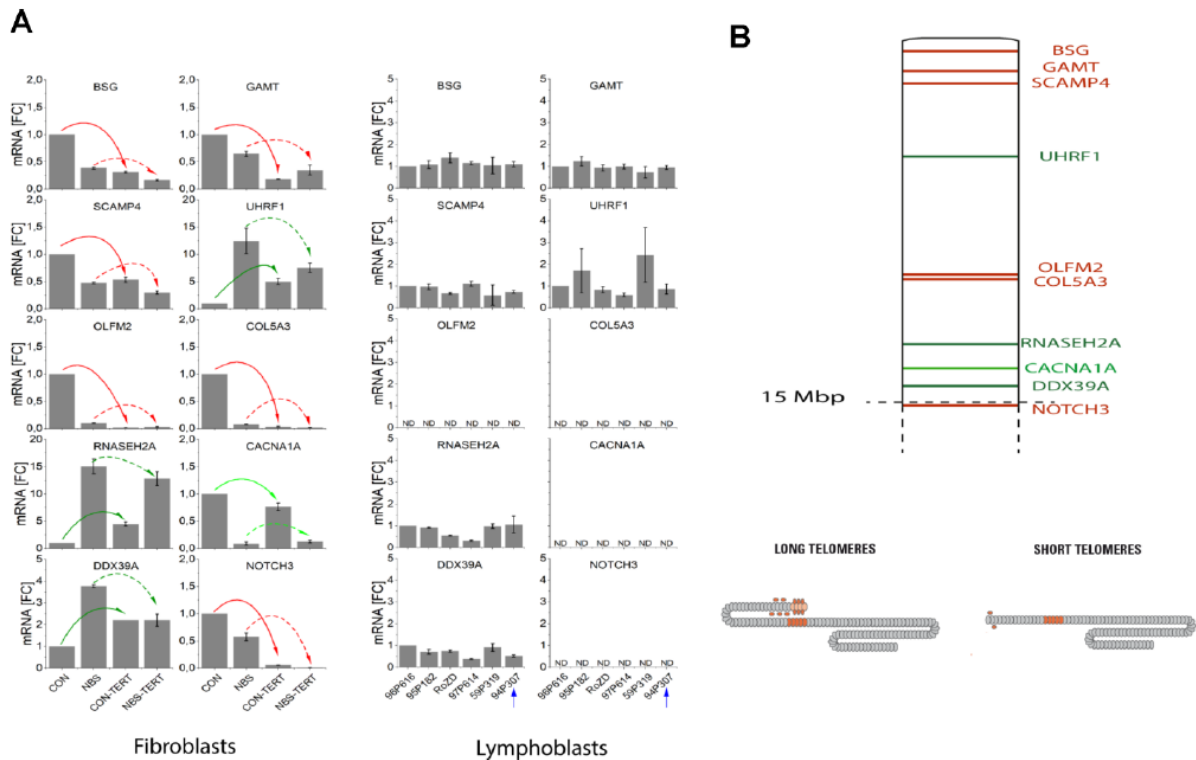


Figure 5. (A) mRNA expression of TPE-OLD candidate genes in cells with normal/short telomeres and artificially elongated telomeres in the presence of hTERT. qPCR analysis was performed in a healthy human fibroblast cell line, a NBS fibroblast cell line, and in all 6 available lymphoblastoid cell lines (LCLs). Total mRNA was extracted from proliferating fibroblasts and from the same cell lines proliferating with experimentally elongated telomeres, after immortalization with hTERT. In LCLs, mRNA from the 6 different donors was compared. One of these cell lines (94P307) showed extremely elongated telomeres on p19. The genes were identified as TPE-OLD candidates by use of Affymetrix gene chip experiments in independent cell lines from healthy controls and HGP patients (as described in Supplementary Tables 7–8 and Supplementary Figures 5–8). All values were normalized to the level (=1-fold) of mRNA in unmodified and pre-senescent control fibroblasts. Each assay was performed in triplicate. Red arrows mark the genes with attenuated regulation in NBS (short telomeres in pre-senescent vs. long telomeres in hTERT infected cells). Green arrows mark the genes with reversed regulation in NBS (dark green: downregulated in pre-senescent in controls; light green upregulated). The blue arrow marks the LCL with extremely long telomeres on 19p. *BSG*: basigin; *GAMT*: guanidinoacetate methyl-transferase; *SCAMP4*: secretory carrier membrane protein 4; *OLFM1*: olfactomedin 1; *UHRF1*: ubiquitin like with PHD and ring finger domains 1; *COL5A3*: collagen type V alpha 3 chain; *RNASEH2A*: ribonuclease H2 subunit A; *CACNA1A*: calcium voltage-gated channel subunit alpha1 A; *DDX39A*: DExD-box helicase 39A; *NOTCH3*: Notch receptor 3. ND, non detectable (mRNA quantifications with Ct values above 35). Borderline Ct values were detected for NOTCH3 for the LCL 95P182 (mean Ct = 34.9) and 59P319 (mean Ct = 34.6), not shown in the figure. **(B)** TPE-OLD concept. Telomeres loop to specific loci to regulate gene expression, a process termed telomere position effect over long distance [31]. The effect may likely extend to a distance of at least 10–15 Mbp from the telomere. The marked TPE-OLD gene candidates on 19p were investigated in experiments shown in Figure 5A: *BSG*, *GAMT*, *SCAMP4*, *OLFM2*, *COL5A3*, *CACNA1A*, *NOTCH3* (upregulated in pre-senescent cells), and *UHRF1*, *DDX39A* and *RNASEH2A* (downregulated in senescent cells). TPE-OLD genes may form clusters with reverse regulation in NBS (green) further away from the telomere.

Table 1. Relationship of telomere length of NBS homozygotes with age at cancer manifestation and age at death.

Telomere length	Origin	ID/DNA	Cancer	Ig Status	Age at cancer manifest.	Mean ± SD	Age at death	Mean ± SD
	Po	94P629	B-NHL	IgA+IgG↓	9		9	
	Po	97P614	B-NHL	normal	7		19	
			DLBCL-1		11			
			DLCBL-5		27			
	Po	8294	T-NHL	unknown	14		16	
	Po	98P222	Pre-B-ALL	unknown	5		6	
	Ge	94P126	NHL	unknown	13?		19?	
	Po	97P081	T-NHL	IgA+IgG↓	24		24	
	Po	94P251	HL	IgA+IgG↓	12		14	
	Po	94P548		IgA+IgG↓			8	
	Po	5567	T-NHL	unknown	34		34	
	Po	96P551		normal				
	Cz	5431	NHL	unknown	24		29	
	Cz	7822	NHL	unknown	7		10	
					6			
					17			
	Po	96P473		IgA+IgG↓				
	Po	97P229	B-NHL	IgA+IgG↓	4		6	
	Po	97P751	Cause of death unclear	unknown			3	
	Po	95P185		IgA+IgG↓				
	Po	95P182	B-NHL	IgA+IgG↓	8		10	
	Po	94P195	T-NHL Precursor TLBL	normal	19		21	
	Po	94P192	TLBL/ALL?	IgG↓	35		36	

*Age-adjusted Po, Poland; Ge, Germany; Cz, Czech Republic.

Table 2. Analysis of caspase-7 and ATM phosphorylation after bleomycin treatment of six NBS lymphoblastoid cell lines with the absolute longest (above) and absolute shortest (below) telomere lengths.

	Survival (y)	Caspase-7 activity after bleomycin treatment (10 µg/ml)				pATM/ATM level after bleomycin (1h)		
		0h	12h	24h	48h	0 µg/ml	10 µg/ml	30 µg/ml
89P0319 ♀	0	0.65±0.26	0.77±0.22	0.78±0.17	0.90±0.13	0.17±0.05	0.56±0.01	0.74±0.03
96P0616 ♀	0.2	0.17±0.01	0.24±0.01	0.41±0.05	0.90±0.08	0.07±0.05	0.24±0.06	0.47±0.06
95P0182 ♀	2.8	0.17±0.14	0.25±0.15	0.46±0.11	0.65±0.10	0.04±0.03	0.28±0.07	0.53±0.06
		0.33±0.28	0.42±0.30	0.55±0.20	0.82±0.14	0.09±0.07	0.36±0.17	0.58±0.14
97P0614 ♂	>12	0.13±0.03	0.16±0.05	0.36±0.09	0.49±0.05	0.04±0.02	0.16±0.07	0.22±0.08
RoZd ♀	>12	0.13±0.08	0.15±0.01	0.27±0.01	0.36±0.05	0.06±0.05	0.30±0.09	0.39±0.04
94P0307 ♂	>12	0.01±0.01	0.02±0.01	0.02±0.01	0.03±0.02	0.11±0.08	0.29±0.06	0.45±0.02
		0.09±0.07	0.11±0.08	0.22±0.18	0.29±0.24	0.07±0.04	0.25±0.08	0.35±0.12
		P=0.22	P=0.16	P=0.09	P=0.03	P=0.62	P=0.38	P=0.10

Each experiment was repeated three times; Mean ± SD.

short or long survival rates. Also, the cell line with low caspase 7 activity had normal ATM function.

DISCUSSION

Accelerated telomere attrition and telomere dysfunction in NBS cells

The main finding of this work is the stronger than expected telomere shortening and functional restriction in NBS patients. NBS homozygotes showed significantly shorter TL in all age groups. TL was reduced in homozygous patients by ~40% (qPCR). TL was ~25% shorter in NBS heterozygotes older than 30 years. The latter result was borderline significant ($p=0.1$) but remarkable in view of the lower age in NBS heterozygotes (42 y vs. 57 y in controls). Even stronger differences in TL were observed with qFISH (60-70%) in a subset of six homozygous NBS patients.

The variability of TL depending on the method suggests that telomeric and subtelomeric sequences are affected. We found only a moderate correlation between qPCR and TRF values, which is plausible insofar as the localization of the subtelomeric region included in the measurement is variable in TRF analysis based on the restriction enzymes used. Similar observations (with comparable correlation coefficients) have been made in other studies [44]. The advantage of the TRF method is the measurement of TL in absolute values (bases); on the other hand there is the disadvantage of being dependent on restriction enzymes with interindividual and intersexual biases [45]. Using qFISH rather short telomeres were found on chromosomes 17, 19, and 20. Yet this pattern was very similar to that of normal diploid cells [26].

In one NBS lymphoblastoid cell line (94P0307), we found striking telomere fusions with extreme telomere elongation in cells with very low *hTERT* expression. There is evidence that in humans the *hTERT* gene is close to the telomere and influenced by TPE-OLD [46]. However, silencing of *hTERT* in this cell line is unlikely because the *hTERT* gene is located on chromosome 5p and the extremely elongated telomere is located on chromosome 19p. We did not search for c-circles and ALT-associated promyelocytic leukemia protein (PML) bodies in this investigation. However, we had some indirect evidence for possible ALT involvement. Telomere dysfunction-driven genome damage associated with chromosomal break-fusion-bridge cycles and double-strand breaks are frequent in ALT cell lines [30], and were also observed in this cell line. This is remarkable insofar as ALT normally requires the activity of the Mre11/Rad50/nibrin recombination complex [14, 47, 48]. However, there are several ALT

mechanisms [14], and ALT may have occurred by homologous recombination and telomere-sister chromatid exchange [14]. Altogether, these *in vitro* experiments are consistent with both the proposed function of nibrin in telomere protection [18–20] and with the occurrence of cancer forms with high ALT prevalence in NBS [49].

Telomere extension was possible with telomerase in cultivated control and NBS fibroblasts. We were able to find expected changes on mRNA levels in control fibroblasts for all TPE-OLD candidate genes investigated on 19p. But we did not find expression changes of telomeric genes for the lymphoblastoid cells with abnormal 19p elongation; the TL-dependent regulation of the genes *BSG*, *GAMT*, *SCAMP4*, *OLFM2*, *COL5A3*, and *NOTCH 3* was attenuated in NBS fibroblasts, and it was reversed for the genes *UHRF1*, *RNASEH2A*, *CACNA1A* and *DDX39A*. These data show that NBS cells are still capable of elongating telomeres. Yet functionally abnormal telomeres may arise.

Possible causes for accelerated telomere attrition in NBS cells

The NBN mutation c.657_661del5 may affect a variety of functions leading to disturbed telomere repair and accelerated telomere attrition. The MRN complex is required for activation of the ATM-dependent repair of dysfunctional telomeres, the resection of telomeric DNA to create the single-stranded 3' overhang and for stabilization of telomeric T-loops [13, 14]. The Mre11-nibrin interaction required for ATM activation [20] may be affected as well as nibrin ubiquitination [19] and/or phosphorylation [18], which is important for cell cycle dependent telomere conservation and repair [18]. In accordance with current concepts (with nibrin as a co-factor for MRN complex assembly and a more indirect activation of ATM [18–20]) ATM phosphorylation was not impaired in our experiments, which does not point to a direct functional interference with ATM activation.

Increased oxidative stress has previously been described for NBS cells [50, 51]. The observation that G:C>A:T is the most frequent spontaneous base mutation in NBS [52] is of interest insofar as the telomeric TTAGGG sequence is sensitive to oxidative modifications and single-strand breaks [53]. Thus a high vulnerability of telomeres to oxidative damage may contribute to accelerated telomere attrition. The occurrence of ALT cells, and persistent DNA replication stress may additionally lead to spontaneous mitotic telomere synthesis, a potential driver of genomic duplications in cancer [14]. Our findings in fetal tissue suggest that substantial TL attrition may occur before birth in NBS

homozygotes, which cannot be explained by the “end replication problem” alone. There were considerable differences in TLs between different fetal tissues. This is in sharp contrast to observations from healthy fetuses showing a very uniform TL in all tissues at all gestational ages [27].

Possible implications of telomere attrition for cancerogenesis

Genetic instability and impaired telomeric repair may synergize with telomere attrition and dysfunction to explain the extremely high cancer incidence in NBS. The “dose dependency” of telomere attrition on the phenotype also account for this possibility. Homozygote NBS patients with marked telomere attrition develop cancer at young age. Heterozygote patients have an increased cancer risk at higher age, and humanized NBS mice with normal TL did not display early tumorigenesis, but showed all other signs of NBS [29]. The higher TL reserve in mice [53, 54] may explain why we observed no significant reduction in TL in the NBS mice. Overall, these data are consistent with epidemiological studies that have demonstrated a strong inverse relationship between TL and cancer incidence in the general population [55–57].

A possible explanation for the high lymphoma incidence in NBS could be the high rate of somatic recombination with associated hypermutability. This hypermutability is required for the extreme degree of somatic recombination of the immunoglobulin and T-cell receptor genes necessary for the vast repertoire of antibodies and T cell receptors [56]. On the other hand, the almost inevitable development of T or B cell lymphoma during childhood and the extreme preference over other types of cancer is striking. Two key steps are important for tumorigenesis: increased mutation rate and clonal selection with a growth advantage. The unique combination of hypermutability and extreme telomere attrition may have contributed to the high incidence of lymphomas at young age. In this context, it is noteworthy that all suggested TPE-OLD genes on p19 are functionally involved in cell senescence or cell growth and that all these TPE-OLD candidates were dysregulated in the NBS fibroblast cell line. Genes with suggested functions in senescence were suppressed, whereas growth promoting genes were rather increased on mRNA level (Figure 5 and Supplementary Table 8). Even if we had not the opportunity to show this dysregulation in cultivated (Epstein-Barr virus transformed) lymphoblastoid cell lines it is possible that TPE-OLD dysregulation favors a growth advantage *in vivo*, which synergizes with the extreme hypermutability and may explain the dramatically increased risk for

developing lymphoma to over 1000-fold in NBS, which was not found in any other disease, including other DNA repair syndromes [56].

Possible implications of telomere attrition for tumor suppression

We did not find an inverse correlation between TL and age of cancer onset. A combination of the TL, the degree of telomere damage, the number of critically short telomeres per cell, and other individual factors may also influence cancer onset. Alternatively, the deleterious effect of TL attrition is to some extent superimposed by some other more beneficial effect. In this context, we found it interesting that individual patients survived their disease for more than a decade. Cultivated lymphoblastoid cells derived from NBS patients with long survival times (>12 years) displayed shorter telomeres and lower caspase 7 activities, compared to cells derived from patients with short survival times (<3 years), suggesting low apoptosis rates and/or increased senescence rates with (at least in these individual patients) effective tumor suppression. The limit on cellular proliferation for cells with short telomeres is considered an initial block to oncogenesis [58]. Data may point to a direct protective effect of short telomeres in these patients.

These results are important to a better understanding of the role of telomere attrition in carcinogenesis *per se*. It is generally accepted that telomere attrition drives genomic instability and that the subsequent acquisition of *hTERT* expression and telomerase activity is involved in cancer immortality [59]. This model is supported by clinical findings showing that short telomeres are an important risk factor for malignant transformation [57]. On the other hand, longer telomeres can be a predictor for poor outcome after a tumor has developed [60]. This, at first glance, contradictory observation is usually attributed to higher telomerase activities (and thus a higher “degree” of immortality) in tumor patients with poor outcome. However, other findings indicate that the activation of telomerase may occur early in tumor development [59, 61]. The exact temporal sequence of telomerase activation, telomere shortening and malignant transformation is not clear. The data presented here illustrate the double-edged sword of telomere shortening in NBN founder mutation carriers with lymphoid malignancies (and thus confirm the current concept) but also show an alternative explanation for the correlation between TL and tumor progression: lower apoptosis and/or increased replicative senescence rates due to short telomeres and thus relative protection against new tumors (summarized in Figure 6). This may have important therapeutic implications. For example,

hematopoietic stem cell transplantation (HSCT) appears to be a promising therapeutic strategy for some but not all NBS patients [62]. From a therapeutic point of view, our data suggest that telomere stabilization should indeed be the goal for NBS (and possibly other tumor) patients *before* cancer onset, but after cancer has already developed, “keeping telomeres short” would probably be more useful. Considering new therapeutic options for influencing telomeres [58] these findings could become clinically relevant for this and other cancer-predisposing mutations with involvement of telomere attrition and/or dysfunction.

Estimating the relative contribution of telomere shortening to cancerogenesis is difficult, especially in view of the bifunctional role of telomere shortening. The DNA repair defect has likely a major contribution to cancerogenesis. According to recent recommendations for a novel nomenclature [21, 22], NBS is clearly a secondary telomeropathy. Our data do not currently warrant the classification of the disease as a classical “impaired telomere maintenance spectrum disorder” (ITM). Secondary telomeropathies include diseases in which it is not clear to what extent the telomere dysfunction is the cause of the pathology.

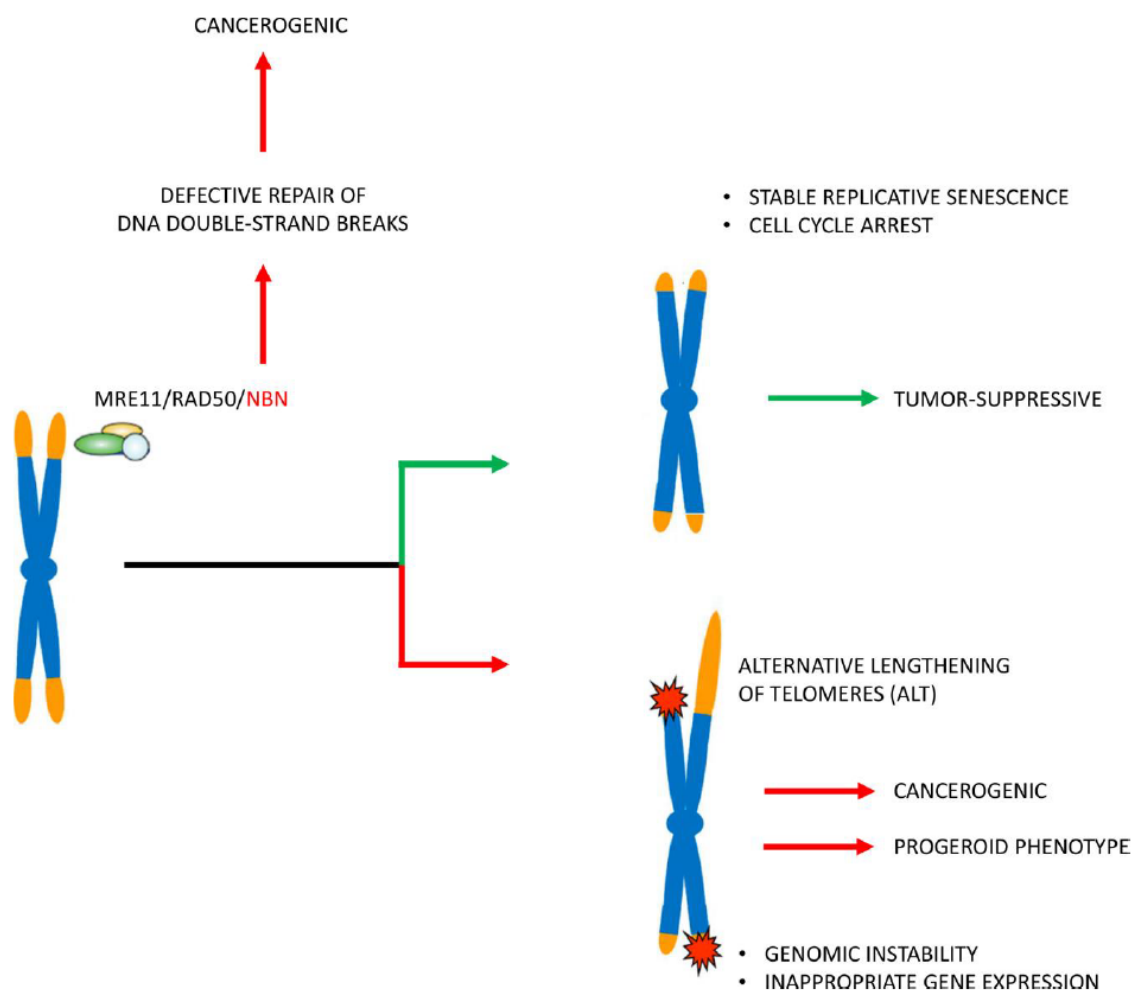


Figure 6. Pathophysiological concept. The patients’ cells in Nijmegen Breakage Syndrome have markedly reduced telomere lengths. Telomere attrition may induce genetic instability and alternative telomere elongation and thus enhance the cancerogenic effect (that is induced by defective repair of DNA double-strand breaks by non-homologous end joining) and also contribute to a progeroid phenotype. Telomere attrition may, however, also mitigate the clinical phenotype by inducing stable replicative senescence and cell cycle arrest. The latter is indicated by cells from patients with long tumor survival times with very short telomeres and little apoptosis.

Possible implications of telomere attrition for the progeroid phenotype

NBS belongs to the progeroid syndromes and patients have symptoms of aging such as decline in mental function, gray hair, teleangiectasia and café au lait spots. It has been shown that transient introduction of telomerase mRNA into progeria cells improves many of the hallmarks of this disorder [63]. It is assumed that telomere dysfunction in Hutchinson Gilford progeria and likely other telomere syndromes is a causative molecular mechanism of pathogenesis [64]. The data presented here expand this concept and show that abnormal TPE-OLD may contribute to the progeroid phenotype in NBS. Using independent methods comparing replicative, stress-inducible and *hTERT* immortalized cells, we identified ten TPE-OLD candidate genes with significant TL-dependent expression changes. Seven of the TPE-OLD candidate genes were upregulated in aged healthy fibroblasts and are involved in senescence pathways or have some functional relation to aging. Three of the genes had rather growth promoting function and were suppressed in normal fibroblasts on mRNA level (Figure 5 and Supplementary Table 8). The TL-dependent response was attenuated for all seven upregulated genes in NBS fibroblasts and was reversed in all three growth promoting genes, suggesting that the normal senescence program is disturbed in these cells and shifted to a rather growth promoting expression pattern.

Thus coordinated regulation of telomeric genes could be important for (patho)physiology. We postulate that the progeroid phenotype in NBS is intimately influenced by TPE-OLD. In the age-associated genetic disease facioscapulohumeral muscular dystrophy *SORBS2* transcription is altered by a telomeric 4.8-Mb loop in patients' myoblasts. *SORBS2* is normally up-regulated by maturation/differentiation of skeletal muscle and is misregulated by TPE-OLD-dependent variegation in myoblasts [65]. NBS is a secondary telomeropathy in which telomere dysregulation occurs at multiple sites. We cannot entirely exclude that some changes on mRNA level occurred secondarily as part of an adaptation mechanism. However, the extremely accelerated telomere attrition is a plausible explanation for abnormal TL-dependent regulation in NBS cells and modulation of the clinical phenotype. A role in pathogenesis is also supported by the significantly milder clinical phenotype in NBS mice with significantly longer telomeres. Humanized NBS mice have less severe immune system defects and are not markedly prone to malignancy.

The pathophysiological role of short telomeres in diseases with short telomeres is mostly attributed to replicative exhaustion, increased DNA damage response,

genetic instability and missing scavenger for oxygen radicals. The studies presented here show another mechanism that could be effective independent from DNA damage response and long before the onset of senescence: an imbalance or dysfunction in telomere position effect.

All progeroid syndromes can be classified into two categories: those caused by alterations in components of the nuclear envelope; and those caused by mutations in components of the telomerase complex. Short telomeres have now been described for almost all progeroid syndromes with mutations in genes involved in DNA-repair pathways, including Rothmund-Thomson syndrome, Werner Syndrome, Dyskeratosis congenita, Ataxia teleangiectasia, Ataxia teleangiectasia like syndrome, Bloom syndrome, and NBS [21, 22]. The progeroid syndromes with short telomeres resemble each other in many aspects and short telomeres are a potential cause or co-factor for symptoms such as nail atrophy, alopecia, gray hair, immunodeficiency and possibly also cancerogenesis. George Martin described the progerias as segmental diseases [66] and characterized their pathology and many molecular defects in pioneering investigations (summarized in reference [67]). In his original definition, each disease captures some, but not all, of the symptoms of aging, each with different (segmental) affected organ systems. The data described here support a more modular instead of a strictly segmental model, in which the aging phenotype is caused by a limited number of modules, as originally proposed by Hofer et al. [68], some of which are unique and some of which overlap the symptoms of other modules. TPE-OLD can provide an explanation for this model on a molecular basis. Depending on the degree of the telomere damage and disease-specific peculiarities, a phenotype variety may result with a more progeroid or more cancerogenic gene expression pattern.

MATERIALS AND METHODS

Cell cultures

The fibroblast cell lines were propagated in Amniomax medium with gentamicin sulfate and L-glutamine supplement. Lymphoblastoid cells (LCLs) were prepared and cultured as described [69].

DNA samples

DNA was isolated from the blood of 27 NBS heterozygotes, 38 NBS homozygotes, a homozygous NBS fetus, and 108 controls. The NBS fetus presented with microcephaly, craniofacial dysmorphism, and signs of immaturity, but no malformation of inner organs. The pregnancy was interrupted in the 32nd week.

Molecular genetics

The founder mutation was analyzed as previously described [6]. Expression of the human telomerase reverse transcriptase gene (*hTERT*) was analyzed by qPCR. GAPDH was used as the internal control gene. The primer sequences for *hTERT* were: 5'- CCG ATT GTG AAC ATG GAC TAC GT -3'(forward); 5'- CGT AGT TGA GCA CGC TGA ACA -3'(reverse). The primer sequences for GAPDH were: 5'-CTC TGC TCC TCC TGT TCG AC-3'(forward); 5'-GCG CCC AAT ACG ACC AAA TC-3'(reverse).

mRNA quantification of TPE-OLD (telomere position effect over long distances) candidate genes was carried in triplicates in a 384-well plate using a BioRad CFX384 real-time C1000 thermal cycler, as described [70]. Human PPIA (Cyclophilin A) (Cat. 4333763F) was used as an endogenous control. The $\Delta\Delta C_t$ method was used for relative quantification [70]. The following gene expression TaqMan assays (Applied Biosystems) were used: BSG (Cat. Hs00936295_m1), CACNA1A (Cat. Hs01579431_m1), COL5A3 (Cat. Hs01555669_m1), DDX39A (Cat. Hs01124952_g1), GAMT (Cat. Hs00355745_g1), NOTCH3 (Cat. Hs01128537_m1), OLFM2 (Cat. Hs01017934_m1), RNASEH2A (Cat. Hs00197370_m1), SCAMP4 (Cat. Hs00365263_m1), and UHRF1 (Cat. Hs01086727_m1). qPCR was applied to determine the relative telomere length as described previously [71]. The relative length of individual telomeres was analyzed by quantitative fluorescence in situ hybridization (Q-FISH) [72]. The fluorescence intensity of single telomeres (*T*) relative to a constant repetitive region in the centromeric region (C) of chromosome 2 (T/C ratio) was measured, using Ikaros software. The T/C ratio of 15 metaphases was estimated, and the mean telomere intensities of the p-arms and q-arms were calculated for each chromosome.

Absolute TL was measured by Terminal Restriction Fragment (TRF) length analysis, using the Roche - TeloTAGGG TL assay and the restriction enzymes *Hinf*I and *Rsa*I [28].

Humanized NBS mice, kindly provided by André Nussenzweig, were generated by reconstitution of *Nbn* knockout mice with the human *NBN* gene carrying the c.657_661del5 mutation or the wild type allele [28].

hTERT immortalization

Fibroblasts were infected with retroviral supernatants from a packaging cell line (PA317-TERT) that stably expresses the human telomerase cloned into a pBabePuro vector, as described previously [73].

Identification of TPE-OLD candidate genes in human fibroblasts

Using an Affymetrix cDNA microarray, we compared the expression profiles of pre-senescent fibroblasts and *hTERT* immortalized fibroblasts. As a model for stress-inducible senescence, we used UV-radiated cells (radiated twice per day, for 3 consecutive days, with a total dose of 528 J/m², using four 20W TL/12 lamps emitting broadband UV-B peaking at 312 nm). Senescence was confirmed by β -galactosidase staining. We analyzed 16 microarrays, each with 54,675 transcripts on an HGU133-A2.0 array from Affymetrix®, in a design with 3 groups. Differentially expressed genes in replicative senescence, up to 15 Mbp telomeric on p19, that were not differentially expressed in UV-B treated cells were viewed as potential TPE-OLD candidates.

Analysis of caspase-7 in western blots

Lymphoblastoid cells were treated in triplicate with 10 μ g/ml bleomycin for 0h, 12h, 24h, and 48h. Caspase fragments were separated by SDS gel electrophoresis, using the primary antibody *cleaved Caspase-7* (Asp 198) and the second antibody (Anti-Mouse IgG Horseradish Peroxidase).

Detection of ATM and phosphorylated ATM (p-ATM) by immunoprecipitation

For examination of phosphorylation of ATM after bleomycin treatment, lymphoblastoid cells in logarithmic growth were treated in triplicate with 0, 10, and 30 μ g/ml bleomycin for 1 h at 37°C. Immunoprecipitation was performed with the FISH-antibody (Anti-ATM, rabbit polyclonal, Novus) and magnetic beads (DynaL Biotech ASA/Invitrogen). The separated proteins were probed with anti-ATM pS1981 (Rockland, monoclonal, mouse), and reprobed with an anti-ATM antibody (Abcam Cambridge, UK) [74].

Statistical analysis

The original data were exported to Excel 2007, GraphPad Prism 5 software, and SPSS 15.0 software for graphs and boxplots. The statistical tests used were Mann-Whitney U test, Fisher's exact test, and the unpaired t-test.

Analysis of chromosome fragility

Chromosome preparations were performed using standard techniques. The lymphoblastoid cell lines were analysed for chromosomal aberrations 4 h after irradiation (Muller MG 150 x ray apparatus; U_A, 100 kV; I, 10 mA; filter, 0.3 mm Ni; dose rate, 2.1 Gy/min;

Seifert, Hamburg, Germany) with 0 Gy, 0.5 Gy and 1.0 Gy including 1h colcemid treatment. 50 cells were analysed each. The types of aberrations were classified as achromatic lesions, chromatid and isochromatid breaks, and chromatid translocations. In order to calculate the total number of chromatid breaks per cell the latter were counted twice, the achromatic lesions and the telomere fusions neglected. Detailed protocols of the cytogenetic and molecular genetic methods are presented in [74].

Ethics statement

All procedures were performed in accordance with the ethical standards of the responsible committee. The cell lines were established with the ethical approval of “The Children’s Memorial Health Institute, Warsaw”, the Ethics Committee of the Second Medical School of Charles University in Prague, and the consent of the subjects, or their parents (for children and the fetus). The mouse studies were approved by the State Office for Health and Social, Berlin (G0438/09).

Data availability statement

The data that supports the findings of this study are available in the supplementary material of this article.

AUTHOR CONTRIBUTIONS

RH analyzed the telomere lengths in the framework of her dissertation (Q-PCR, Q-FISH, hTERT analysis). RK performed the caspase and ATM experiments in the framework of his dissertation. KC and ES took care of the subjects and performed the primary molecular diagnostics. RF provided fetal data and tissues. KJ and MW performed the TPE-OLD analysis and hTERT immortalization. ID performed the TRF analysis. RV performed and analysed array experiments. HN established and characterized the lymphoblastoid cell lines. MD provided resources. KS and MW drafted the paper. All authors read and accepted the manuscript.

ACKNOWLEDGMENTS

We acknowledge the probands and their parents for their participation, Annelore Junge for prenatal cytogenetic diagnostics, and André Nussenzweig for providing the humanized NBS mouse. We thank Antje Gerlach, Mohsen Karbasiyan, Janina Radszewski, and Bastian Salewsky for general technical assistance, Britta Teubner and Brigitte Schröder for cytogenetic assistance, and Dr. Rami Derbas for statistical advice. We would also like to thank Michael Hanna, PhD, (Mercury Medical Research & Writing) for proof-reading the manuscript.

CONFLICTS OF INTEREST

The authors declare that they have no conflicts of interest.

FUNDING

Raneem Habib received a stipend from the University of Damascus, Syria. Ryong Kim received a stipend from the Gottlieb Daimler- und Karl Benz-Stiftung. This work was supported by grants from the German Research Society to K.S. and M.D. (Collaborative Research Center 577, Project B1).

REFERENCES

1. Weemaes CM, Hustinx TW, Scheres JM, van Munster PJ, Bakkeren JA, Taalman RD. A new chromosomal instability disorder: the nijmegen breakage syndrome. *Acta Paediatr Scand.* 1981; 70:557–64. <https://doi.org/10.1111/j.1651-2227.1981.tb05740.x> PMID:7315300
2. Varon R, Demuth I, Chrzanowska KH. GeneReviews®: Nijmegen Breakage Syndrome. Seattle (WA); 1993. PMID:20301355
3. Demuth I, Digweed M. The clinical manifestation of a defective response to DNA double-strand breaks as exemplified by nijmegen breakage syndrome. *Oncogene.* 2007; 26:7792–98. <https://doi.org/10.1038/sj.onc.1210876> PMID:18066092
4. Chrzanowska KH, Gregorek H, Dembowska-Bagińska B, Kalina MA, Digweed M. Nijmegen breakage syndrome (NBS). *Orphanet J Rare Dis.* 2012; 7:13. <https://doi.org/10.1186/1750-1172-7-13> PMID:22373003
5. Saar K, Chrzanowska KH, Stumm M, Jung M, Nürnberg G, Wienker TF, Seemanová E, Wegner RD, Reis A, Sperling K. The gene for the ataxia-telangiectasia variant, nijmegen breakage syndrome, maps to a 1-cM interval on chromosome 8q21. *Am J Hum Genet.* 1997; 60:605–10. PMID:9042920
6. Varon R, Vissinga C, Platzer M, Cerosaletti KM, Chrzanowska KH, Saar K, Beckmann G, Seemanová E, Cooper PR, Nowak NJ, Stumm M, Weemaes CM, Gatti RA, et al. Nibrin, a novel DNA double-strand break repair protein, is mutated in nijmegen breakage syndrome. *Cell.* 1998; 93:467–76. [https://doi.org/10.1016/s0092-8674\(00\)81174-5](https://doi.org/10.1016/s0092-8674(00)81174-5) PMID:9590180
7. Seemanová E, Varon R, Vejvalka J, Jarolim P, Seeman P, Chrzanowska KH, Digweed M, Resnick I, Kremensky I,

- Saar K, Hoffmann K, Dutranoy V, Karbasiyan M, et al. The slavic NBN founder mutation: a role for reproductive fitness? *PLoS One*. 2016; 11:e0167984. <https://doi.org/10.1371/journal.pone.0167984> PMID:27936167
8. Seemanová E, Jarolim P, Seeman P, Varon R, Digweed M, Swift M, Sperling K. Cancer risk of heterozygotes with the NBN founder mutation. *J Natl Cancer Inst*. 2007; 99:1875–80. <https://doi.org/10.1093/jnci/djm251> PMID:18073374
 9. Digweed M, Sperling K. Nijmegen breakage syndrome: clinical manifestation of defective response to DNA double-strand breaks. *DNA Repair (Amst)*. 2004; 3:1207–17. <https://doi.org/10.1016/j.dnarep.2004.03.004> PMID:15279809
 10. Rai R, Hu C, Broton C, Chen Y, Lei M, Chang S. NBS1 phosphorylation status dictates repair choice of dysfunctional telomeres. *Mol Cell*. 2017; 65:801–17.e4. <https://doi.org/10.1016/j.molcel.2017.01.016> PMID:28216226
 11. Oh J, Symington LS. Role of the Mre11 complex in preserving genome integrity. *Genes (Basel)*. 2018; 9:589. <https://doi.org/10.3390/genes9120589> PMID:30501098
 12. Feldser D, Strong MA, Greider CW. Ataxia telangiectasia mutated (atm) is not required for telomerase-mediated elongation of short telomeres. *Proc Natl Acad Sci USA*. 2006; 103:2249–51. <https://doi.org/10.1073/pnas.051143103> PMID:16467146
 13. Stracker TH, Petrini JH. The MRE11 complex: starting from the ends. *Nat Rev Mol Cell Biol*. 2011; 12:90–103. <https://doi.org/10.1038/nrm3047> PMID:21252998
 14. Cesare AJ, Reddel RR. Alternative lengthening of telomeres: models, mechanisms and implications. *Nat Rev Genet*. 2010; 11:319–30. <https://doi.org/10.1038/nrg2763> PMID:20351727
 15. Takai H, Smogorzewska A, de Lange T. DNA damage foci at dysfunctional telomeres. *Curr Biol*. 2003; 13:1549–56. [https://doi.org/10.1016/s0960-9822\(03\)00542-6](https://doi.org/10.1016/s0960-9822(03)00542-6) PMID:12956959
 16. Attwooll CL, Akpinar M, Petrini JH. The mre11 complex and the response to dysfunctional telomeres. *Mol Cell Biol*. 2009; 29:5540–51. <https://doi.org/10.1128/MCB.00479-09> PMID:19667076
 17. Dimitrova N, de Lange T. Cell cycle-dependent role of MRN at dysfunctional telomeres: ATM signaling-dependent induction of nonhomologous end joining (NHEJ) in G1 and resection-mediated inhibition of NHEJ in G2. *Mol Cell Biol*. 2009; 29:5552–63. <https://doi.org/10.1128/MCB.00476-09> PMID:19667071
 18. Verdun RE, Crabbe L, Haggblom C, Karlseder J. Functional human telomeres are recognized as DNA damage in G2 of the cell cycle. *Mol Cell*. 2005; 20:551–61. <https://doi.org/10.1016/j.molcel.2005.09.024> PMID:16307919
 19. Wu J, Zhang X, Zhang L, Wu CY, Rezaeian AH, Chan CH, Li JM, Wang J, Gao Y, Han F, Jeong YS, Yuan X, Khanna KK, et al. Skp2 E3 ligase integrates ATM activation and homologous recombination repair by ubiquitinating NBS1. *Mol Cell*. 2012; 46:351–61. <https://doi.org/10.1016/j.molcel.2012.02.018> PMID:22464731
 20. Kim JH, Grosbart M, Anand R, Wyman C, Cejka P, Petrini JH. The Mre11-Nbs1 interface is essential for viability and tumor suppression. *Cell Rep*. 2017; 18:496–507. <https://doi.org/10.1016/j.celrep.2016.12.035> PMID:28076792
 21. Holohan B, Wright WE, Shay JW. Cell biology of disease: telomeropathies: an emerging spectrum disorder. *J Cell Biol*. 2014; 205:289–99. <https://doi.org/10.1083/jcb.201401012> PMID:24821837
 22. Opresko PL, Shay JW. Telomere-associated aging disorders. *Ageing Res Rev*. 2017; 33:52–66. <https://doi.org/10.1016/j.arr.2016.05.009> PMID:27215853
 23. Siwicki JK, Degerman S, Chrzanowska KH, Roos G. Telomere maintenance and cell cycle regulation in spontaneously immortalized t-cell lines from nijmegen breakage syndrome patients. *Exp Cell Res*. 2003; 287:178–89. [https://doi.org/10.1016/s0014-4827\(03\)00140-x](https://doi.org/10.1016/s0014-4827(03)00140-x) PMID:12799193
 24. Berardinelli F, Sgura A, Di Masi A, Leone S, Cirrone GA, Romano F, Tanzarella C, Antocchia A. Radiation-induced telomere length variations in normal and in nijmegen breakage syndrome cells. *Int J Radiat Biol*. 2014; 90:45–52. <https://doi.org/10.3109/09553002.2014.859400> PMID:24168161
 25. Habib R, Neitzel H, Ernst A, Wong JK, Goryluk-Kozakiewicz B, Gerlach A, Demuth I, Sperling K, Chrzanowska K. Evidence for a pre-malignant cell line

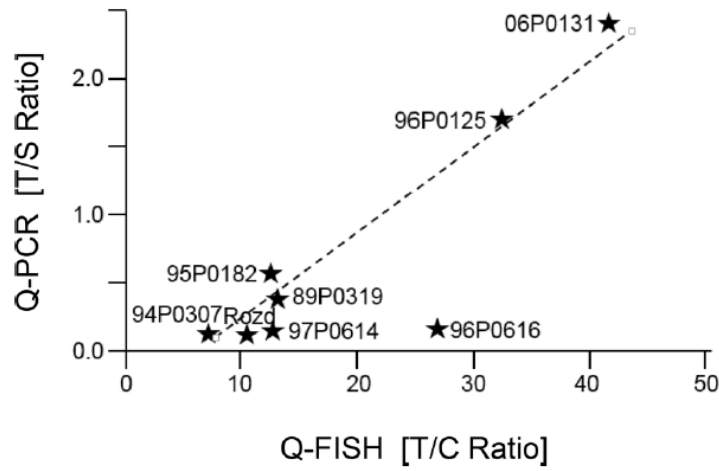
- in a skin biopsy from a patient with nijmegen breakage syndrome. *Mol Cytogenet.* 2018; 11:17.
<https://doi.org/10.1186/s13039-018-0364-6>
 PMID:29445421
26. Lansdorp PM, Verwoerd NP, van de Rijke FM, Dragowska V, Little MT, Dirks RW, Raap AK, Tanke HJ. Heterogeneity in telomere length of human chromosomes. *Hum Mol Genet.* 1996; 5:685–91.
<https://doi.org/10.1093/hmg/5.5.685>
 PMID:8733138
 27. Youngren K, Jeanclos E, Aviv H, Kimura M, Stock J, Hanna M, Skurnick J, Bardeguet A, Aviv A. Synchrony in telomere length of the human fetus. *Hum Genet.* 1998; 102:640–43.
<https://doi.org/10.1007/s004390050755>
 PMID:9703424
 28. Habib R. Analysis of telomere length in patients with chromosomal instability syndromes, particularly Nijmegen Breakage Syndrome (NBS) and its mouse model by complementary technologies; Doctoral thesis Charité - Universitätsmedizin, 2012.
 29. Difilippantonio S, Celeste A, Fernandez-Capetillo O, Chen HT, Reina San Martin B, Van Laethem F, Yang YP, Petukhova GV, Eckhaus M, Feigenbaum L, Manova K, Kruhlak M, Camerini-Otero RD, et al. Role of Nbs1 in the activation of the atm kinase revealed in humanized mouse models. *Nat Cell Biol.* 2005; 7:675–85.
<https://doi.org/10.1038/ncb1270>
 PMID:15965469
 30. Sakellariou D, Chiourea M, Raftopoulou C, Gagos S. Alternative lengthening of telomeres: recurrent cytogenetic aberrations and chromosome stability under extreme telomere dysfunction. *Neoplasia.* 2013; 15:1301–13.
<https://doi.org/10.1593/neo.131574> PMID:24339742
 31. Robin JD, Ludlow AT, Batten K, Magdinier F, Stadler G, Wagner KR, Shay JW, Wright WE. Telomere position effect: regulation of gene expression with progressive telomere shortening over long distances. *Genes Dev.* 2014; 28:2464–76.
<https://doi.org/10.1101/gad.251041.114>
 PMID:25403178
 32. Zavadzka JA, Plyler RA, Bouges S, Koval CN, Rivers WT, Beck CU, Chang EI, Stroud RE, Mukherjee R, Spinale FG. Cardiac-restricted overexpression of extracellular matrix metalloproteinase inducer causes myocardial remodeling and dysfunction in aging mice. *Am J Physiol Heart Circ Physiol.* 2008; 295:H1394–402.
<https://doi.org/10.1152/ajpheart.00346.2008>
 PMID:18689500
 33. Schneider JE, Stork LA, Bell JT, ten Hove M, Isbrandt D, Clarke K, Watkins H, Lygate CA, Neubauer S. Cardiac structure and function during ageing in energetically compromised guanidinoacetate n-methyltransferase (GAMT)-knockout mice - a one year longitudinal MRI study. *J Cardiovasc Magn Reson.* 2008; 10:9.
<https://doi.org/10.1186/1532-429X-10-9>
 PMID:18275592
 34. Herranz N, Gil J. Mechanisms and functions of cellular senescence. *J Clin Invest.* 2018; 128:1238–46.
<https://doi.org/10.1172/JCI95148>
 PMID:29608137
 35. Kim KM, Noh JH, Bodogai M, Martindale JL, Pandey PR, Yang X, Biragyn A, Abdelmohsen K, Gorospe M. SCAMP4 enhances the senescent cell secretome. *Genes Dev.* 2018; 32:909–14.
<https://doi.org/10.1101/gad.313270.118>
 PMID:29967290
 36. Anholt RR. Olfactomedin proteins: central players in development and disease. *Front Cell Dev Biol.* 2014; 2:6.
<https://doi.org/10.3389/fcell.2014.00006>
 PMID:25364714
 37. Zhang X, Zhao G, Zhang Y, Wang J, Wang Y, Cheng L, Sun M, Rui Y. Activation of JNK signaling in osteoblasts is inversely correlated with collagen synthesis in age-related osteoporosis. *Biochem Biophys Res Commun.* 2018; 504:771–76.
<https://doi.org/10.1016/j.bbrc.2018.08.094>
 PMID:30217450
 38. Marinelli S, Eleuteri C, Vacca V, Strimpakos G, Mattei E, Severini C, Pavone F, Luvisetto S. Effects of age-related loss of p/q-type calcium channels in a mice model of peripheral nerve injury. *Neurobiol Aging.* 2015; 36:352–64.
<https://doi.org/10.1016/j.neurobiolaging.2014.07.025>
 PMID:25150573
 39. Cui H, Kong Y, Xu M, Zhang H. Notch3 functions as a tumor suppressor by controlling cellular senescence. *Cancer Res.* 2013; 73:3451–59.
<https://doi.org/10.1158/0008-5472.CAN-12-3902>
 PMID:23610446
 40. Yang J, Liu K, Yang J, Jin B, Chen H, Zhan X, Li Z, Wang L, Shen X, Li M, Yu W, Mao Z. PIM1 induces cellular senescence through phosphorylation of UHRF1 at Ser311. *Oncogene.* 2017; 36:4828–42.
<https://doi.org/10.1038/onc.2017.96>
 PMID:28394343
 41. Hua S, Ji Z, Quan Y, Zhan M, Wang H, Li W, Li Y, He X, Lu L. Identification of hub genes in hepatocellular carcinoma using integrated bioinformatic analysis. *Aging (Albany NY).* 2020; 12:5439–68.
<https://doi.org/10.18632/aging.102969>
 PMID:32213663

42. Park S, Park HEH, Son HG, Lee SJV. The role of RNA helicases in aging and lifespan regulation. *Translational Medicine of Aging*. 2017; 1:24–31. <https://doi.org/10.1016/j.tma.2017.08.001>
43. Zhao S, Weng YC, Yuan SS, Lin YT, Hsu HC, Lin SC, Gerbino E, Song MH, Zdzienicka MZ, Gatti RA, Shay JW, Ziv Y, Shiloh Y, Lee EY. Functional link between ataxia-telangiectasia and nijmegen breakage syndrome gene products. *Nature*. 2000; 405:473–77. <https://doi.org/10.1038/35013083> PMID:10839544
44. Khincha PP, Dagnall CL, Hicks B, Jones K, Aviv A, Kimura M, Katki H, Aubert G, Giri N, Alter BP, Savage SA, Gadalla SM. Correlation of leukocyte telomere length measurement methods in patients with dyskeratosis congenita and in their unaffected relatives. *Int J Mol Sci*. 2017; 18:1765. <https://doi.org/10.3390/ijms18081765> PMID:28805708
45. Meyer A, Salewsky B, Spira D, Steinhagen-Thiessen E, Norman K, Demuth I. Leukocyte telomere length is related to appendicular lean mass: cross-sectional data from the berlin aging study II (BASE-II). *Am J Clin Nutr*. 2016; 103:178–83. <https://doi.org/10.3945/ajcn.115.116806> PMID:26675777
46. Kim W, Ludlow AT, Min J, Robin JD, Stadler G, Mender I, Lai TP, Zhang N, Wright WE, Shay JW. Regulation of the human telomerase gene TERT by telomere position effect-over long distances (TPE-OLD): implications for aging and cancer. *PLoS Biol*. 2016; 14:e2000016. <https://doi.org/10.1371/journal.pbio.2000016> PMID:27977688
47. Compton SA, Choi JH, Cesare AJ, Ozgür S, Griffith JD. Xrcc3 and Nbs1 are required for the production of extrachromosomal telomeric circles in human alternative lengthening of telomere cells. *Cancer Res*. 2007; 67:1513–19. <https://doi.org/10.1158/0008-5472.CAN-06-3672> PMID:17308089
48. Wu G, Jiang X, Lee WH, Chen PL. Assembly of functional ALT-associated promyelocytic leukemia bodies requires nijmegen breakage syndrome 1. *Cancer Res*. 2003; 63:2589–95. PMID:12750284
49. Barthel FP, Wei W, Tang M, Martinez-Ledesma E, Hu X, Amin SB, Akdemir KC, Seth S, Song X, Wang Q, Lichtenberg T, Hu J, Zhang J, et al. Systematic analysis of telomere length and somatic alterations in 31 cancer types. *Nat Genet*. 2017; 49:349–57. <https://doi.org/10.1038/ng.3781> PMID:28135248
50. Krenzlin H, Demuth I, Salewsky B, Wessendorf P, Weidele K, Bürkle A, Digweed M. DNA damage in nijmegen breakage syndrome cells leads to PARP hyperactivation and increased oxidative stress. *PLoS Genet*. 2012; 8:e1002557. <https://doi.org/10.1371/journal.pgen.1002557> PMID:22396666
51. Melchers A, Stöckl L, Radszewski J, Anders M, Krenzlin H, Kalischke C, Scholz R, Jordan A, Nebrich G, Klose J, Sperling K, Digweed M, Demuth I. A systematic proteomic study of irradiated DNA repair deficient Nbn-mice. *PLoS One*. 2009; 4:e5423. <https://doi.org/10.1371/journal.pone.0005423> PMID:19412544
52. Petersen S, Saretzki G, von Zglinicki T. Preferential accumulation of single-stranded regions in telomeres of human fibroblasts. *Exp Cell Res*. 1998; 239:152–60. <https://doi.org/10.1006/excr.1997.3893> PMID:9511733
53. Prowse KR, Greider CW. Developmental and tissue-specific regulation of mouse telomerase and telomere length. *Proc Natl Acad Sci USA*. 1995; 92:4818–22. <https://doi.org/10.1073/pnas.92.11.4818> PMID:7761406
54. Blasco MA, Lee HW, Hande MP, Samper E, Lansdorp PM, DePinho RA, Greider CW. Telomere shortening and tumor formation by mouse cells lacking telomerase RNA. *Cell*. 1997; 91:25–34. [https://doi.org/10.1016/s0092-8674\(01\)80006-4](https://doi.org/10.1016/s0092-8674(01)80006-4) PMID:9335332
55. Widmann TA, Herrmann M, Taha N, König J, Pfreundschuh M. Short telomeres in aggressive non-hodgkin's lymphoma as a risk factor in lymphomagenesis. *Exp Hematol*. 2007; 35:939–46. <https://doi.org/10.1016/j.exphem.2007.03.009> PMID:17533048
56. Chrzanowska KH, Digweed M, Sperling K, Seemanova E, editors. *DNA-repair deficiency and cancer: Lessons from lymphoma*. Fulda: Wiley-VCH Verlag GmbH & Co. KGaA 2009.
57. Wentzensen IM, Mirabello L, Pfeiffer RM, Savage SA. The association of telomere length and cancer: a meta-analysis. *Cancer Epidemiol Biomarkers Prev*. 2011; 20:1238–50. <https://doi.org/10.1158/1055-9965.EPI-11-0005> PMID:21467229
58. Jäger K, Walter M. Therapeutic targeting of telomerase. *Genes (Basel)*. 2016; 7:39. <https://doi.org/10.3390/genes7070039> PMID:27455328
59. Hahn WC. Role of telomeres and telomerase in the pathogenesis of human cancer. *J Clin Oncol*. 2003; 21:2034–43.

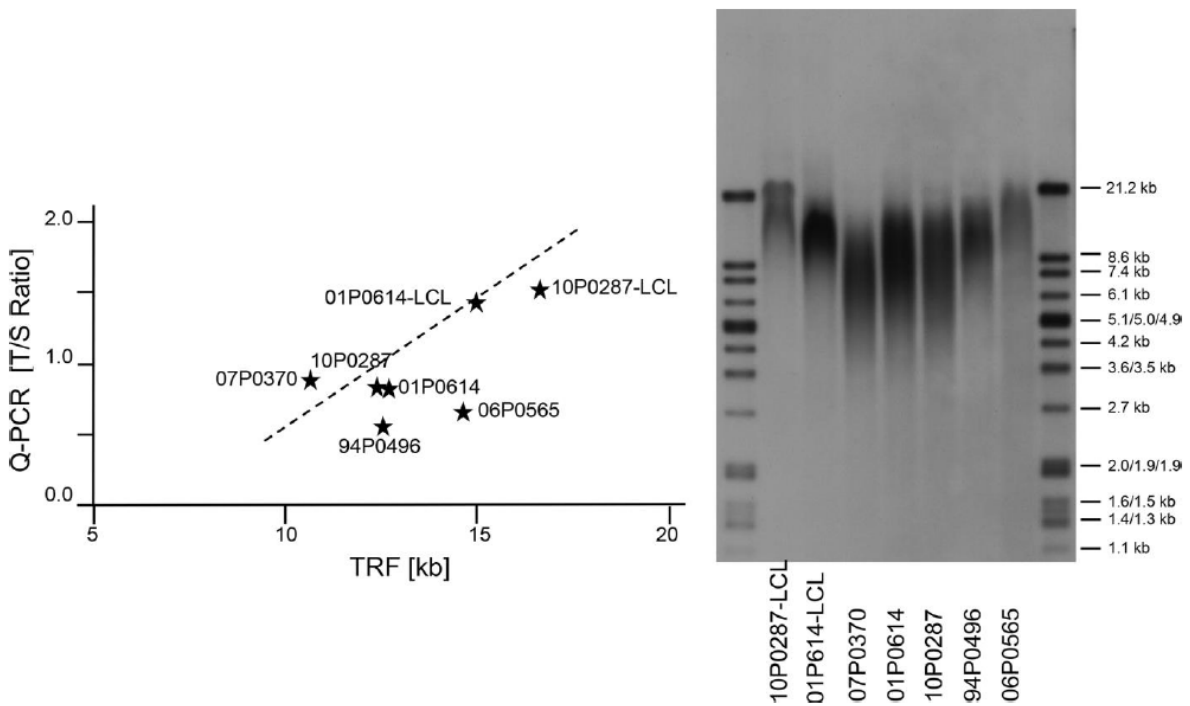
- <https://doi.org/10.1200/JCO.2003.06.018>
PMID:12743159
60. Luo X, Sturgis EM, Yang Z, Sun Y, Wei P, Liu Z, Wei Q, Li G. Lymphocyte telomere length predicts clinical outcomes of HPV-positive oropharyngeal cancer patients after definitive radiotherapy. *Carcinogenesis*. 2019; 40:735–41.
<https://doi.org/10.1093/carcin/bgz019>
PMID:30721961
61. Kolquist KA, Ellisen LW, Counter CM, Meyerson M, Tan LK, Weinberg RA, Haber DA, Gerald WL. Expression of TERT in early premalignant lesions and a subset of cells in normal tissues. *Nat Genet*. 1998; 19:182–86.
<https://doi.org/10.1038/554>
PMID:9620778
62. Wolska-Kuśniercz B, Gregorek H, Chrzanoska K, Piątosza B, Pietrucha B, Heropolitańska-Pliszka E, Pac M, Klaudel-Dreszler M, Kostyuchenko L, Pasic S, Marodi L, Belohradsky BH, Čiznár P, et al, and Inborn Errors Working Party of the Society for European Blood and Marrow Transplantation and the European Society for Immune Deficiencies. Nijmegen breakage syndrome: clinical and immunological features, long-term outcome and treatment options - a retrospective analysis. *J Clin Immunol*. 2015; 35:538–49.
<https://doi.org/10.1007/s10875-015-0186-9>
PMID:26271390
63. Li Y, Zhou G, Bruno IG, Zhang N, Sho S, Tedone E, Lai TP, Cooke JP, Shay JW. Transient introduction of human telomerase mRNA improves hallmarks of progeria cells. *Aging Cell*. 2019; 18:e12979.
<https://doi.org/10.1111/acer.12979> PMID:31152494
64. Aguado J, Sola-Carvajal A, Cancila V, Revêchon G, Ong PF, Jones-Weinert CW, Wallén Arzt E, Lattanzi G, Dreesen O, Tripodo C, Rossiello F, Eriksson M, d'Adda di Fagagna F. Inhibition of DNA damage response at telomeres improves the detrimental phenotypes of hutchinson-gilford progeria syndrome. *Nat Commun*. 2019; 10:4990.
<https://doi.org/10.1038/s41467-019-13018-3>
PMID:31740672
65. Robin JD, Ludlow AT, Batten K, Gaillard MC, Stadler G, Magdinier F, Wright WE, Shay JW. SORBS2 transcription is activated by telomere position effect-over long distance upon telomere shortening in muscle cells from patients with facioscapulohumeral dystrophy. *Genome Res*. 2015; 25:1781–90.
<https://doi.org/10.1101/gr.190660.115>
PMID:26359233
66. Martin GM. Genetic syndromes in man with potential relevance to the pathobiology of aging. *Birth Defects Orig Artic Ser*. 1978; 14:5–39.
PMID:147113
67. Martin GM. Genetic modulation of senescent phenotypes in homo sapiens. *Cell*. 2005; 120:523–32.
<https://doi.org/10.1016/j.cell.2005.01.031>
PMID:15734684
68. Hofer AC, Tran RT, Aziz OZ, Wright W, Novelli G, Shay J, Lewis M. Shared phenotypes among segmental progeroid syndromes suggest underlying pathways of aging. *J Gerontol A Biol Sci Med Sci*. 2005; 60:10–20.
<https://doi.org/10.1093/gerona/60.1.10>
PMID:15741277
69. Neitzel H. A routine method for the establishment of permanent growing lymphoblastoid cell lines. *Hum Genet*. 1986; 73:320–26.
<https://doi.org/10.1007/BF00279094> PMID:3017841
70. Kannenberg F, Gorzelniak K, Jäger K, Fobker M, Rust S, Repa J, Roth M, Björkhem I, Walter M. Characterization of cholesterol homeostasis in telomerase-immortalized tangier disease fibroblasts reveals marked phenotype variability. *J Biol Chem*. 2013; 288:36936–47.
<https://doi.org/10.1074/jbc.M113.500256>
PMID:24196952
71. Neuner B, Lenfers A, Kelsch R, Jäger K, Brüggmann N, van der Harst P, Walter M. Telomere length is not related to established cardiovascular risk factors but does correlate with red and white blood cell counts in a german blood donor population. *PLoS One*. 2015; 10:e0139308.
<https://doi.org/10.1371/journal.pone.0139308>
PMID:26445269
72. Perner S, Bruderlein S, Hasel C, Waibel I, Holdenried A, Ciloglu N, Chopurian H, Nielsen KV, Plesch A, Högel J, Möller P. Quantifying telomere lengths of human individual chromosome arms by centromere-calibrated fluorescence in situ hybridization and digital imaging. *Am J Pathol*. 2003; 163:1751–56.
[https://doi.org/10.1016/S0002-9440\(10\)63534-1](https://doi.org/10.1016/S0002-9440(10)63534-1)
PMID:14578175
73. Walter M, Forsyth NR, Wright WE, Shay JW, Roth MG. The establishment of telomerase-immortalized tangier disease cell lines indicates the existence of an apolipoprotein a-I-inducible but ABCA1-independent cholesterol efflux pathway. *J Biol Chem*. 2004; 279:20866–73.
<https://doi.org/10.1074/jbc.M401714200>
PMID:15001567
74. Kim R. Assoziationsstudie zur klinischen Variabilität bei Patienten mit dem Nijmegen Breakage Syndrom; Doctoral thesis Charité - Universitätsmedizin, 2010.

SUPPLEMENTARY MATERIALS

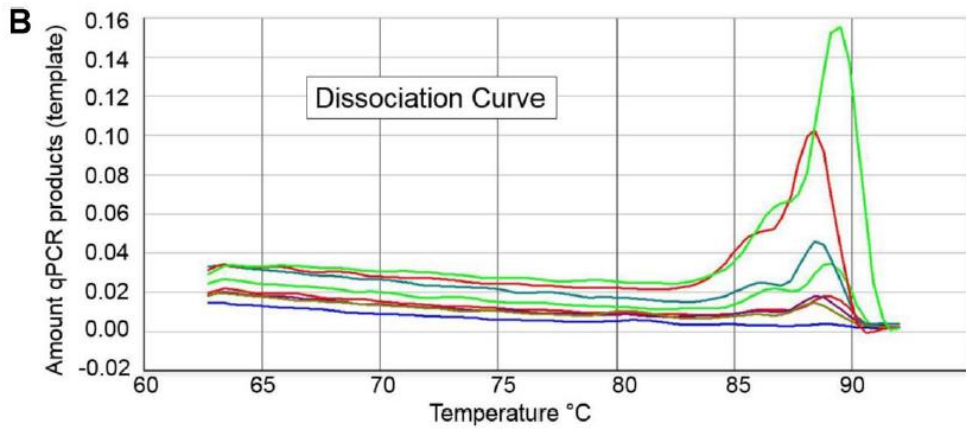
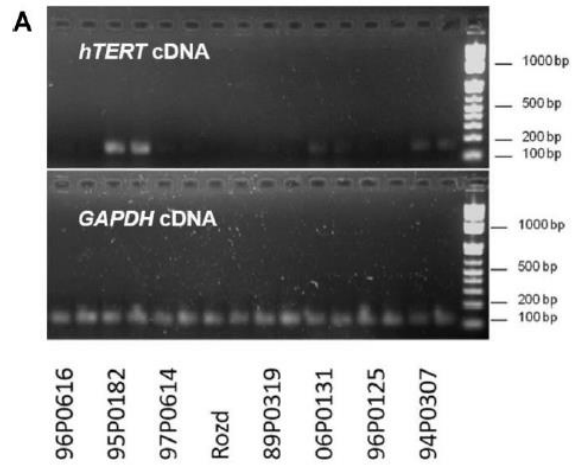
Supplementary Figures

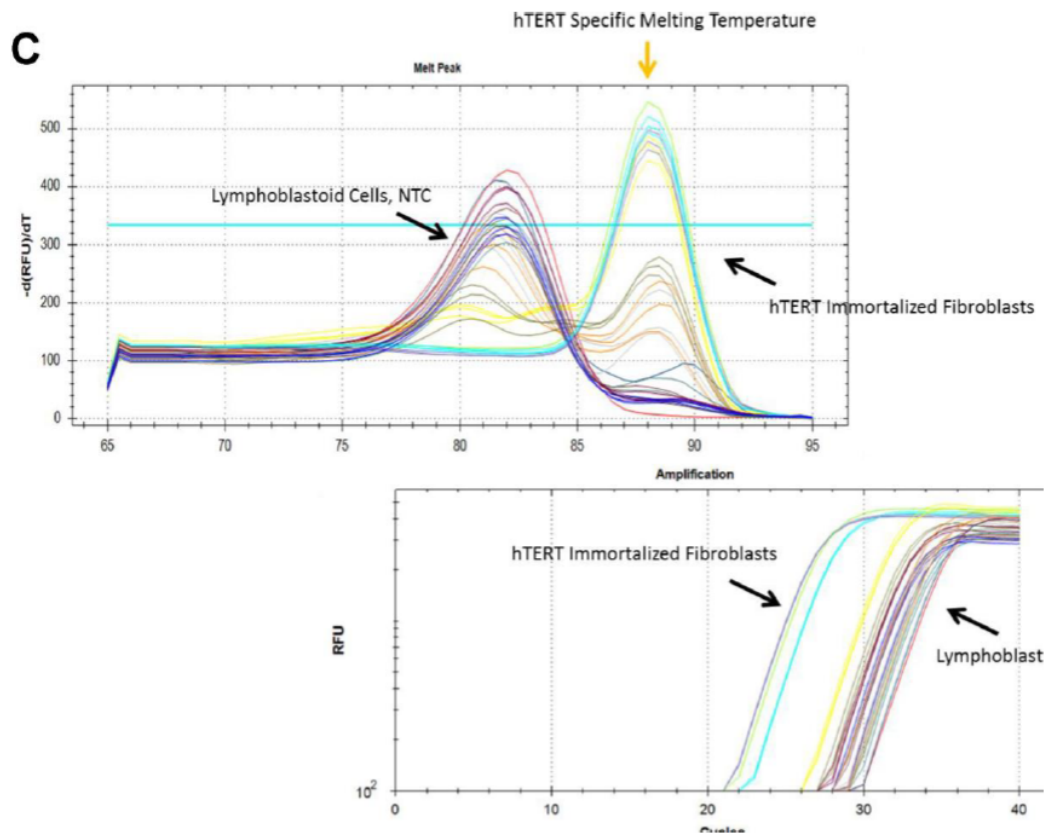


Supplementary Figure 1. Correlation between telomere length analyzed by qPCR and Q-FISH in six NBS lymphoblastoid cell lines and two controls (06P0131,96P0125). Original from [28].

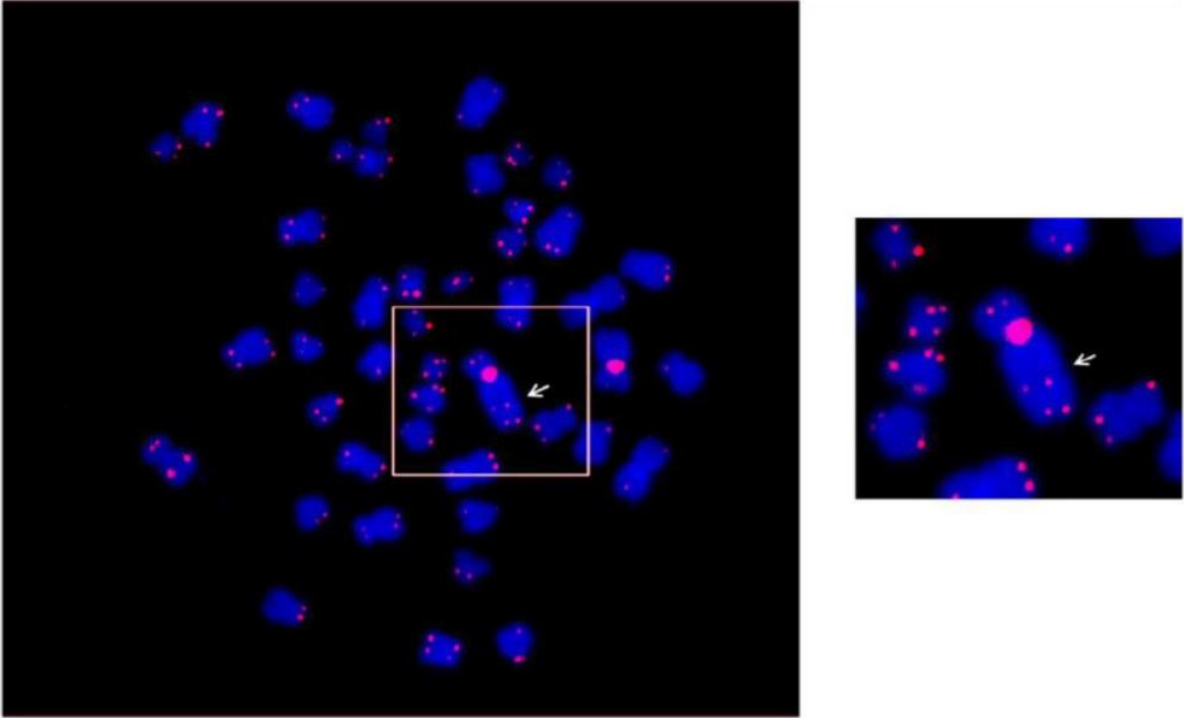


Supplementary Figure 2. Correlation of telomere length measured by qPCR and TRF analysis. The equation of the computed regression line is $y = 3.4(X) + 10.11$ with a correlation coefficient of $r = 0.64$. Mean TRF length has been defined according to the formula described in Roche Application Note No. 12 209 136 001 (April 2018).

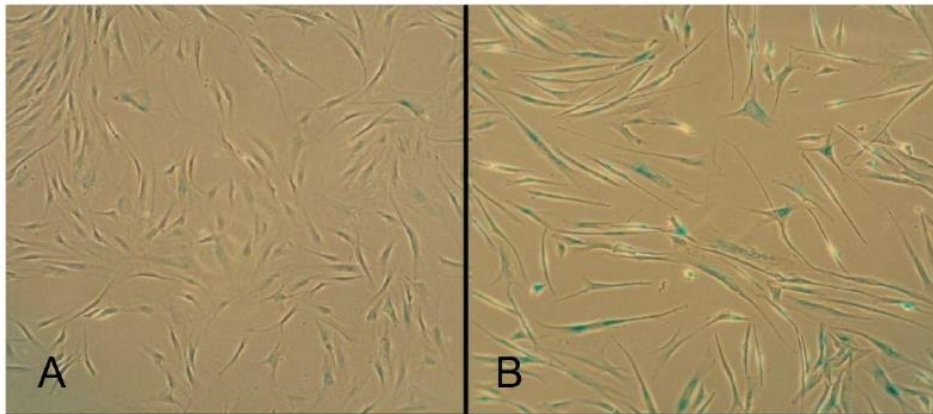
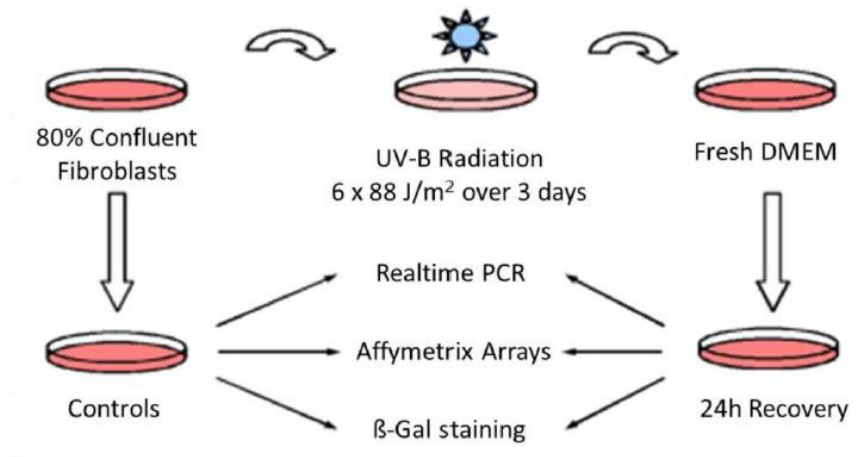




Supplementary Figure 3. (A) Expression of the *hTERT* gene in lymphoblastoid cell lines (LCLs) and *hTERT* immortalized fibroblasts. Agarose gel electrophoresis of the PCR products of the *hTERT* cDNA and the GAPDH cDNA as internal control. 06P0131 and 96P0125 are LCL controls derived from male individuals homozygous for the wild type allele. Original from [28]. (B) Expression of *hTERT* as measured by qPCR. Dissociation curve of qPCR for *hTERT* cDNA (template). The high fluorescent peaks correspond to 95P0182 (green) and 94P0307 (red). The weak fluorescent peaks correspond to 06P0131 (dark green) and 97P0614 (light green). The lower lines (no template) correspond to 89P0319 (purple), 96P0616 (red), Rozd (brown) and 96P0125 (blue). (C) Expression of *hTERT* as measured by qPCR in a separate experiment. Dissociation curve of qPCR for *hTERT* cDNA (template) and non template control (NTC).

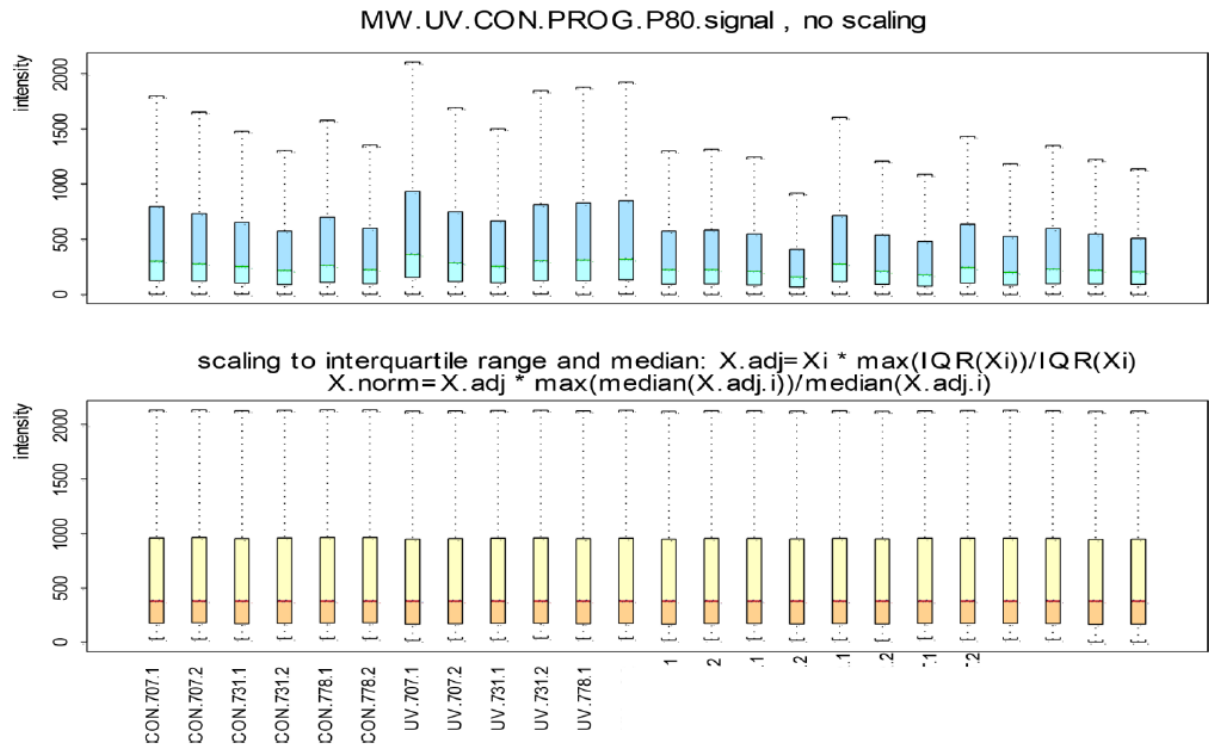


Supplementary Figure 4. Metaphase of NBS-LCL 94P0307 after Q-FISH. The arrow points to the telomere fusion between p telomere of chromosome 2 and an undefined chromosome.

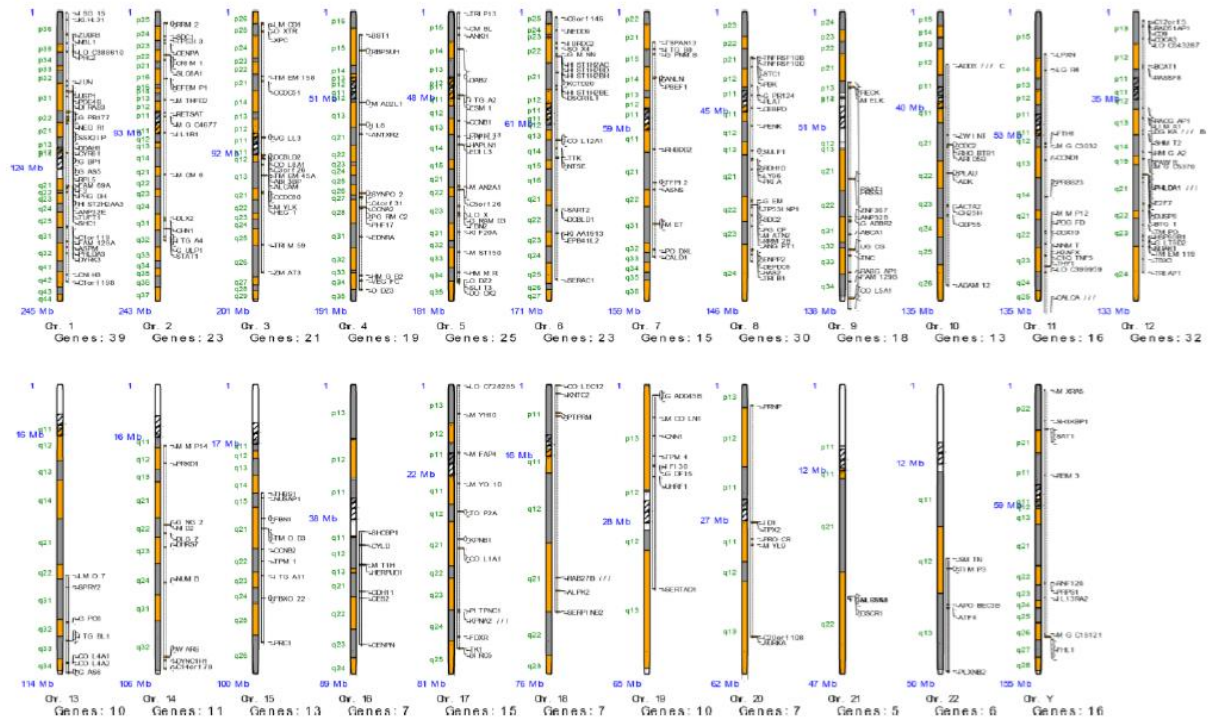


Supplementary Figure 5. TPE-OLD candidate gene approach - UV-Radiation. Human skin fibroblasts at 80 % confluence were exposed to UV-B radiation in a thin layer of DMEM using four 20W TL/12 lamps emitting broadband UV-B peaking at 312 nm. The procedure was performed twice a day for 3 consecutive days with a total dose of 528 J/m². 24 hours after the last irradiation analysis β galactosidase staining was performed. A, pre-treatment. B, senescent cells.

Scaling Data to the Same IQR



Supplementary Figure 6. TPE-OLD candidate gene approach – Statistical analysis. The unnormalized raw data of all experiments were exported in an ASCII format from the Affymetrix GCOS®-Software and imported in the statistical platform S-Plus 8.0® (Insightful Corporation, Seattle, Washington). Ten experiments were assigned two groups based on the characteristics of UV-treatment (6 repeats) and pre-senesence (4 repeats). Both groups were compared to six control experiments. The aim was to identify the most relevant genes discriminating between cells with UV-treatment and cells from pre-senesence, HGP). For this purpose a computer program based on S-Plus which computes the required subsets of genes and simultaneously controls the overall false positive rate was used. 16 microarrays were analyzed, each with 54.675 transcripts on an HGU133-A2.0 array from Affymetrix®, in a design with 3 groups, each with 4-6 replicates. To keep the data at a high quality level we used the GCOS Detection calls to discard all genes (transcripts) with callrates lower than 80% present in at least 13 of 16 repeats in a total of 19.984 transcripts. To make the data of different microarrays comparable, the Affymetrix-GCOS Signal-values were first normalized to have the same interquartile range (IQR) as the maximum IQR of the set and then each chip's median was shifted to the maximum median of the chip set.



Supplementary Figure 7. TPE-OLD candidate gene approach. Differentially expressed genes (DEGs), dependent on chromosomal localization. For simplification only the DEGs with highest significance level are shown.

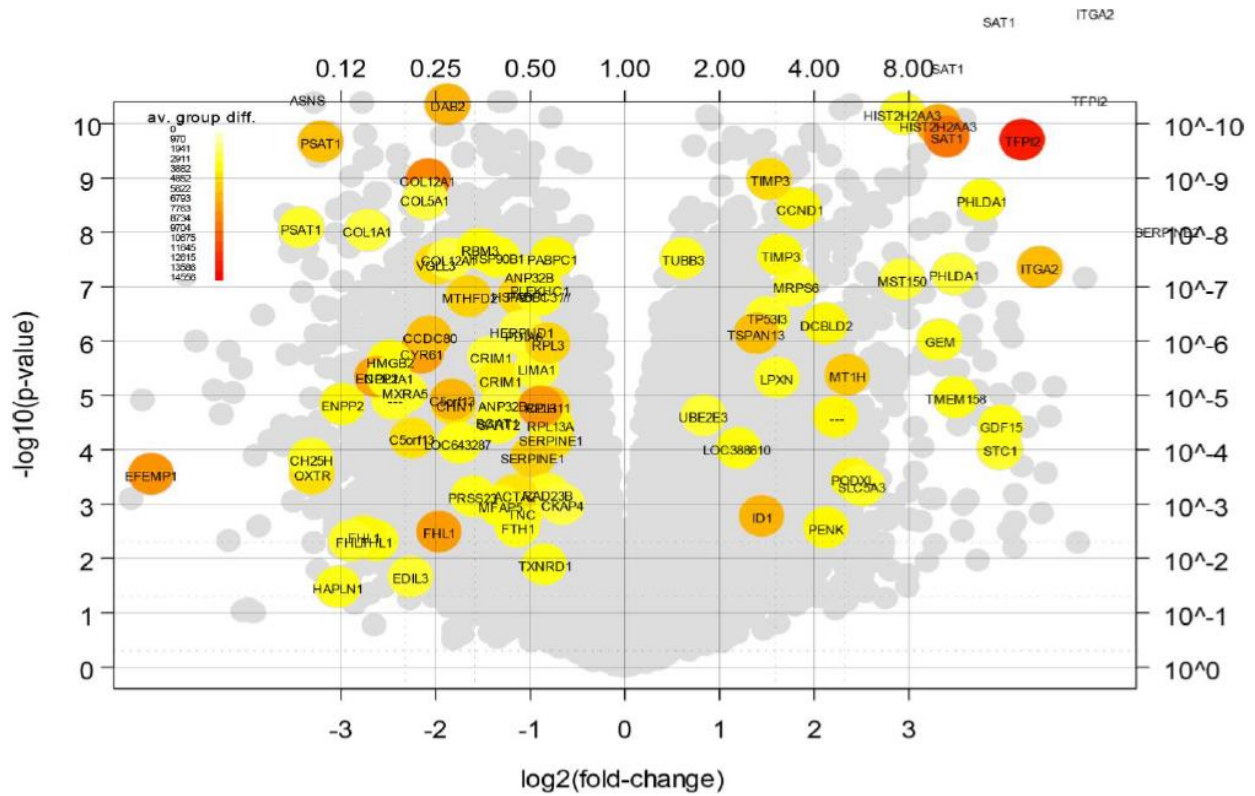


Figure 1 . Volcano plot from MW.UV.CON
 Diff < -3000 , p<= 0.05 , fc < 0.67 , F-p <= 0.05 (n= 60) , diff >= 3000 , fc >= 1.5 (n= 34 entries)
 Comparisons: 54675 , observed differences (pvalue <= 0.05) : 15841 , false detection rate: 0.17

Supplementary Figure 8. TPE-OLD candidate gene approach. Differentially expressed genes (DEGs), visualized as Volcano Plot.

Supplementary Tables

Supplementary Table 1. Telomere length of healthy individuals (controls).

DNA number	relative telomere length	Age (years)	Sex
04P0523	2.16	1	F
04P0862	3.41	1	F
05P0586	1.6	2	M
05P0509	1.12	2	F
04P0535	1.45	3	F
01P0888	0.9	3	M
02P01053	2.25	5	M
04P0216	1.42	9	M
112	1.37	11	F
204	1.29	11	F
166	1.83	12	F
17	1.94	13	F
443	1.93	14	F
444	1.36	15	M
210	0.98	16	F
365	1.51	17	F
247	1.23	18	F
47	1.17	19	F
293	1.58	19	-
193	0.74	20	M
390	1.41	20	M
431	1.25	20	M
423	0.79	20	M
11	1.2	20	M
161	1	20	F
420	0.73	20	F
o2	1	21	M
440	1	21	F
143	1.26	21	F
448	0.83	21	F
129	0.93	21	F
169	1.16	21	F
164	1.18	21	F
13	1.22	21	M
413	0.9	21	F
223	1	22	F
163	0.95	22	M
40	0.91	22	F
188	0.76	22	F
241	1	23	M
246	0.84	23	M
470	1	23	M
280	1.44	23	F
262	0.99	23	F
191	0.89	23	F
328	0.78	24	M
333	1.14	24	F
471	1.39	24	F
464	0.75	24	M
284	1	24	F
150	1	24	F
330	0.85	24	F
292	1.26	24	M
o1	0.97	25	F

425	0.81	25	F
49	1.65	25	F
165	0.99	25	F
189	0.92	25	M
323	1.33	25	M
90	0.84	26	F
320	1.23	26	F
93	1.72	26	F
41	1.52	26	F
388	0.78	27	F
147	0.75	27	F
303	1.34	27	F
445	0.88	27	F
430	0.84	27	F
102	1.3	27	F
32	1	28	M
313	1.54	28	F
160	0.94	28	M
472	0.73	28	F
347	1	28	F
146	0.74	28	M
222	1.1	28	F
Ra	1	28	F
305	1.51	29	F
383	0.92	29	F
207	1	29	F
37	0.81	29	M
73	1.12	29	M
187	0.96	29	M
104	0.74	29	F
23	0.71	29	-
31	0.92	30	F
269	0.84	30	F
1	0.88	30	M
271	1.23	30	F
372	0.93	30	M
27	0.75	30	-
595	1.71	35	M
188	1.21	37	M
596	0.88	38	M
192	0.78	39	M
597	0.94	40	-
194	1	43	F
584	0.79	45	-
591	0.53	60	F
592	0.51	60	M
579	0.4	64	M
590	0.47	66	M
570	0.56	67	M
574	0.5	74	M
588	0.51	75	F
572	0.61	78	F
580	0.61	78	M
587	0.61	80	M

Age group	Number	Mean	SD	Max	Min
1-10	8	1.79	0.80	3.41	0.9
11-20	18	1.30	0.37	1.94	0.73
21-30	65	1.03	0.24	1.72	0.71
31-45	7	1.04	0.33	1.71	0.78
46-80	10	0.53	0.07	0.61	0.4

Supplementary Table 2. Estimation of telomere length of NBS-homozygotes.

DNA number	Relative telomere lengths	Age (years)	Sex
13720	1.62	1	M
12207	1.48	1	M
13424	1.29	1	F
6645	0.3	1	F
5342	0.21	1	M
6018	0.68	2	F
7105	0.44	2	F
3769	0.43	2	M
3772	0.43	2	F
7694	2.1	3	F
11766	2	3	F
8294	2.1	3	F
13607	0.98	5	F
13028	1.55	6	M
3426	1.35	6	F
8165	1	6	M
9990	1.3	6	M
11348	1.17	7	F
5202	0.67	7	F
3201	0.35	7	F
4530	0.22	7	F
8304	0.34	8	M
12557	1.13	8	-
5700	0.99	9	F
11154	1.73	10	M
7822	0.96	10	M
9028	0.78	10	F
5546	0.58	10	M
6023	1.3	12	F
13921	0.76	12	M
2552	0.69	13	M
3197	0.2	13	M
3205	1.3	14	M
3316	0.29	15	M
5567	0.64	15	M
5450	0.56	18	F
10376	0.46	19	F
5431	0.26	20	F

1-10 years:					
Category	Number	Mean	SD	Max	Min
Control	8	1.79	0.80	3.41	0.90
NBS-Homozygote	28	1.01	0.58	2.10	0.21

11-20 years					
Category	Number	Mean	SD	Max	Min
Control	18	1.30	0.37	1.94	0.73
NBS-Homozygote	10	0.65	0.39	1.30	0.20

Supplementary Table 3. Estimation of telomere length of NBS-heterozygotes.

DNA number	Relative telomere lengths	Age (years)	Sex
5343	2	1	F
10130	1.51	2	M
4328	0.89	3	M
8296	1.68	3	M
3221	1	4	M
3223	2	5	F
10133	1.38	5	F
10131	0.99	5	M
10123	2.35	7	M
7234	1.56	8	F
6017	1.77	8	M
3224	1.49	10	M
10120	0.71	12	F
4787	1.31	19	M
8295	0.71	22	F
3222	1	25	F
10124	2	25	M
508	1	27	F
6024	1.3	30	F
466	1.3	30	M
7235	0.79	30	M
7824	0.75	33	M
7823	0.78	35	M
6025	0.32	40	M
4786	0.25	40	M
464	0.6	50	F
463	0.27	54	M

Age	Category	Number	Mean	SD	Max	Min
1 -- 10	Control	8	1.79	0.80	3.41	0.90
	NBS-Heterozygote	12	1.55	0.45	2.35	0.89
11 -- 30	Control	83	1.08	0.29	1.94	0.71
	NBS-Heterozygote	9	1.12	0.41	2.00	0.71
	Control	17	0.74	0.33	1.71	0.40
	NBS-Heterozygote	6	0.50	0.24	0.78	0.25

Supplementary Table 4. Analysis of chromosome fragility after irradiation in six NBS lymphoblastoid cell lines with the absolute longest (above) and absolute shortest (below) telomere lengths.

	Survival (y)	Aberrant mitoses (%)			Breaks (%)		
		0 Gy	0,5 Gy	1,0 Gy	0 Gy	0,5 Gy	1,0 Gy
89P0319 ♀	0	14	69	88	0.16	1.42	2.2
96P0616 ♀	0,2	2	38	42	0.02	0.54	0.68
95P0182 ♀	2,8	0	42	100	0	1.18	3.5
Mean ± SD		5 ± 8	50 ± 7	77 ± 31	0.16 ± 0,02	1.05 ± 0,45	2.13 ± 1,41
97P0614 ♂	>12	2	40	42	0.04	0.52	0.66
RoZd ♀	>12	0	39	59	0	0.48	0.71
94P0307 ♂	>12	0	42	72	0	1.16	1.58
		1 ± 1	40 ± 2	58 ± 15	0.01 ± 0.02	0.72 ± 0.38	0.98 ± 0.52
Control		0	16	10	0	0.2	0.14

Chromatid breaks were distinguished from chromatid translocations. Since the latter are due to two breakage events, they were counted twice for the calculation of the total break events. Dicentric chromosomes were not scored because they cannot be induced in the G2 phase and apparently are due to telomere fusions.

Supplementary Table 5. T/C-FISH data on telomere lengths of NBS-LCL 94P0307.

Chromosome	Median (\pm SD) of p-arm	Median (\pm SD) of q-arm
1	8.7 (\pm 4.8)	8 (\pm 5.9)
2	5.2 (\pm 4.5)	5.1(\pm 8.3)
3	9.0 (\pm 9.3)	9.9 (\pm 6.1)
4	11.2(\pm 10.1)	7.2(\pm 10.5)
5	9.1(\pm 5.7)	11.4(\pm 11.1)
6	9.1(\pm 7.1)	7.8(\pm 4.8)
7	10.6(\pm 6.1)	4.9(\pm 6.7)
8	9.3 (\pm 6.3)	7.1(\pm 6.6)
9	10.7(\pm 5.9)	7.3(\pm 5.5)
10	10.2(\pm 9.4)	17.4(\pm 11.1)
11	9.5(\pm 6.5)	7 (\pm 5.6)
12	8.9(\pm 5.2)	7.5(\pm 5.4)
13	5.6(\pm 6.1)	8.6(\pm 7.3)
14	6.4(\pm 7.3)	9.8(\pm 6.9)
15	5.5(\pm 4.5)	9.7(\pm 4.9)
16	7.5(\pm 6.5)	8.1(\pm 5.1)
17	5 (\pm 4.6)	6.1(\pm 5.7)
18	6.9(\pm 6.2)	5.8(\pm 6.6)
19	13.2(\pm 36.6)	6.2(\pm 5.9)
20	5.3(\pm 4.2)	6.7(\pm 4.1)
21	4.6(\pm 3.2)	6.2(\pm 6.1)
22	5.7(\pm 3.5)	4.9(\pm 3.3)
X	6.6(\pm 7.1)	6.1(\pm 7.9)
Y	6.3(\pm 3.3)	4.5(\pm 5.1)

Supplementary Table 6. Q-FISH analysis of telomere lengths of the p arm of chromosome 19 in 11 metaphases of the NBS lymphoblastoid cell line 94P0307. T/C values are presented for the highly and weakly fluorescent chromosome 19.

Metaphase	1	2	3	4	5	6	7	8	9	10	11	\bar{O}
T/C value: high	85.2	52.6	47.1	44.1	60.5	33.4	79.4	60.2	32.9	68.3	58.6	56.6
T/C value: low	3.2	12.6	2.0	2.1	8.2	1.1	2.1	6.3	2.2	3.5	9.6	4.8

Supplementary Table 7A. TPE-OLD candidate gene approach using Affymetrix expression data in senescent (HGP), *hTERT* immortalized senescent and UV-B-treated fibroblasts for comparison. In yellow those genes with highly significant expression changes in senescent but not in UV-B-treated and/or not in *hTERT* immortalized senescent fibroblasts.

Gene Symbol (Affymetrix ID)	Chromosome location	Gene description	Gene Symbol (Affymetrix ID)	HGP vs. CON				HGP-TERT vs. CON				UV vs. CON			
				P-Value	Fold Change	Fold	Probe Set	P-Value	Fold Change	Fold	Probe Set	P-Value	Fold Change	Fold	Probe Set
BCG	5,121,251-581,495		BCG	0.000001809	682	2.840	205877_x_c0_HGP	BCG	0.000007492	682	2.123	205877_x_c0_HGP-TERT			
BTBD2	1,985,417-2,054,880		BTBD2	0.0000003871	5843	2.024	207722_x_c0_HGP	BTBD2	0.0000042508	5843	2.436	207722_x_c0_HGP-TERT			
CACNA1A	13,517,236-13,734,804		CACNA1A	0.0001904953	775	3.096	203099_x_c0_HGP	CACNA1A	0.0000000000	775	3.096	203099_x_c0_HGP-TERT			
COL3A3	10,970,337-10,121,147		COL3A3	0.0007946944	8009	3.767	210875_c0_HGP	COL3A3	0.0000000000	8009	3.767	210875_c0_HGP-TERT			
DDX3P	14,519,610-14,530,195	DEAD (Rep)	DDX3P	0.0000013000	1012	-0.833	201564_x_c0_HGP	DDX3P	0.0000000000	1012	-0.833	201564_x_c0_HGP-TERT			
KIF9B	18,531,751-18,544,077		KIF9B	0.0000000564	2379	3.040	206255_x_c0_HGP	KIF9B	0.0000465219	2379	2.614	206255_x_c0_HGP-TERT			
KIF9B	18,531,751-18,544,077		KIF9B	0.0000000480	2379	2.710	40852_c0_HGP	KIF9B	0.0000265907	2379	3.055	40852_c0_HGP-TERT			
GAMT	1,397,088-1,402,569		GAMT	0.0000137147	2593	2.071	205534_c0_HGP	GAMT	0.0000000000	2593	2.071	205534_c0_HGP-TERT			
GAMT	1,397,088-1,402,569		GAMT	0.0000000001	2593	2.006	155247_x_c0_HGP	GAMT	0.0000000000	2593	2.006	155247_x_c0_HGP-TERT			
ICAM1	10,381,511-10,397,291		ICAM1	0.0008941400	2683	3.336	202638_x_c0_HGP	ICAM1	0.0004024036	2683	2.718	202638_x_c0_HGP-TERT			
ICAM1	10,381,511-10,397,291		ICAM1	0.0016420465	3363	3.162	202637_c0_HGP	ICAM1	0.0000000000	3363	3.162	202637_c0_HGP-TERT			
SYNA1	18,545,196-18,549,111		SYNA1	0.0004248976	8147	2.104	222242_x_c0_HGP	SYNA1	0.0000420685	8147	3.151	222242_x_c0_HGP-TERT			
SYNA1	18,545,196-18,549,111		SYNA1	0.0000000000	8147	2.104	222242_x_c0_HGP	SYNA1	0.0000420685	8147	3.151	222242_x_c0_HGP-TERT			
MAP2K2	4,990,519-5,124,128		MAP2K2	0.0000007541	5626	2.048	213490_x_c0_HGP	MAP2K2	0.0000000000	5626	2.048	213490_x_c0_HGP-TERT			
MAP2K2	4,990,519-5,124,128		MAP2K2	0.0000000000	5626	2.048	213490_x_c0_HGP	MAP2K2	0.0000000000	5626	2.048	213490_x_c0_HGP-TERT			
MAP2K2	4,990,519-5,124,128		MAP2K2	0.0001449725	8128	2.193	210079_c0_HGP	MAP2K2	0.0000320400	8128	2.099	210079_c0_HGP-TERT			
MAP2K2	4,990,519-5,124,128		MAP2K2	0.0000000000	5626	2.048	213490_x_c0_HGP	MAP2K2	0.0000000000	5626	2.048	213490_x_c0_HGP-TERT			
MAP2K2	4,990,519-5,124,128		MAP2K2	0.0000000000	5626	2.048	213490_x_c0_HGP	MAP2K2	0.0000000000	5626	2.048	213490_x_c0_HGP-TERT			
MAP2K2	4,990,519-5,124,128		MAP2K2	0.0000000000	5626	2.048	213490_x_c0_HGP	MAP2K2	0.0000000000	5626	2.048	213490_x_c0_HGP-TERT			
MAP2K2	4,990,519-5,124,128		MAP2K2	0.0000000000	5626	2.048	213490_x_c0_HGP	MAP2K2	0.0000000000	5626	2.048	213490_x_c0_HGP-TERT			
MAP2K2	4,990,519-5,124,128		MAP2K2	0.0000000000	5626	2.048	213490_x_c0_HGP	MAP2K2	0.0000000000	5626	2.048	213490_x_c0_HGP-TERT			
MAP2K2	4,990,519-5,124,128		MAP2K2	0.0000000000	5626	2.048	213490_x_c0_HGP	MAP2K2	0.0000000000	5626	2.048	213490_x_c0_HGP-TERT			
MAP2K2	4,990,519-5,124,128		MAP2K2	0.0000000000	5626	2.048	213490_x_c0_HGP	MAP2K2	0.0000000000	5626	2.048	213490_x_c0_HGP-TERT			
MAP2K2	4,990,519-5,124,128		MAP2K2	0.0000000000	5626	2.048	213490_x_c0_HGP	MAP2K2	0.0000000000	5626	2.048	213490_x_c0_HGP-TERT			
MAP2K2	4,990,519-5,124,128		MAP2K2	0.0000000000	5626	2.048	213490_x_c0_HGP	MAP2K2	0.0000000000	5626	2.048	213490_x_c0_HGP-TERT			
MAP2K2	4,990,519-5,124,128		MAP2K2	0.0000000000	5626	2.048	213490_x_c0_HGP	MAP2K2	0.0000000000	5626	2.048	213490_x_c0_HGP-TERT			
MAP2K2	4,990,519-5,124,128		MAP2K2	0.0000000000	5626	2.048	213490_x_c0_HGP	MAP2K2	0.0000000000	5626	2.048	213490_x_c0_HGP-TERT			
MAP2K2	4,990,519-5,124,128		MAP2K2	0.0000000000	5626	2.048	213490_x_c0_HGP	MAP2K2	0.0000000000	5626	2.048	213490_x_c0_HGP-TERT			
MAP2K2	4,990,519-5,124,128		MAP2K2	0.0000000000	5626	2.048	213490_x_c0_HGP	MAP2K2	0.0000000000	5626	2.048	213490_x_c0_HGP-TERT			
MAP2K2	4,990,519-5,124,128		MAP2K2	0.0000000000	5626	2.048	213490_x_c0_HGP	MAP2K2	0.0000000000	5626	2.048	213490_x_c0_HGP-TERT			
MAP2K2	4,990,519-5,124,128		MAP2K2	0.0000000000	5626	2.048	213490_x_c0_HGP	MAP2K2	0.0000000000	5626	2.048	213490_x_c0_HGP-TERT			
MAP2K2	4,990,519-5,124,128		MAP2K2	0.0000000000	5626	2.048	213490_x_c0_HGP	MAP2K2	0.0000000000	5626	2.048	213490_x_c0_HGP-TERT			
MAP2K2	4,990,519-5,124,128		MAP2K2	0.0000000000	5626	2.048	213490_x_c0_HGP	MAP2K2	0.0000000000	5626	2.048	213490_x_c0_HGP-TERT			
MAP2K2	4,990,519-5,124,128		MAP2K2	0.0000000000	5626	2.048	213490_x_c0_HGP	MAP2K2	0.0000000000	5626	2.048	213490_x_c0_HGP-TERT			
MAP2K2	4,990,519-5,124,128		MAP2K2	0.0000000000	5626	2.048	213490_x_c0_HGP	MAP2K2	0.0000000000	5626	2.048	213490_x_c0_HGP-TERT			
MAP2K2	4,990,519-5,124,128		MAP2K2	0.0000000000	5626	2.048	213490_x_c0_HGP	MAP2K2	0.0000000000	5626	2.048	213490_x_c0_HGP-TERT			
MAP2K2	4,990,519-5,124,128		MAP2K2	0.0000000000	5626	2.048	213490_x_c0_HGP	MAP2K2	0.0000000000	5626	2.048	213490_x_c0_HGP-TERT			
MAP2K2	4,990,519-5,124,128		MAP2K2	0.0000000000	5626	2.048	213490_x_c0_HGP	MAP2K2	0.0000000000	5626	2.048	213490_x_c0_HGP-TERT			
MAP2K2	4,990,519-5,124,128		MAP2K2	0.0000000000	5626	2.048	213490_x_c0_HGP	MAP2K2	0.0000000000	5626	2.048	213490_x_c0_HGP-TERT			
MAP2K2	4,990,519-5,124,128		MAP2K2	0.0000000000	5626	2.048	213490_x_c0_HGP	MAP2K2	0.0000000000	5626	2.048	213490_x_c0_HGP-TERT			
MAP2K2	4,990,519-5,124,128		MAP2K2	0.0000000000	5626	2.048	213490_x_c0_HGP	MAP2K2	0.0000000000	5626	2.048	213490_x_c0_HGP-TERT			
MAP2K2	4,990,519-5,124,128		MAP2K2	0.0000000000	5626	2.048	213490_x_c0_HGP	MAP2K2	0.0000000000	5626	2.048	213490_x_c0_HGP-TERT			
MAP2K2	4,990,519-5,124,128		MAP2K2	0.0000000000	5626	2.048	213490_x_c0_HGP	MAP2K2	0.0000000000	5626	2.048	213490_x_c0_HGP-TERT			
MAP2K2	4,990,519-5,124,128		MAP2K2	0.0000000000	5626	2.048	213490_x_c0_HGP	MAP2K2	0.0000000000	5626	2.048	213490_x_c0_HGP-TERT			
MAP2K2	4,990,519-5,124,128		MAP2K2	0.0000000000	5626	2.048	213490_x_c0_HGP	MAP2K2	0.0000000000	5626	2.048	213490_x_c0_HGP-TERT			
MAP2K2	4,990,519-5,124,128		MAP2K2	0.0000000000	5626	2.048	213490_x_c0_HGP	MAP2K2	0.0000000000	5626	2.048	213490_x_c0_HGP-TERT			
MAP2K2	4,990,519-5,124,128		MAP2K2	0.0000000000	5626	2.048	213490_x_c0_HGP	MAP2K2	0.0000000000	5626	2.048	213490_x_c0_HGP-TERT			
MAP2K2	4,990,519-5,124,128		MAP2K2	0.0000000000	5626	2.048	213490_x_c0_HGP	MAP2K2	0.0000000000	5626	2.048	213490_x_c0_HGP-TERT			
MAP2K2	4,990,519-5,124,128		MAP2K2	0.0000000000	5626	2.048	213490_x_c0_HGP	MAP2K2	0.0000000000	5626	2.048	213490_x_c0_HGP-TERT			
MAP2K2	4,990,519-5,124,128		MAP2K2	0.0000000000	5626	2.048	213490_x_c0_HGP	MAP2K2	0.0000000000	5626	2.048	213490_x_c0_HGP-TERT			
MAP2K2	4,990,519-5,124,128		MAP2K2	0.0000000000	5626	2.048	213490_x_c0_HGP	MAP2K2	0.0000000000	5626	2.048	213490_x_c0_HGP-TERT			
MAP2K2	4,990,519-5,124,128		MAP2K2	0.0000000000	5626	2.048	213490_x_c0_HGP	MAP2K2	0.0000000000	5626	2.048	213490_x_c0_HGP-TERT			
MAP2K2	4,990,519-5,124,128		MAP2K2	0.0000000000	5626	2.048	213490_x_c0_HGP	MAP2K2	0.0000000000	5626	2.048	213490_x_c0_HGP-TERT			
MAP2K2	4,990,519-5,124,128		MAP2K2	0.0000000000	5626	2.048	213490_x_c0_HGP	MAP2K2	0.0000000000	5626	2.048	213490_x_c0_HGP-TERT			
MAP2K2	4,990,519-5,124,128		MAP2K2	0.0000000000	5626	2.048	213490_x_c0_HGP	MAP2K2	0.0000000000	5626	2.048	213490_x_c0_HGP-TERT			
MAP2K2	4,990,519-5,124,128		MAP2K2	0.0000000000	5626	2.048	213490_x_c0_HGP	MAP2K2	0.0000000000	5626	2.048	213490_x_c0_HGP-TERT			
MAP2K2	4,990,519-5,124,128		MAP2K2	0.0000000000	5626	2.048	213490_x_c0_HGP	MAP2K2	0.0000000000	5626	2.048	213490_x_c0_HGP-TERT			
MAP2K2	4,990,519-5,124,128		MAP2K2	0.0000000000	5626	2.048	213490_x_c0_HGP	MAP2K2	0.0000000						

Supplementary Table 8. Regulation of telomeric 19p genes in normal and NBS fibroblasts with short telomeres (relative to cells with long telomeres).

Gene	Functions in senescence and/or cell growth	Reference	Distance to telomere [Mbp]	Differential gene expression, Affymetrix data	Differential gene expression, qPCR data Control fibroblasts	Differential gene expression, qPCR data NBS fibroblasts	TPE-OLD Effect
					[fold-change]		
BSG	MMP and cytokine production	[32]	0.6	+2.8	+3.2	+2.4	(N)
GAMT	ATP production (SASP?)	[33, 34]	1.4	+2.0	+5.6	+1.9	(N)
SCAMP4	player in SASP	[35]	1.9	+2.3	+1.9	+1.6	(N)
OLFM2	cell differentiation	[36]	9.9	+3.8	+50	+3.3	(N)
UHRF1	neg. regulator of senescence	[40]	4.9	-2.7	-5.0	+1.7	R
COL5A3	age-dependent tissue remodel.	[37]	10.0	+2.4	+25.0	+4.0	(N)
RNASEH2A	migration and invasion	[41]	12.8	-2.1	-4.5	+1.2	R
CACNA1A	calcium entry; nerve function	[38]	13.6	+2.1	+1.3	-1.5	R
DDX39A	role in cancer and longevity	[42]	14.6	-2.0	-2.2	+1.7	R
NOTCH3	pos. regulator of senescence (p21)	[39]	15.2	+4.1	+100.0	+58.0	(N)

BSG, basigin; GAMT, guanidinoacetate methyl-transferase; SCAMP4, secretory carrier membrane protein 4; OLFM2, olfactomedin 2; UHRF1, Ubiquitin like with PHD and ring finger domain 1; COL5A3, collagen type V alpha 3 chain; RNASEH2A, ribonuclease H2 subunit A; CACNA1A, calcium voltage-gated channel subunit alpha1 A; DDX39A, DEXD-box helicase 39A; NOTCH3, Notch Receptor 3; SASP, senescence associated secretory phenotype; MMP, matrix metalloproteinases; (N), TPE-OLD: normal but attenuated regulation; R, TPE-OLD: reversed regulation, compared to regulation (mRNA) in healthy control fibroblasts; grey overlay: upregulation in pre-senescent cells; green overlay, down regulation in pre-senescent cells

Supplementary Table 9. Correlation between telomere length and clinical data of 21 NBS homozygotes.

Telomere length	Age at cancer manifestation		Age at death	
		P		P
Long vs. median		0.07		0.50
Median vs. short		0.52		0.54
Long vs. short		0.41		0.99

The p values are based on the unpaired T- test.

Publication 3: Therapeutic Targeting of Telomerase.

Jäger K, Walter M.

Genes (Basel) 2016; 7(7): 39

DOI: 10.3390/genes7070039

Impact factor (2021): 4.096

Review

Therapeutic Targeting of Telomerase

Kathrin Jäger¹ and Michael Walter^{1,2,*}

¹ Institute of Laboratory Medicine, Clinical Chemistry and Pathobiochemistry, Charité-Universitätsmedizin Berlin, Augustenburger Platz 1, Berlin 13353, Germany; kathrin.jaeger@charite.de

² Labor Berlin-Charité Vivantes Services GmbH, Sylter Str. 2, Berlin 13353, Germany

* Correspondence: m.walter@charite.de; Tel.: +49-30-4050-26505

Academic Editor: Gabriele Saretzki

Received: 1 May 2016; Accepted: 24 June 2016; Published: 21 July 2016

Abstract: Telomere length and cell function can be preserved by the human reverse transcriptase telomerase (hTERT), which synthesizes the new telomeric DNA from a RNA template, but is normally restricted to cells needing a high proliferative capacity, such as stem cells. Consequently, telomerase-based therapies to elongate short telomeres are developed, some of which have successfully reached the stage I in clinical trials. Telomerase is also permissive for tumorigenesis and 90% of all malignant tumors use telomerase to obtain immortality. Thus, reversal of telomerase upregulation in tumor cells is a potential strategy to treat cancer. Natural and small-molecule telomerase inhibitors, immunotherapeutic approaches, oligonucleotide inhibitors, and telomerase-directed gene therapy are useful treatment strategies. Telomerase is more widely expressed than any other tumor marker. The low expression in normal tissues, together with the longer telomeres in normal stem cells versus cancer cells, provides some degree of specificity with low risk of toxicity. However, long term telomerase inhibition may elicit negative effects in highly-proliferative cells which need telomerase for survival, and it may interfere with telomere-independent physiological functions. Moreover, only a few hTERT molecules are required to overcome senescence in cancer cells, and telomerase inhibition requires proliferating cells over a sufficient number of population doublings to induce tumor suppressive senescence. These limitations may explain the moderate success rates in many clinical studies. Despite extensive studies, only one vaccine and one telomerase antagonist are routinely used in clinical work. For complete eradication of all subpopulations of cancer cells a simultaneous targeting of several mechanisms will likely be needed. Possible technical improvements have been proposed including the development of more specific inhibitors, methods to increase the efficacy of vaccination methods, and personalized approaches. Telomerase activation and cell rejuvenation is successfully used in regenerative medicine for tissue engineering and reconstructive surgery. However, there are also a number of pitfalls in the treatment with telomerase activating procedures for the whole organism and for longer periods of time. Extended cell lifespan may accumulate rare genetic and epigenetic aberrations that can contribute to malignant transformation. Therefore, novel vector systems have been developed for a 'mild' integration of telomerase into the host genome and loss of the vector in rapidly-proliferating cells. It is currently unclear if this technique can also be used in human beings to treat chronic diseases, such as atherosclerosis.

Keywords: telomerase; telomeres; aging; senescence; atherosclerosis; cancer; gene therapy; immunotherapy; regenerative medicine; personalized medicine

1. Telomeres and Telomerase in Aging and Cancer

Aging is a complex process, which is accompanied by cycle arrest, remodeling in cell morphology and chromatin structure, functional decline, and extensive shifts in gene expression and metabolism. The aging of human cells can be mediated via stress-related mechanisms and via replicative senescence

induced by telomere shortening. The various senescence triggers interact cooperatively and induce overlapping signaling pathways. Stressors include endogenous substances, exogenous factors, and species-specific mechanisms of aging such as replicative senescence. Replicative aging induced by telomere attrition is a species-specific aging mechanism, which acts as a tumor-suppressor in large, long-lived organisms [1] (Figure 1). Telomere attrition is, however, associated with functional decline and other negative effects that become relevant for the organism beyond the stone-age life span of approximately 50 years. An inverse correlation between telomere length and onset of age-related diseases has been shown in many studies even though the causality is still controversial [2].

Telomeres consist of repetitive non-coding DNA sequences (in humans TTAGGG), which are located at the end of the chromosomes. Telomeres, together with the shelterin complex, form a cap to protect the chromosome ends [3–5]. The shelterin complex consists of six telomere-associated proteins [6]. The telomere sequence is recognized by the subunits TRF1, TRF2, and POT1. These subunits are interconnected by the proteins TIN2, TPP1, and Rap1. The complex allows cells to distinguish telomeres from DNA damage sites. Without this protection, e.g., when telomeres shorten beyond a critical threshold, unprotected telomeres provoke a DNA damage response [7].

Telomere shortening occurs due to the so-called end replication problem, which means that the 3' end of the DNA strand shortens with each cell division, since the DNA polymerase cannot completely replicate the strand [5,8]. At a certain threshold of telomere attrition the damage-repair system recognizes the unprotected DNA double strand as DNA breaks and activates the p53 or the p16INK4a signaling pathway to initiate a senescence or apoptosis program. Reactive oxygen species (ROS) or other environmental stress factors may also lead to telomere damage and accelerate the telomere attrition. Particularly, the GGG triplet within the human telomere sequence TTAGGG is vulnerable to chemical modifications. From a critical telomere length, onwards, telomeres are unable to claim the shelterin complex resulting in loss of the protective inner nucleotide loop, which ultimately leads to genomic instability [9,10] (Figure 1).

In numerous studies, it was observed that a healthy lifestyle is correlated with longer telomeres, likely reflecting protection against age-related diseases [4]. It has been shown in aging mice that cells with short and/or damaged telomeres are accumulating in stress-prone tissues, likely due to replicative exhaustion and/or stress-induced telomere damage. Animal studies suggest that senescence is not only a marker of, but also involved in, the propagation of age-related disorders [5,10].

From an evolutionary point of view, it is thought that the cell division limit was developed as a mechanism for tumor suppression. Indeed, in mice short telomeres are a hindrance to cancer growth. On the other hand, very short and damaged telomeres can also provoke tumor growth when a missing cap leads to chromosomal instability, as it is exemplarily observed in Dyskeratosis congenita [11].

Telomere length and cell function can be preserved by the reserve transcriptase telomerase. The human telomerase consists of two subunits: a RNA templates (TERC, telomerase RNA component), and the catalytic subunit (hTERT, human telomerase reverse transcriptase), which synthesizes the new telomeric DNA from the RNA template [4]. Higher telomerase activities are under normal conditions only detectable in cells that need a high replicative capacity, such as stem cells and progenitor cells [9].

Telomere elongation by telomerase leads to chromosomal stabilization and a change to a more youthful gene expression pattern. In addition to its established role in extending telomeres, hTERT can promote proliferation of resting stem cells through a non-canonical pathway [9] and has direct effects on transcription and cell signaling, e.g., as a cofactor in a β -catenin transcriptional complex [12], which plays a role in embryogenesis and development [13]. Uncontrolled induction of telomerase would, however, have also pitfalls. Telomerase, per se, is no oncogene, but permissive for carcinogenesis and approximately 90% of all tumor cells express the enzyme to elongate the telomeres, which makes its use for systemic applications problematic.

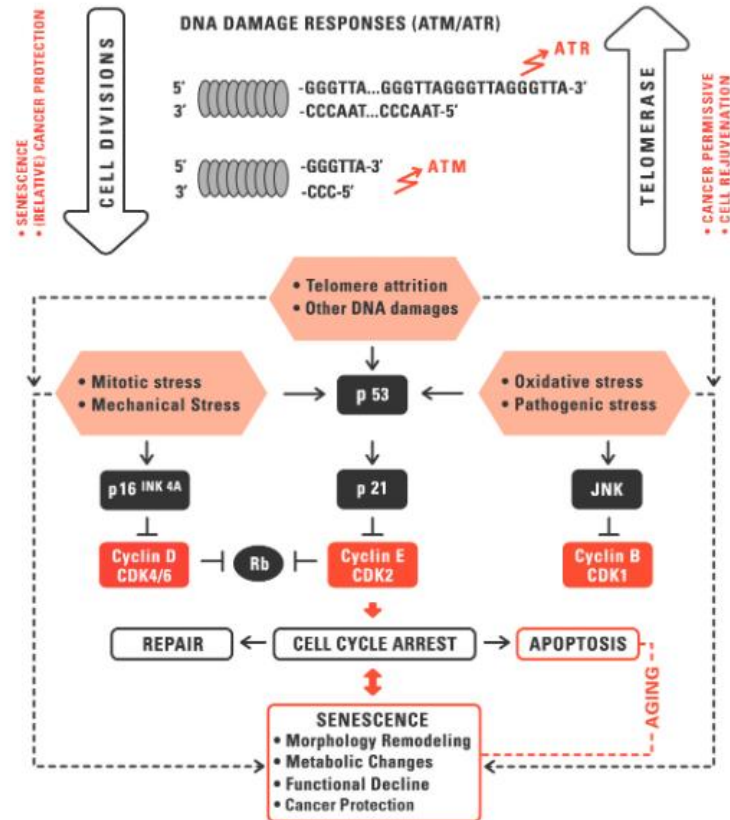


Figure 1. Replicative aging cooperates with other aging mechanisms to activate the p53 and/or Rb signaling pathways. ATM and ATR are sensors of DNA double- and single-strand damage induced by replicative senescence or other DNA damage. Activated ATM and ATR trigger checkpoint responses to induce cell cycle arrest. A stronger stimulation of p53 may lead to apoptosis by activating the mitochondrial pathway of apoptosis. Telomere length and cell function can be preserved by the reserve transcriptase telomerase, which synthesizes the new telomeric DNA from the RNA template. Telomerase may help to avoid senescence and to rejuvenate tissues, but is also permissive for carcinogenesis. Senescence may help to prevent tumor growth but can also be overcome by a process called crisis, and then has paracrine and other pro-tumorigenic effects. With permission, adapted from [1].

The variety in telomere length in individuals of the same age is determined by genetic and environmental factors, leading to telomere damage and accelerated shortening of telomere length [14,15]. Inflammation is thought to contribute to telomere attrition in cells of the immune system by promoting leukocyte turnover and replicative exhaustion, and possibly also by direct modulation of telomerase activity by ROS and other stress factors [16]. For example, increased production of cytokines has been shown to adversely affect telomerase activity and telomere length [17]. C-reactive protein (CRP), a marker of inflammation, is inversely correlated with leukocyte telomere length (LTL) [18]. Shorter telomeres are associated with higher interleukin-6 (IL-6) and C-reactive protein values [19]. Telomerase activity was found to be reduced by psychological and life stress [20,21]. Various stressors trigger increased ROS formation, which leads to telomere attrition both directly and indirectly (by lower hTERT activity), which ultimately leads to a reduction of leukocyte telomere length (LTL) [4]. Smoking is an excellent example for higher ROS formation and, consequently, progressive shortening of telomeres [22].

At the cellular level, senescence serves as a natural tumor suppressor [23]. Senescent cells are no longer capable of replication and shut down their metabolism to a minimum. Only some key pathways are active and only few genes are expressed at higher levels. The senescence normally prevents the replication of abnormal chromosomes. The p16/pRb tumor suppressor pathways are activated in response to DNA damage and telomere dysfunction during senescence [23–25]. This process, however, could be flawed by oncogene activation to bypass senescence. An incorrect removal of senescent cells can lead to malignancy [23]. The alternative lengthening of telomeres (ALT) mechanism enables cancer cells with inactive telomerase the conservation of the telomere structure [26,27]. Approximately 5%–10% of cancer cells maintain their telomeres by ALT, in which sister chromatids exchange their telomeres by non-reciprocal recombination events [28]. Studies have shown that these cancer cells are more sensitive to ROS and drug treatments when they elongate their telomeres by ALT. Apparently these cells are under strong pressure to activate the alternative mechanism to escape senescence and apoptosis [26].

The catalytic subunit hTERT (human telomerase reverse transcriptase) was found to be upregulated in cervical carcinomas [29,30], hepatocellular carcinoma [31], lung tumors [29], breast carcinomas [29], and neuroblastomas [29]. Telomerase in tumor cells is re-expressed on transcriptional, post-transcriptional, post-translational, and epigenetic levels [23]. Under normal conditions, the absence of CAAT and TATA elements in the TERT promoter prevents constitutive activation. However, promoter mutations or unusual epigenetic changes may overcome this barrier [32]. Telomerase also plays a regulatory role in the spread of cancer cells [33]. In the vast majority of investigated tumors an increased expression of human telomerase RNA (hTR) was detected, as well [34].

Telomerase is a target for both anti-cancer and cell rejuvenation strategies with a broad overlap of targets at different cellular and functional levels (Figures 1 and 2).

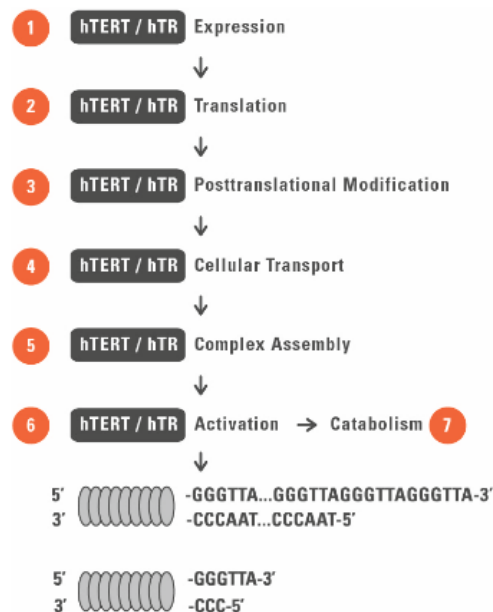


Figure 2. Therapeutic targeting of telomerase. Potential targets of telomerase for antitumor (telomerase suppressing) and rejuvenation (telomerase activation) drugs are shown by numbers 1–7. 1, inhibition/activation of gene transcription; 2, inhibition/activation of protein synthesis; 3, modulation of activity by posttranslational modifications; 4, modulation of telomerase activity by cellular sequestration; 5, interference with telomerase complex assembly; 6, modulation of signaling pathways and molecules involved in enzyme activation, such as Wnt/ β -catenin, PI3K/Akt, and mTOR signaling; and 7, modulation of telomerase complex catabolism including vaccine therapy.

2. Telomerase as a Target for Regenerative Medicine

Replicative senescence contributes to the decline in many physiological functions and in most tissues and, thus, contributes to the pathology of chronic diseases [35,36]. As telomerase activity is not, or only at low levels, detectable in somatic tissues there are many situations and chronic diseases in which the transient rejuvenation by telomerase immortalization could be a therapeutic option [16,37,38]. There are several possible strategies to reconstruct or enhance the enzymatic activity for therapeutic use:

(1). *Classical gene therapy with transfection of telomerase sequences*: This approach can be used for tissue engineering, for in vitro optimization of stem cell transplantation in donor cells with short telomeres [39] and, in principle, also for the treatment of chronic diseases in the whole organism, provided that induction of telomerase is time-limited.

(2). *Re-expression of silenced telomerase*: Cell differentiation normally leads to transcriptional downregulation of telomerase induced by signaling and epigenetic alterations [40,41]. However, telomerase downregulation can, at least in part, be reversed by various substances and mechanisms. Examples are histone deacetylase inhibitors [42] and estrogen receptor agonists, the latter acting by Akt mediated phosphorylation [43]. Many drugs with main targets other than telomerase also influence hTERT on transcriptional and/or posttranslational level. Involved signaling pathways that upregulate hTERT expression and/or activity (see also paragraphs below) are PI3/Akt, MAPK/ERK1/2, and the Wnt/ β -catenin pathway.

(3). *Activation of residual enzymatic activity*: Activation of telomerase activity itself is an option for cells with residual telomerase activity such as stem cells of regenerative tissues and lymphocytes. In lymphocytes' clonal expansion typically activates telomerase activity via enzyme phosphorylation and subsequent nuclear translocation [44]. This function declines with advanced age and leads to exhaustion of memory cells and could be restored by direct interaction with the telomerase holoenzyme or the telomerase activating signaling pathways [45].

(4). *Modulation of the intracellular location*: The sequestration of telomerase is another possible level of regulation on telomerase activity, implicating telomerase localization as a potential target for pharmacotherapy [46]. Telomerase can be translocated between the nucleus and the cytosol. hTERT is also present in mitochondria with yet unknown physiological significance [16,47].

Ectopic expression of telomerase was used to immortalize a wide variety of cell types including human fibroblasts [48–52], dermal fibroblasts [53,54], keratinocytes [55], muscle cells [56–58], vascular endothelial [59–61], myometrial [62], retinal [48–52], bone marrow stromal cells [63–66], osteoblasts [67–69], odontoblasts [70], CD4 and CD8 T cells [71,72], mesenchymal stem cells [72], myoblasts [73], hepatic stellate cells [74,75], fetal neuronal precursors [76], and breast epithelial cells [37]. Some cell types, such as bronchial and corneal cells, were used to form three-dimensional cultures [37].

Telomerase reconstruction was first discussed for treatment of diseases with distorted enzymatic activity of telomerase, namely, dyskeratosis congenital and aplastic anaemia [77]. Potential other applications are production of epithelia for burns or wounds, endothelia for blood vessels, chondrocytes for the treatment of arthritis, osteocytes for bone defects, and hematopoietic cells for bone marrow transplants or for the replacement of immune cells [39,78,79]. By use of this technique human blood vessels have already been engineered in vitro [56].

Transient telomerase activation may also be used for the treatment of other chronic diseases such as cardiac muscle disease, atherosclerosis [15], immunodeficiency, and bone marrow failure [11,80], liver disease [11,81], pulmonary fibrosis [11,82], degenerative cartilage defects [83], cataract [84], rheumatoid arthritis [85], organ transplantation [86], or treatments associated with the accelerated formation of senescent cells such as past cancer therapy or HIV [87,88]. Cartilage defects have become the target of cartilage tissue engineering [83]. Thomas and coworkers have demonstrated that bovine

TERT-modified bovine adrenocortical cells can be transplanted into severe combined immunodeficient mice, and that these cell clones behave like their normal counterparts and form functional tissue after transplantation. This tissue is histologically similar to tissue formed from normal cells and shows a similar rate of cell division, implying a therapeutic role of telomerase in xenotransplantation [86].

The association between telomere length and aging has also led to the development of telomerase activators that may induce hTERT and/or hTR expression, enhance enzyme activity and/or influence cellular location. The idea behind this approach is to reverse normal cellular aging and to treat symptoms of aging. A single molecule telomerase activator, cycloastragenol (commercially available as TA-65, derived from *Astragalus membranaceus* root), has been shown to transiently activate telomerase in T lymphocytes [87], associated with the retardation of telomere shortening, increased proliferative potential, and enhanced functional response [88]. This substance was proposed to be used for the treatment of accelerated immunosenescence in HIV patients to increase the number of senescent memory CD8 T cells [87,88]. Cycloastragenol (TA-65) has been sold as a food supplement since 2013 and has been identified as an effective telomerase activator in immune cells, neonatal keratinocytes, and fibroblasts [87,89], acting via ERK-pathway activation and subsequent enhancement of telomerase expression. It increases the telomere length in mice without increasing the cancer incidence [90]. In a small pilot study it was used for the treatment of age-related macular degeneration [91] and was shown to improve markers of metabolic, bone, and cardiovascular health [92]. A moderate increase in leukocyte telomere length was shown in humans [93]. However, the number of patients in these studies was limited and some effects were of borderline significance. Long-term prospective studies regarding positive or side-effects are lacking.

Other phytochemicals have been shown to activate telomerase. Resveratrol activates telomerase in mammary epithelial [94] and endothelial progenitor cells [95], most likely due to the upregulation of SIRT1 [96]. Current knowledge regarding possible long-term effects is, also for this substance, incomplete [96]. For the treatment of cataracts pharmaceuticals with telomerase activating effects such as N-acetylcarnosine have been proposed since reduced telomere length is intimately involved in opacification, making the lens opaque or cloudy [84]. Another compound (AGS-499) has neuroprotective effects in mice and showed delayed progression of amyotrophic lateral sclerosis and increased survival in SOD1 transgenic mice [97]. Bone marrow mesenchymal stem cells often display premature aging and unstable proliferation. It has recently been shown in a rat model that co-transfection of BMSCs with telomerase and nerve growth factor had a better effect on learning and memory compared to cells lacking these factors [98]. These effects may be used for the development of therapeutic strategies to treat cognitive impairment in vascular dementia.

Indirect strategies to upregulate telomerase activity are described for certain antioxidants, such as N-acetylcysteine, which blocks the nuclear export of telomerase into the cytosol [99] and α -tocopherol, which was shown to retain telomerase activity in brain microvascular endothelial cells [100]. The idea behind this concept is that ROS damage telomeres directly (by damaging the vulnerable GGG triplet of the repetitive telomere sequence) and indirectly (by modulating telomerase activity and cellular location) [101]. HMG-CoA reductase inhibitors may also have telomere lengthening effects [102], by interfering with the redox balance of cells [99] and by increasing expression of the telomere stabilizing protein TRF2 [103]. Finally, Ginkgo biloba was shown to activate telomerase by inducing PI3K/Akt signaling [104].

Telomerase upregulation in skin diseases: The skin is an organ for which some therapeutic approaches of telomerase are already in use. Several therapeutic strategies have been proposed based on in vivo or ex vivo stimulation of stem/progenitor cells for expressing hTERT or telomere RNA component (hTR) and for the replacement of dysfunctional or lost skin [37,105–111]. The application area ranges from reconstructive surgery after severe wounds, burns, deep skin injuries, infections, and decubitus ulcers [106,107] to treatment of diseases with defects in hTERT and/or hTR associated with premature replicative senescence of the skin, e.g., the premature aging Werner syndrome, in Fanconi anaemia, and chronic dysplastic anaemia [37,112]. Positive effects of bone marrow-derived stem/progenitor cells for

skin tissue engineering have been shown in several studies either alone or in combination with artificial skin grafts, thereby reducing the risk of graft rejection [106,108,113]. Ex vivo co-culture of human skin substitutes with circulating endothelial progenitor cells improved survival by formation of functional microvessels [107]. In a rat model transfection of hTERT into hair follicle stem cells by coating polyethylenimine DNA complexes on the skin surface stimulated hair growth [114], presumably by both telomere elongation and/or modulating Wnt/ β -catenin signaling. Recently, optimized three-dimensional culture conditions have been described with enhanced hTERT expression levels, proliferation, and multipotency of human dermal stem/progenitor cells [115].

Telomerase upregulation in atherosclerosis: Despite enormous research and identification of numerous risk factors are the exact causes of atherosclerosis incompletely understood and the exact pathomechanism remains unclear [4,116]. Experimental findings in cell culture and animals suggest that telomere shortening contribute to the pathogenesis of atherosclerosis at advanced age. Numerous findings in humans have shown that telomere shortening correlates with the degree of atherosclerosis in vivo [15]. Experimental data suggest that the activation of telomerase can delay and—at least in part—reverse the senescent phenotype [15,117,118]. The pathologically vicious circle between replicative aging and inflammation by atherosclerosis could be reversed by a telomerase-based therapy [119]. Matsushita et al. have shown that a stable hTERT expression in endothelial cells ensures a younger phenotype and induces improvement of endothelial nitric oxide synthase (eNOS) [120]. Telomerase and vascular endothelial growth (VEGF)-mediated angiogenesis potentially regulate the transcriptional expression of each other, suggesting a role of telomerase in regulating cellular processes other than telomere elongation, such as differentiation and angiogenesis [119]. Development of therapeutic approaches is still on an experimental level due to fear of cancer-promoting side-effects on systemic use.

Telomerase upregulation in psychiatric disorders: Based on experimental and preliminary clinical data it was hypothesized that the mode of action of many psychopharmacological drugs (e.g., antidepressants, lithium, and antipsychotics) is, at least in part, mediated by their influence on telomerase activity. A close correlation between stress-dependent telomerase activity and depression-like behaviors has been shown in mice [121]. Fluoxetine reversed clinical symptoms and increased hippocampal telomerase activity in parallel, raising the possibility that drug effects might be mediated by telomerase-dependent neurogenesis [121]. Smaller pilot studies suggested a close correlation between telomerase activity, clinical symptoms and response to antidepressants [122,123]. Likewise, lithium increased hippocampal telomerase activity in a rat model of depression, accompanied by telomere elongation and reducing clinical symptoms [124]. In patients with bipolar disorder, telomere length correlated with duration of therapy [125]. Antipsychotic drugs may also have some positive influence on telomere length [126]. The modulation of intracellular Wnt/ β -catenin or PI3K/Akt signaling pathways, the interaction with brain-derived neurotrophic factor and 5-HT, and antioxidant properties could represent possible mechanisms by which psychopharmacological drugs could modulate telomerase activity [127]. These pathways are functionally-relevant downstream drug effects and are also activation pathways for telomerase, suggesting a potential (yet unproven) mechanism by which these drugs may mediate neurogenesis via telomerase activation [38,128].

3. Telomerase as a Target for Cancer Treatment

There are several approaches for a telomerase-based gene therapy in the treatment of cancer. Cancer cells have high telomerase activity compared to most other cells [129]. The restriction of hTERT is a potential therapeutic option because telomerase complex components are up regulated in most tumor cells. Moreover, telomerase is a good target for cancer therapy because most somatic cells have no or only low level telomerase activities. Thus, the selective inactivation of telomerase expression in cancer cells does not influence most healthy cells [96]. Different therapeutic approaches for telomerase-based treatment of cancer have been developed or are under investigation [96,130].

(1). *Oligonucleotide inhibitors.* Antisense oligonucleotides and chemically-modified nucleic acids have been shown to inhibit telomerase and to induce telomere shortening [131–135] associated with subsequent onset of senescence and/or apoptosis in cell cultures [134–137]. These inhibitors act directly or indirectly (by inducing apoptosis). Targets include the RNA template, hTERT protein, and associated proteins. For example, the thio-phosphoramidate oligonucleotide inhibitor imetelstat (by Geron Corporation, Menlo Park, CA, USA) targets the RNA template for hTERT by binding to the catalytic site of telomerase [138]. Imetelstat (GRN163L) was successfully tested for glioblastoma tumors [139]. This cancer type ensures that there is sufficient time to permit tumor growth and erosion of telomeres to critical levels that trigger cellular senescence. Clinical phase II studies are planned for breast and lung cancers. Significant side-effects were not observed and possible combinatory therapies with well-established regimes for myeloproliferative neoplasms and acute myeloid leukemia are under investigation [96].

(2). *Small-molecule telomerase inhibitors.* Small-molecule telomerase inhibitors have been identified in screens of chemical libraries or were synthesized based on the structure of natural telomerase inhibitors such as epigallocatechin-3-gallate (EGCG) [140–144]. Moreover, various targets with overlapping functions have been proposed such as the PI3K-Akt-mTOR pathway [145], which is often dysregulated in cancer. The mTOR inhibitor rapamycin was shown to inhibit telomerase activity [146–148] and to counteract carcinogenesis.

(3). *Immunotherapeutic approaches.* The active site of telomerase in cancer cells is a possible target to develop vaccines [149]. Adoptive cell therapy, with the use of high-avidity T lymphocytes reactive against telomerase, has successfully been used in adenocarcinoma mouse prostate mice, which develop androgen-independent prostate cancer [150]. Despite marked temporary autoimmune depletion of B cells as side effect this therapy was not associated with significant immunoglobulin decreases or infections. At least 23 clinical studies, summarized in [151] have investigated hTERT immunotherapy as anticancer strategy in melanoma, acute myeloid leukemia, glioblastoma, prostate, renal, pancreatic, hepatocellular, and non-small-cell lung cancer: 18 phase I/I-II studies [152–168], four phase II studies [169–172], and one phase III trial [173] with pancreatic cancer patients and GV1001. Median survival ranged from 88 to 450 days in non-responders and from 216 to >600 days in responders [157,158,163,166,170,172], with the pancreatic cancer patients showing best survival rates so far. In a phase I trial an hTERT-derived peptide was used as a vaccine in hepatocellular carcinoma patients, with the majority of patients showing recurrence up to 24 weeks after vaccination [174].

Possible reasons for the limited success in many studies are the development of self-tolerance, the limited size of the precursor T-cell repertoire, negative effects of immunosuppressive tumor microenvironment on T cells, and interindividual differences. Various improvements have been proposed for future studies. These include (i) stimulation of cooperation between CD8+ and CD4+ T cells, by immunization with both MHC class I and class II hTERT peptides, in order to expand the pool of persisting memory CD8+ T cells; (ii) limiting the development of immune-tolerance, by immunization with low affinity (mutant) MHC I hTERT peptides, to increase the efficacy of vaccination; (iii) limiting the development of immune-tolerance by parallel immunization with peptides derived from non-self antigens; and (iv) development of personalized approaches with a focus on patients with early stage diseases to avoid negative effects of immunosuppressive cancer microenvironments [151].

(4). *Telomerase-directed gene therapy.* The promoters for telomerase in cancer cells are targets for a tumor specific gene therapy that selectively kills cancer cells and leaves normal cells unharmed by expressing high concentrations of a therapeutic protein only in cancer cells. Adenoviruses are developed that (by use of the hTERT promoter) selectively replicate in cancer cells and, subsequently, kill the cancer cells [175]. Both cytotoxic gene therapy and oncolytic virotherapy approaches have been used to kill cells expressing telomerase and not killing healthy cells [176].

(5). *Phytochemicals*. A wide variety of chemical compounds that occur naturally in plants, or phytochemicals, have been suggested to inhibit telomerase activity in various cancers, summarized in [177]. The substances include allicin, an organophosphate derived from garlic [178]; curcumin, a phenol present in turmeric [178–185]; the flavonolignan silbinin; an organosulfur derived from cruciferous vegetables; epigallocatechin gallate (EGCG), a catechin in green tea [186]. Curcumin [181], genistein [187], EGCG [188], and sulforaphane [189] were tested in breast cancer cells and the non-malignant breast cell line. The mode of action is only partially known and encompasses inhibition of translocation of hTERT to the nucleus [179]; dissociation of Hsp-90 co-chaperone from hTERT [183]; and a decrease of hTERT expression or activity [180–182,190].

Despite extensive studies during prior years on the development of telomerase vaccines, telomerase inhibitors, and telomerase promoter-driven cell killing in oncology, only one therapeutic vaccine went all the way to the clinic (GV1001), and only one telomerase antagonist (imetelstat, GRN163L) is in late preclinical studies. However, numerous drugs with various other targets have been identified with additional off-target effects on telomerase activity. These include substances which act via downregulation of hTERT gene transcription: the tyrosine kinase inhibitors dasatinib, imatinib, gefitinib, and nilotinib [191–193]; the ubiquitin/proteasome pathway inhibitor bortezomib; the cytotoxic drugs 5-azacytidine [194], arsenic trioxide [195] and temozolomide [196]; the chemosensitizer suramin [197]; the non-steroidal anti-inflammatory drugs aspirin [198], indomethacin [198], and celecoxib [199]; the peroxisome proliferator-activated receptor (PPAR) activator troglitazone [200]; the histone deacetylase inhibitors romidepsin [201] and vorinostat [202]; and the mTOR pathway inhibitor rapamycin [203]. The DNA topoisomerase I inhibitor beta-lapachone [204] and the DNA crosslinker cisplatin [205] act via downregulation of hTR gene transcription. The circadian rhythm hormone melatonin downregulates both hTERT and hTR on transcriptional level [206]. Other substances inhibit telomerase activity by unknown mechanisms: perifosine [207], nimesulide [208], auranofin [209], pyrimethamine [210], azidothymidine [211], octreotide [212] and ofloxacin [213]. Quinacrine, bortezomib, etoposide, and doxorubicin directly target the telomere structure proteins TRF1, POT1, shelterin, and TNKS1 [214–217].

Various drugs proposed for skin cancer therapy, including tyrosine kinase and Wnt/ β -catenin signaling inhibitors, also have inhibitory effects on telomerase [218–223]. This is not unexpected because telomerase enzyme activity can be post-transcriptionally regulated by the kinases c-Abl, protein kinase C, ERK1/2, and Akt. [224–234].

Blockade of the epidermal growth factor receptor might be effective in inhibiting telomerase activity of squamous cell carcinomas, which may result in suppression of tumor growth [235]. The recent finding of a germline mutation in the promoter of hTERT in a melanoma-prone family further suggests the importance of telomerase as an important target in skin cancer therapy [236]. Resveratrol, by contrast is, at least in mouse models, a potent chemopreventive agent against melanoma [237,238] but rather increases telomerase activity.

4. Advantages, Pitfalls, and Outlook

There are many advantages for using telomerase as an anti-cancer target. First, it is an essential and specific component for most cancer cells [129,138] and more widely expressed than any other tumor marker. Approximately 90% of all human cancers have elevated telomerase levels relative to normal cells. Second, telomerase is the most efficient mechanism for replicative immortality with only one (less robust) compensatory mechanism (ALT), which limits the risk for development of resistance to telomerase-based therapies. Third, the very low expression of telomerase in normal tissues, together with the longer telomeres in normal stem cells versus cancer cells, provides at least some degree of specificity with low risk of toxicity in normal cells [239], and limited risk in stem cells, provided that telomerase inhibition is limited in time.

There are also various pitfalls for a use of telomerase as a therapeutic target in cancer treatment. First, the anti-proliferative effects of telomerase inhibition are induced in cells with short telomeres only, which requires some time of tumor growth until the drug can be effective. Second, telomerase inhibition may elicit negative effects in highly proliferative cells which need telomerase for survival, namely, stem cells, etc. [240]. Despite shorter telomeres in cancer cells, these two points may restrict the therapeutic option for a narrow telomere length window. Moreover, it has been shown that stress induces a shift of telomerase from the nucleus to mitochondria, suggesting a telomere-independent physiological function and possible risks in long term inhibition of telomerase [16]. There are also caveats to the therapeutic strategy of senescence induction, per se. On one hand, both telomere-driven replicative senescence and stress-inducible senescence are tumor-suppressive [241–247]. On the other hand, senescence can be reversed by a process called crisis and then has pro-tumorigenic paracrine effects. By induction of telomere dysfunction and attrition chromosomal instability occurs and may result in activation of oncogenes and/or silencing of tumor suppressor genes, which may counteract the original therapeutic intention and cooperate to promote malignant transformation and drug resistance [248–252]. Finally, the currently available drugs and substances are often unspecific and have a wide variety of actions and different cellular targets that may counteract replicative immortality but may also exacerbate other cancer hallmarks such as chromosomal instability. Some studies are promising but also suggest that for complete eradication of all subpopulations of cancer cells a simultaneous targeting of several mechanisms will be needed. It is unlikely that a single target will provide lasting remission.

Approximately 5%–10% of cancer cells maintain their telomeres by ALT [28]. This process is only partially understood but may offer new therapeutic options by modulating the involved factors such as the shelterin complex or the telomere sequences themselves to induce telomere deprotection.

There are also a number of pitfalls in the treatment with telomerase-activating procedures or substances. Immortality is not intrinsically essential for malignancy [253]. However, an extended lifespan may accumulate rare genetic and epigenetic aberrations that can contribute to malignant transformation. Constitutive telomerase expression in mice increased tissue fitness and delay of aging at the expense of slightly increased cancer incidence [254–256]. In mice with cancer resistant backgrounds (by increased expression of tumor suppressors p16, Arf, and p53) transgenic telomerase expression extends lifespan by 43% [254]. Interestingly, the cancer-promoting activity in transgenic mouse models is not observed when telomerase is re-activated later in life.

In this context, a recently described methodological advance is of interest. Bernardes de Jesus et al. have designed a potential therapeutic approach in which telomerase is induced temporarily and selectively in old cells without promoting cancer growth. The special feature of recombinant adeno-associated virus (rAAV) vector is its 'mild' integration into the host genome. By use of rAAV vectors, which expressed the catalytic subunit of mouse telomerase (mTERT) it was integrated into the host genome at very low rates but, in mice, did not induce cancer growth. A possible explanation is the loss of the vector in rapidly proliferating cells such as cancer cells. Thus, this method might be used to treat age-related diseases, such as atherosclerosis or diabetes [257]. In short-lived organisms, such as mice, this strategy seems to be an excellent approach for a telomerase-based gene therapy. For long-lived organisms it is currently unknown if cancer can be promoted by rare integration events of constitutively-overexpressed hTERT [257].

Acknowledgments: The authors acknowledge the financial support of the Sonnenfeldstiftung (to Kathrin Jäger) and Katja Tränkner (WriteNow, Berlin, Germany) for preparing the drawings.

Author Contributions: Kathrin Jäger and Michal Walter wrote this review.

Conflicts of Interest: The authors declare no conflict of interest.

Abbreviations

The following abbreviations are used in this manuscript:

ALT	alternative lengthening of telomeres
CRP	C-reactive protein
hTERT	human telomerase reverse transcriptase
hTR	human telomerase RNA
IL-6	interleukine-6
LTL	leucocyte telomere length
mTERT	mouse telomerase reverse transcriptase
rAAV	recombinant adeno-associated virus
ROS	reactive oxygen species
TERC	telomerase RNA component
TERT	telomerase reverse transcriptase
VEGF	vascular endothelial growth

References

1. Walter, M. Interrelationships among HDL metabolism, aging, and atherosclerosis. *Arterioscler Thromb. Vasc. Biol.* **2009**, *29*, 1244–1250. [[CrossRef](#)] [[PubMed](#)]
2. Fyhrquist, F.; Saijonmaa, O.; Strandberg, T. The roles of senescence and telomere shortening in cardiovascular disease. *Nat. Rev. Cardiol.* **2013**, *10*, 274–283. [[CrossRef](#)] [[PubMed](#)]
3. To-Miles, F.Y.L.; Backman, C.L. What telomeres say about activity and health: A rapid review. *Can. J. Occup. Ther.* **2016**. [[CrossRef](#)] [[PubMed](#)]
4. Zhu, H.; Blecher, M.; van der Harst, P. Healthy aging and disease: Role for telomere biology? *Clin. Sci.* **2011**, *120*, 427–440. [[CrossRef](#)] [[PubMed](#)]
5. Boccardi, V.; Herbig, U. Telomerase gene therapy: A novel approach to combat aging. *EMBO Mol. Med.* **2012**. [[CrossRef](#)] [[PubMed](#)]
6. Xin, H.; Liu, D.; Songyang, Z. The telosome/shelterin complex and its functions. *Genome Biol.* **2008**. [[CrossRef](#)] [[PubMed](#)]
7. De Lange, T. Shelterin: The protein complex that shapes and safeguards human telomeres. *Genes Dev.* **2005**, *19*, 2100–2110. [[CrossRef](#)] [[PubMed](#)]
8. Artandi, S.E.; DePinho, R.A. Telomeres and telomerase in cancer. *Carcinogenesis* **2010**, *31*, 9–18. [[CrossRef](#)] [[PubMed](#)]
9. Sarin, K.Y.; Cheung, P.; Gilson, D.; Lee, E.; Tennen, R.I.; Wang, E.; Artandi, M.K.; Oro, A.E.; Artandi, S.E. Conditional telomerase induction causes proliferation of hair follicle stem cells. *Nature* **2005**, *436*, 1048–1052. [[CrossRef](#)] [[PubMed](#)]
10. Baker, D.J.; Wijshake, T.; Tchkonja, T.; LeBrasseur, N.K.; Childs, B.G.; van de Sluis, B.; Kirkland, J.L.; van Deursen, J.M. Clearance of p16Ink4a-positive senescent cells delays ageing associated disorders. *Nature* **2001**, *409*, 232–236. [[CrossRef](#)] [[PubMed](#)]
11. Stanley, S.E.; Armanios, M. The short and long telomere syndromes: Paired paradigms for molecular medicine. *Curr. Opin. Gen. Dev.* **2015**, *33*, 1–9. [[CrossRef](#)] [[PubMed](#)]
12. Park, J.I.; Venteicher, A.S.; Hong, J.Y.; Choi, J.; Jun, S.; Shkreli, M.; Chang, W.; Meng, Z.; Cheung, P.; Ji, H.; et al. Telomerase modulates Wnt signalling by association with target gene chromatin. *Nature* **2009**, *460*, 66–72. [[CrossRef](#)] [[PubMed](#)]
13. Rao, T.P.; Kuhl, M. An updated overview on Wnt signaling pathways: A prelude for more. *Circ. Res.* **2010**, *106*, 1798–1806. [[CrossRef](#)] [[PubMed](#)]
14. Von Zglinicki, T. Oxidative stress shortens telomeres. *Trends Biochem. Sci.* **2001**, *27*, 339–344. [[CrossRef](#)]
15. Nazari-Shafti, T.Z.; Cooke, J.P. Telomerase therapy to reserve cardiovascular senescence. *Methodist Debaquey Cardiovasc. J.* **2015**, *11*, 172–175. [[CrossRef](#)] [[PubMed](#)]
16. Babizhayev, M.A.; Yegorov, Y.E. Tissue formation and tissue engineering through host cell recruitment or a potential injectable cell-based biocomposite with replicative potential: Molecular mechanisms controlling cellular senescence and the involvement of controlled transient telomerase activation therapies. *J. Biomed. Mater. Res. Part A* **2015**, *103A*, 3993–4023.

17. Xu, D.; Erickson, S.; Szeps, M.; Gruber, A.; Sangfelt, O.; Einhorn, S.; Pisa, P.; Grandér, D. Interferon α down-regulates telomerase reverse transcriptase and telomerase activity in human malignant and nonmalignant hematopoietic cells. *Blood* **2000**, *96*, 4313–4318. [[PubMed](#)]
18. Aviv, A.; Valdes, A.; Gardner, J.P.; Swaminathan, R.; Kimura, M.; Spector, T.D. Menopause modifies the association of leukocyte telomere length with insulin resistance and inflammation. *J. Clin. Endocrinol. Metab.* **2006**, *91*, 635–640. [[CrossRef](#)] [[PubMed](#)]
19. Carrero, J.J.; Stenvinkel, P.; Fellstrom, B.; Qureshi, A.R.; Lamb, K.; Heimbürger, O.; Bárány, P.; Radhakrishnan, K.; Lindholm, B.; Soveri, I.; et al. Telomere attrition is associated with inflammation, low fetuin—a levels and high mortality in prevalent haemodialysis patients. *J. Intern. Med.* **2008**, *263*, 302–312. [[CrossRef](#)] [[PubMed](#)]
20. Deng, W.; Cheung, S.T.; Tsao, S.W.; Wang, X.M.; Tiwari, A.F. Telomerase activity and its association with psychological stress, mental disorders, lifestyle factors and interventions: A systematic review. *Psychoneuroendocrinology* **2016**, *64*, 150–163. [[CrossRef](#)] [[PubMed](#)]
21. Oliveira, B.S.; Zunzunegui, M.V.; Quinlan, J.; Fahmi, H.; Tu, M.T.; Guerra, R.O. Systematic review of the association between chronic social stress and telomere length: A life course perspective. *Ageing Res. Rev.* **2016**, *26*, 37–52. [[CrossRef](#)] [[PubMed](#)]
22. Nawrot, T.S.; Staessen, J.A.; Holvoet, P.; Struijker-Boudier, H.A.; Schiffrin, P.; van Bortel, L.M.; Fagard, R.H.; Gardner, J.P.; Kimura, M.; Aviv, A. Telomere length and its associations with oxidized-LDL, carotid artery distensibility and smoking. *Front. Biosci.* **2010**, *2*, 1164–1168.
23. Yaswen, P.; MacKenzie, K.L.; Keith, W.N.; Hentosh, P.; Rodier, F.; Zhu, J.; Firestone, G.L.; Matheu, A.; Carnero, A.; Bilsland, A.; et al. Therapeutic targeting of replicative immortality. *Sem. Cancer Biol.* **2015**, *35*, S104–S128. [[CrossRef](#)] [[PubMed](#)]
24. Jacobs, J.J.L.; de Lange, T. Significant Role for p16^{INK4a} in p53-Independent Telomere-Directed Senescence. *Curr. Biol.* **2004**, *14*, 2302–2308. [[CrossRef](#)] [[PubMed](#)]
25. Jacobs, J.J.L. Loss of Telomere Protection: Consequences and Opportunities. *Front. Oncol.* **2013**. [[CrossRef](#)] [[PubMed](#)]
26. Chang, S.; Khoo, C.M.; Naylor, M.L.; Maser, R.S.; DePinho, R.A. Telomere-based crisis: Functional differences between telomerase activation and ALT in tumor progression. *Genes Dev.* **2003**, *17*, 88–100. [[CrossRef](#)] [[PubMed](#)]
27. Hu, J.; Hwang, S.S.; Liesa, M.; Gan, B.; Sahin, E.; Jaskelioff, M.; Ding, Z.; Ying, H.; Boutin, A.T.; Zhang, H.; et al. Antitelomerase Therapy Provokes ALT and Mitochondrial Adaptive Mechanisms in Cancer. *Cell* **2012**, *148*, 651–663. [[CrossRef](#)] [[PubMed](#)]
28. O'Sullivan, R.; Almouzni, G. Assembly of telomeric chromatin to create ALTERNATIVE endings. *Trends Cell Biol.* **2014**, *24*, 675–685. [[CrossRef](#)] [[PubMed](#)]
29. Zhang, A.; Zheng, C.; Lindvall, C.; Hou, M.; Ekedahl, J.; Lewensohn, R.; Yan, Z.; Yang, X.; Henriksson, M.; Blennow, E.; et al. Frequent Amplification of the Telomerase Reverse Transcriptase Gene in Human Tumors. *Cancer Res.* **2000**, *60*, 6230–6235. [[PubMed](#)]
30. Zhang, A.; Zheng, C.; Hou, M.; Lindvall, C.; Wallin, K.L.; Angström, T.; Yang, X.; Hellström, A.C.; Blennow, E.; Björkholm, M.; et al. Amplification of the Telomerase Reverse Transcriptase (hTERT) Gene in Cervical Carcinomas. *Genes Chromos. Cancer* **2002**, *34*, 269–275. [[CrossRef](#)] [[PubMed](#)]
31. Takuma, Y.; Nouse, K.; Kobayashi, Y.; Nakamura, S.; Tanaka, H.; Matsumoto, E.; Fujikawa, T.; Suzuki, M.; Hanafusa, T.; Shiratori, Y. Telomerase reverse transcriptase gene amplification in hepatocellular carcinoma. *J. Gastroenterol. Hepatol.* **2004**, *19*, 1300–1304. [[CrossRef](#)] [[PubMed](#)]
32. Rousseau, P.; Autexier, C. Telomere biology: Rationale for diagnostics and therapeutics in cancer. *RNA Biol.* **2016**, *12*, 1078–1082.
33. Terali, K.; Yilmazer, A. New surprises from an old favourite: The emergence of telomerase as a key player in the regulation of cancer stemness. *Biochimie* **2016**, *121*, 170–178. [[CrossRef](#)] [[PubMed](#)]
34. Soder, A.I.; Hoare, S.F.; Muir, S.; Going, J.J.; Parkinson, E.K.; Keith, W.N. Amplification, increased dosage and in situ expression of the telomerase RNA gene in human cancer. *Oncogene* **1997**, *14*, 1013–1021. [[CrossRef](#)] [[PubMed](#)]
35. Shay, J.W.; Wright, W.E. Hallmarks of telomeres in ageing research. *J. Pathol.* **2007**, *211*, 114–123. [[CrossRef](#)] [[PubMed](#)]

36. Sahin, E.; Depinho, R.A. Linking functional decline of telomeres, mitochondria and stem cells during ageing. *Nature* **2010**, *464*, 520–528. [[CrossRef](#)] [[PubMed](#)]
37. Shay, J.W.; Wright, W.E. Use of telomerase to create bioengineered tissues. *Ann. N. Y. Acad. Sci.* **2005**, *1057*, 479–491. [[CrossRef](#)] [[PubMed](#)]
38. Jaskelioff, M.; Muller, F.L.; Paik, J.H.; Thomas, E.; Jiang, S.; Adams, A.C.; Sahin, E.; Kost-Alimova, M.; Protopopov, A.; Cadiñanos, J.; et al. Telomerase reactivation reverses tissue degeneration in aged telomerase-deficient mice. *Nature* **2011**, *469*, 102–106. [[CrossRef](#)] [[PubMed](#)]
39. Allsopp, R.C.; Weissman, I.L. Replicative senescence of hematopoietic stem cells during serial transplantation: Does telomere shortening play a role? *Oncogene* **2002**, *21*, 3270–3273. [[CrossRef](#)] [[PubMed](#)]
40. Pendino, F.; Tarkanyi, I.; Dudognon, C.; Hillion, J.; Lanotte, M.; Aradi, J.; Segal-Bendirdjian, S. Telomeres and telomerase: Pharmacological targets for new anticancer strategies? *Curr. Cancer Drug Targets* **2006**, *6*, 147–180. [[CrossRef](#)] [[PubMed](#)]
41. Atkinson, S.P.; Hoare, S.F.; Glasspool, R.M.; Keith, W.N. Lack of telomerase gene expression in alternative lengthening of telomere cells is associated with chromatin remodeling of the hTR and hTERT gene promoters. *Cancer Res.* **2005**, *65*, 7585–7590. [[PubMed](#)]
42. Serenicki, N.; Hoare, S.F.; Kassem, M.; Atkinson, S.P.; Keith, W.N. Telomerase promoter reprogramming and interaction with general transcription factors in the human mesenchymal stem cell. *Regen. Med.* **2006**, *1*, 125–131.
43. Doshida, M.; Ohmichi, M.; Tsutsumi, S.; Kawagoe, J.; Takahashi, T.; Du, B.; Mori-Abe, A.; Ohte, T.; Saitoh-Sekiguchi, M.; Takahashi, K.; et al. Raloxifene increases proliferation and up-regulates telomerase activity in human umbilical vein endothelial cells. *J. Biol. Chem.* **2006**, *281*, 24270–24278. [[CrossRef](#)] [[PubMed](#)]
44. Liu, K.; Hodes, R.J.; Weng, N. Cutting edge: Telomerase activation in human T lymphocytes does not require increase in telomerase reverse transcriptase (hTERT) protein but is associated with hTERT phosphorylation and nuclear translocation. *J. Immunol.* **2001**, *166*, 4826–4830. [[CrossRef](#)] [[PubMed](#)]
45. Tarkanyi, I.; Aradi, J. Pharmacological intervention strategies for affecting telomerase activity: Future prospects to treat cancer and degenerative disease. *Biochimie* **2008**, *90*, 156–172. [[CrossRef](#)] [[PubMed](#)]
46. Stewart, S.A. Multiple levels of telomerase regulation. *Mol. Interv.* **2002**, *2*, 481–483. [[CrossRef](#)] [[PubMed](#)]
47. Sharma, N.K.; Reyes, A.; Green, P.; Caron, M.J.; Bonini, M.G.; Gordon, D.M.; Holt, I.J.; Santos, J.H. Human telomerase acts as a hTR-independent reverse transcriptase in mitochondria. *Nucleic Acids Res.* **2012**, *40*, 712–725. [[CrossRef](#)] [[PubMed](#)]
48. Bodnar, A.G.; Ouellette, M.; Frolkis, M.; Holt, S.E.; Chiu, C.P.; Morin, G.B.; Harley, C.B.; Shay, J.W.; Lichtsteiner, S.; Wright, W.E. Extension of life-span by introduction of telomerase into normal human cells. *Science* **1998**, *279*, 349–352. [[CrossRef](#)] [[PubMed](#)]
49. Counter, C.M.; Meyerson, M.; Eaton, E.N.; Ellisen, L.W.; Caddle, S.D.; Haber, D.A.; Weinberg, R.A. Telomerase activity is restored in human cells by ectopic expression of hTERT (hEST2), the catalytic subunit of telomerase. *Oncogene* **1998**, *16*, 1217–1222. [[CrossRef](#)] [[PubMed](#)]
50. Vaziri, H.; Benchimol, S. Reconstitution of telomerase activity in normal human cells leads to elongation of telomeres and extended replicative life span. *Curr. Biol.* **1998**, *8*, 279–282. [[CrossRef](#)]
51. Jiang, X.R.; Jimenez, G.; Chang, E.; Frolkis, M.; Kusler, B.; Sage, M.; Beeche, M.; Bodnar, A.G.; Wahl, G.M.; Tlsty, T.D.; et al. Telomerase expression in human somatic cells does not induce changes associated with a transformed phenotype. *Nat. Genet.* **1999**, *21*, 111–114. [[CrossRef](#)] [[PubMed](#)]
52. Morales, C.P.; Holt, S.E.; Ouellette, M.; Kaur, K.J.; Yan, Y.; Wilson, K.S.; White, M.A.; Wright, W.E.; Shay, J.W. Absence of cancer-associated changes in human fibroblasts immortalized with telomerase. *Nat. Genet.* **1999**, *21*, 115–118. [[CrossRef](#)] [[PubMed](#)]
53. Funk, W.D.; Wang, C.K.; Shelton, D.N.; Harley, C.B.; Pagon, G.D.; Hoeffler, W.K. Telomerase expression restores dermal integrity to in vitro-aged fibroblasts in a reconstituted skin model. *Exp. Cell Res.* **2000**, *258*, 270–278. [[CrossRef](#)] [[PubMed](#)]
54. Wyllie, F.S.; Jones, C.J.; Skinner, J.W.; Haughton, M.F.; Wallis, C.; Wynford-Thomas, D.; Faragher, R.G.; Kipling, D. Telomerase prevents the accelerated cell ageing of Werner syndrome fibroblasts. *Nat. Genet.* **2000**, *24*, 16–17. [[PubMed](#)]
55. Harada, H.; Nakagawa, H.; Takaoka, M.; Lee, J.; Herlyn, M.; Diehl, J.A.; Rustgi, A.K. Cleavage of MCM2 licensing protein fosters senescence in human keratinocytes. *Cell Cycle* **2008**, *7*, 3534–3538. [[CrossRef](#)] [[PubMed](#)]

56. McKee, J.A.; Banik, S.S.; Boyer, M.J.; Hamad, N.M.; Lawson, J.H.; Niklason, L.E.; Counter, C.M. Human arteries engineered in vitro. *EMBO Rep.* **2003**, *4*, 633–638. [[CrossRef](#)] [[PubMed](#)]
57. Oh, H.; Taffet, G.E.; Youker, K.A.; Entman, M.L.; Overbeek, P.A.; Michael, L.H.; Schneider, M.D. Telomerase reverse transcriptase promotes cardiac muscle cell proliferation, hypertrophy, and survival. *Proc. Natl. Acad. Sci. USA* **2001**, *98*, 10308–10313. [[CrossRef](#)] [[PubMed](#)]
58. Wootton, M.; Steeghs, K.; Watt, D.; Munro, J.; Gordon, K.; Ireland, H.; Morrison, V.; Behan, W.; Parkinson, E.K. Telomerase alone extends the replicative life span of human skeletal muscle cells without compromising genomic stability. *Hum. Gene Ther.* **2003**, *14*, 1473–1487. [[CrossRef](#)] [[PubMed](#)]
59. Yang, J.; Chang, E.; Cherry, A.M.; Bangs, C.D.; Oei, Y.; Bodnar, A.; Bronstein, A.; Chiu, C.P.; Herron, G.S. Human endothelial cell life extension by telomerase expression. *J. Biol. Chem.* **1999**, *274*, 26141–26148. [[CrossRef](#)] [[PubMed](#)]
60. Gu, X.; Zhang, J.; Brann, D.W.; Yu, F.S. Brain and retinal vascular endothelial cells with extended life span established by ectopic expression of telomerase. *Invest. Ophthalmol. Vis. Sci.* **2003**, *44*, 3219–3225. [[CrossRef](#)] [[PubMed](#)]
61. Yang, J.; Nagavarapu, U.; Relloma, K.; Sjaastad, M.D.; Moss, W.C.; Passaniti, A.; Herron, G.S. Telomerized human microvasculature is functional in vivo. *Nat. Biotechnol.* **2001**, *19*, 219–224. [[CrossRef](#)] [[PubMed](#)]
62. Condon, J.; Yin, S.; Mayhew, B.; Word, R.A.; Wright, W.E.; Shay, J.W.; Rainey, W.E. Telomerase immortalization of human myometrial cells. *Biol. Reprod.* **2002**, *67*, 506–514. [[CrossRef](#)] [[PubMed](#)]
63. Shi, S.; Gronthos, S.; Chen, S.; Reddi, A.; Counter, C.M.; Robey, P.G.; Wang, C.Y. Bone formation by human postnatal bone marrow stromal stem cells is enhanced by telomerase expression. *Nat. Biotechnol.* **2002**, *20*, 587–591. [[CrossRef](#)] [[PubMed](#)]
64. Simonsen, J.L.; Rosada, C.; Serakinci, N.; Justesen, J.; Stenderup, K.; Rattan, S.I.; Jensen, T.G.; Kassem, M. Telomerase expression extends the proliferative life-span and maintains the osteogenic potential of human bone marrow stromal cells. *Nat. Biotechnol.* **2002**, *20*, 592–596. [[CrossRef](#)] [[PubMed](#)]
65. Gronthos, S.; Chen, S.; Wang, C.Y.; Robey, P.G.; Shi, S. Telomerase accelerates osteogenesis of bone marrow stromal stem cells by upregulation of CBFA1, osterix, and osteocalcin. *J. Bone Miner Res.* **2003**, *18*, 716–722. [[CrossRef](#)] [[PubMed](#)]
66. Kawano, Y.; Kobune, M.; Yamaguchi, M.; Nakamura, K.; Ito, Y.; Sasaki, K.; Takahashi, S.; Nakamura, T.; Chiba, H.; Sato, T.; et al. Ex vivo expansion of human umbilical cord hematopoietic progenitor cells using a coculture system with human telomerase catalytic subunit (hTERT)-transfected human stromal cells. *Blood* **2003**, *101*, 532–540. [[CrossRef](#)] [[PubMed](#)]
67. Darimont, C.; Avanti, O.; Tromvoukis, Y.; Vautravers-Leone, P.; Kurihara, N.; Roodman, G.D.; Colgin, L.M.; Tullberg-Reinert, H.; Pfeifer, A.M.; Offord, E.A.; et al. SV40 T antigen and telomerase are required to obtain immortalized human adult bone cells without loss of the differentiated phenotype. *Cell Growth Differ.* **2002**, *13*, 59–67. [[PubMed](#)]
68. Yudoh, K.; Matsuno, H.; Nakazawa, F.; Katayama, R.; Kimura, T. Reconstituting telomerase activity using the telomerase catalytic subunit prevents the telomere shorting and replicative senescence in human osteoblasts. *J. Bone Miner Res.* **2001**, *16*, 1453–1464. [[CrossRef](#)] [[PubMed](#)]
69. Yudoh, K.; Nishioka, K. Telomerized presenescent osteoblasts prevent bone mass loss in vivo. *Gene Ther.* **2004**, *11*, 909–915. [[CrossRef](#)] [[PubMed](#)]
70. Hao, J.; Narayanan, K.; Ramachandran, A.; He, G.; Almushayt, A.; Evans, C.; George, A. Odontoblast cells immortalized by telomerase produce mineralized dentin-like tissue both in vitro and in vivo. *J. Biol. Chem.* **2002**, *277*, 19976–19981. [[CrossRef](#)] [[PubMed](#)]
71. Luiten, R.M.; Pene, J.; Yssel, H.; Spits, H. Ectopic hTERT expression extends the life span of human CD4 helper and regulatory T-cell clones and confers resistance to oxidative stress-induced apoptosis. *Blood* **2003**, *101*, 4512–4519. [[CrossRef](#)] [[PubMed](#)]
72. Kobune, M.; Kawano, Y.; Ito, Y.; Chiba, H.; Nakamura, K.; Tsuda, H.; Sasaki, K.; Dehari, H.; Uchida, H.; Honmou, O. Telomerized human multipotent mesenchymal cells can differentiate into hematopoietic and cobblestone area-supporting cells. *Exp. Hematol.* **2003**, *31*, 715–722. [[CrossRef](#)]
73. Di Donna, S.; Mamchaoui, K.; Cooper, R.N.; Seigneurin-Venin, S.; Tremblay, J.; Butler-Browne, G.S.; Mouly, V. Telomerase can extend the proliferative capacity of human myoblasts, but does not lead to their immortalization. *Mol. Cancer Res.* **2003**, *1*, 643–653. [[PubMed](#)]

74. Schnabl, B.; Choi, Y.H.; Olsen, J.C.; Hagedorn, C.H.; Brenner, D.A. Immortal activated human hepatic stellate cells generated by ectopic telomerase expression. *Lab. Invest.* **2002**, *82*, 323–333. [[CrossRef](#)] [[PubMed](#)]
75. Watanabe, T.; Shibata, N.; Westerman, K.A.; Okitsu, T.; Allain, J.E.; Sakaguchi, M.; Totsugawa, T.; Maruyama, M.; Matsumura, T.; Noguchi, H. Establishment of immortalized human hepatic stellate scavenger cells to develop bioartificial livers. *Transplantation* **2003**, *75*, 1873–1880. [[CrossRef](#)] [[PubMed](#)]
76. Roy, N.S.; Nakano, T.; Keyoung, H.M.; Windrem, M.; Rashbaum, W.K.; Alonso, M.L.; Kang, J.; Peng, W.; Carpenter, M.K.; Lin, J.; et al. Telomerase immortalization of neuronally restricted progenitor cells derived from the human fetal spinal cord. *Nat. Biotechnol.* **2004**, *22*, 297–305. [[CrossRef](#)] [[PubMed](#)]
77. Townsley, D.M.; Dumitriu, B.; Young, N.S. Bone marrow failure and the telomeropathies. *Blood* **2014**, *124*, 2775–2783. [[CrossRef](#)] [[PubMed](#)]
78. Shay, J.W.; Wright, W.E. The use of telomerized cells for tissue engineering. *Nat. Biotechnol.* **2000**, *18*, 22–23. [[CrossRef](#)] [[PubMed](#)]
79. Ulaner, G.A. Telomere Maintenance in Clinical Medicine. *Am. J. Med.* **2004**, *117*, 262–269. [[CrossRef](#)] [[PubMed](#)]
80. Bär, C.; Povedano, J.M.; Serrano, R.; Benitez-Buelga, C.; Popkes, M.; Formentini, I.; Bobadilla, M.; Bosch, F.; Blasco, M.A. Telomerase gene therapy rescues telomere length, bone marrow aplasia, and survival in mice with aplastic anemia. *Blood* **2016**, *127*, 1770–1779. [[CrossRef](#)] [[PubMed](#)]
81. Donati, B.; Valenti, L. Telomeres, NAFLD and Chronic Liver Disease. *Int. J. Mol. Sci.* **2016**. [[CrossRef](#)] [[PubMed](#)]
82. Calado, R.T. Telomeres in lung diseases. *Prog. Mol. Biol. Transl. Sci.* **2014**, *125*, 173–183. [[PubMed](#)]
83. Li, J.; Pei, M. Cell senescence: A challenge in cartilage engineering and regeneration. *Tissue Eng. Part B Rev.* **2012**, *18*, 270–287. [[CrossRef](#)] [[PubMed](#)]
84. Babizhayev, M.A.; Yegorov, Y.E. Telomere attrition in lens epithelial cells—A target for N-acetylcarnosine therapy. *Front. Biosci.* **2010**, *15*, 934–956. [[CrossRef](#)]
85. Weyand, C.M.; Fujii, H.; Shao, L.; Goronzy, J.J. Rejuvenating the immune system in rheumatoid arthritis. *Nat. Rev. Rheumatol.* **2009**, *5*, 583–588. [[CrossRef](#)] [[PubMed](#)]
86. Thomas, M.; Yang, L.; Hornsby, P.J. Formation of functional tissue from transplanted adrenocortical cells expressing telomerase reverse transcriptase. *Nat. Biotechnol.* **2000**, *18*, 39–42. [[PubMed](#)]
87. Fauce, S.R.; Jamieson, B.D.; Chin, A.C.; Mitsuyasu, R.T.; Parish, S.T.; Ng, H.L.; Kitchen, C.M.; Yang, O.O.; Harley, C.B.; Effros, R.B. Telomerase-based pharmacologic enhancement of antiviral function of human CD8+ T lymphocytes. *J. Immunol.* **2008**, *181*, 7400–7406. [[CrossRef](#)] [[PubMed](#)]
88. Dock, J.N.; Effros, R.B. Role of CD8 T Cell Replicative Senescence in Human Aging and in HIV-mediated Immunosenescence. *Aging Dis.* **2011**, *2*, 382–397. [[PubMed](#)]
89. Harley, C.B.; Liu, W.; Blasco, M.; Vera, E.; Andrews, W.H.; Briggs, L.A.; Raffaele, J.M. A natural product telomerase activator as part of a health maintenance program. *Rejuven. Res.* **2011**, *14*, 45–56. [[CrossRef](#)] [[PubMed](#)]
90. Bernardes de Jesus, B.; Schneeberger, K.; Vera, E.; Tejera, A.; Harley, C.B.; Blasco, M.A. The telomerase activator TA-65 elongates short telomeres and increases health span of adult/old mice without increasing cancer incidence. *Aging Cell* **2011**, *10*, 604–621. [[CrossRef](#)] [[PubMed](#)]
91. Dow, C.T.; Harley, C.B. Evaluation of an oral telomerase activator for early age-related macular degeneration—A pilot study. *Clin. Ophthalmol.* **2016**, *10*, 243–249. [[CrossRef](#)] [[PubMed](#)]
92. Harley, C.B.; Liu, W.; Flom, P.L.; Raffaele, J.M. A natural product telomerase activator as part of a health maintenance program: Metabolic and cardiovascular response. *Rejuven. Res.* **2013**, *16*, 386–395. [[CrossRef](#)] [[PubMed](#)]
93. Salvador, L.; Singaravelu, G.; Harley, C.B.; Flom, P.; Suram, A.; Raffaele, J.M. A Natural Product Telomerase Activator Lengthens Telomeres in Humans: A Randomized, Double Blind, and Placebo Controlled Study. *Rejuven. Res.* **2016**. [[CrossRef](#)] [[PubMed](#)]
94. Pearce, V.P.; Sherrell, J.; Lou, Z.; Kopelovich, L.; Wright, W.E.; Shay, J.W. Immortalization of epithelial progenitor cells mediated by resveratrol. *Oncogene* **2008**, *27*, 2365–2374. [[CrossRef](#)] [[PubMed](#)]
95. Xia, L.; Wang, X.X.; Hu, X.S.; Guo, X.G.; Shang, Y.P.; Chen, H.J.; Zeng, C.L.; Zhang, F.R.; Chen, J.Z. Resveratrol reduces endothelial progenitor cells senescence through augmentation of telomerase activity by Akt-dependent mechanisms. *Br. J. Pharmacol.* **2008**, *155*, 387–394. [[CrossRef](#)] [[PubMed](#)]

96. Sprouse, A.A.; Steding, C.E.; Herbert, B.-S. Pharmaceutical regulation of telomerase and its clinical potential. *J. Cell. Mol. Med.* **2012**, *16*, 1–7. [[CrossRef](#)] [[PubMed](#)]
97. Eitan, E.; Tichon, A.; Gazit, A.; Gitler, D.; Slavin, S.; Priel, E. Novel telomerase-increasing compound in mouse brain delays the onset of amyotrophic lateral sclerosis. *EMBO Mol. Med.* **2012**, *4*, 313–329. [[CrossRef](#)] [[PubMed](#)]
98. Wang, F.; Chang, G.; Geng, X. NGF and TERT co-transfected BMSCs improve the restoration of cognitive impairment in vascular dementia rats. *PLoS ONE* **2014**, *9*, e98774. [[CrossRef](#)] [[PubMed](#)]
99. Haendeler, J.; Hoffman, J.; Diehl, J.F.; Vasa, M.; Spyridopoulos, I.; Zeiher, A.M.; Dimmeler, S. Antioxidants inhibit nuclear export of telomerase reverse transcriptase and delay replicative senescence of endothelial cells. *Circ. Res.* **2004**, *94*, 768–775. [[CrossRef](#)] [[PubMed](#)]
100. Tanaka, Y.; Moritoh, Y.; Miva, N. Age-dependent telomere-shortening is repressed by phosphorylated alpha-tocopherol together with cellular longevity and intracellular oxidative-stress reduction in human brain microvascular endotheliocytes. *J. Cell Biochem.* **2007**, *102*, 689–703. [[CrossRef](#)] [[PubMed](#)]
101. Passos, J.F.; Saretzki, G.; Ahmed, S.; Nelson, G.; Richter, T.; Peters, H.; Wappler, I.; Birket, M.J.; Harold, G.; Schaeuble, K.; et al. Mitochondrial dysfunction accounts for the stochastic heterogeneity in telomere-dependent senescence. *PLoS Biol.* **2007**, *5*, e110. [[CrossRef](#)] [[PubMed](#)]
102. Brouillette, S.W.; Moore, J.S.; McMahon, A.D.; Thompson, J.R.; Ford, L.; Shepherd, J.; Packard, C.J.; Samani, N.J. Telomere length, risk of coronary heart disease, and statin treatment in the West of Scotland Primary Prevention Study: A nested case-control study. *Lancet* **2007**, *369*, 107–114. [[CrossRef](#)]
103. Spyridopoulos, I.; Haendeler, J.; Urbich, C.; Brummendorf, T.H.; Oh, H.; Schneider, M.D.; Zeiher, A.M.; Dimmeler, S. Statins enhance migratory capacity by upregulation of the telomere repeat binding factor TRF2 in endothelial progenitor cells. *Circulation* **2004**, *110*, 3136–3142. [[CrossRef](#)] [[PubMed](#)]
104. Dong, X.X.; Hui, Y.J.; Xiang, W.X.; Rong, Z.F.; Jian, S.; Zhu, C.J. Ginkgo Biloba extract reduces endothelial progenitor-cell senescence through augmentation of telomerase activity. *J. Cardiovasc. Pharmacol.* **2007**, *49*, 111–115. [[CrossRef](#)] [[PubMed](#)]
105. Mimeault, M.; Batra, S.K. Recent advances on the significance of stem cells in tissue regeneration and cancer therapies. *Stem Cells* **2006**, *24*, 2319–2345. [[CrossRef](#)] [[PubMed](#)]
106. Yoshikawa, T.; Mitsuno, H.; Nonaka, I.; Sen, Y.; Kawanishi, K.; Inada, Y.; Takakura, Y.; Okuchi, K.; Nonomura, A. Wound therapy by marrow mesenchymal cell transplantation. *Plast. Reconstr. Surg.* **2008**, *121*, 860–877. [[CrossRef](#)] [[PubMed](#)]
107. Kung, E.F.; Wang, F.; Schechner, J.S. In vivo perfusion of human skin substitutes with microvessels formed by adult circulating endothelial progenitor cells. *Dermatol. Surg.* **2008**, *34*, 137–146. [[PubMed](#)]
108. Zhang, C.P.; Fu, X.B. Therapeutic potential of stem cells in skin repair and regeneration. *Chin. J. Traumatol.* **2008**, *11*, 209–221. [[CrossRef](#)]
109. Park, B.S.; Jang, K.A.; Sung, J.H.; Park, J.S.; Kwon, Y.H.; Kim, K.J.; Kim, W.S. Adipose-derived stem cells and their secretory factors as a promising therapy for skin aging. *Dermatol. Surg.* **2008**, *34*, 1323–1326. [[PubMed](#)]
110. Branski, L.K.; Gauglitz, G.G.; Herndon, D.N.; Jeschke, M.G. A review of gene and stem cell therapy in cutaneous wound healing. *Burns* **2008**, *35*, 171–180. [[CrossRef](#)] [[PubMed](#)]
111. Kim, D.S.; Cho, H.J.; Yang, S.K.; Shin, J.W.; Huh, C.H.; Park, K.C. IGFBP-2 Contributes to the proliferation of less proliferative cells in forming skin equivalents. *Tissue Eng. Part A* **2009**, *15*, 1075–1080. [[CrossRef](#)] [[PubMed](#)]
112. Siegl-Cachedenier, I.; Flores, I.; Klatt, P.; Blasco, M.A. Telomerase reverses epidermal hair follicle stem cell defects and loss of longterm survival associated with critically short telomeres. *J. Cell Biol.* **2007**, *179*, 277–290. [[CrossRef](#)] [[PubMed](#)]
113. Wu, Y.; Wang, J.; Scott, P.G.; Tredget, E.E. Bone marrow-derived stem cells in wound healing: A review. *Wound Repair Regen.* **2007**, *15*, S18–S26. [[CrossRef](#)] [[PubMed](#)]
114. Jan, H.M.; Wei, M.F.; Peng, C.L.; Lin, S.J.; Lai, P.S.; Shieh, M.J. The use of polyethylenimine-DNA to topically deliver hTERT to promote hair growth. *Gene Ther.* **2012**, *19*, 86–93. [[CrossRef](#)] [[PubMed](#)]
115. Shim, J.H.; Lee, T.R.; Shin, D.W. Novel in vitro culture condition improves the stemness of human dermal stem/progenitor cells. *Mol. Cells* **2013**, *36*, 556–563. [[CrossRef](#)] [[PubMed](#)]
116. Neuner, B.; Lenfers, A.; Kelsch, R.; Jäger, K.; Brüggmann, N.; van der Harst, P.; Walter, M. Telomere length is not related to established cardiovascular risk factors but does correlate with red and white blood cell counts in a German blood donor population. *PLoS ONE* **2015**, *10*, e0139308. [[CrossRef](#)] [[PubMed](#)]

117. Walter, M.; Forsyth, N.R.; Wright, W.; Shay, J.W.; Roth, M.G. The establishment of telomerase-immortalized Tangier disease cell lines indicates the existence of an apolipoprotein A-I-inducible but ABCA1-independent cholesterol efflux pathway. *J. Biol. Chem.* **2004**, *279*, 20866–20873. [[CrossRef](#)] [[PubMed](#)]
118. Kannenberg, F.; Gorzelniak, K.; Jäger, K.; Fobker, M.; Rust, S.; Repa, J.; Roth, M.; Björkhem, I.; Walter, M. Characterization of cholesterol homeostasis in telomerase-immortalized Tangier disease fibroblasts reveals marked phenotype variability. *J. Biol. Chem.* **2013**, *288*, 36936–36947. [[CrossRef](#)] [[PubMed](#)]
119. Hartwig, F.P.; Nedel, F.; Collares, T.V.; Tarquinio, S.B.; Nör, J.E.; Demarco, F.F. Telomeres and tissue engineering: The potential roles of TERT in VEGF-mediated angiogenesis. *Stem Cell Rev.* **2012**, *8*, 1275–1281. [[CrossRef](#)] [[PubMed](#)]
120. Matsushita, H.; Chang, E.; Glassford, A.J.; Cooke, J.P.; Chiu, C.P.; Tsao, P.S. eNOS Activity Is Reduced in Senescent Human Endothelial Cells Preservation by hTERT Immortalization. *Circ. Res.* **2001**, *89*, 793–798. [[CrossRef](#)] [[PubMed](#)]
121. Zhou, Q.G.; Hu, Y.; Wu, D.L.; Zhu, L.J.; Chen, C.; Jin, X.; Luo, C.X.; Wu, H.Y.; Zhang, J.; Zhu, D.Y. Hippocampal telomerase is involved in the modulation of depressive behaviors. *J. Neurosci.* **2011**, *31*, 12258–12269. [[CrossRef](#)] [[PubMed](#)]
122. Wolkowitz, O.M.; Mellon, S.H.; Epel, E.S.; Lin, J.; Reus, V.I.; Rosser, R.; Burke, H.; Compagnone, M.; Nelson, J.C.; Dhabhar, F.S.; et al. Resting leukocyte telomerase activity is elevated in major depression and predicts treatment response. *Mol. Psychiatry* **2012**, *17*, 164–172. [[CrossRef](#)] [[PubMed](#)]
123. Simon, N.M.; Walton, Z.E.; Bui, E.; Prescott, J.; Hoge, E.; Keshaviah, A.; Schwarz, N.; Dryman, T.; Ojsekis, R.A.; Kovachy, B.; et al. Telomere length and telomerase in a well-characterized sample of individuals with major depressive disorder compared to controls. *Psychoneuroendocrinology* **2015**, *58*, 9–22. [[CrossRef](#)] [[PubMed](#)]
124. Wei, Y.B.; Backlund, L.; Wegener, G.; Mathé, A.A.; Lavebratt, C. Telomerase dysregulation in the hippocampus of a rat model of depression. Normalization by lithium. *Int. J. Neuropsychopharmacol.* **2015**. [[CrossRef](#)] [[PubMed](#)]
125. Martinsson, L.; Wei, Y.; Xu, D.; Melas, P.A.; Mathé, A.A.; Schalling, M.; Lavebratt, C.; Backlund, L. Long-term lithium treatment in bipolar disorder is associated with longer leukocyte telomeres. *Transl. Psychiatry* **2013**. [[CrossRef](#)] [[PubMed](#)]
126. Yu, W.Y.; Chang, H.W.; Lin, C.H.; Cho, C.L. Short telomeres in patients with chronic schizophrenia who show a poor response to treatment. *J. Psychiatry Neurosci.* **2008**, *33*, 244–247. [[PubMed](#)]
127. Bersani, F.S.; Lindqvist, D.; Mellon, S.H.; Penninx, B.W.; Verhoeven, J.E.; Révész, D.; Reus, V.I.; Wolkowitz, O.M. Telomerase activation as a possible mechanism of action for psychopharmacological interventions. *Drug Discov. Today* **2015**, *20*, 1305–1309. [[CrossRef](#)] [[PubMed](#)]
128. Duman, R.S.; Malberg, J.; Nakagawa, S. Regulation of adult neurogenesis by psychotropic drugs and stress. *J. Pharmacol. Exp. Ther.* **2001**, *299*, 401–407. [[PubMed](#)]
129. Kim, N.W.; Piatyszek, M.A.; Prowse, K.R.; Harley, C.B.; West, M.D.; Ho, P.L.; Coviello, G.M.; Wright, W.E.; Weinrich, S.L.; Shay, J.W. Specific association of human telomerase activity with immortal cells and cancer. *Science* **1994**, *266*, 2011–2015. [[CrossRef](#)] [[PubMed](#)]
130. Podlevsky, J.D.; Chen, J.J. It all comes together at the ends: Telomerase structure, function, and biogenesis. *Mutat. Res.* **2012**, *730*, 3–11. [[CrossRef](#)] [[PubMed](#)]
131. Feng, J.; Funk, W.D.; Wang, S.-S.; Weinrich, S.L.; Avilion, A.A.; Chiu, C.P.; Adams, R.R.; Chang, E.; Allsopp, R.C.; Yu, J.; et al. The RNA component of human telomerase. *Science* **1995**, *269*, 1236–1241. [[CrossRef](#)] [[PubMed](#)]
132. Norton, J.C.; Piatyszek, M.A.; Wright, W.E.; Shay, J.W.; Corey, D.R. Inhibition of human telomerase activity by peptide nucleic acids. *Nat. Biotechnol.* **1996**, *14*, 615–619. [[CrossRef](#)] [[PubMed](#)]
133. Kondo, S.; Tanaka, Y.; Kondo, Y.; Hitomi, M.; Barnett, G.H.; Ishizaka, Y.; Liu, J.; Haqqi, T.; Nishiyama, A.; Villeponteau, B.; et al. Antisense telomerase treatment: Induction of two distinct pathways, apoptosis and differentiation. *FASEB J.* **1988**, *12*, 801–811.
134. Pitts, A.E.; Corey, D.R. Inhibition of human telomerase by 2'-O-methyl-RNA. *Proc. Natl. Acad. Sci. USA* **1988**, *95*, 11549–11554. [[CrossRef](#)]
135. Herbert, B.; Pitts, A.E.; Baker, S.I.; Hamilton, S.E.; Wright, W.E.; Shay, J.W.; Corey, D.R. Inhibition of human telomerase in immortal human cells leads to progressive telomere shortening and cell death. *Proc. Natl. Acad. Sci. USA* **1999**, *96*, 14276–14281. [[CrossRef](#)] [[PubMed](#)]

136. Corey, D.R. Telomerase inhibition, oligonucleotides, and clinical trials. *Oncogene* **2002**, *21*, 631–637. [[CrossRef](#)] [[PubMed](#)]
137. Asai, A.; Oshima, Y.; Yamamoto, Y.; Uochi, T.A.; Kusaka, H.; Akinaga, S.; Yamashita, Y.; Pongracz, K.; Pruzan, R.; Wunder, E.; et al. A novel telomerase template antagonist (GRN163) as a potential anticancer agent. *Cancer Res.* **2003**, *63*, 3931–3939. [[PubMed](#)]
138. Harley, C.B. Telomerase and cancer therapeutics. *Nat. Rev. Cancer* **2008**, *8*, 167–179. [[CrossRef](#)] [[PubMed](#)]
139. Marian, C.O.; Cho, S.K.; McEllin, B.M.; Maher, E.A.; Hatanpaa, K.J.; Madden, C.J.; Mickey, B.E.; Wright, W.E.; Shay, J.W.; Bachoo, R.M. The telomerase antagonist, imetelstat, efficiently targets glioblastoma tumor-initiating cells leading to decreased proliferation and tumor growth. *Clin. Cancer Res.* **2010**, *16*, 154–163. [[CrossRef](#)] [[PubMed](#)]
140. Naasani, I.; Seimiya, H.; Yamori, T.; Tsuruo, T. FJ5002: A potent telomerase inhibitor identified by exploiting the disease-oriented screening program with COMPARE analysis. *Cancer Res.* **1999**, *59*, 4004–4011. [[PubMed](#)]
141. Hayakawa, N.; Nozawa, K.; Ogawa, A.; Kato, N.; Yoshida, K.; Akamatsu, K.I.; Tsuchiya, M.; Nagasaka, A.; Yoshida, S. Isothiazolone derivatives selectively inhibit telomerase from human and rat cancer cells in vitro. *Biochemistry* **1999**, *38*, 11501–11507. [[CrossRef](#)] [[PubMed](#)]
142. Damm, K.; Hemmann, U.; Garin-Chesa, P.; Huel, N.; Kauffmann, I.; Priepke, H.; Niestroj, C.; Daiber, C.; Enenkel, B.; Guilliard, B.; et al. A highly selective telomerase inhibitor limiting human cancer cell proliferation. *EMBO J.* **2001**, *20*, 6958–6968. [[CrossRef](#)] [[PubMed](#)]
143. Kleideiter, E.; Piotrowska, K.; Klotz, U. Screening of telomerase inhibitors. *Methods Mol. Biol.* **2007**, *405*, 167–180. [[PubMed](#)]
144. Wong, L.H.; Unciti-Broceta, A.; Spitzer, M.; White, R.; Tyers, M.; Harrington, L. A yeast chemical genetic screen identifies inhibitors of human telomerase. *Chem. Biol.* **2013**, *20*, 333–340. [[CrossRef](#)] [[PubMed](#)]
145. Sengupta, S.; Peterson, T.R.; Sabatini, D.M. Regulation of the mTOR complex 1 pathway by nutrients, growth factors, and stress. *Mol. Cell* **2010**, *40*, 310–322. [[CrossRef](#)] [[PubMed](#)]
146. Bu, X.; Jia, F.; Wang, W.; Guo, X.; Wu, M.; Wei, L. Coupled down-regulation of mTOR and telomerase activity during fluorouracil-induced apoptosis of hepatocarcinoma cells. *BMC Cancer* **2007**. [[CrossRef](#)] [[PubMed](#)]
147. Sundin, T.; Peffley, D.M.; Gauthier, D.; Hentosh, P. The isoprenoid perillyl alcohol inhibits telomerase activity in prostate cancer cells. *Biochimie* **2012**, *94*, 2639–2648. [[CrossRef](#)] [[PubMed](#)]
148. Sundin, T.; Peffley, D.M.; Hentosh, P. Disruption of an hTERT-mTOR-RAPTOR protein complex by a phytochemical perillyl alcohol and rapamycin. *Mol. Cell Biochem.* **2013**, *375*, 97–104. [[CrossRef](#)] [[PubMed](#)]
149. Liu, J.P.; Chen, W.; Schwarzer, A.P.; Li, H. Telomerase in cancer immunotherapy. *Biochim. Biophys. Acta* **2010**, *1805*, 35–42. [[CrossRef](#)] [[PubMed](#)]
150. Ugel, S.; Scarselli, E.; Iezzi, M.; Mennuni, C.; Pannellini, T.; Calvaruso, F.; Cipriani, B.; De Palma, R.; Ricci-Vitiani, L.; Peranzoni, E. Autoimmune B-cell lymphopenia after successful adoptive therapy with telomerase-specific T lymphocytes. *Blood* **2010**, *115*, 1374–1384. [[CrossRef](#)] [[PubMed](#)]
151. Zanetti, M. A second chance for telomerase reverse transcriptase in anticancer immunotherapy. *Nat. Rev. Clin. Oncol.* **2016**. [[CrossRef](#)] [[PubMed](#)]
152. Su, Z.; Dannull, J.; Heiser, A.; Yancey, D.; Pruitt, S.; Madden, J.; Coleman, D.; Niedzwiecki, D.; Gilboa, E.; Vieweg, J. Immunological and clinical responses in metastatic renal cancer patients vaccinated with tumor RNA-transfected dendritic cells. *Cancer Res.* **2003**, *63*, 2127–2133. [[PubMed](#)]
153. Parkhurst, M.R.; Riley, J.P.; Igarashi, T.; Li, Y.; Robbins, P.F.; Rosenberg, S.A. Immunization of patients with the hTERT: 540–548 peptide induces peptide-reactive T lymphocytes that do not recognize tumors endogenously expressing telomerase. *Clin. Cancer Res.* **2004**, *10*, 4688–4698. [[CrossRef](#)] [[PubMed](#)]
154. Vonderheide, R.H.; Domchek, S.M.; Schultze, J.L.; George, D.J.; Hoar, K.M.; Chen, D.Y.; Stephans, K.F.; Masutomi, K.; Loda, M.; Xia, Z.; et al. Vaccination of cancer patients against telomerase induces functional antitumor CD8+ T lymphocytes. *Clin. Cancer Res.* **2004**, *10*, 828–839. [[CrossRef](#)] [[PubMed](#)]
155. Su, Z.; Dannull, J.; Yang, B.K.; Dahm, P.; Coleman, D.; Yancey, D.; Sichi, S.; Niedzwiecki, D.; Boczkowski, D.; Gilboa, E.; et al. Telomerase mRNA-transfected dendritic cells stimulate antigen-specific CD8+ and CD4+ T cell responses in patients with metastatic prostate cancer. *J. Immunol.* **2005**, *174*, 3798–3807. [[CrossRef](#)] [[PubMed](#)]
156. Cortez-Gonzalez, X.; Zanetti, M. Telomerase immunity from bench to bedside: Round one. *J. Transl. Med.* **2007**. [[CrossRef](#)] [[PubMed](#)]

157. Brunsvig, P.F.; Aamdal, S.; Gjertsen, M.K.; Kvalheim, G.; Markowski-Grimsrud, C.J.; Sve, I.; Dyrhaug, M.; Trachsel, S.; Møller, M.; Eriksen, J.A.; et al. Telomerase peptide vaccination: A phase I/II study in patients with non-small cell lung cancer. *Cancer Immunol. Immunother.* **2006**, *55*, 1553–1564. [[CrossRef](#)] [[PubMed](#)]
158. Bernhardt, S.L.; Gjertsen, M.K.; Trachsel, S.; Møller, M.; Eriksen, J.A.; Meo, M.; Buanes, T.; Gaudernack, G. Telomerase peptide vaccination of patients with non-resectable pancreatic cancer: A dose escalating phase I/II study. *Br. J. Cancer* **2006**, *95*, 1474–1482. [[CrossRef](#)] [[PubMed](#)]
159. Mavroudis, D.; Bolonakis, I.; Cornet, S.; Myllaki, G.; Kanellou, P.; Kotsakis, A.; Galanis, A.; Nikoloudi, I.; Spyropoulou, M.; Menez, J.; et al. A phase I study of the optimized cryptic peptide TERT572y in patients with advanced malignancies. *Oncology* **2006**, *70*, 306–314. [[CrossRef](#)] [[PubMed](#)]
160. Bolonaki, I.; Kotsakis, A.; Papadimitraki, E.; Aggouraki, D.; Konsolakis, G.; Vagia, A.; Christophylakis, C.; Nikoloudi, I.; Magganas, E.; Galanis, A.; et al. Vaccination of patients with advanced non-small-cell lung cancer with an optimized cryptic human telomerase reverse transcriptase peptide. *J. Clin. Oncol.* **2007**, *25*, 2727–2734. [[CrossRef](#)] [[PubMed](#)]
161. Berntsen, A.; Trepiakas, R.; Wenandy, L.; Geertsen, P.F.; thor Straten, P.; Andersen, M.H.; Pedersen, A.E.; Claesson, M.H.; Lorentzen, T.; Johansen, J.S.; et al. Therapeutic dendritic cell vaccination of patients with metastatic renal cell carcinoma: A clinical phase 1/2 trial. *J. Immunother.* **2008**, *31*, 771–780. [[CrossRef](#)] [[PubMed](#)]
162. Hunger, R.E.; Kernland Lang, K.; Markowski, C.J.; Trachsel, S.; Møller, M.; Eriksen, J.A.; Rasmussen, A.M.; Braathen, L.R.; Gaudernack, G. Vaccination of patients with cutaneous melanoma with telomerase-specific peptides. *Cancer Immunol. Immunother.* **2011**, *60*, 1553–1564. [[CrossRef](#)] [[PubMed](#)]
163. Kyte, J.A.; Gaudernack, G.; Dueland, S.; Trachsel, S.; Julsrud, L.; Aamdal, S. Telomerase peptide vaccination combined with temozolomide: A clinical trial in stage IV melanoma patients. *Clin. Cancer Res.* **2011**, *17*, 4568–4580. [[CrossRef](#)] [[PubMed](#)]
164. Rapoport, A.P.; Aqui, N.A.; Stadtmauer, E.A.; Vogl, D.T.; Fang, H.B.; Cai, L.; Janofsky, S.; Chew, A.; Storek, J.; Akpek, G.; et al. Combination immunotherapy using adoptive T-cell transfer and tumor antigen vaccination on the basis of hTERT and survivin after ASCT for myeloma. *Blood* **2011**, *117*, 788–797. [[CrossRef](#)] [[PubMed](#)]
165. Vik-Mo, E.O.; Nyakas, M.; Mikkelsen, B.V.; Moe, M.C.; Due-Tønnesen, P.; Suso, E.M.; Sæbøe-Larsen, S.; Sandberg, C.; Brinchmann, J.E.; Helseth, E.; et al. Therapeutic vaccination against autologous cancer stem cells with mRNA-transfected dendritic cells in patients with glioblastoma. *Cancer Immunol. Immunother.* **2013**, *62*, 1499–1509. [[CrossRef](#)] [[PubMed](#)]
166. Fenoglio, D.; Traverso, P.; Parodi, A.; Tomasello, L.; Negrini, S.; Kalli, F.; Battaglia, F.; Ferrera, F.; Sciallero, S.; Murdaca, G.; et al. A multi-peptide, dual-adjuvant telomerase vaccine (GX301) is highly immunogenic in patients with prostate and renal cancer. *Cancer Immunol. Immunother.* **2013**, *62*, 1041–1052. [[CrossRef](#)] [[PubMed](#)]
167. Staff, C.; Mozaffari, F.; Frodin, J.E.; Mellstedt, H.; Liljefors, M. Telomerase (GV1001) vaccination together with gemcitabine in advanced pancreatic cancer patients. *Int. J. Oncol.* **2014**, *45*, 1293–1303. [[CrossRef](#)] [[PubMed](#)]
168. Davoli, T.; de Lange, T. Telomere-driven tetraploidization occurs in human cells undergoing crisis and promotes transformation of mouse cells. *Cancer Cell* **2012**, *21*, 765–776. [[CrossRef](#)] [[PubMed](#)]
169. Greten, T.F.; Forner, A.; Korangy, F.; N'Kontchou, G.; Barget, N.; Ayuso, C.; Ormandy, L.A.; Manns, M.P.; Beaugrand, M.; Bruix, J. A phase II open label trial evaluating safety and efficacy of a telomerase peptide vaccination in patients with advanced hepatocellular carcinoma. *BMC Cancer* **2010**. [[CrossRef](#)] [[PubMed](#)]
170. Brunsvig, P.F.; Kyte, J.A.; Kersten, C.; Sundstrøm, S.; Møller, M.; Nyakas, M.; Hansen, G.L.; Gaudernack, G.; Aamdal, S. Telomerase peptide vaccination in NSCLC: A phase II trial in stage III patients vaccinated after chemoradiotherapy and an 8-year update on a phase I/II trial. *Clin. Cancer Res.* **2001**, *17*, 6847–6857. [[CrossRef](#)] [[PubMed](#)]
171. Ellebaek, E.; Engell-Noerregaard, L.; Iversen, T.Z.; Froesig, T.M.; Munir, S.; Hadrup, S.R.; Andersen, M.H.; Svane, I.M. Metastatic melanoma patients treated with dendritic cell vaccination, interleukin-2 and metronomic cyclophosphamide: Results from a phase II trial. *Cancer Immunol. Immunother.* **2012**, *61*, 1791–1804. [[CrossRef](#)] [[PubMed](#)]

172. Kotsakis, A.; Vetsika, E.K.; Christou, S.; Hatzidaki, D.; Vardakis, N.; Aggouraki, D.; Konsolakis, G.; Georgoulas, V.; Christophyllakis, C.; Cordopatis, P.; et al. Clinical outcome of patients with various advanced cancer types vaccinated with an optimized cryptic human telomerase reverse transcriptase (TERT) peptide: Results of an expanded phase II study. *Ann. Oncol.* **2012**, *23*, 442–449. [[CrossRef](#)] [[PubMed](#)]
173. Middleton, G.; Silcocks, P.; Cox, T.; Valle, J.; Wadsley, J.; Propper, D.; Coxon, F.; Ross, P.; Madhusudan, S.; Roques, T.; et al. Gemcitabine and capecitabine with or without telomerase peptide vaccine GV1001 in patients with locally advanced or metastatic pancreatic cancer (TeloVac): An open-label, randomised, phase 3 trial. *Lancet Oncol.* **2014**, *15*, 829–840. [[CrossRef](#)]
174. Mizukoshi, E.; Nakagawa, H.; Kitahara, M.; Yamashita, T.; Arai, K.; Sunagozaka, H.; Iida, N.; Fushimi, K.; Kaneko, S. Phase I trial of multidrug resistance-associated protein 3-derived peptide in patients with hepatocellular carcinoma. *Cancer Lett.* **2015**, *369*, 242–249. [[CrossRef](#)] [[PubMed](#)]
175. Nemunaitis, J.; Tong, A.W.; Nemunaitis, M.; Senzer, N.; Phadke, A.P.; Bedell, C.; Adams, N.; Zhang, Y.A.; Maples, P.B.; Chen, S.; et al. A phase I study of telomerase-specific replication competent oncolytic adenovirus (telomelysin) for various solid tumours. *Mol. Ther.* **2010**, *18*, 429–434. [[CrossRef](#)] [[PubMed](#)]
176. Keith, W.N.; Bilisland, A.; Hardie, M.; Evans, T.R. Drug insight: Cancer cell immortality-telomerase as a target for novel cancer gene therapies. *Nat. Clin. Pract. Oncol.* **2004**, *1*, 88–96. [[CrossRef](#)] [[PubMed](#)]
177. Chen, Y.; Zhang, Y. Functional and mechanistic analysis of telomerase: An antitumor drug target. *Pharmacol. Ther.* **2016**, *163*, 24–47. [[CrossRef](#)] [[PubMed](#)]
178. Sun, L.; Wang, X. Effects of allicin on both telomerase activity and apoptosis in gastric cancer SGC-7901 cells. *World J. Gastroenterol.* **2003**, *9*, 1930–1934. [[CrossRef](#)] [[PubMed](#)]
179. Chakraborty, S.; Ghosh, U.; Bhattacharyya, N.P.; Bhattacharya, R.K.; Roy, M. Inhibition of telomerase activity and induction of apoptosis by curcumin in K-562 cells. *Mutat. Res.* **2006**, *596*, 81–90. [[CrossRef](#)] [[PubMed](#)]
180. Yokoyama, M.; Noguchi, M.; Nakao, Y.; Ysunaga, M.; Yamasaki, F.; Iwasaka, T. Antiproliferative effects of the major tea polyphenol, (–)-epigallocatechin gallate and retinoic acid in cervical adenocarcinoma. *Gynecol. Oncol.* **2008**, *108*, 326–331. [[CrossRef](#)] [[PubMed](#)]
181. Ramachandran, C.; Fonseca, H.B.; Jhabvala, P.; Escalon, E.A.; Melnick, S.J. Curcumin inhibits telomerase activity through human telomerase reverse transcriptase in MCF-7 breast cancer cell line. *Cancer Lett.* **2002**, *184*, 1–6. [[CrossRef](#)]
182. Hsin, I.L.; Sheu, G.T.; Chen, H.H.; Chiu, L.Y.; Wang, H.D.; Chan, H.W.; Hsu, C.P.; Ko, J.L. N-acetyl cysteine mitigates curcumin-mediated telomerase inhibition through rescuing of Sp1 reduction in A549 cells. *Mutat. Res.* **2010**, *688*, 72–77. [[CrossRef](#)] [[PubMed](#)]
183. Lee, J.H.; Chung, I.K. Curcumin inhibits nuclear localization of telomerase by dissociating the Hsp90 co-chaperone p23 from hTERT. *Cancer Lett.* **2010**, *290*, 76–86. [[CrossRef](#)] [[PubMed](#)]
184. Singh, M.; Singh, N. Molecular mechanism of curcumin induced cytotoxicity in human cervical carcinoma cells. *Mol. Cell Biochem.* **2009**, *325*, 107–119. [[CrossRef](#)] [[PubMed](#)]
185. Mukherjee Nee Chakraborty, S.; Ghosh, U.; Bhattacharyya, N.P.; Bhattacharya, R.K.; Dey, S.; Roy, M. Curcumin-induced apoptosis in human leukemia cell HL-60 is associated with inhibition of telomerase activity. *Mol. Cell Biochem.* **2007**, *297*, 31–39. [[CrossRef](#)] [[PubMed](#)]
186. Berletch, J.B.; Liu, C.; Love, W.K.; Andrews, L.G.; Katiyar, S.K.; Tollefsbol, T.O. Epigenetic and genetic mechanisms contribute to telomerase inhibition by EGCG. *J. Cell Biochem.* **2008**, *103*, 509–519. [[CrossRef](#)] [[PubMed](#)]
187. Li, Y.; Liu, L.; Andrews, L.G.; Tollefsbol, T.O. Genistein depletes telomerase activity through cross-talk between genetic and epigenetic mechanisms. *Int. J. Cancer* **2009**, *125*, 286–296. [[CrossRef](#)] [[PubMed](#)]
188. Meeran, S.M.; Patel, S.N.; Chan, T.H.; Tollefsbol, T.O. A novel prodrug of epigallocatechin-3-gallate: Differential epigenetic hTERT repression in human breast cancer cells. *Cancer Prev. Res. (Phila)* **2011**, *4*, 1243–1254. [[CrossRef](#)] [[PubMed](#)]
189. Moon, D.O.; Kang, S.H.; Kim, K.C.; Kim, M.O.; Choi, Y.H.; Kim, G.Y. Sulforaphane decreases viability and telomerase activity in hepatocellular carcinoma Hep3B cells through the reactive oxygen species-dependent pathway. *Cancer Lett.* **2010**, *295*, 260–266. [[CrossRef](#)] [[PubMed](#)]
190. Mittal, A.; Pate, M.S.; Wylie, R.C.; Tollefsbol, T.O.; Katiyar, S.K. EGCG down-regulates telomerase in human breast carcinoma MCF-7 cells, leading to suppression of cell viability and induction of apoptosis. *Int. J. Oncol.* **2004**, *24*, 703–710. [[CrossRef](#)] [[PubMed](#)]

191. Shapira, S.; Granot, G.; Mor-Tzuntz, R.; Raanani, P.; Uziel, O.; Lahav, M.; Shpilberg, O. Second-generation tyrosine kinase inhibitors reduce telomerase activity in K562 cells. *Cancer Lett.* **2012**, *323*, 223–231. [[CrossRef](#)] [[PubMed](#)]
192. Mor-Tzuntz, R.; Uziel, O.; Shpilberg, O.; Lahav, J.; Raanani, P.; Bakhanashvili, M.; Rabizadeh, E.; Zimra, Y.; Lahav, M.; Granot, G. Effect of imatinib on the signal transduction cascade regulating telomerase activity in K562 (BCR-ABL-positive) cells sensitive and resistant to imatinib. *Exp. Hematol.* **2010**, *8*, 27–37. [[CrossRef](#)] [[PubMed](#)]
193. Moon, D.O.; Kim, M.O.; Heo, M.S.; Lee, J.D.; Choi, Y.H.; Kim, G.Y. Gefitinib induces apoptosis and decreases telomerase activity in MDA-MB-231 human breast cancer cells. *Arch. Pharm. Res.* **2009**, *32*, 1351–1360. [[CrossRef](#)] [[PubMed](#)]
194. Zhang, Y.; Sun, M.; Shi, W.; Yang, Q.; Chen, C.; Wang, Z.; Zhou, X. Arsenic trioxide suppresses transcription of hTERT through down-regulation of multiple transcription factors in HL-60 leukemia cells. *Toxicol. Lett.* **2015**, *232*, 481–489. [[CrossRef](#)] [[PubMed](#)]
195. Zhang, X.; Li, B.; de Jonge, N.; Bjorkholm, M.; Xu, D. The DNA methylation inhibitor induces telomere dysfunction and apoptosis of leukemia cells that is attenuated by telomerase over-expression. *Oncotarget* **2015**, *6*, 4888–4900. [[CrossRef](#)] [[PubMed](#)]
196. Kanzawa, T.; Germano, I.M.; Kondo, Y.; Ito, H.; Kyo, S.; Kondo, S. Inhibition of telomerase activity in malignant glioma cells correlates with their sensitivity to temozolomide. *Br. J. Cancer* **2003**, *89*, 922–929. [[CrossRef](#)] [[PubMed](#)]
197. Gan, Y.; Lu, J.; Yeung, B.Z.; Cottage, C.T.; Wientjes, M.G.; Au, J.L. Pharmacodynamics of telomerase inhibition and telomere shortening by noncytotoxic suramin. *AAPS J.* **2015**, *17*, 268–276. [[CrossRef](#)] [[PubMed](#)]
198. He, H.; Xia, H.H.; Wang, J.D.; Gu, Q.; Lin, M.C.; Zou, B.; Lam, S.K.; Chan, A.O.; Yuen, M.F.; Kung, H.F.; et al. Inhibition of human telomerase reverse transcriptase by nonsteroidal antiinflammatory drugs in colon carcinoma. *Cancer* **2006**, *106*, 1243–1249. [[CrossRef](#)] [[PubMed](#)]
199. Zhao, Y.-Q.; Feng, H.-W.; Jia, T.; Chen, X.-M.; Zhang, H.; Xu, A.-T.; Zhang, H.L.; Fan, X.-L. Antiproliferative effects of celecoxib in Hep-2 cells through telomerase inhibition and induction of apoptosis. *Asian Pac. J. Cancer Prev.* **2014**, *15*, 4919–4923. [[CrossRef](#)] [[PubMed](#)]
200. Rashid-Kolvear, F.; Taboski, M.A.; Nguyen, J.; Wang, D.Y.; Harrington, L.A.; Done, S.J. Troglitazone suppresses telomerase activity independently of PPARgamma in estrogen-receptor negative breast cancer cells. *BMC Cancer* **2011**. [[CrossRef](#)]
201. Kiran, K.G.; Palaniswamy, M.; Angayarkanni, J. Human telomerase inhibitors from microbial source. *World J. Microbiol. Biotechnol.* **2015**, *31*, 1329–1341. [[CrossRef](#)] [[PubMed](#)]
202. Li, C.T.; Hsiao, Y.M.; Wu, T.C.; Lin, Y.W.; Yeh, K.T.; Ko, J.L. Vorinostat, SAHA, represses telomerase activity via epigenetic regulation of telomerase reverse transcriptase in non-small cell lung cancer cells. *J. Cell Biochem.* **2011**, *112*, 3044–3053. [[CrossRef](#)] [[PubMed](#)]
203. Zhao, Y.M.; Zhou, Q.; Xu, Y.; Lai, X.Y.; Huang, H. Antiproliferative effect of rapamycin on human T-cell leukemia cell line Jurkat by cell cycle arrest and telomerase inhibition. *Acta Pharmacol. Sin.* **2008**, *29*, 481–488. [[CrossRef](#)] [[PubMed](#)]
204. Woo, H.J.; Choi, Y.H. Growth inhibition of A549 human lung carcinoma cells by beta-lapachone through induction of apoptosis and inhibition of telomerase activity. *Int. J. Oncol.* **2005**, *26*, 1017–1023. [[PubMed](#)]
205. Burger, A.M.; Double, J.A.; Newell, D.R. Inhibition of telomerase activity by cisplatin in human testicular cancer cells. *Eur. J. Cancer* **1997**, *33*, 638–644. [[CrossRef](#)]
206. Leon-Blanco, M.M.; Guerrero, J.M.; Reiter, R.J.; Calvo, J.R.; Pozo, D. Melatonin inhibits telomerase activity in the MCF-7 tumor cell line both in vivo and in vitro. *J. Pineal. Res.* **2003**, *35*, 204–211. [[CrossRef](#)] [[PubMed](#)]
207. Holohan, B.; Hagiopian, M.M.; Lai, T.P.; Huang, E.; Friedman, D.R.; Wright, W.E.; Shay, J.W. Perifosine as a potential novel anti-telomerase therapy. *Oncotarget* **2015**, *6*, 21816–21826. [[CrossRef](#)] [[PubMed](#)]
208. Baoping, Y.; Guoyong, H.; Jieping, Y.; Zongxue, R.; Hesheng, L. Cyclooxygenase-2 inhibitor nimesulide suppresses telomerase activity by blocking Akt/PKB activation in gastric cancer cell line. *Dig. Dis. Sci.* **2004**, *49*, 948–953. [[CrossRef](#)] [[PubMed](#)]
209. Kim, N.-H.; Park, H.J.; Oh, M.-K.; Kim, I.-S. Antiproliferative effect of gold (I) compound auranofin through inhibition of STAT3 and telomerase activity in MDA-MB 231 human breast cancer cells. *BMB Rep.* **2013**, *46*, 59–64. [[CrossRef](#)] [[PubMed](#)]

210. Khorramizadeh, M.R.; Saadat, F.; Vaezzadeh, F.; Safavifar, F.; Bashiri, H.; Jahanshiri, Z. Suppression of telomerase activity by pyrimethamine: Implication to cancer. *Iran Biomed. J.* **2007**, *11*, 223–228. [[PubMed](#)]
211. Brown, T.; Sigurdson, E.; Rogatko, A.; Broccoli, D. Telomerase inhibition using azidothymidine in the HT-29 colon cancer cell line. *Ann. Surg. Oncol.* **2003**, *10*, 910–915. [[CrossRef](#)] [[PubMed](#)]
212. Gao, S.; Yu, B.P.; Li, Y.; Dong, W.G.; Luo, H.S. Antiproliferative effect of octreotide on gastric cancer cells mediated by inhibition of Akt/PKB and telomerase. *World J. Gastroenterol.* **2003**, *9*, 2362–2365. [[CrossRef](#)] [[PubMed](#)]
213. Yamakuchi, M.; Nakata, M.; Kawahara, K.; Kitajima, I.; Maruyama, I. New quinolones, ofloxacin and levofloxacin, inhibit telomerase activity in transitional cell carcinoma cell lines. *Cancer Lett.* **1997**, *119*, 213–219. [[CrossRef](#)]
214. Sun, H.; Xiang, J.; Li, Q.; Liu, Y.; Li, L.; Shang, Q.; Xu, G.; Tang, Y. Recognize three different human telomeric G-quadruplex conformations by quinacrine. *Analyst* **2012**, *137*, 862–867. [[CrossRef](#)] [[PubMed](#)]
215. Ci, X.; Li, B.; Ma, X.; Kong, F.; Zheng, C.; Björkholm, M.; Jia, J.; Xu, D. Bortezomib-mediated down-regulation of telomerase and disruption of telomere homeostasis contributes to apoptosis of malignant cells. *Oncotarget* **2015**, *6*, 38079–38092. [[PubMed](#)]
216. Kato, M.; Nakayama, M.; Agata, M.; Yoshida, K. Gene expression levels of human shelterin complex and shelterin-associated factors regulated by the topoisomerase II inhibitors doxorubicin and etoposide in human cultured cells. *Tumour Biol.* **2013**, *34*, 723–733. [[CrossRef](#)] [[PubMed](#)]
217. Zhang, B.; Qian, D.; Ma, H.H.; Jin, R.; Yang, P.X.; Cai, M.Y.; Liu, Y.H.; Liao, Y.J.; Deng, H.X.; Mai, S.J.; et al. Anthracyclines disrupt telomere maintenance by telomerase through inducing PinX1 ubiquitination and degradation. *Oncogene* **2012**, *31*, 1–12. [[CrossRef](#)] [[PubMed](#)]
218. Mimeault, M.; Hauke, R.; Mehta, P.P.; Batra, S.K. Recent advances on cancer stem/progenitor cell research: Therapeutic implications for overcoming resistance to the most aggressive cancers. *J. Mol. Cell Med.* **2007**, *11*, 981–1011. [[CrossRef](#)] [[PubMed](#)]
219. Mimeault, M.; Batra, S.K. Recent advances on the development of novel anti-cancer drugs targeting cancer stem/progenitor cells. *Drug Dev. Res.* **2008**, *69*, 415–430. [[CrossRef](#)]
220. Tang, J.Y.; So, P.L.; Epstein, E.H., Jr. Novel Hedgehog pathway targets against basal cell carcinoma. *Toxicol. Appl. Pharmacol.* **2006**, *224*, 257–264. [[CrossRef](#)] [[PubMed](#)]
221. Singh, B.; Schneider, M.; Knyazev, P.; Ullrich, A. UV-induced EGFR signal transactivation is dependent on proligand shedding by activated metalloproteases in skin cancer cell lines. *Int. J. Cancer* **2009**, *124*, 531–539. [[CrossRef](#)] [[PubMed](#)]
222. Stecca, B.; Mas, C.; Clement, V.; Zbinden, M.; Correa, R.; Piguat, V.; Beermann, F.; Ruiz, I.; Altaba, A. Melanomas require HEDGEHOG-GLI signaling regulated by interactions between GLI1 and the RAS-MEK/AKT pathways. *Proc. Natl. Acad. Sci. USA* **2007**, *104*, 5895–5900. [[CrossRef](#)] [[PubMed](#)]
223. Hoffmeyer, K.; Raggioli, A.; Rudloff, S.; Anton, R.; Hierholzer, A.; Del Valle, I.; Hein, K.; Vogt, R.; Kemler, R. Wnt/ β -catenin signaling regulates telomerase in stem cells and cancer cells. *Science* **2012**, *336*, 1549–1554. [[CrossRef](#)] [[PubMed](#)]
224. Calado, R.T.; Young, N.S. Telomere maintenance and human bone marrow failure. *Blood* **2008**, *111*, 4446–4455. [[CrossRef](#)] [[PubMed](#)]
225. Yamamoto, K.; Nihrane, A.; Aglipay, J.; Sironi, J.; Arkin, S.; Lipton, J.M.; Ouchi, T.; Liu, J.M. Upregulated ATM gene expression and activated DNA crosslink-induced damage response checkpoint in Fanconi anemia: Implications for carcinogenesis. *Mol. Med.* **2008**, *14*, 167–174. [[CrossRef](#)] [[PubMed](#)]
226. Meshorer, E.; Gruenbaum, Y. Gone with the Wnt/Notch: Stem cells in laminopathies, progeria, and aging. *J. Cell Biol.* **2008**, *181*, 9–13. [[CrossRef](#)] [[PubMed](#)]
227. Scaffidi, P.; Misteli, T. Lamin A-dependent misregulation of adult stem cells associated with accelerated ageing. *Nat. Cell Biol.* **2008**, *10*, 452–459. [[CrossRef](#)] [[PubMed](#)]
228. Bergoglio, V.; Magnaldo, T. Nucleotide excision repair and related human diseases. *Genome Dyn.* **2006**, *1*, 35–52. [[PubMed](#)]
229. Stout, G.J.; Blasco, M.A. Genetic dissection of the mechanisms underlying telomere-associated diseases: Impact of the TRF2 telomeric protein on mouse epidermal stem cells. *Dis. Model Mech.* **2009**, *2*, 139–156. [[CrossRef](#)] [[PubMed](#)]
230. Aubert, G.; Lansdorp, P.M. Telomeres and aging. *Physiol. Rev.* **2008**, *88*, 557–579. [[CrossRef](#)] [[PubMed](#)]

231. Mason, P.J.; Wilson, D.B.; Bessler, M. Dyskeratosis congenital—A disease of dysfunctional telomere maintenance. *Curr. Mol. Med.* **2005**, *5*, 159–170. [[CrossRef](#)] [[PubMed](#)]
232. Kenyon, J.; Gerson, S.L. The role of DNA damage repair in aging of adult stem cells. *Nucleic Acids Res.* **2007**, *35*, 7557–7565. [[CrossRef](#)] [[PubMed](#)]
233. Nijnik, A.; Woodbine, L.; Marchetti, C.; Dawson, S.; Lambe, T.; Liu, C.; Rodrigues, N.P.; Crockford, T.L.; Cabuy, E.; Vindigni, A.; et al. DNA repair is limiting for haematopoietic stem cells during ageing. *Nature* **2007**, *447*, 686–690. [[CrossRef](#)] [[PubMed](#)]
234. Chigancas, V.; Lima-Bessa, K.M.; Stary, A.; Menck, C.F.; Sarasin, A. Defective transcription/repair factor IIIH recruitment to specific UV lesions in trichothiodystrophy syndrome. *Cancer Res.* **2008**, *68*, 6074–6083. [[CrossRef](#)] [[PubMed](#)]
235. Budiyo, A.; Bito, T.; Kunisada, M.; Ashida, M.; Ichihashi, M.; Ueda, M. Inhibition of the epidermal growth factor receptor suppresses telomerase activity in HSC-1 human cutaneous squamous cell carcinoma cells. *J. Invest. Dermatol.* **2003**, *121*, 1088–1094. [[CrossRef](#)] [[PubMed](#)]
236. Horn, S.; Figl, A.; Rachakonda, P.S.; Fischer, C.; Sucker, A.; Gast, A.; Kadel, S.; Moll, I.; Nagore, E.; Hemminki, K.; et al. TERT promoter mutations in familial and sporadic melanoma. *Science* **2013**, *339*, 959–961. [[CrossRef](#)] [[PubMed](#)]
237. Baur, J.A.; Sinclair, D.A. Therapeutic potential of resveratrol: The in vivo evidence. *Nat. Rev. Drug Discov.* **2006**, *5*, 493–506. [[CrossRef](#)] [[PubMed](#)]
238. Athar, M.; Back, J.H.; Tang, X.; Kim, K.H.; Kopelovich, L.; Bickers, D.R.; Kim, A.L. Resveratrol: A review of preclinical studies for human cancer prevention. *Toxicol. Appl. Pharmacol.* **2007**, *224*, 274–283. [[CrossRef](#)] [[PubMed](#)]
239. Shay, J.W.; Wright, W.E. Telomeres and telomerase in normal and cancer stem cells. *FEBS Lett.* **2010**, *584*, 3819–3825. [[CrossRef](#)] [[PubMed](#)]
240. Hahn, W.C.; Counter, C.M.; Lundberg, A.S.; Beijersbergen, R.L.; Brooks, M.W.; Weinberg, R.A. Creation of human tumor cells with defined genetic elements. *Nature* **1999**, *400*, 464–468. [[PubMed](#)]
241. Braig, M.; Lee, S.; Loddenkemper, C.; Rudolph, C.; Peters, A.H.; Schlegelberger, B.; Stein, H.; Dörken, B.; Jenuwein, T.; Schmitt, C.A. Oncogene-induced senescence as an initial barrier in lymphoma development. *Nature* **2005**, *436*, 660–665. [[CrossRef](#)] [[PubMed](#)]
242. Chen, Z.; Trotman, L.C.; Shaffer, D.; Lin, H.K.; Dotan, Z.A.; Niki, M.; Koutcher, J.A.; Scher, H.I.; Ludwig, T.; Gerald, W.; et al. Crucial role of p53-dependent cellular senescence in suppression of Pten-deficient tumorigenesis. *Nature* **2005**, *436*, 725–730. [[CrossRef](#)] [[PubMed](#)]
243. Collado, M.; Serrano, M. The power and the promise of oncogene-induced senescence markers. *Nat. Rev. Cancer* **2006**, *6*, 472–476. [[CrossRef](#)] [[PubMed](#)]
244. Xue, W.; Zender, L.; Miething, C.; Dickins, R.A.; Hernandez, E.; Krizhanovskiy, V.; Cordon-Cardo, C.; Lowe, S.W. Senescence and tumour clearance is triggered by p53 restoration in murine liver carcinomas. *Nature* **2007**, *445*, 656–660. [[CrossRef](#)] [[PubMed](#)]
245. Ventura, A.; Kirsch, D.G.; McLaughlin, M.E.; Tuveson, D.A.; Grimm, J.; Lintault, L.; Newman, J.; Reczek, E.E.; Weissleder, R.; Jacks, T. Restoration of p53 function leads to tumour regression in vivo. *Nature* **2007**, *445*, 661–665. [[CrossRef](#)] [[PubMed](#)]
246. Ewald, J.A.; Desotelle, J.A.; Wilding, G.; Jarrard, D.F. Therapy-induced senescence in cancer. *J. Natl. Cancer Inst.* **2010**, *102*, 1536–1546. [[CrossRef](#)] [[PubMed](#)]
247. Te Poele, R.H.; Okorokov, A.L.; Jardine, L.; Cummings, J.; Joel, S.P. DNA damage is able to induce senescence in tumor cells in vitro and in vivo. *Cancer Res.* **2002**, *62*, 1876–1883. [[PubMed](#)]
248. Rudolph, K.L.; Millard, M.; Bosenberg, M.W.; DePinho, R.A. Telomere dysfunction and evolution of intestinal carcinoma in mice and humans. *Nat. Genet.* **2001**, *28*, 155–159. [[CrossRef](#)] [[PubMed](#)]
249. Chin, L.; Artandi, S.E.; Shen, Q.; Tam, A.; Lee, S.-L.; Gottlieb, G.J.; Greider, C.W.; DePinho, R.A. p53 deficiency rescues the adverse effects of telomere loss and cooperates with telomere dysfunction to accelerate carcinogenesis. *Cell* **1999**, *97*, 527–538. [[CrossRef](#)]
250. Artandi, S.E.; Chang, S.; Lee, S.L.; Alson, S.; Gottlieb, G.J.; Chin, L.; DePinho, R.A. Telomere dysfunction promotes non-reciprocal translocations and epithelial cancers in mice. *Nature* **2000**, *406*, 641–645. [[PubMed](#)]
251. O'Sullivan, J.N.; Bronner, M.P.; Brentnall, T.A.; Finley, J.C.; Shen, W.T.; Emerson, S.; Emond, M.J.; Gollahan, K.A.; Moskowitz, A.H.; Crispin, D.A.; et al. Chromosomal instability in ulcerative colitis is related to telomere shortening. *Nat. Genet.* **2002**, *32*, 280–284. [[CrossRef](#)] [[PubMed](#)]

252. Romanov, S.R.; Kozakiewicz, B.K.; Holst, C.R.; Stampfer, M.R.; Haupt, L.M.; Tlsty, T.D. Normal human mammary epithelial cells spontaneously escape senescence and acquire genomic changes. *Nature* **2001**, *409*, 633–637. [[CrossRef](#)] [[PubMed](#)]
253. Seger, Y.R.; García-Cao, M.; Piccinin, S.; Cunsolo, C.L.; Doglioni, C.; Blasco, M.A.; Hannon, G.J.; Maestro, R. Transformation of normal human cells in the absence of telomerase activation. *Cancer Cell* **2002**, *2*, 401–413. [[CrossRef](#)]
254. Tomas-Loba, A.; Flores, I.; Fernandez-Marcos, P.J.; Cayuela, M.L.; Maraver, A.; Tejera, A.; Borrás, C.; Matheu, A.; Klatt, P.; Flores, J.M.; et al. Telomerase reverse transcriptase delays aging in cancer resistant mice. *Cell* **2008**, *135*, 609–622. [[CrossRef](#)] [[PubMed](#)]
255. Blasco, M.A. Telomeres and human disease: Ageing, cancer and beyond. *Nat. Rev. Genet.* **2005**, *6*, 611–622. [[CrossRef](#)] [[PubMed](#)]
256. Gonzalez-Suarez, E.; Geserick, C.; Flores, J.M.; Blasco, M.A. Antagonistic effects of telomerase on cancer and aging in K5-mTert transgenic mice. *Oncogene* **2005**, *24*, 2256–2270. [[CrossRef](#)] [[PubMed](#)]
257. Bernardes de Jesus, B.; Vera, E.; Schneeberger, K.; Tejera, A.M.; Ayuso, E.; Bosch, F.; Blasco, M.A. Telomerase gene therapy in adult and old mice delays aging and increases longevity without increasing cancer. *EMBO Mol. Med.* **2012**, *4*, 691–704. [[CrossRef](#)] [[PubMed](#)]



© 2016 by the authors; licensee MDPI, Basel, Switzerland. This article is an open access article distributed under the terms and conditions of the Creative Commons Attribution (CC-BY) license (<http://creativecommons.org/licenses/by/4.0/>).

Curriculum vitae

Mein Lebenslauf wird aus datenschutzrechtlichen Gründen in der elektronischen Version meiner Arbeit nicht veröffentlicht.

Mein Lebenslauf wird aus datenschutzrechtlichen Gründen in der elektronischen Version meiner Arbeit nicht veröffentlicht.

List of publication

1. Haj Ali J, Abdeen Z, Azmi K, Berman T, **Jäger K**, Barnett-Itzhaki B, Walter M. Influence of exposure to pesticides on telomere length and pregnancy outcome: diethylphosphates but not dimethylphosphates are associated with accelerated telomere attrition in a Palestinian cohort. *Ecotoxicol Environ Saf.* **2023**; 27;256:114801. Doi: 10.1016/j.ecoenv.2023.114801

Impact Factor 7.129

2. Lin H, Mensch J, Haschke M, **Jäger K**, Koettgen B, Dervedde J, Orsó E, Walter M. Establishment and Characterization of hTERT Immortalized Hutchinson-Gilford Progeria Fibroblast Cell Lines. *Cells* **2022**; 11(18):2784. DOI: 10.3390/cells11182784

Impact Factor 2022 6.70

3. **Jäger K**, Mensch J, Grimmig ME, Neuner B, Gorzelniak K, Türkmen S, Demuth I, Hartman A, Hartmann C, Wittig F, Sporbert A, Hermann A, Fuellen G, Möller S, Walter M. A Conserved Long-Distance Telomeric Silencing Mechanism Suppresses mTOR Signaling in Aging Human Fibroblasts. *Science advances* **2022**; 8 (33): eabk2814. DOI: 10.1126/sciadv.abk2814

Impact factor 2022 14.136

4. Hecker M, Fitzner B, **Jäger K**, Bühring J, Schwartz M, Hartmann A, Walter M, Zettel UK. Leukocyte Telomere Length in Patients with Multiple Sclerosis and Its Association with Clinical Phenotypes. *Mol Neurobiol.* **2021**; 58(6): 2886-2896. DOI: 10.1007/s12035-021-02315-y

Impact factor 2021 5.682

5. Habib R, Kim E, Neitzel H, Demuth I, Chrzanowska K, Seemanova E, Faber R, Digweed M, Voss R, **Jäger K**, Sperling K, Walter M. Telomere attrition and dysfunction: a potential trigger of the progeroid phenotype in nijmegen breakage syndrome. *Aging* **2020**;12(12):12342-12375. DOI: 10.18632/aging.103453

Impact factor 2021 5.955

6. **Jäger K**, Walter M. Therapeutic Targeting of Telomerase. *Genes (Basel)* **2016**; 7(7): 39. DOI: 10.3390/genes7070039

Impact factor 2021 4.096

7. Neuner B, Lenfers A, Kelsch R, **Jäger K**, Brüggmann N, van der Harst P, Walter M. Telomere Length Is Not Related to Established Cardiovascular Risk Factors but Does Correlate with Red and White Blood Cell Counts in a German Blood Donor Population. *PLoS ONE* **2015**; 10: e0139308.

Impact factor 2022 3.24

8. Kannenberg F, Gorzelniak K, **Jäger K**, Fobker M, Rust S, Repa J, Roth M, Björkhem I, Walter M. Characterization of cholesterol homeostasis in telomerase-immortalized Tangier disease fibroblasts reveals marked phenotype variability. *J Biol Chem.* **2013**; 288:36936-47.

Impact factor 2022 5.157

Acknowledgement

My special thanks go to my doctoral advisor Prof. Michael Walter, MD, for the always warm and collegial supervision and for the enormous support throughout the work.

Special thanks go to Juliane Mensch, who accompanied me both professionally and personally with a lot of understanding, humor and patience through the project and became a very good friend.

I would also like to thank all the members of Prof. Michael Walter's research group for their help.

I would also like to thank all co-authors, Bruno Neuner for his active support with the statistics; Seval Türkmen and Anje Sporbart for their help with the 3D-FISH experiments; Ilja Demuth for the samples of the BASE-II study; Steffen Möller and Georg Fuellen for the biostatistical analyses; Alexander Hartmann, Christiane Hartmann, Andreas Hermann, and Elisabeth Grimmig for their final contributions.

Finally, a big thanks to my family and friends who move me every day with their courage, love, and strength.